

Impact of Salinity Stress on Chloroplast Biogenesis and Photosynthesis

Thesis submitted to

JAWAHARLAL NEHRU UNIVERSITY

For the award of the Degree of

Doctor of Philosophy

SATPAL



**SCHOOL OF LIFE SCIENCES
JAWAHARLAL NEHRU UNIVERSITY
NEW DELHI-110067**

INDIA

2009

*Dedicated to My Family
& Teachers*

CONTENTS

Certificate	
Acknowledgements	
Abbreviations	
Introduction	1-2
Literature review	3-54
Salt stress	3
Salt movement through plants	3
Halophyte and glycophyte comparisons	4
Genetic Diversity for Salt Tolerance in Plants	5
Mechanism of Salt Stress Tolerance in Plants	6
Osmolytes and Osmoprotectants	8
Ion Homeostasis	9
Ion transport Systems that mediate Na ⁺ homeostasis	9
Na ⁺ Influx and Efflux across the Plasma Membrane	10
Na ⁺ Vacuolar Compartmentalization	10
Ca ²⁺ Signaling and SOS signal Transduction Pathway	11
Chloroplast biogenesis: A brief overview	12
Chlorophyll biosynthesis in higher plants: A brief overview	13
Glutamate 1-semialdehyde aminotransferase	17
Porphobilinogen deaminase	18
Uroporphyrinogen III cosynthetase	19
Coproporphyrinogen oxidase	19
Mg-chelatase	21
Protochlorophyllide oxidoreductase	26
Chlorophyll a oxygenase	32
Regulation of chlorophyll biosynthesis pathway	36
Oxidative stress and reactive oxygen species	40
Non-photochemical quenching and photochemical quenching.	43
Chl a fluorescence OJIP curve	42
Components of Thylakoids membranes:	43

Materials and Methods	55-83
Plant material and chemicals	55
Plant growth conditions	55
Chl and carotenoid estimation	56
Element Analysis	57
ALA content	57
GSA content	57
Pchlide content	58
ALAD activity	58
PBGD activity	58
Protox activity	59
Mg- Chelatase activity	59
RNA gel	62-63
RT-PCR	64
Northern	64
Probe preparation	65-66
Primer used	66-67
TEM	68
Fluorescence spectra	69-70
Chl a measurement	70-71
Thylakoid isolation	71
SDS-PAGE	72-74
Antibodies used	75-76
Antioxidative enzymes	76-79
2-Dimensional gel electrophoresis	80 -83
Results	84-104
Chlorophyll and Carotanooids Contents	84
Chlorophyll contents	84
Carotenoid contents	85
Protein	85
Sodium contents	85
Potassium contents	86
Na ⁺ /K ⁺ Ratio	86
Calcium contents	86
Glutamate -1-semialdehyde (GSA) accumulation	87

ALA contents	87
Pchlide contents	87
ALAD activity	88
PBGD activity	88
Coprox activity	88
Protox activity	88
Mg chelatase activity	89
POR activity	89
Immunoblot of photosynthetic proteins	90-91
Gene expression of Chl biosynthetic enzymes	91
Shibata shift	91-92
Chl a fluorescence	92-94
Photosynthetic electron transport reactions	94-95
Light saturation curve	95-96
Room and low temperature fluorescence spectra	96-97
Immunoblot of photosynthetic proteins	97-98
Gene expression of PSII proteins	99
Ultrastructure of chloroplast	99
Antioxidative enzymes	99-101
Gene expression of antioxidative enzymes	101
MDA content	101
H ₂ O ₂ content	101
Tocopherols	102
Gene expression of salt related proteins	102
Proteomics	102-104
Discussion	105-120
Summary	121-126
References	127-200

JAWAHARLAL NEHRU UNIVERSITY

NEW DELHI-110067



DECLARATION

*The research work embodied in this thesis entitled “**Impact of Salinity Stress on Chloroplast Biogenesis and Photosynthesis**” has been carried out in the School of Life Sciences, Jawaharlal Nehru University, New Delhi. This work is original and has not been submitted so far, in part or in full, for the award of any other degree or diploma of any university.*



SATPAL

Candidate



PROF. B. C. TRIPATHY

Supervisor



PROF. R. MADHUBALA

Dean

School of Life Sciences

ACKNOWLEDGEMENTS

I owe my sincere gratitude to my Supervisor, Prof. B. C. Tripathy for his constant support, encouragement, supervision and freedom to realize my scientific pursuit and having shown faith in my abilities. I owe him lots of gratitude for having me shown the path of research. His vision and generosity has seen me through all ordeals. This piece of work would have been a distant dream for me without him. Thank you very much, Sir.

I am extremely thankful to the present and the former Deans of the School of Life Sciences for generating all necessary facilities and conducive environment for carrying out the present work.

I am very indebted to Prof V. Rajamani from Environmental Sciences for providing me Element analysis facility.

I am thankful to Dr. R.K Singh and Dr R.K. Gautam from CSSRI Karnal for not only providing but helping me in getting seeds from CSSRI Karnal. Thanks a lot to both of you sir. I am also thankful to Sanjay from CSSRI Karnal.

I am thankful to Jogindre and Mahfooj for their help in MALDI TOF-TOF beyond their capacity.

Thank you very much Saini sir. My thesis glows only because of your beautiful photographs. The necessary technical support from Mr S K Mishra, Mr. Alexander, Mr Khan, and Mr Sharma helped me to continue my work uninterruptedly. My special thanks to all these gentlemen.

I am very thankful to Nerender Chaudry from IIT making my spectral data presentable.

No words suffice to thank my incredible lab members Dr B S Tiwary, Dr Ardendu Dash, Dr Maya, Dr Suchi, Dr Versha, Dr Sasmita, Dr Gopal, Dr Rupesh, Dr Ajay, Ansuman, Dr Siddhartha, Chhavi, Rajneesh, Vijay, Naveen, Namrata, Siva, Manas, Vivek, Parteek, Rahul, Priyanka, Deepika, Chitra and several summer trainees for their affection, care, support in lab management and sometimes tolerating my erratic behavior and annoyance. Dr Budhi's encouraging and helpful nature always inspired me. Enjoyment of his company during

morning and evening tea is memorable. Positive attitude of Dr Rupesh always inspired me for not getting despaired. Thanks for your company during several adventurous trips.

I am thankful to Ratnakarn for REAL-TIME experiments.

I am thankful to Rahul, Rekha, Bhavna, Superva and Ansu who helped me a lot during their summer trainings

This part of work would have never started without the love, affection and support of my friends O P Siwach, Vineet, Surender, Krishan, Rahul, Rakesh. The encouraging words, the emotional support and a long association with you charmed my life. In my most tiring and difficult times your company brought volumes of smile. I miss all of you a lot and will fondly remember your company. Wishing you all a happy, prosperous and a great life ahead.

I wish to express my thanks to Mr. Sumer Singh for his full cooperation in official hassles. Day to day help of Naresh, Ramesh and Baljit, Joshi, Natthu- is duly acknowledged.

The services of JNU Canteens: Ajay and Gopalan uncle (Library), Ashok, Manoj and Babuva (Godavari Dhaba), Panditji, Ali, Shadeek (SSS canteen) are duely acknowledged. Thank you friends for your love, care and service.

I am very thankful to Pandit Ji (Parveen Traders) for providing me necessary lab chemicals and other things of experimental use at any time.

My friends, colleagues and juniors at the School of Life Sciences: Special thanks to all of you, and I really mean all of you, have contributed to my thesis.

The financial assistance DBT and CSIR in the form of fellowship is duly acknowledged.

I am thankful to my family and especially my father who gave me money in the situation when Govt funding agencies CSIR and DBT financial help failed to reach me. I am thankful to my younger brother Jaipal who helped me in my everyday life.

-SATPAL

ABBREVIATIONS

ALA	5-aminolevulinic acid
ALAD	5-aminolevulinic acid dehydratase
APS	Ammonium persulphate
ATP	Adenosine-5'-triphosphate
BCIP	5-bromo-4-chloro-3-indolyl phosphate
BSA	Bovine Serum Albumine
β -ME	β -mercaptoethanol
CAO	Chlorophyllide A oxygenase
CBB	Coomassie brilliant blue
Chl	Chlorophyll
Chlide	Chlorophyllide
ChIP	Geranyl-geranyl reductase
ChII	Magnesium chelatase subunit-I
CHS	Chalcone synthase
CPO	Coproporphyrinogen III
Coprox	Coproporphyrinogen III oxidase
D	Dark
dA/dt	Change in absorbance with time
DEPC	Diethyl pyrocarbonate
DTT	Dithiotreitol
DV	Divinyl
DW	Dry weight
EDTA	Ethylenediaminetetraacetic acid
EtBR	Ethidium bromide
ETR	Electron transport rate
FC1	Ferrochelatase 1
F ₀	Minimum fluorescence, when all reaction centers are open
F _m	Maximum fluorescence, when all reaction centers are open
F _v	Variable fluorescence
FW	Fresh weight
GluTR	Glutamyl tRNA reductase
GSA	Glutamate-1-semialdehyde
GSAT	Glutamate-1-semialdehyde aminotransferase
h	Hour
HEPES	(N-[2-Hydroxyethyl] piperazine-N'-[2-ethanesulphonic acid])
HEAR	Hexane extracted acetone residue
kb	Kilobase
kDa	Kilodalton
l	Liter

LHCP	Light-Harvesting-Chlorophyll-Protein Complex
LL	Low-light
µg	Microgram
µl	Microliter
ml	milliliter
min	Minute
MES	(2-[N-morpholino] ethane sulfonic acid)
MOPS	3-[N-Morpholino] propane sulphonic acid
MDA	Malondialdehyde
MS	Murishage and Skoog
Mg-Proto IX	Mg-protoporphyrin
MP(E)	Magnesium protoporphyrin IX monomethyl (ester)
MV	Monovinyl
nm	Nanometer
NADPH	Reduced form of nicotinamide adenine dinucleotide phosphate
NBT	Nitroblue tetrazolium
NPQ	Non-photochemical quenching
ORF	Open reading frame
¹ O ₂	Singlet oxygen
O ₂ ^{·-}	Superoxide radical
PAGE	Polyacrylamide gel electrophoresis
PBG	Porphobilinogen
PBGD	Porphobilinogen deaminase
Pchl _a	Protochlorophyllide
PCD	Programmed cell death
PCR	Polymerase chain reaction
PEG	Polyethylene glycol
POR	Protochlorophyllide oxidoreductase
PMSF	Phenylmethylsulphonyl fluoride
Proto IX	Protoporphyrin IX
Protox	Protoporphyrinogen oxidase
PSI	Photosystem I
PSII	Photosystem II
□PSII	Quantum yield of photosystemII
P ₆₈₀	Reaction center of PSII
P ₇₀₀	Reaction center of PSI
PUFA	Polyunsaturated fatty acid
qP	Photochemical quenching
qN	Non- photochemical quenching
RNA	Ribonucleic acid
rpm	revolutions per minute
RT	Room temperature
RT-PCR	Reverse transcriptase Polymerase chain reaction
SD	Standard deviation

SDS	Sodium dodecyl sulphate
TAE	Tris acetate EDTA
TBA	Thiobarbituric acid
TCA	Trichloroacetic acid
TE	Tris EDTA
TBST	Tris buffer saline with Tween-20
T-DNA	Transfer DNA
TLC	Thin layer chromatography
TPD	Tetraphenylbutadiene
Tris	Tris (hydroxymethyl) aminomethane
UroD	Uroporphyrinogen decarboxylase
Urogen	Uroporphyrinogen III
UV	Ultraviolet
Vol	Volume
ECe	The electrical conductivity of the saturated paste extract; equivalent to the concentration of salts in saturated soil or in a hydroponic solution

Introduction

INTRODUCTION

Plants are exposed to various environmental stresses during their lifetime. Salt stress is the most typical abiotic stress affecting plants. Soil salinity is a serious problem in world's agriculture. This is due to heavy irrigation in the hot, dry area where there is an excessive water loss through a combination of evaporation and transpiration. Soil salinity is the major constraint to the food production because it limits crop yield and restricts use of land. The greatest challenges faced by plants cultivated in the presence of excess salt are osmotic regulation, ion toxicity and oxidative stress. Super-oxide detoxifying enzymes such as superoxide dismutase, ascorbate peroxidase, catalase, glutathione reductase are important components of the cellular response to salt stress (Meloni et al, 2003). The synthesis of 'osmolytes' is an important stress response for osmotic adjustment and stabilization of the cellular structure.

Chloroplasts are the hallmark organelles of plants and are responsible for essential plant functions such as the fixation of CO₂, manufacture of carbon skeletons, fatty acids and pigments, and the synthesis of amino acids from inorganic nitrogen, among others (Staehelein and Newcomb, 2000). Chloroplast biogenesis is a complex process. Seeds germinate in dark, and the small, undifferentiated plastids enlarge and develop into etioplasts with a large internal structure termed the prolamellar body. Subsequently when the aerial portion of the developing seedling is exposed to light, the etioplast of the cotyledons and primary leaves develop into photosynthetically active chloroplast. In higher plants, chloroplasts develop from proplastids, small organelles (0.2–0.5 mm diameter) that lack thylakoid membranes and that are present primarily in meristematic cells and in young postmitotic cells (Vothknecht and Westhoff, 2001). As meristematic cells begin to differentiate into mesophyll and palisade cells, proplastids coordinately differentiate into chloroplasts. This differentiation process is modulated by environmental cues such as light and other abiotic stresses like salt stress.

Chloroplast development involves the biosynthesis of components of photosynthetic apparatus involving synthesis of pigments (chlorophyll and carotenoids etc.), lipids and proteins. Chloroplast development is governed in a coordinated manner by chloroplast and nuclear genomes (Leon et al, 1998). High salt stress is a major environmental factor that limits plant growth and productivity. Photosynthesis is profoundly affected by salinity stress. Chloroplast

biogenesis and chlorophyll biosynthesis are interrelated and essential for photosynthetic function.

Rice is an important crop of India and several other countries. It is severely affected by salinity stress. Different cultivars respond differently to salts stress. To produce salt tolerant lines by classical breeding or by means of genetic engineering it is of utmost importance to know physiology and photosynthetic efficiencies of different cultivars. Therefore to better understand the mechanism of tolerance to salt stress two cultivars i.e., a salt sensitive cultivar Pusa Basmati-1 and a salt tolerant rice genotype CSR-10 are taken for comparative study.

More specifically the following objectives were set:

1. To estimate Chl, carotenoids, tocopherols and tetrapyrrole intermediates of Chl biosynthetic pathway in rice seedlings exposed to salt stress.
2. To study the effect of salt stress on ion-homeostasis, Na, K and Ca accumulation in rice seedlings.
3. To understand effect of salinity stress on Chl a fluorescence parameters i.e., F_0 , F_m , F_v/F_m , ETR, qP, qN and quantum yield of PSII.
4. To understand effect of salinity stress on electron transport of whole chain, PSII and PSI in rice seedlings.
5. To study effects of salt stress on Chl a fluorescence spectra at room (298 K) as well as low temperature (77 K).
6. To measure the activities, gene and protein expression of some of the major enzymes of Chl biosynthetic pathway in rice seedlings in response to salt stress.
7. To understand antioxidative response in plants exposed to salt stress for different time period.
8. To understand differential protein expression in plants in response to salt stress by 2-Dimensional-gel electrophoresis and mass spectrometry.

Literature Review

REVIEW OF LITERATURE

Salt Stress

Plants are subjected to various abiotic stresses such as low temperature, salt, drought, flooding, heat, oxidative stress and heavy metal toxicity during their life cycle among those, salinity stress is the most typical abiotic stress (Mahajan et al, 2005). It is estimated that 6% of the world's total land and 30% of the world's irrigated areas already suffer from salinity problems (Unesco Water Portal, 2007). Salinity is a soil condition characterized by a high concentration of soluble salts. Soils are classified as saline when the EC_e is 4 dS/m or more (USDA-ARS.2008), which is equivalent to approximately 40 mM NaCl and generates an osmotic pressure of approximately 0.2 MPa. This definition of salinity derives from the EC_e that significantly reduces the yield of most crops (Munns and Tester, 2008). Because NaCl is the most soluble and widespread salt, it is not surprising that all plants have evolved mechanisms to regulate its accumulation and to select against it in favor of other nutrients commonly present in low concentrations, such as K⁺ and NO₃⁻. In most plants, Na⁺ and Cl⁻ are effectively excluded by roots while water is taken up from the soil (Munns R, 2005). Salinity stress negatively impacts agricultural yield throughout the world affecting production whether it is for subsistence or economic gain. The plant response to salinity consists of numerous processes that function in coordination to alleviate both cellular hyper osmolarity and ion disequilibrium. High Salinity causes both hyperionic and hyper osmotic stress effects, and the consequence of these can be plant demise (Glenn, et al., 1999, Niu et al., 1995, Yeo; 1998). Most commonly, the stress is caused by high Na⁺ and Cl⁻ concentrations in the soil solution. Altered water status most likely brings about initial growth reduction; however the precise contribution of subsequent process to inhibition of cell division and expansion and acceleration of cell death has not been well elucidated (Munns; 1993, Yeo, 1998). Membrane disorganization, reactive oxygen species, metabolic toxicity, inhibition of photosynthesis, and attenuated nutrient acquisition are factors that initiate more catastrophic events (Flowers et al., 1977, Greenway and Munns; 1980).

Salt Movement through Plants

Movement of salt into roots and to shoots is a product of the transpiration flux required to maintain the water status of the plant (Flowers and Yeo; 1992, Yeo; 1998). Unregulated transpiration can result in toxic levels of ion accumulation in the aerial parts of the plant. An

immediate response to salinity, which mitigates ion flux to the shoot, is stomatal closure. However, because of the water potential difference between the atmosphere and leaf cells, and the need for carbon fixation, this is an untenable long-term strategy of tolerance (Munns and Termaat; 1986, Yeo; 1998).

To protect actively growing and metabolizing cells, plants regulate ion movement into tissues (Flowers and Yeo; 1992, Munns; 1993). One mode by which plants control salt flux to the shoot is the entry of ions into the xylem stream. Still debated is the extent to which symplastic ion transport through the epidermis and cortical cells contributes to a reduction in Na^+ that is delivered to the xylem (Clarkson, 1991, Flowers and Yeo; 1992). The accumulation of large quantities of ions in mature and old leaves, which then dehisce, has often been observed under salt stress (Flowers and Yeo; 1992, Munns, 1993). The solutes content of tissues containing cells with little vacuolation (e.g. meristematic regions) predominated by organic osmolytes and in tissues with highly vacuolated cells by ions (Bizel et al. 1988; Wyn, 1981).

Halophyte and Glycophyte Comparisons

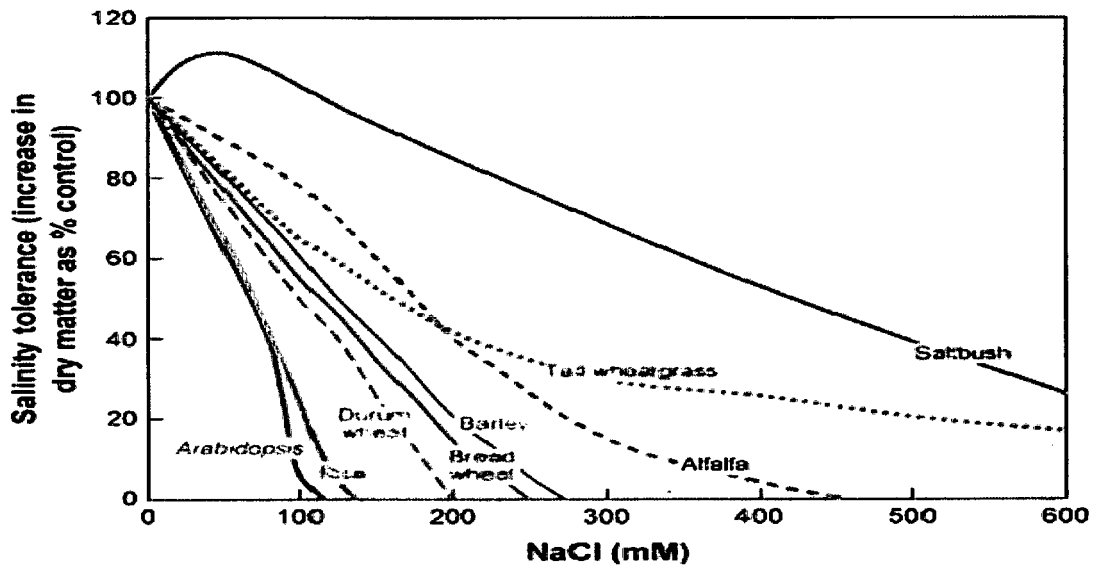
Halophyte for optimal growth require electrolyte (typically Na^+ and Cl^-) in concentrations higher or much higher than those found in nonsaline soils. How and within which range of NaCl (roughly defined from 20 to 500 mM NaCl) these plants respond best is complex, and has led to a number of classification attempts (Flower et al., 1977, Glenn et al.; 1999, Greenway and Munns; 1980). Halophytes seem to lack unique metabolic machinery that is insensitive to or achieved by high Na^+ and Cl^- (Flowers et al.; 1977, Nelson et. al; 1998, Niu et al.; 1995, Rhodes; 1987). Instead, plants ultimately survive and grow in saline environments because of osmotic adjustment through intracellular compartmentation that partitions toxins away from the cytoplasm through the energy-dependent transport into the vacuole (Apse et al., 1999, Binzel et al., 1988). Some halophytes exclude Na^+ and Cl^- through glands and bladders, which are specialized structure that seems to be evolutionarily late inventions by which halophytes gain an edge over glycophytes. Osmotic adjustment of both halophytes and glycophytes is also achieved through the accumulation of organic solutes in the cytosol, and the lumen, matrix, or stoma of organelles (Niu et al.; 1995, Rhodes and Samaras; 1994, Yeo; 1998).

A principal difference between halophytes and glycophytes is the capacity of the former to survive salt shock. This capacity allows halophytes to more readily establish metabolic steady

state for growth in saline environment (Braun et al.; 1986, Cacas et al.; 1991, Cushman et al.; 1990). Responsiveness to salinity and at least some ability to establish an adapted new steady state is not unique, however, to halophytes in as much as both glycophyte cells and plants exhibit substantial capacity for salt tolerance provided that stress imposition is gradual. (Amzallag et al.; 1990, Bressan et al., 1990) whereas glycophytes restrict ion movement to the shoot by attempting control of ion influx into root xylem, halophytes tend more readily to take up Na^+ such that roots typically much lower NaCl concentrations than the rest of plant. It seems that a major advantage that halophytes have over glycophytes is not only more responsive Na^+ partitioning but more effective capacity to co-ordinate this partitioning with processes controlling growth, and ion flux across the plasma-membrane, in both cellular and organismal contents (Adams et al.; 1992), Bressan et al.; 1990, Glenn et al.; 1999).

Genetic Diversity for Salt Tolerance in Plants

Plants differ greatly in their tolerance of salinity, as reflected in their different growth responses. Of the cereals, rice (*Oryza sativa*) is the most sensitive and barley (*Hordeum vulgare*) is the most



AR Munns R, Tester M. 2008. *Annu. Rev. Plant Biol.* 59:651–81.

Fig.1

tolerant (Figure 1). tolerant and durum wheat (*Triticum turgidum* ssp. *durum*) is less so. Tall wheat grass (*Thinopyrum ponticum*, syn. *Agropyron elongatum*) is a halophytic relative of wheat

and is one of the most tolerant of the monocotyledonous species (**Figure 1**); its growth proceeds at concentrations of salt as high as in seawater. The variation in salinity tolerance in dicotyledonous species is even greater than in monocotyledonous species. Some legumes are very sensitive, even more sensitive than rice (L'ouchli A, 1984); alfalfa or lucerne (*Medicago sativa*) is very tolerant, and halophytes such as saltbush (*Atriplex* spp.) continue to grow well at salinities greater than that of seawater (**Figure 1**). Many dicotyledonous halophytes require a quite high concentration of NaCl (100– 200 mM) for optimum growth (Flowers et al, 1977). *Arabidopsis*, when compared with other species under similar conditions of light and humidity (that is, at high transpiration rates), is a salt-sensitive species (**Figure 1**). This sensitive plant may provide limited insights into mechanisms of salinity tolerance unless it is compared with a tolerant relative such as *Thellungiella halophila*. The differences between these two species are highlighted by their responses to 100 mM NaCl under conditions of high transpiration. Continued exposure to 100 mM does not allow *Arabidopsis* to complete its life cycle (Sickler CM et al, 2007), but has little effect on the growth rate of *Thellungiella* (James RA et al, 2006). Plant Bread wheat (*Triticum aestivum*) is moderatelyGenetic diversity for salt tolerance that exists in plant taxa is distributed over numerous genera (Flowers et al.; 1986; Greenway and Munns, 1980). Most crops are salt sensitive or hypersensitive plants (glycophytes) in contrast to halophytes, which are native flora of saline environments. Some halophytes have the capacity to accommodate extreme salinity because of very special anatomical and morphological adaptations or avoidance mechanisms (Flowers et al.; 1986). However these are rather unique characteristics for which genes are not likely to be easily introgressed into plants. Research of recent decades has established that most halophytes and glycophytes tolerate salinity by rather similar strategies often using analogous tactical process (Hasegawa et al.; 2000b). The cytotoxic ions in saline environments, typically Na⁺ and Cl⁻, are compartmentalized into vacuoles and used as solutes (Blumwald et al.; 2000; Niu et al.; 1995). It follows then that many of rare molecular entities that mediate ion homeostasis and salt stress signaling are similar in all plants (Hasegawa et al.; 2000b).

Mechanism of Salt Stress Tolerance in Plants

The mechanisms of salinity tolerance fall into three categories

Tolerance to osmotic stress: The osmotic stress immediately reduces cell expansion in root tips and young leaves, and causes stomatal closure. A reduced response to the osmotic stress would result in greater leaf growth and stomatal conductance, but the resulting increased leaf area would benefit only plants that have sufficient soil water. Greater leaf area expansion would be productive when a supply of water is ensured such as in irrigated food production systems, but could be undesirable in water-limited systems, and cause the High salinity causes hyper osmotic stress and ion disequilibrium that produce secondary effects or pathologies (Hasegawa et al., 2000; Zhu, 2001). Fundamentally, plants cope by either avoiding or tolerating salt stress. That is plants are either dormant during the salt episode or there must be cellular adjustment to tolerate the saline environment. Tolerance mechanism can be categorized as those that function to minimize osmotic stress or ion disequilibrium or alleviate the consequent secondary effects caused by these stresses. The chemical potential of the Saline soil initially establishes a water potential imbalance between the apoplast and symplast that leads to turgor decrease, which if severe enough can cause growth reduction (Bohnert et al, 1995). Soil water to be used up before the grain is fully matured (Abebe T, 2003).

Na⁺ exclusion from leaf blades: Na⁺ exclusion by roots ensures that Na does not accumulate to toxic concentrations within leaves. A failure in Na⁺ exclusion manifests its toxic effect after days or weeks, depending on the species, and causes premature death of older leaves (Munns R, 2008).

Tissue tolerance, i.e., tolerance of tissue to accumulated Na⁺, or in some species, to Cl⁻: Tolerance requires compartmentalization of Na⁺ and Cl⁻ at the cellular and intracellular level to avoid toxic concentrations within the cytoplasm, especially in mesophyll cells in the leaf. Toxicity occurs with time, after leaf Na⁺ increases to high concentrations in the older leaves (Munns R, 2008).

Growth cessation occurs when turgor is reduced below the yield threshold of the cell wall. Cellular dehydration begins when the potential difference is greater than can be compensated for by turgor loss. (Taiz and Zeiger, 1998).

The cellular response to turgor reduction is osmotic adjustment. The cytosolic and organellar machinery of glycophyte and halophyte is equivalently Na^+ and Cl^- sensitive; so osmotic adjustment is achieved in these compartments by accumulation of compatible osmolytes and osmoprotectants (Bohnert et al, 1995, Bohnert and Jenson, 1996). However, Na^+ and Cl^- are energetically efficient osmolytes for osmotic adjustment and are compartmentalized into the vacuole to minimize cytotoxicity (Blumwald et al., 2000; Niu et al.; 1995). Movement of ions into the vacuole might occur directly from the apoplast into the vacuole through membrane vesiculation or a cytological process that juxtaposes the plasma membrane to the tonoplast (Hasegawa et al., 2000). Then compartmentalization would be achieved with minimal or no exposure of the cytosol or toxic ions. The bulk of Na^+ and Cl^- movement from the apoplast to the vacuole likely is mediated through ion transport systems located in the plasma membrane and tonoplast. Presumably, tight coordinate regulation of these ion transport system is required in order to control net influx across the plasma membrane and vacuolar compartmentalization. The SOS signal pathway is a pivotal regulator of; at least some, key transport systems required for ion homeostasis (Hasegawa et al., 2000; Sanders, 2000; Zhu 2000). CaMV 35S promoter driven overexpression of the *Arabidopsis thaliana* SOS1 gene, which encodes a plasma membrane Na^+/H^+ antiporter, improves plant salt tolerance in *A. thaliana* (Shi et al., 2003).

Osmolytes and Osmoprotectants

Salt tolerance requires that compatible solutes accumulate in the cytosol and organelles where these function in osmotic adjustment and osmoprotection (Rhoder and Hanson, 1993). Some compatible osmolytes are essential elemental ions such as K^+ , but the majorities are organic solutes. A major category of organic osmotic solutes consists of simple sugars (mainly fructose and glucose), sugar alcohols (glycerol and methylated inositols) and complex sugars (trehalose, raffinose and fructans) (Bohnert and Jensen, 1996). The addition of glucosylglycerol (GG) to the culture medium protected cyanobacterium *Synechocystis* sp. PCC 6803 cells against salt stress and reversed the adverse effects of NaCl on cell division and cell size (Ferjani et al., 2003). Trehalose-producing, transgenic rice (*Oryza sativa*) plants showed increased tolerance to drought, salt, and cold, as shown by chlorophyll fluorescence and growth inhibition analyses (Jang et al., 2003). Others osmolytes include quaternary amino acid derivatives (proline, glycine betaine, β -alanine betaine, proline betaine), tertiary amines (1, 4, 5, 6- tetrahydro-2-methyl-4-

carboxyl pyrimidine), and sulfonium compounds (choline o-sulfate, dimethyl sulfonium propionate) (Nuccio et al.; 1999). NaCl alleviated the inhibitory effect of UV-B on PSII activity. Proline accumulated under salt stress conditions might be one of the reasons for the observed tolerance of barley seedlings to UV-B radiation (Fedina et al., 2003). Many osmolytes are presumed to be osmoprotectants, as their levels of accumulation are insufficient to facilitate osmotic adjustment. Glycine betaine preserves thylakoid and plasma membrane integrity after exposure to saline solutions or to freezing or high temperatures (Rhodes and Hanson, 1993). A common feature of compatible solutes is that these compounds can accumulate to high levels without disturbing intracellular biochemistry (Bohnert and Jensen, 1996).

Ion Homeostasis

Since NaCl is the principal soil salinity stress, a research focus has been the transport system that is involved in utilization of Na^+ as an osmotic solute (Blumwald et al., 2000; Hasegawa et al., 2000; Niu et al., 1995). Research of more than 30 years previously, established that Ca^{2+} modulates intracellular Na^+ homeostasis and salt tolerance. High $[\text{Na}^+]_{\text{ext.}}$ negatively affects K^+ acquisition (Rains and Epstein, 1967). Na^+ competes with K^+ for uptake through common transport system and does this effectively since the $[\text{Na}^+]_{\text{ext.}}$ in saline environments is usually considerably greater than $[\text{K}^+]_{\text{ext.}}$. Ca^{2+} enhances K^+/Na^+ selective intracellular accumulation. (Maathuis et al, 1996; Rains and Epstein, 1967). Recently, the SOS stress signaling pathway was identified to be pivotal regulator of plant ion homeostasis and salt tolerance (Hasegawa et al.; 2000; Sanders, 2000). This signaling pathway functionally resembles that yeast calcineurin cascade that controls Na^+ influx and efflux across the plasma membrane (Bressan et al.; 1998).

Ion transport Systems that mediate Na^+ homeostasis

H^+ - pumps. H^+ -Pumps in the plasma membrane and tonoplast energize solute transport necessary to compartmentalize cytotoxic ions away from the cytoplasm and to facilitate the functions of ions as signal determinants (Maeshima, 2000; Maeshima, 2001; Morsomme and Boutry, 2000; Ratajczak, 2000). These pumps provide the driving force (H^+ electrochemical potential) for secondary active transport and function to establish membrane potential gradients that facilitate electrophoretic ion flux. The plasma membrane localized H^+ pump is a P-type ATPase and is primarily responsible for the large (pH and membrane potential gradient across this membrane (Morsomme and Boutry, 2000). A vacuolar H^+ -ATPase and vacuolar

pyrophosphates generate the ΔpH and membrane potential across the tonoplast (Drozdowicz and Rea, 2001; Maeshima 2001). The activity of these H^+ pumps is increased by salt treatment and induced gene expression may account for some of the up regulation (Hasegawa et al., 2000b; Maeshima, 2001).

Na^+ influx and Efflux across the Plasma Membrane

Recently, much insight has been gained about Na^+ transport system that is involved in the net flux of the cation across the plasma membrane (Amtman and Sanders; 1999; Blumwald et al.; 2000; Hasegawa et al., 2000). Transport systems with greater selectivity for K^+ are presumed to facilitate Na^+ “Leakage” into cells. Specifically, Na^+ is a competitor for uptake through plasma membrane K^+ inward rectifying channels, such as those that are in Shaker type family, e.g. AKT1 (Schachtman, 2000). K^+ outward rectifying channels also may facilitate Na^+ influx (Schachtman, 2000). Recently the properties of HKT proteins from *Arabidopsis* (Kato et al., 2001; Uozumi et al., 2000), rice (Horie et al.; 2001) and *eukalyptus* (Fairbairn et al., 2000) have been characterized. At HKT1 is the only member of the *Arabidopsis* gene family while both rice and *eukalyptus* have at least two genes. (Uozumi et al.. 2000). Rice (*Oryza sativa* L. India) OsHKT1 and OsHKT2 were identified based on sequence similarity with wheat HKT (Horie et al. 2001). OsHKT1 and 2 transcripts accumulate in response to low K^+ but their steady state abundance is reduced by treatment with 30mm NaCl. Identification of sos3-1 hkt1 double mutation in *Arabidopsis* has confirmed the existence of a Na^+ entry system(s) different than HKT1 that functions *in Planta*. (Amtmann and Sanders, 1999). Energy-dependent Na^+ transport across the plasma membrane of plant cells is mediated by the secondary active Na^+ / H^+ antiporter SOS1. Phylogenetically, SOS1 is similar to SOD2 of *Saccharomyces pombe*, NHA1 of *S. cerevisiae* and Nha A and Nha P of *Pseudomonas aeruginosa* (Shi et al.; 2000).

Na^+ Vacuolar Compartmentalization

A Na^+/H^+ antiporter that is energized by the ΔpH across the tonoplast facilitates vacuolar compartmentalization of the cation. The *Arabidopsis* AtNHX1 was isolated by functional genetic complementation of yeast mutant detected for the endosomal Na^+/H^+ antiporter yeast (ScNHX1) and has sequence similarity to mammalian NHE transporters (Apse et al., 1999; Gaxiola et al., 1999, Quintero et al., 2000). Transgenic *Arabidopsis* and tomato plants that overexpress AtNHX1 accumulate abundant quantities of the transporter in the tonoplast and exhibit

substantially enhanced salt tolerance (Apse et al.; 1999; Quintero et al., 2000; Zhang and Blum Wald, 2001).

Ca²⁺ Signaling and SOS signal Transduction Pathway

Jian-Kang Zhu and Currosbess identified three genetically linked *Arabidopsis* loci (SOS1, SOS2 and SOS3), which are components of a stress signaling pathway that controls ion homeostasis and salt tolerance (Hasegawa et al. 2000; Sanders, 2000; Zhu, 2000; 2001). Genetic analysis of Na⁺/Li⁺ sensitivity established that *sos1* is epistatic to *sos2* and *sos3* (Zhu, 2000). SOS3 encodes a Ca²⁺ binding protein with sequence similarity to the regulatory B subunit of calcineurin and neuronal Ca²⁺ sensors (Ishitani et al., 2000, Liu and Zhu, 1998). SOS codes for a serine / threonine kinase (446 amino acids) which has a 267 amino acid N-terminal catalytic domain that is similar in sequence to yeast SNF1 (Sucrose non-fermenting) kinase and the mammalian AMPK (AMP-activated protein kinase (Liu et al.; 2000; Zhu, 2000). Kinase activity of SOS2 is essential for its salt tolerance determinant function (Zhu, 2000) Ca²⁺ binds to SOS3, which leads to interaction with SOS2 and activation of kinase. The plasma membrane sited Na⁺/H⁺ antiporter SOS1 is controlled by the SOS pathway at the transcriptional and post transcriptional level (Guo et al., 2001; Zhu, 2001).

Cell Signaling during Salt Stress

High salinity, low temperature and drought are common stress conditions that adversely affect plant growth and crop production. The cellular and molecular responses of plants to environmental stress have been studied intensively (Thomashow, 1999; Hasegawa et al.; 2000). Signal transduction during salt stress is not completely understood. A generic signal transduction pathway starts with signal perception, followed by the generation of second messengers (e.g., inositol phosphates and reactive oxygen species [ROS]). Second messengers can modulate intracellular Ca²⁺ levels, often initiating a protein phosphorylation cascade that finally targets proteins directly involved in cellular protection or transduction factors controlling specific set of stress related genes. Products of these genes may participate in the generation of regulatory molecules like plant hormones abscisic acid (ABA), ethylene, and salicylic acid (SA). These regulatory molecules can, in turn initiate a second round of signaling that may follow the same pathway, although different components are often involved (Xiong and Zhu, 2002). Signal transduction requires the proper spatial and temporal co-ordination of all signaling molecules.

Thus there are certain molecules that participate in the modification, delivery, or assembly of signaling components, but do not directly relay the signal. These are protein modifiers (e.g. enzymes for protein lipidation, methylation, glycosylation and ubiquitination), scaffolds and adapters (Xiong and Zhu, 2001).

Chloroplast biogenesis: A brief overview

Chloroplast is the hallmark organelle of plant. It performs photosynthesis and is therefore required for photoautotrophic plant growth. Chloroplasts are double membrane organelles which originated when a photosynthetic prokaryote was engulfed by the non photosynthetic eukaryotic ancestor of green and red algae and land plants. (Dyall et al, 2004; Martin et al, 2002). Chloroplast not only the site of photosynthesis but also carry out other non photosynthetic functions no less important than photosynthesis. They manufacture fatty acids, aromatic and nonaromatic amino acids (essential for protein synthesis, but also for a vast array of plant secondary metabolites), purine and pyrimidine bases, isoprenoids (like carotenoids and sterols) and tetrapyrroles (like haem and chlorophyll). Most of these functions are essential for every cell type, and chloroplasts have integrated into cellular development pathways by differentiating into a variety of other, interconvertible, non-photosynthetic plastid types (Waters et al, 2004). Thylakoids are dominating structure inside fully mature chloroplasts. In dark grown plants in the absence of light proplastids turn into etioplasts which contain very few internal membranes but a characteristic prolemellar body. Prolemellar body is paracrystalline structure consisting of lipids and essentially a single protein, the NADPH-dependent protochlorophyllide oxidoreductase. Shortly after the onset of illumination the prolemellar body is dispersed and thylakoids begin to form (Vothknecht and Westhoff, 2001). Chloroplast biogenesis is a complex process and is co-ordinated by both nuclear and plastid genome. Only 5-10 % proteins of chloroplast are encoded by its own genome remaining proteins are nuclear encoded so translated into cytoplasm and then imported into chloroplast. (Jarvis and Soll, 2002) So the chloroplast biogenesis involves the biosynthesis of many lipids, proteins and pigments including chlorophyll. Pigments and proteins unite to form dominating complexes of thylakoids, Photosystem I and Photosystem II and their associated light harvesting antenna, the cytochrome b_6f complex and the proton translocating ATP synthase (Vothknecht and Westhoff, 2001).

Chlorophyll biosynthesis in higher plants: A brief overview

The Chl biosynthesis pathway in higher plants is much more complex and the metabolic flux is regulated by 17 enzymes (Fig. 2). However the formation of Chlorophyll can be subdivided into three parts, (i) formation of 5-aminolevulinic acid (ALA), the committed step for all tetrapyrroles, (ii) formation of protoporphyrin IX (Proto) from eight molecules of ALA, and (iii) formation of Chl in the magnesium branch. Enzymes catalyzing early steps in the synthesis are highly soluble and located mostly in the chloroplast stroma, whereas enzymes of the late steps are associated with thylakoid or inner envelope membranes. All of the enzymes of the pathway are encoded by nuclear genes and are synthesized in the cytoplasm as precursor polypeptides with amino-terminal extensions (transit peptides) that enable them to pass through the double membrane of the chloroplast envelope and to their site of function within the organelle. The only molecule required for Chl biosynthesis that is synthesized within the organelle is tRNA^{Glu}, which is encoded on the chloroplast genome (Eckhardt et al, 2004; Tanaka and Tanaka, 2007).

ALA formation from glutamate:

δ -Aminolevulinic acid (ALA), the first universal tetrapyrrole precursor, can be formed by two different pathways. members of the α proteobacterial: group (which includes photosynthetic bacteria of the *Rhodobacter* and *Rhodospseudomonas*, and *Rhodospirillum* genera as well as the nonphotosynthetic genera *Agrobacterium*, *Rhizobium* and *Bradyrhizobium*), and all eukaryotic organisms that do not contain chloroplasts (animals, yeasts, fungi), form ALA by condensation of succinyl-coenzyme A with glycine in a reaction catalyzed by the pyridoxal-P-containing enzyme ALA synthase (EC 2.3.1.37) (Gibson et al. 1958; Kikuchi et al. 1958). In contrast, all plants and algae, and all bacteria that are not in the α proteobacterial group, including cyanobacteria, many photosynthetic bacteria, and archaea, form ALA by a different route that begins with the five-carbon precursor, glutamate (Beale and Castelfranco 1974; Beale et al. 1975; Meller et al. 1975), which is activated ligation to tRNA^{Glu} (Kannangara et al. 1984), followed by reduction of the α carboxyl group of the activated glutamate to form glutamate 1-semialdehyde (GSA) (Pontoppidan and Kannangara 1994), and transamination of GSA to form ALA (Kannangara and Gough 1978). The fact that ALA biosynthesis in all plants and most bacteria differs from that in animals suggests that it may be possible to develop herbicides and

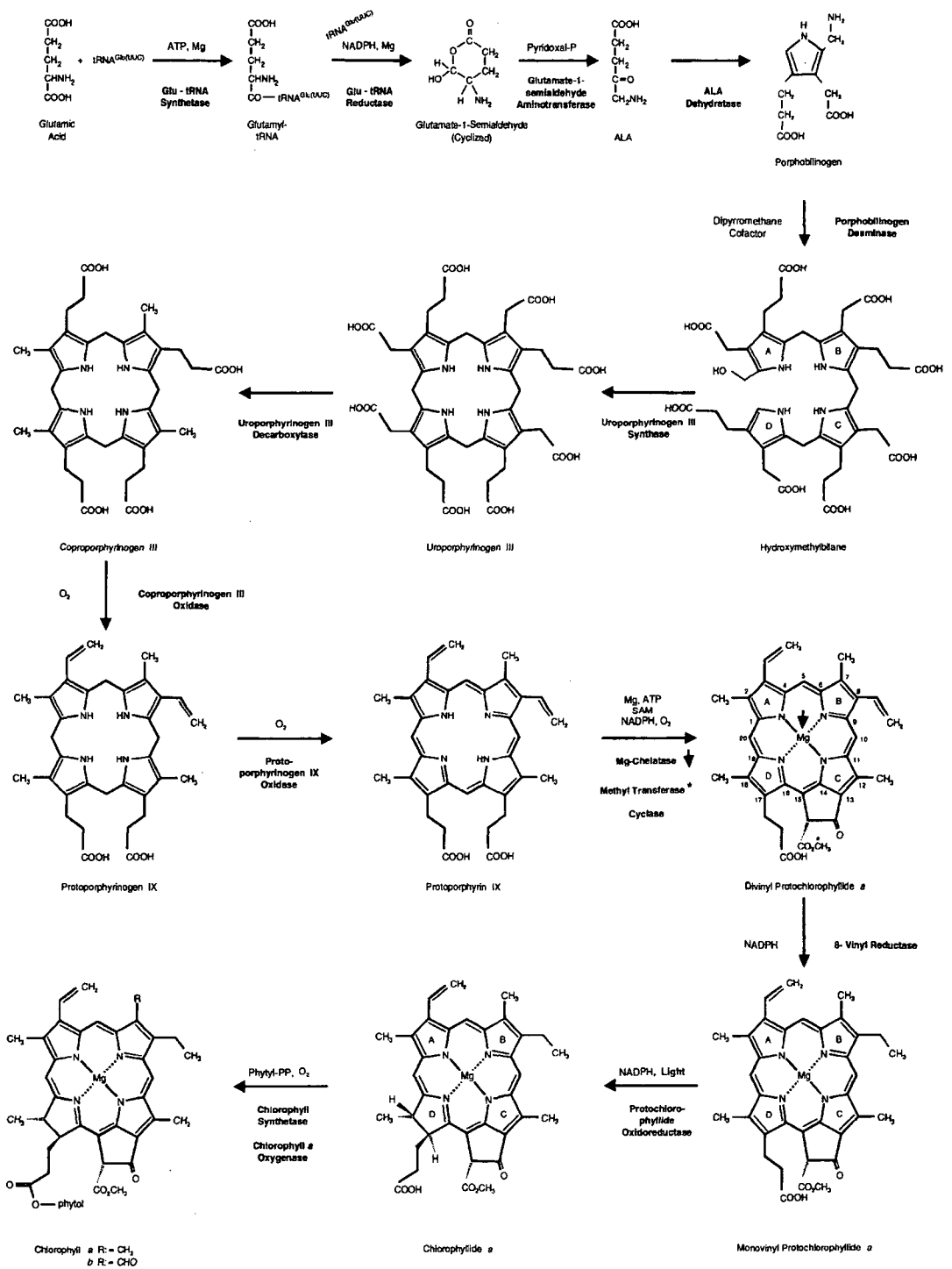


Figure 2 A scheme of tetrapyrrole biosynthetic pathway (Smith and Griffiths, 1993, modified)

Table-A. List of enzymes involved in tetrapyrrole biosynthesis and their respective gene names and localization in the cell. **M:** Mitochondria, **P:** Plastid

Step	Enzyme name	Localization	Gene name(s)
1	Glutamyl-tRNA synthase	P	<i>GluRS</i>
2	Glutamyl-tRNA reductase	P	<i>HEMA1</i> <i>HEMA2</i> <i>HEMA3</i>
3	Glutamate-1-semialdehyde aminotransferase	P	<i>GSAT1</i> <i>GSAT2</i>
4	Porphobilinogen synthase		<i>AlaD/HEMB</i> <i>HEMB1</i> <i>HEMB2</i>
5	Porphobilinogen deaminase	P	<i>PbgD/HEMC</i>
6	Uroporphyrinogen III synthase	P	<i>UroS/HEMD</i>
7	Uroporphyrinogen III decarboxylase	P	<i>UroD/HEME</i> <i>HEME1</i> <i>HEME2</i>
8	Coproporphyrinogen oxidase	P	<i>CPO/HEMF</i> <i>HEMF1</i> <i>HEMF2</i>
9	Protoporphyrinogen oxidase	P/M	<i>PPX/HEMG</i> <i>HEMG1</i> <i>HEMG2</i>
10	Mg-chelatase	P	<i>CHL D</i> <i>CHLH</i> <i>CHLI 1</i> <i>CHLI 2</i>
11	Mg-protoporphyrin IX methyltransferase	P	<i>CHLM</i>
12	Mg-protoporphyrinogen IX monomethyl ester cyclase	P	<i>CRD1</i>
13	Divinyl reductase	P	<i>DVR</i>
14	NADPH-protochlorophyllide oxidoreductase	P	<i>PORA</i> <i>PORB</i> <i>PORC</i>
15	Geranylgeranyl reductase	P	<i>Chl P</i>
16	Chlorophyll synthase	P	<i>Chl G</i>
17	Chlorophyllide a oxygenase	P	<i>CAO</i>

antibiotics that specifically target steps in the five-carbon ALA biosynthetic pathway and that are nontoxic to animals.

Glutamyl t-RNA synthetase:

Glutamyl-tRNA synthetase (EC 6.1.1.17) has been studied in connection with its role in protein synthesis. Like all aminoacyl-tRNA synthetases, the enzyme requires the cognate amino acid and tRNA as substrates, and the reaction requires the energy of ATP hydrolysis. There is no evidence to suggest that the glutamyl-tRNA synthetase that charges tRNAGlu for ALA biosynthesis differs from the one involved in protein synthesis. The single glutamyltRNA synthetase found in barley chloroplasts has a subunit molecular mass of 54 kDa (Beale S I, 1999). Glutamyl-tRNA (Glu-tRNA) synthetase (GluRS), which forms Glu-tRNA by the esterification of glutamate to the 3' end of tRNA, is found in different organisms in two forms: a discriminating enzyme (D-GluRS) that recognizes exclusively tRNAGlu and a relaxed specificity nondiscriminating enzyme that recognizes both tRNAGln and tRNAGlu (ND-GluRS). This ND-GluRS produces Glu-tRNAGln in the many organisms (most bacteria and all archaea and eukaryotic organelles) that lack GluRS; the mischarged Glu-tRNAGln is then transformed by a tRNA-dependent amidotransferase to Gln-tRNAGln. Genomewide analysis revealed that many bacteria contain duplicated GluRSs (GluRS1, GluRS2). In addition, some organisms contain a truncated version of GluRS (GluQRS) that is involved in the modification of tRNA^{Asp} (Levican et al, 2007).

Glutamyl-tRNA reductase

Glutamyl-tRNA reductase, the second enzyme of the pathway, reduces the activated α -carboxyl group of glutamyl-tRNA (Glu-tRNA) in the presence of NADPH and releases glutamate 1-semialdehyde (GSA). Pyridine nucleotides are required for this reaction (Hooper *et al.*, 1988). In addition, the enzyme is subject to feedback regulation by heme and appears to be a major control point of porphyrin biosynthesis (Wang *et al.*, 1987; Kannangara *et al.*, 1988). Micromolar concentrations of Zn^{2+} , Cu^{2+} and Cd^{2+} inhibit barley glutamyl-tRNA reductase (Pontoppidan and Kannangara, 1994). In green barley plants, this enzyme is stimulated by GTP (Kannagara *et al.*, 1988).

Two clones of GluTR, *hemA1* and *hemA2* from cucumber have been cloned (Tanaka *et al.* 1996). Of these, *hemA1* accumulation increases upon illumination. The *hemA1* mRNA

accumulated in response to demand of Chl synthesis in photosynthesising tissues, whereas *hemA2* mRNA was expressed in response to the demand of synthesis of porphyrins other than chlorophylls. *Arabidopsis* plants expressing antisense *HEMA1* mRNA, showed less chlorophyll, decreased ALA levels and decreased glutamyl-tRNA levels (Kumar and Soll, 2000). In *Arabidopsis* GluTR interacts with FLU, a negative regulator of chlorophyll biosynthesis pathway (Meskauskiene *et al.*, 2001, 2002).

Glutamate 1-semialdehyde aminotransferase

The formation of δ -aminolevulinate from GSA is catalyzed by glutamate 1-semialdehyde aminotransferase. This enzyme is functionally an aminomutase, which transfers the amino group on carbon 2 of the glutamate- semialdehyde to the neighbouring carbon atom i.e., carbon 5 of ALA. During the conversion of GSA to ALA, amino group from pyridoxamine phosphate is donated to GSA, leading to formation of an intermediate, 4, 5-diaminovalerate. The enzyme then releases amino group from position-4 of this intermediate, releasing 5-ALA. The enzyme is inhibited rapidly by gabaculine (Gough *et al.*, 1992). Tolerant GABA mutant of GSA-AT, resulted from a point mutation, Met-248-Ile, in the middle of the polypeptide chain accompanied by a deletion of three amino acids (serine, proline, and phenylalanine) close to the NH₂ terminus but can also be affected by the point mutation alone (Grimm *et al.*, 1991; Smith & Grimm, 1992).

Light is reported to stimulate transcription of the gene encoding the enzyme in *Arabidopsis* (Ilag *et al.*, 1994) and *Chlamydomonas reinhardtii* (Matters and Beale, 1994). The gene has been isolated from *Hordeum vulgare* (Kannangara *et al.*, 1994), *Pisum sativum* (Pugh *et al.*, 1992), *E.coli*, *Synechococcus* (Grimm *et al.*, 1991), *Salmonella* (Elliot *et al.*, 1990), *Arabidopsis* (*gsa1* and *gsa2*) (Ilag *et al.*, 1994), *Glycine max* (Sangwan and O'Brian, 1993), *Nicotiana tabacum* (Hofgen *et al.*, 1994) and *Brassicca napus* (Tsang *et al.*, 2003). The gene have also been cloned in *Bacillus subtilis* and purified and crystallized from *E. coli* (Lv *et al.*, 2006). The amino acid sequences of these genes show extensive homology among themselves.

5-Aminolevulinic acid dehydratase

This enzyme is also known as PBG synthase. It is a homooctameric metalloenzyme that catalyzes the condensation of two 5-aminolevulinic acid molecules to form the tetrapyrrole

precursor porphobilinogen. The mechanism of action of ALAD was first proposed by (Shemin, 1976). The aldol condensation between two ALA molecules involves the initial binding of two substrate molecules and a five membered heterocyclic ring of PBG is formed with the help of a lysine and a histidine residue (Nandi, 1978; Jordan and Shemin, 1980; Spencer and Jordan, 1994, 1995). Pea ALAD has a distinct metal binding domain based on aspartate and an active site domain of lysine, which is highly conserved (Boese *et al.*, 1991).

This enzyme has been isolated from wheat (Nandi and Waygood, 1967), tobacco (Shetty and Miller, 1969), radish (Shibata and Ochiai, 1977), spinach (Liedgens *et al.*, 1980) and tomato (Polking, 1995). In pea, the *ALAD* expression was high in dark grown tissues as compared to light grown samples (Li *et al.*, 1991). ALA dehydratase was detectable in embryonic leaves whether the plants were grown in darkness or under continuous white-light illumination. In the leaves of dark-grown seedlings, the highest levels of message accumulation were observed at approximately 8 to 10 d postgermination, and, thereafter, a steady decline in mRNA levels was observed. In the leaves of light-grown seedlings, steady-state levels of mRNA encoding the three chlorophyll biosynthetic enzymes were inversely correlated with leaf age (He *et al.*, 1994). In contrast, light is not essential for expression of *ALAD* in leaves of dark-grown plants of soybean (Kaczor *et al.*, 1994).

Porphobilinogen deaminase

The enzyme, which is a soluble chloroplast protein (Castelfracco *et al.*, 1988) catalyses the formation of the linear tetrapyrrole, hydroxymethylbilane, from four molecules of Porphobilinogen (PBG). The tetrapyrrole is either converted to uroporphyrinogen III by uroporphyrinogen cosynthetase or non-enzymatically cyclized to uroporphyrinogen I (Frydman and Frydman, 1978 a, b). Porphobilinogen deaminase enzyme has been purified from *A. thaliana*, which is a monomer of 35 kDa. It is inactivated by arginine-, histidine-, lysine-specific reagents and also by the substrate analogue 2-bromoporphobilinogen (Jones and Jordan, 1994).

A cDNA clone for porphobilinogen deaminase from *Arabidopsis* encodes a precursor protein of 382 residues, which is then imported to the isolated chloroplasts and processed to a mature protein (Lim *et al.*, 1994). The enzyme was encoded by a single gene and is expressed in both leaves and roots (Witty *et al.*, 1996). Northern blot analysis has shown that the *PsPBGD* is expressed in chlorophyll-containing tissues and is subjected to light induction. The enzyme has

an acidic isoelectric point and is a single polypeptide showing different levels of sensitivity to divalent cations, being most sensitive to Fe^{2+} . The synthesis of PBGD is regulated by light (Smith, 1988; Spano and Timko, 1991; Shashidhara and Smith, 1991; He *et al.*, 1994). In *Euglena gracilis*, PBGD transcript levels regulated at the post-transcriptional level (Vacula *et al.*, 2001).

Uroporphyrinogen III cosynthetase

This enzyme catalyses formation of uroporphyrinogen III from hydroxymethylbilane. The enzyme has been isolated from *E. gracilis* (Hart and Battersby, 1985) and wheat germ (Higuchi and Bogorad, 1975). The enzyme was found to be heat labile and Na^+ and K^+ enhanced its activity. The enzyme PBGD and cosynthase may be present as a complex (Tsai *et al.*, 1987). *HemD* gene encodes for the enzyme and has been cloned and isolated from various organisms. The enzyme from *A. nidulans* has an inferred amino acid sequence which shows 43-50% homology to that from *B. subtilis*, *E. coli* (Jones *et al.*, 1994). The inferred amino acid sequence has conserved arginine residue at codon 146, which has been implicated to be important for cosynthase activity (Hansson *et al.*, 1991). Gene for uroporphyrinogen synthase has been identified and characterized in *A. thaliana*. A precursor protein of 34 kDa when was imported to chloroplast produce mature protein of 29 kDa (Tan 2008). The first gene encoding UROS was isolated from *Escherichia coli* (Sasarman *et al.*, 1987) with those from human (Tsai *et al.* 1988) *Bacillus subtilis* (Hansson *et al.* 1991) *Pseudomonas aeruginosa* (Mohr *et al.* 1994) *Anacystis nidulans* R2 (now reclassified as *Synechococcus* PCC 7942) (Jones *et al.* 1994) mouse (Bensidhoum *et al.* 1994) and budding yeast *Saccharomyces cerevisiae* (Amillet *et al.* 1995).

Coproporphyrinogen oxidase

This enzyme catalyses the oxidative decarboxylation of propionate side chains on ring A and B to yield protoporphyrinogen IX. In aerobic organisms, oxygen is utilized as the sole electron acceptor for enzymatic activity while in anaerobic organisms NADP^+ is used (Seehra *et al.*, 1983). The coprogen oxidase was first purified from tobacco (Hsu and Miller, 1970). Yeast enzyme is a homodimer of 70 kDa (Camadro *et al.*, 1986). It has shown that tobacco plants containing antisense RNA for coprogen oxidase are more resistant to tobacco mosaic virus (Mock *et al.*, 1999). Tobacco plants containing antisense coprogen oxidase RNA showed decreased enzyme levels of coprogen oxidase and were characterized by growth retardation and

necrosis, showing that these plants were damaged due to oxidative stress (Kruse *et al.*, 1995a). The full-length cDNA from barley and tobacco were cloned and found that these encode for precursor proteins of 43.6 and 44.9 kDa respectively (Kruse *et al.*, 1995b). These proteins were processed to 39 kDa after import into pea chloroplast and accumulated in the stroma.

There are two isoforms of coprogen oxidase (*Cpx1* and *Cpx2*) was found in maize. The *Cpx1* fused with GFP showed that it was localized in plastid, whereas in case of *Cpx2*, it appeared to localize to mitochondria (Williams *et al.*, 2006). Mutants defective in the enzyme have been isolated from *R. sphaeroides* (Coomber *et al.*, 1982), defective in two genes, *hemN* and *hemF*, which encode alternative forms of coprogen oxidase (Xu *et al.*, 1992). An *Arabidopsis* mutant defective *LIN2* gene encoding coprogen oxidase develops lesions on leaves, in a developmentally regulated and light dependent manner (Ishikawa *et al.*, 2001).

Protoporphyrinogen oxidase

Protoporphyrinogen oxidase catalyzes the final reaction of the common branch of the heme and chlorophyll biosynthesis pathways, i.e., conversion of Protoporphyrinogen IX (Proto IX) to Protoporphyrin IX (Proto IX) in plants. Proto IX is unstable and spontaneously undergoes oxidation in presence of oxygen and its oxidation is enhanced by light (Jacobs and Jacobs, 1979). Enzyme catalyzed reaction mechanism of Proto IX oxidation consists of three consecutive dehydrogenations and a subsequent tautomerization yielding the porphyrin through the stereospecific loss of the fourth *meso* hydrogen as a proton (Akhtar, 1994). Proto IX is active only if there are no polar groups on ring A and B and is quite stable towards acids and bases.

Proto IX was isolated from yeast mitochondrial membranes (Camadro *et al.*, 1994), from spinach, where proto IX was both found in chloroplast and mitochondria respectively (Watanabe *et al.*, 2001), from *Arabidopsis* where transcripts of plastidal proto IX were very high in leaves, where as it was low in roots and floral buds (Narita *et al.*, 1996), from tobacco (*PPX1* and *PPX2*) where transcripts of both genes were expressed synchronously during tobacco plant development and diurnal and circadian growth (Lermontova *et al.*, 1997), purified from barley etioplasts (Jacobs and Jacobs, 1987), localized in the envelope (stromal side) and thylakoid membranes (stromal side) of chloroplasts (Matringe *et al.*, 1992a; Che *et al.*, 2000). Dailey *et al.*, 1994 have expressed *hemY* gene of the *B. subtilis* in *E. coli* and found the protein was capable of oxidizing coprogen III and proto IX. Yamato *et al.*, 1995 have shown that amino acid sequences of

protox purified from tobacco-cultured cells have shown homology to acid/base catalysis and heme binding regions of plant peroxidases. When human protoporphyrinogen IX oxidase was overexpressed in rice resulted in severe necrotic leaf and growth retardation. Tetrapyrrole-induced photooxidation was confirmed by increased lipid peroxidation and subsequent cell death (Jung *et al* 2008).

Mg-chelatase

The chelation of Mg^{2+} into protoporphyrin IX, which is catalyzed by the enzyme Mg-chelatase, is the key reaction unique to chlorophyll biosynthesis. In photosynthetic organisms, Mg-chelatase is a three component enzyme and catalyses the insertion of Mg^{2+} in two steps, with an ATP-dependent activation followed by an ATP-dependent chelation step (Walker and Willows 1997; Walker and Weinstein, 1994). The optimal ATP concentration for activation is found to be higher than that of chelation step. The activation step requires interaction of subunits D and I. Since D subunit occurs as an aggregate, this step involves dissociation of a single D subunit from the aggregate. ATP and a kinase-mediated phosphorylation are also involved in this step. The second step (chelation) of catalysis is Mg^{2+} insertion, and involves the H subunit along with the $I_2.D$ complex. The subunit of $I_2.D$ complex then drives the release of a water molecule from the Mg^{2+} ion's co-ordination sphere, by using water as a substrate for hydrolysis of ATP. The released Mg^{2+} , co-coordinated to a histidine residue on the H subunit, promotes dissociation of hydrogen ions from the pyrrole nitrogen atoms and is then itself co-coordinated into porphyrin macrocycle (Walker and Willows, 1997). The stoichiometry of H: $I_2.D$ complex has been shown as 4:1 (Willows *et al.*, 1996). In tobacco, only a 110 amino acid long part of ChlH is required for interaction with partner subunits and maintenance of the enzymatic activity (Grafe *et al.*, 1999).

In the purple bacteria *R. capsulatus* and *R. sphaeroides*, Mg-chelatase is encoded by the *bchD*, *I* and *H* genes (Gibson *et al.*, 1995; Willows *et al.*, 1996). The *bchH* and *bchD* gene pair have been expressed separately in *E. coli* and insertion of Mg^{2+} into proto IX was obtained by combining soluble extracts from induced cells and supplying substrate, ATP and Mg^{2+} (Willows *et al.*, 1996). BchlH (140 kDa) binds the substrate protoporphyrin IX in a molar ratio of 1:1, while Bchl with its ATP binding domain functions as a homodimer. BchD participates as a polymer with an apparent Mr of 550 kDa. The complex catalyses an activation step requiring

TH-16996



571.2
Sa 835
I m

Bchl, BchD and Mg-ATP and a metal insertion step involving protoporphyrin IX and BchH (Gibson *et al.*, 1995). Structural analyses have shown that Bchl forms hexamers and belongs to ATPases associated with various (AAA (+) families of proteins. AAA (+) proteins are Mg (2+)-dependent ATPases that normally form oligomeric ring structures in the presence of ATP. It has been suggested that ATP hydrolysis of each Bchl within the hexamer causes a conformational change of the hexamer as a whole (Hansson *et al.*, 2002).

Jung *et al.*, 2003 isolated the *chlH* mutant from rice, where they have shown that *ChlH* is light inducible and the mutant is defective in thylakoid development. Depending upon the concentration of Mg²⁺ in lysis buffer, the ChlH migrated between stroma and the envelope membrane and was localized in the envelope membrane at very higher concentrations of Mg²⁺ (above 5mM), indicating that the activity of Mg-chelatase was regulated by the expression and subchloroplastidic localisation of ChlH protein (Nakayama *et al.*, 1998).

Transgenic tobacco plants expressing antisense RNA for Mg-chelatase *ChlH* were chlorophyll deficient. In these plants, less protoporphyrin IX and heme accumulated, and a decrease in 5-aminolevulinate synthesizing capacity was seen (Papenbrock *et al.*, 2000b). Virus-induced gene silencing of *ChlH* in tobacco led to lowering of *ChlD* and *Chl I* mRNAs along with less chlorophyll content (Hiriart *et al.*, 2002). Mochizuki *et al.*, 2001 have isolated one Mg-chelatase subunit H mutant of *Arabidopsis*, which they named *GUN5* (Genome Uncoupled). Mutation in this gene had repressed expression of *lhcb* whereas those with mutations in *ChlI*, *ChlD* gene did not show any *lhcb1* repression. This comparison suggests a specific function for ChlH protein in the plastid-signaling pathway (Mochizuki *et al.*, 2001; Strand *et al.*, 2003).

The *ChlI* gene was cloned from soybean by Nakayama *et al.*, 1995. It is localized in stroma and has an ATP-binding motif. The *ChlI* mRNA was reversibly induced by light in cell cultures of soybean. In *Arabidopsis*, a second *ChlI* gene, *ChlI-2* has been identified that supports limited chlorophyll synthesis in a T-DNA knockout mutant of the chlorina locus (*chlI*) (Rissler *et al.*, 2002). Using transformants of tobacco with sense and antisense mRNA for *ChlI*, it has shown that both elevated and decreased levels of *ChlI* mRNA and ChlI protein led to reduced Mg-chelatase activity and in these plants chlorophyll synthesis was also reduced (Papenbrock *et al.*, 2000a). In *Arabidopsis* double-knockout mutant of *chlI1/chlI1 chlI2/chlI2* was albino. Comparison with the pale-green phenotype of a *chlI1/chlI1* single-knockout mutant indicates that

CHLI2 could support some chlorophyll biosynthesis in the complete absence of CHLI1 (Huang and Li, 2009). The tobacco *ChlD* cDNA sequence was isolated and cloned (Papenbrock *et al.*, 1997). The amino terminal half of *ChlD* cDNA was 46% homologous to that of *ChlI*, indicating gene duplication from an ancestral gene. Reconstitution experiments using yeast protein extract expressing the three subunits of tobacco Mg-chelatase showed additional requirement of ATP (Papenbrock *et al.*, 1997). ChlD in pea is associated with the membranes in the presence of MgCl₂. It was 89 kDa protein expressed in soluble form and was active in a Mg-chelatase reconstitution assay (Luo *et al.*, 1999). CHLH gene encoding the H subunit of Mg-chelatase was induced by light under all conditions with an initial peak after 2-4 h light. The other Mg-chelatase subunit genes CHLI and CHLD genes were not strongly regulated at the level of transcript abundance (Stephenson and Terry, 2008).

The *chlH* subunit of *Synechocystis* stimulates magnesium protoporphyrin methyltransferase (ChlM) activity (Shepherd *et al.*, 2005). The ATPase activity of recombinant CHLI1 in *Arabidopsis thaliana* was found to be fully inactivated by oxidation and easily recovered by thioredoxin-assisted reduction, suggesting that CHLI1 is a target protein of thioredoxin (Ikegami *et al.* 2007).

S-adenosyl-l-methionine: Mg-protoIX methyltransferase

This enzyme catalyzes the conversion of Mg-protoporphyrin IX to Mg-protoporphyrin monomethyl ester (MPE) by transferring of a methyl group to the carboxyl group of the C13-propionate side chain of MgProto (Gibson *et al.*, 1963) where, SAM acts as a methyl group donor. This enzyme belongs to the broad family of S-Adenosyl-L-Methionine (SAM)-dependent methyltransferases (Kagan and Clarke, 1994), which contains the S-adenosyl- methionine (SAM)-binding domain, a seven-stranded b-sheet (Jones, 1999). The *Synechocystis* PCC 6803 *chlM* was over expressed in *E. coli* and the protein has been purified which is a 20 kDa protein (Shepherd *et al.*, 2003). Taking the purified protein steady state kinetic assays were performed using Magnesium deuteroporphyrin IX (MgD), a substrate analogue of Magnesium protoporphyrin IX where the initial rate studies showed that the reaction proceeds via a ternary complex, a rapid binding of the substrate and the enzyme preceded by slower isomerization of the enzyme (Shepherd *et al.*, 2004). Co-expression of Mg-chelatase (all subunits) and *chlM* from *Synechocystis* in *E. Coli* yielded soluble protein extracts that converted protoporphyrin IX to Mg-protoporphyrin IX monomethyl ester (Jensen *et al.*, 1999).

In *Arabidopsis* and spinach, this protein has a dual localization in chloroplast membranes as well as thylakoids. Averina *et al.*, 2002 showed that SAM-MgPdxMT was located not only in prothylakoids but also in prolamellar bodies of barley containing photoactive Pchl_a. *ChlM* from tobacco encodes a 35-kDa protein. The amount of ALA, Mg-proto and heme were reduced in antisense *chlM* plants of tobacco. The Mg chelatase activity was reduced in antisense plants whereas the Fe-chelatase activity was increased. The gene expression of *chlH*, *GluTR*, *GSAT* was less in antisense plants and more in sense plants. Western analysis of these corresponding proteins revealed a direct correlation between RNA levels and protein amounts (Alawady and Grimm, 2005).

Ferrochelatase

The chelation of Fe²⁺ to make heme is a crucial branch point of the tetrapyrrole synthesis pathway, which is catalyzed by ferrochelatase where Fe²⁺ gets inserted into protoporphyrin IX to generate protoheme. The ferrochelatase gene has been isolated from *Arabidopsis* (Smith *et al.*, 1994), barley & cucumber (Miyamoto *et al.*, 1994), soybean & *E. coli* (Kanjo *et al.*, 2001), and tobacco (Papenbrock *et al.*, 2001).

Though plastids are the major site of heme biosynthesis, mitochondria have also the capacity for heme production (Cornah *et al.*, 2002). In higher plants, ferrochelatase activity has been detected in bean cotyledons, oat seedlings and spinach leaves (Jones 1968; Porra and Lascelles, 1968) and barley etiolated seedlings where the ferrochelatase activity was found to be associated with mitochondria, etioplasts and plasma membranes (Little and Jones, 1976; Jacobs and Jacobs, 1995). In pea chloroplasts, the activity was shown to be associated with thylakoid membranes (Matringe *et al.*, 1994). Suzuki *et al.*, 2000 have shown that CsFeC1 protein from cucumber was present in hypocotyls and roots but not in cotyledons and targeted both to chloroplast and mitochondria (Masuda *et al.*, 2003) and CsFeC2 is localized predominantly in thylakoids and in very minor quantity in envelope membrane. It is detected in all tissues and was light responsive in cotyledons. Chow *et al.*, 1998 have shown the presence of two types (*AtFC-I*, *AtFC-II*) of ferrochelatases in *Arabidopsis*. One form was shown to be expressed in leaves, stems, roots and flowers and imported into chloroplasts and mitochondria whereas the other one was expressed in leaves, stems and flowers and targeted solely to chloroplasts (Lister *et al.*, 2001). *AtFC-I* was found to induce in response to TMV infection suggesting the requirement of

heme synthesis as part of defence response (Singh *et al.*, 2002). Impaired expression of plastidic ferrochelatase led to necrotic phenotype of antisense RNA transformed tobacco plants indicating that it plays a role in Chl biosynthesis (Papenbrock *et al.*, 2001). PIF1, members of a basic helix–loop–helix family of transcription factors regulates expression of a *ferrochelatase FeChII* in dark (Moon *et al.*, 2008). Expression of ferrochelatase upregulated in light whereas downregulated in chill and heat stress (Mohanty *et al.*, 2006).

Vinyl reductase

The 8-vinyl reductase reduces the 8-vinyl group on the tetrapyrrole to an ethyl group (Parham and Rebeiz, 1995) using NADPH as the reductant. This activity has been detected with isolated plastid membranes, in intact chloroplasts (Parham and Rebeiz, 1995; Tripathy and Rebeiz, 1988) from Cucumber (*Cucumis sativus*) and Barley respectively and also in solubilized crude extracts (Kolossoff and Rebeiz, 2001).

Nagata *et al.*, 2005 followed by Nakanishi *et al.*, 2005 isolated the mutant of *Arabidopsis*, which accumulates divinyl chlorophyll. The mutant is pale green and the chlorophyll a/b ratio varies in between 6 and 10 depending on the developmental stage and growth conditions (the chlorophyll a/b ratios of the wild type were between 3 and 3.8). This mutant is capable of photosynthesizing and growing under low-light conditions (70 to 90 $\mu\text{mole m}^{-2} \text{s}^{-1}$); but rapidly died under highlight conditions (1000 $\mu\text{mole m}^{-2} \text{s}^{-1}$) (Nagata *et al.*, 2005). The thylakoid membranes were in a disorderly fashion having no distinct grana stacks in the mutant but no distinct differences in the size and the number of chloroplasts between the wild type and the mutant. Starch granules were not found in the mutant chloroplasts, suggesting the reduction of photosynthetic activity in the mutant (Nakanishi *et al.*, 2005). The transcript level of DVR expression is high in leaves, stems and flower buds, and low in roots and localized in mesophyll cells of the chloroplast.

Though DVR genes were found in both higher plants and green algae, complete genomic sequence data from the unicellular red alga *Cyanidioschyzon merolae* (Matsuzaki *et al.*, 2004), which accumulates monovinyl chlorophylls, suggested that it lacks DVR homologs. These data suggest that another type of enzyme is involved in the reduction of the 8-divinyl groups in this organism. In cyanobacteria, a DVR gene was found in *Synechococcus* sp WH1802 but was not found in other cyanobacterial lineages. The knock-out mutant of gene Slr1923 lost its ability to

synthesize monovinyl chlorophyll and accumulated 3,8-divinyl chlorophyll instead. It was concluded that Slr1923 encodes the vinyl reductase or a subunit essential for monovinyl chlorophyll synthesis (Ito et al, 2008). [3, 8-DV]-Chlide a is the major substrate of DVR. Accordingly, name of the enzyme was from [3, 8-DV]-Pchlide a 8-vinyl reductase to [3, 8-DV]-Chlide a 8-vinyl reductase (Nagata 2007).

Protochlorophyllide oxidoreductase

It is the first light-requiring enzyme of the chlorophyll biosynthesis pathway. It catalyses the conversion of protochlorophyllide (Pchlide) to chlorophyllide (Chlide) by using light as a substrate along with protochlorophyllide (Pchlide) and NADPH as a cofactor. As a result of its requirement for light, this reaction is an important regulatory step in chlorophyll biosynthesis pathway and subsequently assembly of the photosynthetic apparatus. The initial binding of NADPH involves three distinct steps, which appear to be necessary for the optimal alignment of the cofactor in the enzyme active site. This is followed by the binding of the Pchlide substrate and subsequent substrate-induced conformational changes within the enzyme that occur prior to the formation of the final "poised" conformational state. These studies, which provide important information on the formation of the reactive conformation, reveal that ternary complex formation is the rate-limiting step in the overall reaction and is controlled by slow conformational changes in the protein (Heyes *et al*, 2008). The role of conformational changes in explaining the huge catalytic power of enzymes has been solved using using the chlorophyll biosynthetic enzyme NADPH: protochlorophyllide (Pchlide) oxidoreductase, which catalyses a unique light-driven reaction involving hydride and proton transfers (Sytina *et al*, 2008). Pchlide reduction occurs by dynamically coupled nuclear quantum tunneling of a hydride anion followed by a proton on the microsecond time scale in the Pchlide excited and ground states, respectively (Heyes *et al*, 2009). POR is nuclear encoded, translated as a precursor protein in the cytosol and ultimately transported into plastids (Apel, 1981). POR converts Pchlide to Chlide, by adding two hydrogen atoms at C17 and C18 on ring D (Figure II). The fact that POR is light-activated means the enzyme-substrate complex can be formed in the dark, removing the diffusive components out of the reaction. This has recently been exploited by studying Pchlide reduction at low temperatures to trap intermediates in the reaction pathway (Heyes *et al.*, 2002, 2003; Heyes and Hunter, 2004). As a result, the reaction has been shown to consist of at least three distinct steps: an initial light-

driven step, followed by a series of 'dark' reactions. An initial photochemical step can occur below 200 K (Heyes *et al.*, 2002), whereas two 'dark' steps were identified for *Synechocystis* POR, which can only occur close to or above the 'glass transition' temperature of proteins (Heyes *et al.*, 2003). This implies a role for protein motions during these stages of the catalytic mechanism. A thermophilic form of the enzyme has been used to identify two additional 'dark' steps, which were shown to represent a series of ordered product release and cofactor binding events. First, NADP⁺ is released from the enzyme and then replaced by NADPH, before release of the Chlide product and subsequent binding of Pchlde have taken place (Heyes and Hunter, 2004). Monovinyl protochlorophyllide (MV-Pchlde) and Divinyl protochlorophyllide (Dv-Pchlde) don't influence differentially the enzyme kinetics or the steps involved in the reaction pathway (Heyes *et al.*, 2006). The POR activity in different species is also temperature dependent. In *Synechocystis* the optimum temperature for POR activity is 30⁰C, whereas in thermophilic cyanobacterium *Thermosynechococcus elongates* the optimum temperature for POR activity is in between 50⁰C- 55⁰C and is much less active at room temperature (McFarlane *et al.*, 2005).

The absorption of light by the tetrapyrrole may produce torsional strain in the molecule providing favorable conditions for hydride/ hydrogen transfer from NADPH. Tyr and Lys are absolutely conserved among all members of the short chain alcohol dehydrogenase family and these residues are important for catalysis. The Tyr may be deprotonated, acting as a general acid to facilitate hydride transfer to or from NAD (P)⁺/H (Bohren *et al.*, 1994). The proton at the C-18 position of Pchlde is derived from Tyr-275 (numbering of Pea POR) and the hydride transferred to the C-17 position is derived from the *pro-S* face of NADPH. The proximity of the Lys residue may be important for lowering the apparent pKa of the phenolic group (around 10) of the Tyr to facilitate deprotonation (Figure III). It may also play a role in ensuring that the nicotinamide ring of NAD (P)⁺/H is in the correct orientation for *pro-S* hydride transfer (Varughese *et al.*, 1994). Spectroscopic studies of the dark grown bean seedlings gave the idea about two forms of protochlorophyllide, a main component with a red absorption band at 650 nm and a minor component absorbing at 636nm (Shibata, 1957). Again by fluorescence study it has been shown that there are two main forms of protochlorophyllide absorbing at 650nm and 638 nm and a minor form which absorbs at 628nm. The 650-nm and 638-nm forms are photoconvertible to chlorophyll at room temperature but the 628-nm form was not photoconvertible. Griffiths, 1975

observed in the barley-etiolated membranes, the non-photoactive protochlorophyllide could be converted into photoactive form (P638/652) by an NADPH requiring reaction.

At least three different spectral forms of Pchl_{id}e are recognized in intact tissues based on their fluorescence emission maximum (in nm): Pchl_{id}e F631 (due to the pigment structural arrangements), Pchl_{id}e F644 (due to association of POR), and Pchl_{id}e F655 (due to localization in PLBs and/or prothylakoids) (Böddi *et al.*, 1992, 1993). Fluorescence lifetime of Pchl_{id}e measured in plants showed that short- and long-wavelength Pchl_{id}e forms have fast (0.3 to 0.8 ns) and slow (5.1 to 7.1 ns) components with different proportions depending on plant species (Mysliwa-Kurdziel *et al.*, 2003). Short-wavelength Pchl_{id}e forms are thought to be located in the prothylakoids, bound in a monomeric form to proteins other than POR (Böddi *et al.*, 1998; Kis-Petik *et al.*, 1999). The main photoactive form present in etiolated plants is Pchl_{id}e F655, which after illumination, is converted to Chl_{id}e and subsequently to Chl (F682) through the formation of several, long wavelength intermediates (Böddi and Franck, 1997; Schoefs *et al.*, 2000a). After flash illumination, photoactive Pchl_{id}e complex can be regenerated by reloading with non-photoactive Pchl_{id}e on a fast time-scale with concomitant release of Chl_{id}e (Franck *et al.*, 1999; Schoefs *et al.*, 2000b).

Full-length cDNA clones of *POR* were isolated from Barley (Schulz *et al.*, 1989; Holtorf *et al.*, 1995), from Oat (Darrah *et al.*, 1990), from Pea (Spano *et al.*, 1992), from Wheat (Teakle and Griffiths, 1993), from *Arabidopsis* (Benli *et al.*, 1991; Armstrong *et al.*, 1995; Oosawa *et al.*, 2000), cyanobacterium *Plectonema boryanum* and *Phormidium lamonosum* (Fujita *et al.*, 1998; Rowe and Griffiths, 1995), from Liverwort (Takio *et al.*, 1998), from *Chlamydomonas* (Li and Timko, 1996), *Synechocystis* (Suzuki and Bower, 1995), Tobacco (Masuda *et al.*, 2002), Cucumber (Kuroda *et al.*, 2000) and from Banana (Coemans *et al.*, 2005). The high degree of sequence similarity among *POR*s from different taxonomic group implies a common mechanism of the enzyme action.

A characteristic feature of *POR* accumulating in dark is its sensitivity to illumination. The *POR* mRNA expression was also decreased (Santel and Apel, 1981). Red and far-red light treatment also inhibits *POR* mRNA expression indicating that *POR* expression was controlled by phytochrome (Apel, 1981; Batschauer and Apel 1984; Mosinger *et al.*, 1985). The negative effect of light on *POR* enzyme and its mRNA was observed in different dicotyledons like Bean,

Pea, Tomato, *Arabidopsis* (Forreiter *et al.*, 1991; Spano *et al.*, 1992; Armstrong *et al.*, 1995) and in monocotyledonous plants maize and barley (Forreiter *et al.*, 1991; Holtorf *et al.*, 1995). However some flowering plants have isoforms of POR. In *Arabidopsis* (Armstrong *et al.*, 1995; Oosawa *et al.*, 2000; Pattanayak and Tripathy, 2002; Su *et al.*, 2001), in Barley (Holtorf *et al.*, 1996a) and in Tobacco (Masuda *et al.*, 2002) there are different PORs present. In *Arabidopsis* there are three isoforms of POR, namely PORA, PORB and PORC. These three isoforms are differentially regulated by light. The level of *porA* mRNA and protein decreases on illumination of etiolated plants (Holtroff and Apel, 1996b) while that of *porC* increases and was dominantly expressed in both mature and immature tissues (Oosawa *et al.*, 2000). *PorB* transcript and protein levels remain constant in both dark and on illumination (Armstrong *et al.*, 1995, Holtrof *et al.*, 1995; Holtrof and Apel, 1996a). Both *porB* and *porC* of *Arabidopsis thaliana* exhibited diurnal fluctuation but only the *porB* mRNA of *Arabidopsis* exhibits circadian regulation (Su *et al.*, 2001). *PorC* mRNA and protein expression also increased under high light intensity (Su *et al.*, 2001; Masuda *et al.*, 2003). In cucumber the levels of the *POR* mRNA increased etiolated cotyledons when they were illuminated with continuous light and even matured leaves (Kuroda *et al.*, 1995, 2000; Fusada *et al.*, 1995) via transcriptional activation (Fusada *et al.*, 1995). In Tobacco, two *POR* isoforms have been isolated, the expression of which was not negatively regulated by light, persisted in mature green tissue and showed diurnal fluctuations with a similar oscillation phase (Masuda *et al.*, 2002). The plant hormone cytokinin also regulates cucumber *POR* gene expression by binding to the *cis*-elements present at 5' region of the *POR* promoter.

Degradation of PORA is specific and controlled by nuclear-encoded proteases. The mechanism of light-activation of protease expression is unknown. Mapleston and Griffiths, 1980 observes that *POR* activity decreased after illumination. Reinbothe *et al.*, 1995d showed that barley pPORA-Pchl_a complex was resistant to protease treatment independent of the presence or absence of NADPH. In contrast pPORA-Chl_a complex was rapidly degraded. The naked pPORA without its substrate or products was less sensitive to proteolysis than the pPORA-Chl_a complex suggesting that both substrate binding and product formation had caused differential changes in protein conformation (Reinbothe *et al.*, 1995d). PORB was not degraded by the protease. The *PORA* degrading protein is assumed to be nuclear encoded, energy dependent and plastid localized protein in barley (Reinbothe *et al.*, 1995d). But the study of post-import degradation of radiolabeled barley pPORA and pPORB on incubation with stroma

enriched fractions from etiolated and light grown barley or wheat did not show any protease activity (Dahlin *et al.*, 2000).

The import of the precursor of barley PORA (pPORA) into chloroplasts was totally dependent on envelope bound Pchl_{ide}, the substrate for the enzyme's catalytic activity (Reinbothe *et al.*, 1995 b, c). During the light induced transformation of etioplasts into chloroplasts, the concentration of Pchl_{ide} dramatically declined, and chloroplasts rapidly lost the ability to import pPORA. However ALA feeding restored the capacity to import pPORA. Exogenously applied Pchl_{ide} competitively released the envelope-bound pPORA into the cytosol (Reinbothe *et al.*, 1996c). The role of the transit peptide of pPORA was further analyzed by production of chimeric constructs, in which the transit sequences of pPORA and pPORB were exchanged and fused to either their cognate mature polypeptides or to a reporter protein of cytosolic dihydrofolate reductase (DHFR) from mouse. The transit peptide of pPORA conferred Pchl_{ide}-dependent import of both the mature PORB and DHFR, while that of pPORB directed the mature PORA and DHFR into chloroplasts even without the endogenous Pchl_{ide} (Reinbothe *et al.*, 1997), suggesting that the transit peptide of pPORA directly interacts with Pchl_{ide} in the plastid envelope for translocation. The Pchl_{ide}-dependent import of the transit peptide of barley pPORA and DHFR chimeric construct was also shown in chloroplasts of tobacco, *Arabidopsis*, and five other tested monocotyledonous and dicotyledonous plant species (Reinbothe *et al.*, 2000). pPORA also interacts with Toc33/34, one 16 kDa plastid envelop protein (ORP16) and Pchl_{ide} a oxygenase during its posttranslational import into isolated barley chloroplasts (Reinbothe *et al.*, 2004a,b). Again Reinbothe *et al.*, 2005 showed that Plastids of the *ppi1* mutant of *Arabidopsis* lacking Toc33, were unable to import pPORA in darkness but imported the small subunit precursor of ribulose-1, 5-bisphosphate carboxylase/oxygenase (pSSU), precursor ferredoxin (pFd) as well as pPORB. In white light, photooxidative membrane damage, induced by excess Pchl_{ide} accumulating in *ppi1* chloroplasts because of the lack of pPORA import, to be the cause of the general drop of protein import. Kim and Apel, 2004 also showed the POR import is substrate dependent. They found that the homozygous *xantha2* (*xantha2* is devoid of Pchl_{ide} and even also after ALA feeding in dark no Pchl_{ide} accumulation) mutants (where GFP fusion protein was stably expressed) failed to accumulate PORA-GFP, which may be caused by the lack of Pchl_{ide}. Using transgenic *flu* mutants that express the various GFP fusion proteins tested the uptake of PORA into plastids further. In cotyledons of *flu* and wild-type seedlings kept

under continuous light, SSU-GFP and PORB-GFP, but not PORA-GFP, accumulated within chloroplasts. Soon after these seedlings were transferred to the dark, *flu* started to accumulate Pchl_{ide} and PORA-GFP began to appear in plastids of this mutant, whereas in wild-type control seedlings, the fusion protein was not detected. However the Pchl_{ide} dependent PORA import is confined to the cotyledons but not to the matured green leaves. Again Kim *et al.*, 2005 showed, PORA and PORB import into plastids of intact seedlings (mutant lines of Toc34, Toc33, Toc159) revealed an unexpected multiplicity of import routes that differed by their substrate, cell, tissue and organ specificities.

On the contrary, several reports indicated that Pchl_{ide} is not required for the import of POR in vitro (Teakle and Griffiths, 1993 in wheat), (Dahlin *et al.*, 1995; Aronsson *et al.*, 2000, 2001b, 2003a in pea), (Jarvis *et al.*, 1998; Jarvis and Soll, 2001 in *Arabidopsis*). The absence or presence of Pchl_{ide} did not significantly affect the capacity to import pPORA and pPORB in barley (Dahlin *et al.*, 1995; Aronsson *et al.*, 2000).

POR disrupted mutant has been constructed and characterized in *Synechocystis* sp. PCC 6803, (Wu and Vermaas, 1995) and *P. boryanum* (Fujita *et al.*, 1998). Although DPOR contribute to Chl synthesis in *Synechocystis*, but POR plays the major role in the cells grown under strong light (Fujita *et al.*, 1998). The repression of *POR* gene expression in *A. tricolor* resulted in loss of Chl synthesis activity (Iwamoto *et al.*, 2001).

Light-independent protochlorophyllide oxidoreductase

Light-independent chlorophyll (Chl) biosynthesis is a prerequisite for the assembly of photosynthetic pigment–protein complexes in the dark (Demko V *et al.*, 2009). In contrast to angiosperms' dependence on light for Pchl_{ide} photoreduction, nonflowering land plants, algae and photosynthetic bacteria have a distinct enzyme known as light-independent protochlorophyllide reductase (DPOR) that catalyzes reduction of Pchl_{ide} in the dark. Spectral investigation of chlorophyll a formation during greening process in chlL(-) and chlN(-) mutants and downregulation of chlL and chlN in green light in wild type strain of cyanobacteria suggests that the regulation of dark-operative protochlorophyllide oxidoreductase (DPOR) in the transcriptional level is essential for cyanobacteria to synthesize appropriate chlorophyll for acclimating in various light colour environments (Gao Y *et al.*, 2009). The light-independent

protochlorophyllide reductase genes have been isolated from different species i.e. from *R. capsulatus* (*bchN*, *bchB* and *bchL*), from cyanobacteria (*chlN*, *chlB* and *chlL*) and several gymnosperms (Choquet *et al.*, 1992; Li *et al.*, 1993). *ChlN* was identified coding for a 545 amino acid protein, involved in reduction of Pchlde to Chlide (Choquet *et al.*, 1992). The protein product of *C. reinhardtii* chloroplast gene *chlL* has 53% homology to *bchL* gene product in *Rhodobacter* (Suzuki and Bauer, 1992). Dark POR activity was dependent on the presence of all three subunits, ATP and the reductant dithionite in *R. capsulatus* (Fujita and Bauer, 2000). In *R. capsulatus*, ferredoxin functioned as an electron donor to DPOR for its activity (Nomata *et al.*, 2005). In *Rhodobacter capsulatus*, mutations in genes known to completely block reduction of protochlorophyllide to chlorophyllide (*bchN*, *bchB*, *bchL*) accumulate a pool of monovinyl and divinyl forms of protochlorophyllide; but, *bchJ*-disrupted strains accumulate reduced levels of bacteriochlorophyll concomitant with the accumulation of divinyl Pchlde and thus have an altered ratio of monovinyl to divinyl Pchlde (Suzuki and Bauer, 1995).

Studies in yellow-in-the-dark mutants of *Chlamydomonas* indicated that synthesis of *ChlL* subunit is controlled by light intensity whereas the synthesis of *ChlB* and *ChlN* seem not to be influenced by light intensity (Cahoon and Timko, 2000). *ChlB* gene encoding one of the subunits of light-independent POR was cloned by Richard *et al.*, 1994; from *Ginkgo biloba*. *ChlB* mRNA starts to accumulate at the beginning of each dark phase (Richard *et al.*, 1994). The cyanobacterium *Plectonema boryanum* devoid of the *chlL* gene is unable to synthesize Chl in the dark (Kada *et al.*, 2003). There is a decrease in PSI activity in this mutant, however the PSII activity remained unchanged.

Chlorophyllide a oxygenase

Chlorophyll b is one of the major light-harvesting pigments produced by land plants, green algae and several cyanobacterial species. It is synthesized from chlorophyll a by chlorophyllide a oxygenase (CAO), which in higher plants consists of three domains, namely, A, B, and C (Kanematsu *et al.*, 2008). The transgenic plants overexpressing the A-domain-deleted CAO accumulated an excess amount of chlorophyll b during greening. The transgenic plants which lacked the A domain either died or were obviously retarded when they were exposed to continuous light immediately after etiolation (Yamasato *et al.*, 2008). The A domain of CAO is essential in the control of chlorophyll biosynthesis and in the survival of seedlings during de-

etiolation especially under strong illumination (Yamasato et al, 2008). B domain is not involved in the regulation of CAO protein level as there was no effect on protein level in transgenics overexpressing deleted CAO in chlorophyll b less mutants of *Arabidopsis* (Sakuraba et al, 2007). Tanaka *et al.*, 1998 isolated and characterized a gene from *Chlamydomonas reinhardtii* using insertional mutational studies, which they found to be encoding CAO enzyme, an enzyme involved in conversion of Chl a to b. The enzyme was found to be similar to methyl monooxygenases and its coding sequence of 463 amino acids was found to contain domains for a [2Fe-2S] Rieske center and for a mononuclear nonheme iron-binding site. Chl b is synthesized by oxidation/ conversion of methyl group on the D ring of the porphyrin molecule to a formyl group at that position. During conversion of Chl a to Chl b the electron is transferred from Rieske centre to the mononuclear iron with subsequent activation of molecular oxygen for oxygenation of the Chl a methyl group (Beale and Weinstein, 1990; Porra *et al.*, 1993). Since CAO is chloroplast localized and present in both thylakoid and envelop membrane (Eggink *et al.*, 2004), it could accept electrons from ferredoxin-NADPH oxidoreductase or from ferredoxin itself. Using the conserved motifs of CAO of *Chlamydomonas* as probe Espineda *et al.*, 1999 isolated the same gene from *Arabidopsis* that has 8 introns and coding sequence of 537 aminoacids. The hydropathic profiles of *AtCAO* suggested that there were no transmembrane helices. Tomitani *et al.*, 1999 isolated Chl b-synthesizing genes (*CAO*) from two prochlorophytes and from some major chlorophytes. The alignment of the deduced amino acid sequences showed 51 % to 83 % identity among the sequences and all the sequences shared typical motifs for [2Fe-2S] centre and for the mononuclear iron-binding site.

Oster *et al.*, 2000 have shown that, a recombinant CAO enzyme produced in *E. coli* catalyses an unusual two-step oxygenase reaction that is the 'missing link' in the chlorophyll cycle of higher plants. Overexpression of the CAO gene in *Arabidopsis* led to an increase in the Chl b level leading to reduction of the Chl a: b ratio from 2.85 to 2.65 in full green rosette leaves and at the same time there is 10-20 % increase in antenna size (Tanaka *et al.*, 2001). Expression of the CAO gene from *Arabidopsis* in *Synechocystis sp.* resulted in production of Chl b up to about 10 % of total Chl in this organism and these expressed chl-b pigments efficiently incorporated into the P700-chlorophyll a-protein- complex (Sato *et al.*, 2001). Duncan *et al.*, 2003 also showed that chl b can bind to CP43 protein. Chl b up to 80 % of total Chl was produced in *Synechocystis sp.* when higher plant gene coding for LHCP II was incorporated into

its genome together with the *CAO* gene although LHC II did not accumulate (Xu *et al.*, 2001). These studies indicate that there must be a communication between regulation of Chl b synthesis and synthesis of Chl b-binding proteins. Masuda *et al.*, 2002, 2003 showed that *CAO* gene responded to the level of irradiance. After a high light to low light shift of the *Dunaliella salina* culture, both the *CAO* and *lhcb* transcripts were rapidly induced. In higher plants light plays a major role in regulating the *CAO* gene and protein expression. Both transcript and protein level of CAO increased when *Arabidopsis* plants were transferred from moderate to shade light (Harper *et al.*, 2004). Over expression of *CAO* in tobacco plants resulted in 20% increase in Chl b in low light whereas 72% increase in Chl b under high light. The Chl a/b ratio decreased from 3.38 in WT plants to 2.33 in transgenic plants when grown in high-light (Pattanayak *et al.*, 2005). In *Arabidopsis* plants also there is decrease in Chl a/b ratio (Tanaka and Tanaka, 2005). The *CAO* sequence has been classified into 4 parts, the N-terminal sequence predicted to be a transit peptide, the successive conserved sequence unique in land plants (A-domain), a less-conserved sequence (B-domain) and the C-terminal conserved sequence common in chlorophytes and prochlorophytes (C-domain) (Nagata *et al.*, 2004). The C-domain is sufficient for catalytic activity and the N-terminal A domain confers protein instability by sensing the presence of Chl b and regulate the accumulation of CAO protein (Yamasato *et al.*, 2005). Lee *et al.*, 2005 isolated and characterized two isoforms (*OsCAO1*, *OsCAO2*) from Rice where *OsCAO1* transcript is less in dark and induced by light. *OsCAO2* mRNA levels are higher under dark conditions, and its expression is down regulated by exposure to light.

Geranyl-geranyl reductase

This enzyme catalyses the reduction of geranylgeranyl diphosphate to phytyl diphosphate. The cDNA encoding a pre-geranyl-geranyl reductase (mature protein is of 47 kDa) from *Arabidopsis thaliana* was isolated and characterized. This gene when expressed in *E.coli* sequentially catalyzed the reduction of geranyl-geranyl-chlorophyll a into phytyl-chlorophyll a as well as the reduction of free geranyl-geranyl diphosphate into phytyl diphosphate, suggesting that this is a multifunctional gene. The transcript level is up-regulated during etioplast to chloroplast and chloroplast to chromoplast development (Keller *et al.*, 1998).

The decrease in CHLP activity affects the chlorophyll and tocopherol contents (Tanaka *et al.*, 1999). Using the transgenic *Tobacco* plants expressing antisense RNA for geranyl geranyl

reductase (1.51 kb, mature protein of 47kDa) they have shown that chlorophyll content decreases in high light-intensity. They have also shown that CHLP provides phytol for both chlorophyll and tocopherol synthesis and is present at a branchpoint of tocopherol and chlorophyll biosynthesis. The reduced chlorophyll content in *chlP* antisense plants resulted in the reduction of electron transport chains per leaf area without a concomitant effect on the stoichiometry, composition and activity of both photosystems. However the reduced tocopherol content of the thylakoid membrane is a limiting factor for defensive reactions to photo-oxidative stress (Grasses *et al.*, 2001). PSII was severely photo-inhibited in mature leaves of all *chlP* antisense tobacco plants. Lipid peroxidation was also more in antisense plants and accumulation of xanthophylls cycle pigments was observed which could be a compensatory mechanism for tocopherol deficiency (Havaux *et al.*, 2003). A *bchP* gene coding for *chlP* has been detected from *Rhodobacter capsulatus* as a part of photosynthetic gene cluster (Mars, 1981; Zsebo and Hearst, 1984). Addelee *et al.*, 1996 cloned and sequenced *chlP* (1.224 kb, 44.87 kDa) from *Synechocystis* sp. PCC 6803 and complement the *bchP* mutant of *R. sphaeroides*. Inactivation of the *chlP* in *Synechocystis* sp. PCC 6803 resulted in decreased Chl and carotenoid contents. The mutant is also unable to grow photoautotrophically due to instability and rapid degradation of photosystems because of photooxidative stress caused by the accumulation of geranylgeranylated chlorophyll a. (Shpilyov *et al.*, 2005)

Chlorophyll synthetase

Chlorophylls are esterified with a long chain C-20 alcohol, phytol. The reaction is catalyzed by enzyme chlorophyll synthetase, where both Chlide a and Chlide b were equally esterified (Rüdiger *et al.*, 1980). The PChlide and Bchlide (bacterial chlorophyllide) are not accepted by the plant enzyme indicating that reduction of the 17, 18 double bond on the ring D was essential but reduction of 7, 8 double bond on ring B was unacceptable (Benz and Rüdiger, 1981b). Helfrich *et al.*, 1994 conclude that compounds which have the 13 (2)-carbomethoxy group at the same side of the macrocycle as the propionic side chain of ring D are neither substrates nor competitive inhibitors. Only compounds having the 13(2)-carbomethoxy group at the opposite site are substrates for the enzyme. Domanskii *et al.*, 2003 and Schmid *et al.*, 2002 showed that esterification kinetics of chlorophyllide is a rapid phase, leading to esterification of 15% of total chlorophyllide within 15-30 sec, followed by a lag-phase of nearly 2 min and a subsequent main phase.

In etioplasts, geranyl geranyl pyrophosphate (GGPP) is used as a substrate (Rüdiger *et al.*, 1980), while in chloroplasts; the preferential substrate is phytyl diphosphate (PhPP) (Soll *et al.*, 1983). Chlorophyll synthetase in chloroplast thylakoid membranes incorporates phytol in presence of ATP and a stromal kinase (Benz and Rüdiger, 1981a). The chlorophyll synthetase was found to be present in heat-bleached, ribosome-deficient plastids from rye and oat (Hess *et al.*, 1992), indicating its nuclear origin and synthesis by cytoplasmic ribosomes. The enzyme was not affected by the developmental stage of the plastids. In etiolated wheat, the enzyme was found in latent form in prolamellar bodies (Lindsten *et al.*, 1990). In photosynthetic bacteria *Rhodobacter*, the essential loci involved in bacteriochlorophyll a biosynthesis are clustered in a 46 kb region of the chromosomes (Bauer *et al.*, 1993). *BchG* in bacteria (Bollivar *et al.*, 1994b) and *G4* (Gaubier *et al.*, 1995) in *A. thaliana* encode for the enzyme and show a homology of 60-75% in amino acid sequences.

The final product of the reaction is Chl a, which differs from Chl b only by the presence of a methyl group at pyrrole ring II in place of formyl group (Beale and Weinstein, 1990). In *C. vulgaris* and greening maize respectively (Schneegurt and Beale, 1992; Porra *et al.*, 1993, 1994), the 7-formyl oxygen of Chl b is derived from O₂ by an oxygenase mechanism and these oxygenase reactions are irreversible (Hayaishi O., 1987). Despite the irreversibility the 7-formyl group, Chl b can be reduced to a 7-methyl group leading to synthesis of Chl a (Ito *et al.*, 1996; Ohtsuka *et al.* 1997).

It was shown that the conversion of Chlide to chlorophyll is a four-step process including three intermediates i.e., Chlide geranylgeraniol, Chlide dihydrogeranylgeraniol and Chlide tetrahydrogeranylgeraniol before the formation of Chlide phytol or chlorophyll (Shoefs and Bertrand, 2000).

Regulation of chlorophyll biosynthesis pathway

Chlorophyll, the most abundant tetrapyrrole in plants, responsible for harvesting and trapping light during photosynthesis are ubiquitously distributed in all plant species and perform a multitude of functions throughout development. The genes responsible for the pathway have been identified and the enzymatic steps of the pathways are well characterized. The steady-state levels of transcripts and the encoded enzymes were determined in many organisms with respect to response to environmental stimuli, tissue specific and developmental program and revealed

novel insights into the variation of the expression profiles in this pathway. All enzymes of the Chl biosynthetic pathway are nuclear encoded and so a tight regulation is expected at various levels of gene expression (Smith and Griffiths, 1993; Beale, 1999). Chl synthesis is highly synchronized with the formation of other pigments like heme, carotenoid, quinines etc and pigment-binding proteins to ensure the coordination between the different organelles in plants.

There are three main reasons for higher plants to control the chlorophyll biosynthesis pathway:

1. Since other tetrapyrroles except chlorophyll molecules are present in different parts of plants and essential for plant development, regulation at the branch point particularly at the Mg^{2+} insertion step is essential.
2. Chlorophyll biosynthetic pathway intermediates, the porphyrin molecules which are photodynamic in nature generate singlet oxygen species when they accumulate during skotomorphogenesis to photomorphogenesis. The singlet oxygen endogenously inhibits many metabolic pathways of the plants. The major control is at the production of the initial precursor ALA.
3. Since chloroplast development is a complex process and depends upon a lot of proteins, co-factors along with the chlorophyll pigments, a careful co-ordination between the synthesis of chlorophyll pigments and apoproteins should be occurred. The coupling of pigment synthesis and the assembly should be tightly regulated so that there won't be any free chlorophyll molecules, which are phototoxic.

The initial part of the pathway i.e. ALA formation is crucial for metabolic flow through the pathway and is generally accepted as the rate limiting in Chl synthesis. In maize, a lag-phase of about 3h for ALA synthesis exists prior to the formation of porphyrins suggesting an inhibition of ALA synthesis by Pchl_{ide} (Stobart and Ameen-bukhari, 1984) or heme.

GluTR, one of the enzymes of ALA production from glutamyl-tRNA is the major regulatory point in the pathway. The gene encoding for GluTR, that is; *HEMA* is regulated by hormones, the circadian clock (Kruse *et al.*, 1997), by light, through the action of phytochrome and cryptochrome (McCormac and Terry, 2002; McCormac *et al.*, 2001), and sugars (Ujwal *et al.*, 2002). Thus multiple external factors can influence the flux through the tetrapyrrole pathway, by the synthesis of the initial precursor.

There is also evidence that heme, whose synthesis may be enhanced in the dark by the accumulation of pathway intermediates behind the block at POR, acts to repress ALA synthesis, since GluTR activity is inhibited by haem (Vothknecht *et al.*, 1996). This is supported by the observation that phytochrome chromophore- deficient mutants, such as *hyl* and *hy2*, have reduced protochlorophyllide and ALA synthesis in the dark (Papenbrock *et al.*, 2001). The reduced ability to turnover haem may cause an increase in its levels. Tobacco plants transformed with antisense ferrochelatase RNA exhibited necrotic lesions induced by an accumulation of protoporphyrin IX (Papenbrock *et al.*, 1999), whereas tobacco plants antisense for subunits of magnesium chelatase had a decrease in chlorophyll content in leaves, but did not show necrotic lesions, suggesting that porphyrin accumulation was prevented by haem feedback (Papenbrock *et al.*, 2000a, 2000b).

The *Arabidopsis flu* mutant accumulates very high levels of Pchlde in the dark, and if the plants are exposed to white light, photobleaching is observed due to the phototoxicity of Pchlde (Goslings *et al.*, 2004; Danon *et al.*, 2005). Subsequently, FLU was shown to interact directly with GluTR in the yeast two-hybrid system (Goslings *et al.*, 2004) and was specific for the GluTR. *ulf3*, a suppressor of *flu* gene was isolated which reduced ALA synthesis and Pchlde accumulation. It was found to be allelic to *hyl*; supporting the model that haem antagonizes the effect of the *flu* mutation by inhibiting GluTR independently (Goslings *et al.*, 2004).

The branch point for proto IX represents another regulatory step at which the quantitative distribution of intermediate is controlled in the direction of Chl and heme. In plastids, the insertion of Mg^{2+} or Fe^{2+} into the porphyrin ring determines the flux to either Chl or heme. Magnesium chelatase has a higher affinity for proto IX than Fe- chelatase (Guo *et al.*, 1998). It suggested that while both the chelatases contribute to a coordinated allocation of proto IX, the excessive flow of proto IX is towards Chl synthesis in irradiated plants. Ferrochelatase is inhibited by ATP (Cornah *et al.*, 2002), so in the light, when ATP levels are higher, the magnesium branch of the pathway would be favored; conversely, in the dark, magnesium chelation would be reduced. The steady- state level of total heme increases in tobacco plants during the dark period and corresponds to the Fe-chelatase activity (Papenbrock *et al.*, 1999). In *Arabidopsis*, the magnesium chelatase subunit *ChlH* reaches a peak at the beginning of the light

phase and ferrochelatase reaches a peak at the end of the light phase, indicating a diurnal rhythm (Harmer *et al.*, 2000).

The most important external modulator of the tetrapyrrole pathway in plants is light. In angiosperms, it plays a direct role in the chlorophyll branch, because POR requires light for activity. Although plants require freshly synthesized Chl molecules throughout their lifetimes to meet the demands of growth and pigment turnover, light exerts a rapid and dramatic negative regulation on POR-mediated light-dependent Pchlide reduction at the level of enzyme activity and protein accumulation (Forreiter *et al.*, 1990). Different *POR* isoforms express differently in light, *porA* is present in dark but absent in light, *porB* is constitutively expressed both in dark and light but *porC* is absent in dark and light inducible (Armstrong *et al.*, 1995; Oosawa *et al.*, 2000; Su *et al.*, 2001). The light-activated reduction of Pchlide to Chlide and the simultaneous photo conversion of Pr form of phytochrome to the Pfr form trigger plant photomorphogenesis which includes changes in gene expression, formation of chloroplasts, cotyledon expansion, leaf development and inhibition of stem elongation (Chory, 1991).

Light also strongly regulates *POR* mRNA level during greening of most of the monocot plants (Darrah *et al.*, 1990). *POR-A* is rapidly degraded in etiolated seedlings upon illumination but if complexed with its product, Chlide, it becomes highly sensitive to proteolysis (Reinbothe *et al.*, 1995a, 1995b). A light- induced plastid protease activity degrades the *POR-Chlide* complex. This *POR*-degrading protease, composed of both Asp-type and Cys- type proteinases, is not found in etioplasts but is highly active in chloroplasts (Reinbothe *et al.*, 1995a, 1995b), as some of its constituents are encoded by light-responsive nuclear genes (Reinbothe *et al.*, 1995a).

Regulation of tetrapyrrole biosynthesis in higher plants has been attributed to negative feedback control of steps prior to delta-aminolevulinic acid (ALA) formation. One of the first mutants with a defect in this control had been identified in barley. The tigrina (*tig*) *d* mutant accumulates 10-15-fold higher amounts of Pchlide than wild type, when grown in the dark. The identity of the *TIGRINA d* protein and its mode of action are not known yet. Initially this protein had been proposed to act as a repressor of genes that encode enzymes involved in early steps of ALA formation. The *TIGRINA d* gene of barley is an ortholog of the *FLU* gene of *Arabidopsis thaliana* (Lee *et al.*, 2003). Phytochrome-interacting factor1 (*PIF1*) negatively regulates Chl biosynthesis in dark and its activity is negatively regulated by light (Huq *et al.*, 2004). *pif1*

mutant seedlings accumulate excess free protochlorophyllide when grown in the dark, with consequent lethal bleaching upon exposure to light.

In *Synechocystis* sp PCC 6803, a Chl binding 'chelator' protein binds to newly synthesized Chl and provides Chl for new photosynthetic reaction centers and antenna molecules (Wu and Vermaas, 1995). The FLP (flu like protein) proteins act as regulators of chlorophyll synthesis in response to light and plastid signals in *Chlamydomonas*. Reduction of the FLP proteins by RNA interference leads to the accumulation of several porphyrin intermediates and to photobleaching when cells are transferred from the dark to the light (Falciatore *et al.*, 2005)

Nuclear genes control plastid differentiation in response to developmental and environmental signals. Chlorophyll biosynthesis pathway intermediates plays crucial role in plastid development and signaling between chloroplast to nucleus. Susek and Chory, 1992 isolated mutants which do not repress *Lhcb* transcription completely in *Arabidopsis* seedlings, in which chloroplast development is prevented due to photooxidative damage by norflurazon treatment. This group of mutants is referred to as *gun* for *genomes uncoupled* (Susek *et al.*, 1993; Mochizuki *et al.*, 2001). The *lhcb1* expression is not repressed in norflurazone treated GUN5 mutant, as compared to wild type (Mochizuki *et al.*, 2001). Interestingly transgenic *Arabidopsis* lines overexpressing *porA* or *porB* restored the loss of nuclear gene expression due to the norflurazon treatment, indicating that the transgenic lines phenotypically resemble *gun* mutants (McCormac and Terry 2002, 2004).

In return, plastids emit signals that are essential for proper expression of many nuclear encoded photosynthetic proteins. Accumulation of Mg-protoporphyrin IX is a plastid signal (Strand *et al.*, 2003) that represses nuclear transcription through a signaling pathway in *Arabidopsis* that requires the GUN4 gene. GUN4 binds the product and substrate of Mg-chelatase and activates it, thus participating in plastid-to-nucleus signaling by regulating Mg-proto synthesis or trafficking (Larkin *et al.*, 2003). Cyanobacterial *gun4* mutant cells exhibit lower Chl contents, accumulate protoporphyrin IX and show less activity not only of Mg-chelatase but also of Fe-chelatase (Wilde *et al.*, 2004).

Oxidative stress and reactive oxygen species

There are many potential sources of ROIs (Reactive oxygen intermediates) in plants. Some are reactions involved in normal metabolism, such as photosynthesis and respiration. These are in line with the traditional concept, considering ROIs as unavoidable byproducts of aerobic metabolism (Asada and Takahashi, 1987). Other sources of ROIs belong to pathways enhanced during abiotic stresses, such as glycolate oxidase in peroxisomes during photorespiration. However, in recent years, new sources of ROIs have been identified in plants, including NADPH oxidases, amine oxidases and cell-wall-bound peroxidases. These are tightly regulated and participate in the production of ROIs during processes such as programmed cell death (PCD) and pathogen defense (Dat et al, 2000; Hammond-Kosack and Jones, 1996; Polle, 2001). Whereas, under normal growth conditions, the production of ROIs in cells is low ($240 \mu\text{M s}^{-1} \text{O}_2^-$ and a steady-state level of $0.5 \mu\text{M H}_2\text{O}_2$ in chloroplasts) (Polle, 2001), many stresses that disrupt the cellular homeostasis of cells enhance the production of ROIs ($240\text{--}720 \mu\text{M s}^{-1} \text{O}_2^-$ and a steady-state level of $5\text{--}15 \mu\text{M H}_2\text{O}_2$) (Polle, 2001). These include drought stress and desiccation, salt stress, chilling, heat shock, heavy metals, ultraviolet radiation, air pollutants such as ozone and SO_2 , mechanical stress, nutrient deprivation, pathogen attack and high light stress (Dat et al, 2000; Bowler et al, 1992; Orozco-Cardenas and Ryan, 1999). The production of ROIs during these stresses results from pathways such as photorespiration, from the photosynthetic apparatus and from mitochondrial respiration. In addition, pathogens and wounding or environmental stresses (e.g. drought or osmotic stress) have been shown to trigger the active production of ROIs by NADPH oxidases (Hammond-Kosack and Jones, 1996; Orozco-Cardenas and Ryan, 1999; Pei et al, 2000). The enhanced production of ROIs during stress can pose a threat to cells but it is also thought that ROIs act as signals for the activation of stress-response and defense pathways (Desikin et al, 2001; Knight and Knight, 2001). Thus, ROIs can be viewed as cellular indicators of stress and as secondary messengers involved in the stress-response signal transduction pathway. Although the steady-state level of ROIs can be used by plants to monitor their intracellular level of stress, this level has to be kept under tight control because over-accumulation of ROIs can result in cell death (Dat et al, 2000; Hammond-Kosack and Jones, 1996; Polle, 2001). ROI-induced cell death can result from oxidative processes such as membrane lipid peroxidation, protein oxidation, enzyme inhibition and DNA and RNA damage (the traditional concept). Alternatively, enhanced levels of ROIs can activate a PCD pathway, as

was recently demonstrated by the inhibition of oxidative stress (paraquat)-induced cell death in tobacco by anti-apoptotic genes (Mitsuhara et al, 1999). Because ROIs are toxic but also participate in signaling events, plant cells require at least two different mechanisms to regulate their intracellular ROI concentrations by scavenging of ROIs: one that will enable the fine modulation of low levels of ROIs for signaling purposes, and one that will enable the detoxification of excess ROIs, especially during stress. In addition, the types of ROIs produced and the balance between the steady-state levels of different ROIs can also be important. These are determined by the interplay between different ROI-producing and ROI scavenging mechanisms, and can change drastically depending upon the physiological condition of the plant and the integration of different environmental, developmental and biochemical stimuli.

Chl a Fluorescence and OJIP transient

Chlorophyll a (Chl a) fluorescence induction observed in plants, algae and cyanobacteria, known also as the fluorescence transient or Kautsky effect (Stirbet et al., 1998), has been extensively studied (Govindjee & Papageorgiou, 1971; Fork & Mohanty, 1986; Govindjee, 1995). It consists of light intensity dependent polyphasic changes in Chl a fluorescence emission when a dark-adapted leaf, or a suspension of isolated chloroplasts or intact photosynthetic cells, is illuminated with the continuous light. In the first phase of the transient (time scale from zero to one or several seconds, depending on the light intensity) the fluorescence intensity rises quickly from an initial low value, F_0 (The O level), to a higher one F_P (The P level). Under low light fluorescence rises to an intermediary step denoted as F_{P1} . But under high light, typically over 500 Wm^{-2} , two intermediary step denoted as F_J (the “J” or I_1 , level) and F_I (the “J” or I_2 level) normally appear (Strasser & Govindjee, 1991, 1992; Neubauer & Schreiber, 1987). The F_P level becomes saturated from 100 Wm^{-2} and is then denoted as F_m . A dip between I and P is sometimes present in the fluorescence transient and is denoted as D (Munday & Govindjee, 1969)

The variable fluorescence $F_v(t)$ [defined as $F(t) - F_0$, where $F(t)$ is the fluorescence intensity at any time t] is related mainly to the fluorescence of antenna chlorophyll of photosystem II, and is due to the variation of the quantum yield of fluorescence emission (between 2 and 10 %) (Latimer et al, 1956). Fluorescence induction measurements are now frequently used in different *in vivo* studies of plants, such as stress, pollution and productivity (Schreiber & Bilger, 1993). Chl a fluorescence emission *in vivo* comes from both PSI and PSII

photosystems, the contribution of PS1 being smaller [10-25% of F_0] (Lavergne & Trissl, 1995). PS1 does not contribute to the variable fluorescence (Butler, 1978). The first phase of Chl a fluorescence induction is mainly related to the photochemical process and charge separation reactions that take place at the PSII level (Dau, 1994; Govindjee, 1995; Joshi and Mohanty, 1995). The PSII unit catalyses the light- induced electron transport from water to the plastoquinone (PQ) pool molecules (mobile electron carriers between PSI & PSII). The electron transport system at PSII level starts with the excitation trapping by the photochemical reaction centre chlorophyll a (P 680) which induces the primary charge separation: $P\ 680^+ Phe^-$ (Greenfield & Wasielewski, 1996) This primary radical pair can decay by several pathways: transfer of the electron from the Phe^- to Q_A (the secondary charge separation), recombination and reformation of singlet excited state of the photochemical reaction centre $P\ 680^*$, formation of the $P\ 680$ triplet state, and other non-radiative pathways.

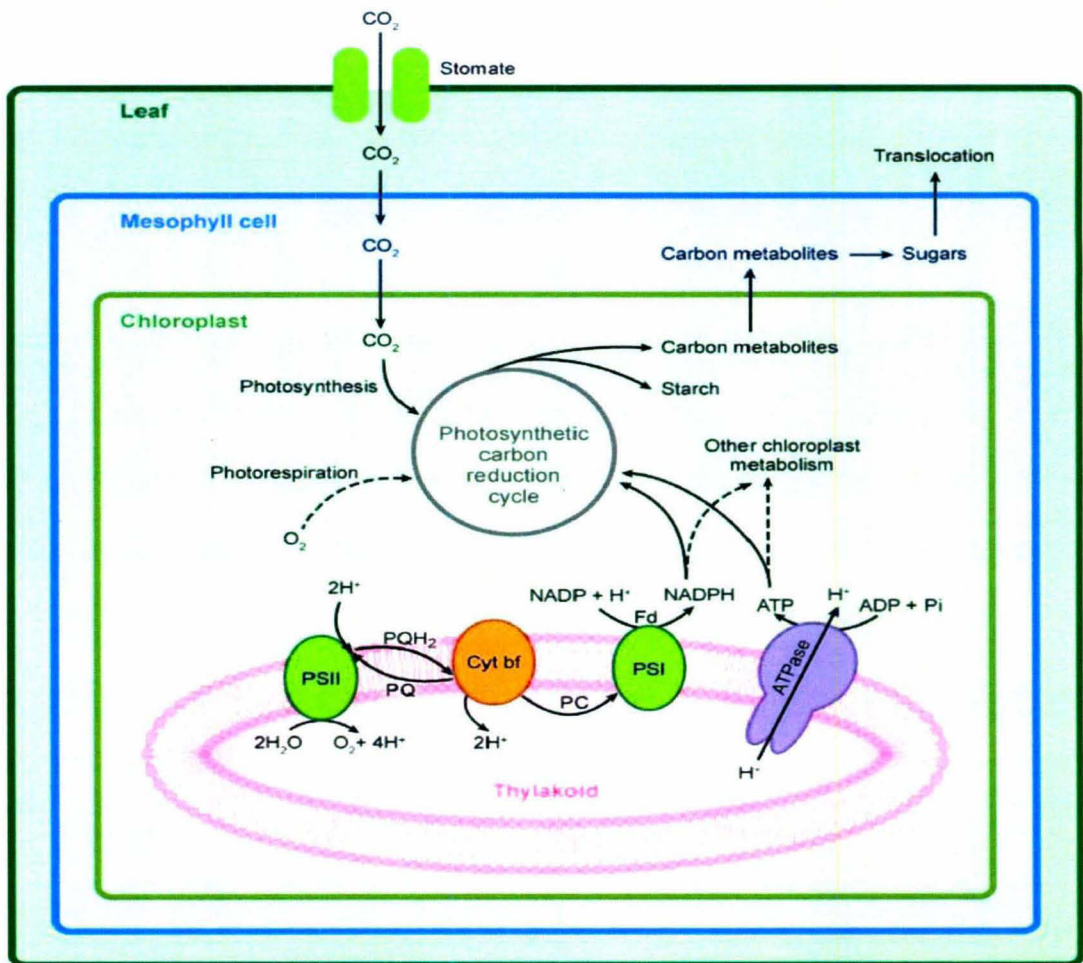
Non-photochemical quenching and photochemical quenching.

Chlorophyll fluorescence quenching is measured with a commercial fluorometer that can measure fluorescence yield in the presence of varying background white light as shown in Fig.III. Over a wide range of light intensities, plants are able to maintain a low steady state fluorescence yield and chl^* yield due to a combination of qP and NPQ. Thus qP and NPQ help to minimize production of O_2^* in the PSII antenna. The quenching due solely to NPQ can be determined periodically by measuring the fluorescence during a brief (<1s) pulse of light that saturates photochemistry so that there is no more quenching due to qP (Muller et al, 2001). Non-photochemical quenching can be divided into at least three components according to their relaxation kinetics in darkness following a period of illumination, as well as their response to different inhibitors (Horton and Hague 1998). The major and most rapid component in most algae and plants is the pH or energy dependent component, qE. A second component, qT, relaxes within minutes and is more important in algae, but rather negligible in most plants during exposure to excess light. This component is due to the phenomenon of state transition, the uncoupling of LHCs from PSII. The third component of NPQ shows the slowest relaxation and is the least defined. It is related to the photoinhibition of photosynthesis and is therefore called qI (Muller et al, 2001).

Components of Thylakoids membranes:

Thylakoids membranes are unique structure present in chloroplast. Sunlight is trapped by a photosystem unit of thylakoids membranes (Fig.3) consisting of PSI, PSII, Cytbf complex and converted into chemical energy producing reducing power in the form of NADPH which in turn utilized for CO₂ fixation (Baker 2008).

Photosystem II complex



 Baker NR. 2008. *Annu. Rev. Plant Biol.* 59:89–113.

Fig.3

Photosystem II contains at least nine different redox components (chlorophyll, pheophytin, plastoquinone, tyrosine, manganese, iron, cytochrome b559, carotenoid and histidine), which have been shown to undergo light induced electron transfer. However, only five of these redox

components are known to be involved in transferring electrons from water to plastoquinone pool: the water oxidizing manganese cluster (Mn)₄, the amino acid tyrosine (Yz), the reaction centre chlorophyll (P680), pheophytin and the two plastoquinone molecules, Q_A and Q_B. (Whitmarsh and Govindjee, 2002). PS II, a multisubunit complex consisting of 25 different polypeptides, is embedded in the thylakoid membrane of higher plants, algae and cyanobacteria (Hankamer et al., 1997). It uses light energy to catalyze a series of electron transfer reactions resulting in the splitting of water into molecular oxygen and reduction of PQ for which it is also known as water-plastoquinone oxidoreductase. The polypeptide composition of the oxygen evolving PSII complex with their associated functions is shown in table.1. All PSII proteins are believed to be present as one copy per P680 reaction center (RC). The primary photochemical reaction that generates redox potential to oxidize water and reduce PQ occurs in PSII RC. The RC consists of two highly hydrophobic proteins D1 and D2, which are conserved in higher plants species and have a significant degree of homology with the primary sequence of the L and M subunits of purple bacteria (Nanba & Satoh, 1987; Satoh, 1996). The excitation energy derived from the absorption of light by chls is used to convert the primary oxidant, P680* to P680 (Nanba & Satoh, 1987; Satoh, 1996). P680 is thought to consist of two chl molecules ligated to D1 and D2 proteins (Durrant et al., 1995). The excited state, P680*, donates a single high-energy unpaired electron to a molecule of pheophytin (Pheo), thereby forming the radical pair, P680⁺ Phea⁻ (Nanba & Satoh, 1987; Satoh, 1996). Each time P680⁺ is formed, it accepts an electron from a specific amino acid residue (D1-Tyr₁₆₁) and therefore is reduced to P680 (Babcock, 1987; Britt, 1996). As D1-Tyr₁₆₁ donates an electron to P680⁺, it accepts another electron from water via a four atoms manganese cluster associated with the luminal side of PSII (Joliot et al., 1969; Kok et al., 1970). Pheo, after accepting electrons from P680 passes them onto a PQ molecule (Q_A), tightly bound to D2 protein (Trebst, 1986; Diner et al., 1991). Q_A⁻ passes its electron onto a second PQ molecules associated with the Q_B site of D1 protein. (Trebst, 1986; Dostani et al., 1988; Diner et al., 1991). This electron transfer is aided by the presence of a nonheme iron localized between Q_A and Q_B (Diner et al., 1991). Each PQ associated with the Q_B site can accept two electrons derived from water and two protons from stroma before being released into the lipid matrix in the form of reduced PQ.

The electron extraction from water required for the reduction of D1-Tyr₁₆₁ is facilitated by involvement of four manganese associated with the luminal surface of PSII. The process of

water oxidation is known to involve the accumulation of four oxidizing equivalents on manganese leading to four electron oxidation of water (Joliot et al., 1969; Kok et al., 1970). These manganese are stabilized by three extrinsic proteins associated with the PSII. The 33 kDa subunit stabilizes the manganese cluster while the 23 and 17 kDa subunits allow PSII to evolve oxygen under Ca^{2+} and Cl^- limiting conditions respectively (Ghanotakis et al., 1984; Miyao et al., 1984a; 1984b).

Photosystem I complex

PSI complex consists minimum of 13 different polypeptides in chloroplast of higher plants (Chitnis, 1996). It uses light energy to catalyze the photo oxidation of plastocyanin, a copper protein present in the lumen of thylakoid membrane and the photo reduction of Fd, a [2Fe-2S] protein in chloroplast stroma. The polypeptide composition of PSI complex with their associated functions is shown in table. All proteins are believed to be present as one copy per P700 RC. The co-factors of PSI are bound to the PsaA, PsaB, and PsaC proteins (Chitnis et al., 1995; Chitnis, 1996).

The primary photochemical reaction that generates redox potential to oxidize plastocyanin and reduce Fd occurs in PSI RC. The excitation energy absorbed by the chls is transferred to the primary electron donor P700 that is a dimer of chl a molecules (Norris et al., 1971). Excitation of P700 leads to the charge separation, which is stabilized by spatial displacement of electrons through a series of redox centers. In forward reaction, an electron from the excited P700 is transferred to the primary acceptor A_0 , a chl a monomer (Shuvalov et al., 1986) and then to an intermediate acceptor A_1 , which is one of the two phylloquinone molecules found in PSI (Thurnauer & Gast, 1985). The next acceptor of electrons in the sequence is the [4Fe-4S] cluster Fx. The subsequent path of electrons through F_A/F_B remains an unresolved area in the electron transfer pathway in PSI (Jung et al., 1995; Mannen et al., 1996). The electrons may travel in a series: Fx to $F_{B/A}$ to $F_{A/B}$ to Fd. Alternatively, the electrons from Fx may be transferred to F_A or F_B and then one or two of these reduced clusters can donate electrons to Fd. The electron lost by P700 is gained by oxidizing plastocyanin.

Cytochrome b_6f complex

The cyt b_6f complex is the simplest and the best characterized of the multisubunit complex that catalyses the light reaction of photosynthesis in the thylakoid membrane. It mediates the transfer

of electrons from plastoquinone to plastocyanin, and is involved in noncyclic electron flow from PSII to PSI (Wood & Bendall, 1976; Hurt & Hauska, 1981) as well as in cyclic electron flow around PSI (Lam & Malkin, 1982).

The precise manner in which cyt b_6f complex transfer electrons from reduced PQ to plastocyanin is yet to be worked out, but the most popular models are based on the Q-cycle scheme of Mitchel (1975). It is believed to contain two PQ-binding sites C and site Z, which are located near the two surfaces of the membrane. It seems that first electron is passed to the Rieske center, which then reduces cyt f. The second electron can be passed either to the Rieske center or donated to the low potential form of cyt b_6f , since the semiquinone species is a strong reductant. If the later occurs, the electron on cyt b_6LP ($E_m = -150$ mV) is probably passed to the high potential cyt b_6HP ($E_m = -50$ mv) and then then used to reduce a bound plastoquinol to a semiquinone at site C. Further reduction of this semiquinone bound at site C could occur in several different ways, either another plastoquinol molecule is reduced at the Z site, making a second electron available via a reduction of cyt b_6HP , or electron donation may come directly from PSII or indirectly from PSI via reduced Fd. If site C is near the outer surface, then the effect of the cyt b_6 -catalysed Q cycle is to pump protons across the membrane and shift the proton /electron stoichiometry from 1 to 2 for plastoquinol oxidation.

Effect of salt stress on chloroplast biogenesis and photosynthesis

Chloroplasts are the most sensitive organelles affected by the salt stress (Lapiana & Popov, 1970). Any change in structure and function of the chloroplast will affect the function of the organelle, which in turn affects the ultimate yield of the plants. Genes or proteins associated with photosynthetic pathways were in general not among the most altered by the stress. For example, in *Thellungiella* (a stress-tolerant plant), photosynthesis genes correspond to 15% of all genes down-regulated (Wong et al., 2006), while in rice alterations in photosynthesis-related genes are mostly associated with stress recovery (Zhou et al., 2007). The effect of salinity and drought on genes associated with photosynthesis (AraCyc Pathways, www.arabidopsis.org/tools/aracyc) was checked in arabidopsis seedlings using the expression profiles available (generated with the Affymetrix ATH1 chip; Kilian et al., 2007). The imposed stresses were evaluated for 24 h. Although no information on the physiological status of the seedlings was given, the imposed stresses may be considered as mild. Of the 139 photosynthesis-related genes (AraCyc Pathways)

the AtGenExpress salt and drought microarray has information for 102 genes. As a general trend, both stresses led to gene down-regulation, most of the changes being small possibly reflecting the mild stress (Stitt et al, 2007).

Pigment contents: Various pigments contents are affected differently by the salinity stress depending upon the halophytic or glycophytic nature of the plants and algae. Photosynthetic pigments are reported to change with the plant genotypes, the system used and the time period of the stress imposed (Misra et al., 1995, 1996). Chlorophyll decreased in salt susceptible crops but increased in salt tolerant crops (Misra et al., 1997; Lapiana & Popov, 1970). Ma et al. (1977) have shown that in *P.euphratica* Olive with increasing salt levels chlorophyll a contents and chlorophyll a/b ratio increased, while chlorophyll b and carotenoid content decreased. According to Lu et al. (2002) salt in halophyte *Suaeda salsa* does not affect neoxanthin, leutin, β -carotene, violaxanthin, antheraxanthin, and chlorophyll a and b contents. Tezara et al. (2003) have shown that salt stress has no significant effect on chlorophyll content in *Lycium nodosum* while according to Kovach et al. (1992) chlorophyll a/b ratio increased with salinity treatment in *Hydrophila Polysperma* (Roxb.) Anders. (Acanthaceae). Singh & Kshatriya et al. (2002) have shown that graded concentrations of NaCl (20-200 mM) show decrease in the chlorophyll 'a' contents of *Anabaena* with increasing concentration of NaCl except at extremely low concentration of NaCl (5-20 mM).

Chloroplast structure: High salinity causes ion imbalance and osmotic stress in plants. Plastids from *Triticum aestivum* cv. Giza 168 had swollen prothylakoids however the prolamellar bodies were regular (Abdelkader, 2007). According to Barhoumi et al, 2007 NaCl affected the ultrastructure of the chloroplast, especially in the mesophyll. The chloroplasts of mesophyll cells from control plants were discoidal and exhibited well compartmentalised grana stacks. Little or no starch was present. Salinity caused the development of an undulating thylakoid system and numerous plastoglobuli in most of the mesophyll chloroplasts. The thylakoids were often greatly distended, leading to the appearance of vesicles in the stroma. In some cases, the disorganisation of thylakoid membranes was accompanied by the disappearance of grana stacking. Occasionally, the chloroplast envelope was disrupted in several places and the stroma very lightly stained. Salinity affects the chloroplast ultrastructure (Boyer, 1976). According to Hernandez et al. (1995) in *Pisum sativum* L. salt treated leaves showed disorganized thylakoid structure of the chloroplast, an increase in the number and size of plastoglobule in sensitive plants and decrease

in starch content in salt tolerant plants. Sairam & Srivastava (2002) have shown that membrane stability index (MSI) decreased with salt stress but decline was more in wheat genotype HD2687 (susceptible) than in Kharchia 65 (tolerant). NaCl-induced changes in the thylakoid membrane of wild-type *Anabaena variabilis* and its NaCl(r) mutant strain as indicated by difference in its absorption and fluorescence spectra at different wavelength (Chauhan et al., 2000).

Reactive oxygen species and super-oxide detoxifying enzymes: Salt stress affects enzymatic activities of chloroplast enzymes. According to Hernandez et al. (1995) in salt treated *Pisum sativum* L., chloroplast from tolerant plants showed significant increase of Cu Zn-SODII and ascorbate peroxidase activities as well as in ascorbate content, while those in from sensitive plants showed increase in H₂O₂ content and lipid peroxidation. In *Lotus japonicas* gene expression of dehydroascorbate reductase, superoxide dismutase and glutathione peroxidase increased in response to NaCl stress. (Rubio MC *et al*, 2008)

Superoxide dismutase (SOD) is one of the crucial enzymes that protect cells against the oxidative damages (Raychqudhuri and Deng, 2000; Fridovich *et al*, 1986). There are three main isoforms SODs in eukaryotic cells: Mn-SOD in mitochondria, Cu/Zn-SOD in chloroplast and cytoplasm, and Fe-SOD in plastid. Unlike Cu/Zn-SOD and Fe-SOD, Mn-SOD, whose activity is not inhibited by H₂O₂ and cyanide, exists only in mitochondria (Bowler *et al*, 1992, 1994), in which the over-produced ROS could cause mitochondrial diseases and aging (Wei and Lee, 2002). The roles of SODs under environmental stresses have been studied extensively (Raychqudhuri and Deng, 2000; Yu and Rengel, 1999). Mn-SOD overexpressed in *Arabidopsis* played a pivotal role in preventing the over accumulation of ROS and protecting the cells against ROS caused by salt stress, as a result, enhanced salt-tolerance of the transgenic plants (Wang *et al*, 2006).

Two cytosolic (OsAPx1 and OsAPx2), two peroxisomal (OsAPx3 and OsAPx4), and four chloroplastic (OsAPx5, OsAPx6, OsAPx7, and OsAPx8) isoforms identified in the rice genome. NaCl at 150 mM and 200 mM increased the expression of OsAPx8 and the activities of APx, but had no effect on the expression of OsAPx1, OsAPx2, OsAPx3, OsAPx4, OsAPx5, OsAPx6, and OsAPx7 in rice roots. However, NaCl at 300 mM up-regulated OsAPx8 expression, increased APx activity, and down-regulated OsAPx7 expression, but had no effect on the expression of OsAPx1, OsAPx2, OsAPx3, OsAPx4, OsAPx5, and OsAPx6 (Hong *et al*, 2007).

Wheat genotype Kharachia 65(tolerant) exhibited less decrease in Ascorbic acid content, less increase in H₂O₂, thiobarbituric (TBARS) measure of lipid peroxidation and higher increase in superoxide dismutase (SOD) and its isozymes, ascorbate peroxidase (APOX) and glutathione reductase (GR) in all subcellular fraction than salt sensitive HD2687 in response to salinity stress. Chloroplast fraction showed higher total SOD, APOX and GR activity than mitochondrial and and cytosolic fraction. Cu/Zn-SOD and Fe-SOD were observed in all the subcellular fractions; however the activities were higher in chloroplastic fractions for both the isoforms. Susceptibility of HD2687 to long term salinity stress seems to be due to less induction of SOD enzymes, no induction in chloroplastic and mitochondrial APOX and the cytosolic GR and decrease in chloroplastic and GR under salt stress resulting in higher oxidative stress in the form of H₂O₂ and TBARS contents (Sairam & Srivastava, 2002). Separation of the isoforms of leaf SOD, APX and CAT by polyacrylamide gel electrophoresis followed by in-gel activity staining revealed that the salt-induced activities of APX and CAT were the result of increases in activities of all the isoenzymes in *P. euphratica* (Wang *et al*, 2008).

Meloni *et al.* (2003) have shown that two cultivars of cotton, Guazuncho and Pora showed different response to salt stress. The superoxide dismutase (SOD: EC 1.15.1.1) activity in Pora increases with increase in the intensity of NaCl stress, but salt treatment has no significant effect on this enzyme activity in Guazuncho. The peroxidase (POD) and glutathione reductase (GR) activities showed similar trends under salt stress, in both cultivars. Net photosynthesis and stomatal conductance decreased in response to salt stress, but Pora showed a smaller reduction in photosynthesis than Guazuncho. Stomatal aperture limited leaf photosynthetic activity in the NaCl treated plants of both cultivars. However significant reduction in the leaf chlorophyll contents due to NaCl stress was observed only in Guazuncho. This suggests that salt tolerant cotton varieties may have a better protection against reactive oxygen species (ROS) by increasing the activity of antioxidant enzymes under salt stress. Wang *et al.* (2004) have shown that in *Suaeda salsa* L. Photosynthetic capacity was not decreased by NaCl treatment but seven SOD activity bands were detected in *S. salsa* leaf extracts, including a Mn-SOD and several isoforms of Fe-SOD and CuZn-SOD indicating that *S. salsa* possesses an effective antioxidative response system for avoiding oxidative damage. According to Badawi *et*

al. (2004) over-expression of ascorbate peroxidase in tobacco chloroplasts enhances the tolerance to salt stress and water deficit.

Photosynthesis: Photosynthetic response to drought and salinity stress is highly complex. It involves the interplay of limitations taking place at different sites of the cell/leaf and at different time scales in relation to plant development. The intensity, duration and rate of progression of the stress will influence plant responses to water scarcity and salinity, because these factors will dictate whether mitigation processes associated with acclimation will occur or not. Acclimation responses to salinity include synthesis of compatible solutes as well as adjustments in ion transport (such as uptake, extrusion and sequestration of ions). These responses will eventually lead to restoration of cellular homeostasis, detoxification and therefore survival under stress. (Chaves *et al.*, 2009).

Chloroplast is essential for photosynthetic function. Chloroplast biogenesis and photosynthesis are interrelated. Photosynthesis is highly affected by salinity stress. Saline irrigation in tropical spiny shrub *Lycium nodosum* causes more than 80% reduction in photosynthetic rate, carboxylation efficiency and stomatal conductance (Tizara *et al.*, 2003). According to Kovach *et al.* (1992) salt stressed plants of *Hygrophila polysperma* grew longer, had more total internodes, mature nodes, leaves and roots but have a slight lower level of photosynthesis than control plants.

Salt stress greatly enhanced phosphoenolpyruvate carboxylase-kinase (PEPCase-k) activity in leaves of sorghum. Salinization also increased the phosphorylation state of PEPCase-k in darkened sorghum leaves. This fact, together with increased malate production during the dark period, suggests a shift towards mixed C₄ plants and Crassulacean acid metabolism types of photosynthesis in response to salt stress. (Garcia-Maurino *et al.*, 2002). According to Adams *et al.* (1992) Common ice plant (*Mesembryanthemum crystallinum*) shows developmentally programmed inducibility for a switch from C₃-photosynthesis to CAM (Crassulacean Acid Metabolism). This metabolic switch is enhanced by salinity. CAM induction is dependent on organized leaf tissue and cannot be elicited by salt stress in suspension culture cells. It suggests that cells in culture mimic only the partly the stress response mechanism of intact plants and communication between different tissue is required to mount a complete environmental response. According to Iglesias *et al.* (2004) salt stress reduced total plant biomass by 27-38%, whereas potassium nitrate supplementation partially counteracted this effect by increasing dry matter and

new leaf area. Salinized *Carrizo citrange* had the greatest response to nitrate supplementation, whereas the effects on salinized *Cleopatra mandarin* and *C. macrophylla* were less apparent. Nitrogen and chlorophyll contents and photosynthetic activity also increased in leaves of the nitrate-supplemented salinized plants. In salinized plants, nitrate supplementation reduced leaf abscission, stimulated photosynthetic activity and increased growth of new leaves.

Effect of salt stress on photosynthesis and salt protection of plant is mediated by various enzymes. Polyamines have been suggested to play an important role in stress protection. However, attempts to determine the function of polyamines have been complicated by the fact that, dependent on the conditions, polyamine contents increase or decrease during stress. Kasinathan & Wingler (2004) have shown the accumulation of polyamines in control and mutated plants of *Arabidopsis thaliana* with reduced activity of arginine decarboxylase (EC 4.1.1.19). Polyamines accumulated in wild-type that were pre-treated with 100 mM NaCl before transfer to 125 mM NaCl, but not in plants that were directly transferred to 125 mM NaCl without prior treatment with 100 mM NaCl. This shows that polyamine accumulation depends on acclimation to salinity. The salt treatment that induced polyamine accumulation in wild-type plants did not lead to polyamine accumulation in mutants. Decreased fresh weight, chlorophyll content and photosynthetic efficiency indicated that mutants were more severely affected by salt stress than the wild type. Morant-Manceau et al. (2004) have shown that salinity decreased the net photosynthesis and transpiration rates in wheat as compared to control plants, but induced no significant change in chlorophyll a fluorescence parameters.

Photochemical parameters: The growth of the plant is reduced by salinity stress although plant species differ in their tolerance to salinity (Munns & Termaat, 1986). The decline in growth observed in many plants subjected to salinity stress is often associated with decrease in their photosynthetic capacity. PhotosystemII (PSII) plays a key role in the response of photosynthesis to environmental perturbations (Baker, 1991). The results of salinity stress on PSII photochemistry are conflicting. Some studies have shown that salt stress inhibits PSII activity (Bongi and Loreto, 1989; Mishra et al., 1991; Masojidek & Hall, 1992; Baelkhodja., 1994; Everard et al., 1994), whereas other studies have indicated that salt stress has no effects on PSII (Robinson et al., 1983; Brugnoli and Bjorkman, 1992; Morales et al., 1992; Abdia et al. ., 1999). Under natural conditions more than one environmental stresses co-occur frequently. Thus plants grown under natural conditions are subjected to the interaction of multiple environmental

stresses. It has been reported that responses of the plants to several simultaneous stresses are complex and usually not predictable by a single factor analysis and that a combination of different environmental stress factors can result in intensification, overlapping or antagonistic effects (Osmond et al., 1986). The effects of interaction of salinity stress and high light on PSII have shown that salinity stress predisposes PSII photoinhibitory damage (Mishra et al., 1991; Masojidek & Hall, 1992).

High salt concentration lead to stomatal closure, inhibition of PSII and CO₂ fixation, increased non-photochemical quenching in *A. thaliana*. However gas exchange and PSI was unaffected (Stepien and Johnson, 2009). Chl and carotenoids contents decreased in halophyte *Cakile maritime* at extreme salt concentration (Debez et al, 2008). However anthocyanin content increased with increasing salt concentration. Net photosynthetic rate (A), stomatal conductance, maximum quantum efficiency of PSII and quantum yield increased at lower salt concentration but decreased at higher (≥ 200 mM) salt concentration and it was accompanied with increase in non-photochemical quenching (Debez et al, 2008). Moderate salinity stress (200 mM) increases plant growth, PSII and carboxylation efficiency in halophyte *A. portulacoides* (Redondo-Gómez, 2007).

Salinity treatment shows no effects on PSII photochemistry, photochemical quenching (qP) and non-photochemical quenching (NPQ), but increases the resistance of photosystem II to heat stress in halophyte *Suaeda salsa*. Salt stress (400 mM NaCl) resulted in a significant accumulation of sodium and chloride in leaves of halophyte *Suaeda salsa* and neither effect on the maximal efficiency PSII (Φ PSII). Also *S.salsa* showed high resistance not only to salinity stress but also to photoinhibition even when treated with high salinity as high as 400 mM NaCl and exposed to full sunlight (Lu et al., 2002, 2003). According to Delfine et al. (1998) PSII is unaffected by the low level of salt accumulation in spinach leaves but is likely to be more sensitive than PSI when salt accumulation is high. Chen et al. (2004) have shown that NaCl treatment in *Rumex* leaves alone had no effect on the maximal photochemistry of PII or the polyphasic rise of chlorophyll fluorescence but prompted heat resistance of the O₂-evolving complex (OEC) and also causes lesser heat-induced decrease in photochemical quenching (qP), efficiency of excitation energy capture by open PSII reaction centers (F_v'/F_m'), and quantum yield of PSII electron transport (Φ PSII). According to Allakhvediv et al. (2000) salt stress modified heat stress on PSII photochemistry by causing lesser heat-induced decrease in

photochemical quenching (qP), efficiency of excitation energy capture by open PSII reaction centers (F_v'/F_m'), and quantum yield of PSII electron transport (Φ_{PSII}). According to Meloni et al. (2003) photochemical efficiency of PSII was not affected in either of the cotton cultivar with salt stress.

Effects of light and salt stress on photosystem II (PSII) in the cyanobacterium *Synechocystis* sp. PCC 6803 are completely different. Strong light induced photodamage to PSII, whereas salt stress inhibited the repair of the photodamaged PSII and did not accelerate damage to PSII directly. The combination of light and salt stress appeared to inactivate PSII very rapidly as a consequence of their synergistic effects. Radioactive labeling of cells revealed that salt stress inhibited the synthesis of proteins de novo and, in particular, the synthesis of the D1 protein (Allakhverdiev et al., 2002). In *Lycium nodosum* no evidence of chronic photoinhibition due to salinity was observed, since maximum quantum yield of PSII, F_v/F_m did not change due to salinity. Nevertheless, saline irrigation causes decrease in photochemical quenching (qP) coefficients relative to controls (Tizara et al., 2003). In *Spirulina platensis* cells Salinity stress induced a decrease in oxygen evolution activity, which correlated with the decrease in the quantum yield of PSII electron transport (Φ_{PSII}) and induced an increase in non-photochemical quenching (qN) and a decrease in photochemical quenching (qP) (Lu & Vonshak, 2002).

Materials & Methods

MATERIALS AND METHODS

PLANT MATERIALS AND CHEMICALS:

Plant Material

Rice (*Oryza sativa* L.) two cultivars CSR10 and Pusa Basmati1 (PB1) were used as an experimental material. Seeds of CSR10 were obtained from Central Soil Salinity Research Institute (C.S.S.R.I.) Karnal, Haryana and that of PB1 were obtained from Indian Agricultural Research Institute (I.A.R.I.), New Delhi.

Chemicals:

Chemicals were purchased from different companies like Sigma, Invitrogen, MDI, GE Health Care, Bio-Rad, Fluka, Qiagens, Gene, Qualigen, S.D.Fine and BDH etc.

PLANT GROWTH CONDITIONS:

The seeds without dehusking were washed with tap water several times and soaked in water for 24 h. Seeds were grown in vermiculite using half strength Murashige and Skoog (MS) liquid media having no agar and vitamins as nutrient solution. Seeds were grown first in complete darkness for five days at 28⁰C before giving NaCl salt stress. Salt stress was given in dark 12 h prior transfer to white fluorescent light of constant intensity of 100 μ moles photons $m^{-2} s^{-1}$, 28⁰C temperature and 75% relative humidity.

Nutrient Sol. used for Growth of Rice Seedlings:

For the growth of rice seedlings half strength Murashige and Skoog basal salt medium was prepared. Following is the composition of full strength MS medium used (Murashige and Skoog 1962).

Ammonium nitrate (NH_4NO_3) 1,650 mg/ml

Boric acid (H_3BO_3) 6.2 mg/ml

Calcium chloride ($CaCl_2 \cdot 2H_2O$) 440 mg/ml

Cobalt chloride ($CoCl_2 \cdot 6H_2O$) 0.025 mg/ml

Magnesium sulfate ($MgSO_4 \cdot 7H_2O$) 370 mg/ml

Cupric sulfate ($CuSO_4 \cdot 5H_2O$) 0.025 mg/ml

Potassium phosphate (KH_2PO_4) 170 mg/ml

Ferrous sulfate ($\text{FeSO}_4 \cdot 7\text{H}_2\text{O}$) 27.8 mg/ml
Potassium nitrate (KNO_3) 1,900 mg/ml
Manganese sulfate ($\text{MnSO}_4 \cdot 4\text{H}_2\text{O}$) 22.3 mg/ml
Potassium iodide (KI) 0.83 mg/ml
Sodium molybdate ($\text{Na}_2\text{MoO}_4 \cdot 2\text{H}_2\text{O}$) 0.25 mg/ml
Zinc sulfate ($\text{ZnSO}_4 \cdot 7\text{H}_2\text{O}$) 8.6 mg/ml
NaEDTA.2H₂O 37.2 mg/ml

Spectrophotometry:

Spectrophotometric studies were done on UV-160A (Shimadzu Corporation, Kyoto, Japan), Lambda-35 (Perkin Elmer) and Cary 300 Bio uv-visible (Varian) double-beam spectrophotometers.

Chl and carotenoid estimation:

Leaf seedlings were homogenized in 90% chilled ammonical acetone (10 ml) in a pre-chilled mortar and pestle under green safe light. For preparing 90% ammonical acetone, 1 N ammonia solution (7.48 ml in 100 ml distilled water) was prepared and then diluted ten times. This 0.1N ammonia solution was taken and acetone was added so as to obtain 90% ammonical solution. Three replicates were taken for each batch. Homogenate was centrifuged at 10,000 rpm for 10 min at 4°C. Supernatant was taken for estimating Chl and carotenoids. Absorbance was taken at 663 nm, 645 nm and 470 nm. Reference cuvette contained 90% ammonical acetone. Chl was calculated as described by Porra *et al.*, 1989 and carotenoids were calculated as described by Welburn and Lichenthaler, 1984.

$$\text{Chl a} = (14.21 \times \text{OD}_{663} - 3.01 \times \text{OD}_{645}) \text{ V/W}$$

$$\text{Chl b} = (25.23 \times \text{OD}_{645} - 5.16 \times \text{OD}_{663}) \text{ V/W}$$

$$\text{Chl (a+b)} = (9.05 \times \text{OD}_{663} + 22.2 \times \text{OD}_{645}) \text{ V/W}$$

$$\text{Carotenoids} = (1000 \times \text{OD}_{470} - \{3.27 \times \text{Chl a} - 1.04 \times \text{Chl b}\} / 5) \text{ V} / 227 \times \text{W}$$

Protein estimation:

Protein estimation was done according to Bradford (1976). Bradford reagent was prepared by mixing 40 mg of coomassie G in 20 ml of absolute alcohol with stirring for 20 min. To this 40 ml of orthophosphoric acid and 340 ml of double distilled water was added and the

solution was filtered twice using whatman filter paper no.1 and was stored in dark bottle. Standard curve was made by using different dilutions of BSA ranging from 1 to 10 µg / ml. To 950 µl of Bradford reagent 50 µl of water was added containing different concentrations of BSA, it was vortexed vigorously and OD was recorded immediately at 595nm.

Element Analysis:

Element analysis of sodium, potassium and calcium was done by inductively coupled plasma atomic emission spectrometry (ICP-AES). Leaf samples were harvested at desired time points and dried at 80°C for 48 h in oven and dry wt. was measured. Dried tissues were imbibed in 0.1N KNO₃ and kept overnight. Extract was filtered and element analysis was done.

GSA Content:

Leaf samples (200 mg) were taken, weighed and one set was processed immediately for GSA estimation and another set was incubated in 500 µM Gabaculine in MES 0.1 M, PH 7.0 for 4 h in light. The tissue were hand homogenized in prechilled mortar and pestle in 5.0 ml of 0.1N HCl and centrifuged in sorvall centrifuge in SS-34 at 10,000 rpm for 10 min. at 4°C. Supernatant was taken for estimation. Reaction mixture contained: 400 µl of supernatant, 360 µl of HCl 0.1N, 80 µl of 3-methyl-2-benzothiazolinonehydrazone (MBTH) 2%. This was then incubated in boiling water bath for two minutes. Boiling was done in capped tubes. This was then cooled rapidly Reference cuvette contains 400 µl of 0.1N HCl and no supernatant was added to it. After cooling 760 µl of distilled water and 40 µl of 20.% FeCl₃ was added, mixed by vortexing and read at 620 nm. Extinction coefficient used was 16.9 mM⁻¹ (Sood et al, 2005).

ALA Content:

Plant leaf samples (200 mg) were taken at different time points and one set was kept in 60 mM Levulinic acid for 4 h in light and other set was processed immediately for ALA estimation. Tissues were hand homogenized in a prechilled mortar and pestle in 5 ml of 1 M sodium acetate buffer (pH 4.6). The homogenate was centrifuged at 10,000 rpm (12,000g) for 10 min and supernatant was taken for assay. The assay mixture consisted of 1 ml of supernatant, 4 ml of distilled water, and 250 µl of acetylacetone. The assay medium was mixed properly and heated in a boiling water bath for 10 min. Then the extract was cooled at room temperature, and an equal volume of modified Ehrlich's reagent was added and vortexed for 2 min. After 10 min

of incubation, absorbance of the extract was measured at 555 nm. Standard curve was prepared from known conc. of ALA. ALA content was determined from the standard curve of ALA (Sood et al, 2005).

Pchlride Content:

Leaf tissues from plants were homogenized in 90% chilled ammonical acetone (10 ml) in a pre-chilled mortar and pestle. The homogenate was centrifuged in Sorvall centrifuge in SS 34 rotor at 10,000 rpm for 10 min at 4⁰C. Supernatant was taken and HEAR was prepared. For preparing HEAR, acetone extract of the sample was taken in a separating funnel and equal volume of ice cold hexane was added to it. This was mixed properly and the two layers were allowed to separate. Lower layer was taken. To this layer 1/3 rd volume of hexane was added. Again the two layers were mixed and allowed to separate. Lower layer was taken. This layer was hexane-extracted acetone-residue solvent mixture (HEAR). Emission spectra E440, E420, E400 from HEAR were recorded from 580 nm to 700 nm and were corrected for photomultiplier tube response. Pchlride contents were calculated (Tewari and Tripathy, 1998; Hukmani and Tripathy, 1992).

ALAD

Preparation of Ehrlich reagent: Ehrlich reagent was prepared as described by Mauzerall and Granick (1956). For preparing Ehrlich reagent 2 g of dimethyl amino benzaldehyde (DMAB) was dissolved in 30 ml of glacial acetic acid and 16 ml of 70% perchloric acid (4N) was added. Final volume was made to 50.0 ml with glacial acetic acid.

ALAD assay was done as described by Tiwari and Tripathy, 1998. Three replicates of 200 mg leaves were taken from seedlings grown in white light. Leaves were homogenized at 4⁰C in 5 ml of 0.1M tris pH 7.6, 0.01 M 2-mercaptoethanol in mortar and pestle. The homogenate was centrifuged at 10,000 rpm for 10 min. at 4⁰C in sorvall SS-34 rotor. Supernatant was taken for enzyme assay. Reaction mixture contained tris 300 µmoles pH 8.5, ALA 12 µmoles, 2-mercaptoethanol 15 µmoles, KCL 150 µmoles. To this 0.5 ml protein was added. Final volume was made to 3.0 ml with distilled water. Reaction mixture was incubated at 37⁰C for one h and 1.0 ml of 20 % TCA with 0.1M mercuric chloride was added to stop the reaction. This was then centrifuged at 5000 rpm for 10 min. in sorvall SS-34 rotor to settle down precipitated protein. Supernatant was taken. 1.0 ml of aliquot was taken and 1.0 ml of Ehrlich reagent was added to it.

Absorbance was taken at 555 nm. For calculations absorption coefficient was $6.2 \times 10^4 \text{ M}^{-1}$ (Tiwari and Tripathy, 1998). Reference cuvette contained water and Ehrlich in ratio of 1:1.

PBGD

Leaves tissue (250 mg) were taken and enzyme was assayed as described by (Tiwari and Tripathy, 1998). Leaves were hand homogenized in mortar and pestle in 5.0 ml of phosphate buffer (pH 8.0) and 0.6 mM EDTA at 4°C and passed through 4 layers of cheesecloth. Homogenate was centrifuged at 10,000 rpm for 10 min in sorvall SS-34 rotor at 4°C. Supernatant was taken for assay. Enzyme activity was assayed as amount of porphyrin synthesized in 3.0 ml of reaction mixture having following composition as final concentrations: - Freshly prepared 0.6 ml PBG (550 μM), 90 μl EDTA solution (0.6 mM), 428 μl phosphate buffer (pH 8.0), 1.8 ml of enzyme extract and 82 μl distilled water. In blank distilled water was added instead of enzyme. The reaction mixture was incubated at 37°C for 1 h. 750 μl of this reaction mixture was taken to which 1.7 ml of TCA (7.1%) was added to stop the reaction. Centrifuge at 10,000 rpm for 10 min in sorvall SS-34 at 4°C. Then 10 μl of iodine solution (1 %) was added and incubated for 5 min at 37°C. Finally 20 μl of freshly prepared Sodium thiosulphate (2 %) was added to reduce iodine. Absorbance was measured at 406 nm. Extinction coefficient used at 406 nm was $5.48 \times 10^5 \text{ M}^{-1} \text{ cm}^{-1}$. Absorbance of all samples was taken from 400-700 nm to check for a peak at 405.5 or 406 nm.

Protoporphyrinogen oxidase

Preparation of sodium amalgam: Sodium amalgam was prepared as described by Vogel (1974). 3 % sodium amalgam solution was prepared 0.55 g sodium metal was heated slowly with continuous shaking. Once both were mixed properly, amalgam was taken out in a pestle and mortar and grounded to a fine powder. This process was done very fast, as sodium amalgam is hygroscopic. Whole process was done in presence of N_2 gas. Sodium amalgam was prepared freshly before use.

Preparation of proto IX solution: 1 mg of proto IX was dissolved in 0.1N KOH in 20 % ethanol.

Reduction of proto IX: Porphyrin is reduced with freshly grounded 3 % sodium amalgam (1mg / ml solution) under N_2 gas to protoporphyrinogen. This can be seen as color of proto IX solution changes from pink to colorless. The solution was centrifuged and pH was adjusted immediately

to 7.5-7.8 with 40 % orthophosphoric acid. After adjusting the pH centrifugation was done and the supernatant was used immediately as substrate. This process was done slowly and in dark.

Assay of protoporphyrinogen oxidase: Assay was done as described by Tiwari and Tripathy, 1998. Leaves were taken from 5 day old seedlings and hand homogenized in prechilled mortar and pestle in isolation buffer containing sucrose 0.5 M, Hepes 20 mM pH 7.7, MgCl₂ 1 mM, EDTA 1 mM, BSA 0.2 % and passed through 8 layers of cheese cloth and 1 layer of miracloth. Homogenate was centrifuged at 4000 rpm for 7 min. at 4⁰C in sorvall SS-34 rotor. Pellet consisting of plastids was suspended in lysis buffer containing tris 0.01 M pH 7, MgCl₂ 20 mM, EDTA 2.5 mM and kept on ice for 10 min. This was then centrifuged at 10,000 rpm for 10 min. at 4⁰ C in sorvall SS-34 rotor. Supernatant was taken for assay. Reaction mixture contained 100 µl of reaction buffer (containing final concentration of tris 0.01 M pH 7.7, MgCl₂ 20 mM, EDTA 2.5 mM, ATP 6 mM and DTT 5 mM), 55 µl of protogen, 45 µl of distilled water and 100 µl of chloroplast suspension. Blank contained heat killed enzyme. Heat killed enzyme was obtained by keeping supernatant in boiling water bath for 10 min. Reaction mixture was incubated at room temperature (30⁰C) for 1 hour. Reaction was stopped by adding 1.7 ml of 90 % ammoniacal acetone. Samples were centrifuged and supernatant was taken for fluorimetry. HEAR was prepared as described earlier. Emission spectra were recorded from 600nm-700nm at 400 nm and 440 nm excitation. Calculations were done as described by (Tiwari and Tripathy 1998, 1999; Hukmani and Tripathy 1992).

Coproporphyrinogen oxidase

For estimation of coprogen oxidase oxidized coporphyrinogen IX was reduced with 3 % sodium amalgam as described before. Plastids were isolated from leaves excised from 5-day-old seedlings grown under different light regimes. Plastids were suspended in lysis buffer containing 0.01 M tris pH 7.7, 20 mM MgCl₂, 2.5 mM EDTA and kept on ice for 10 min. This was then centrifuged at 5000 rpm for 5 min at 4⁰C in sorvall SS-34 rotor. Supernatant was taken for assay. Reaction mixture for coprogen oxidase assay consisted of 100 µl of reaction buffer containing final concentrations of 0.05 M tris pH 7.7, 20 mM MgCl₂, 2.5 mM EDTA, 6 mM ATP and 5 mM DTT, 55 µl of coprogen, 45 µl of distilled water and 100 µl of enzyme supernatant. Blank contained heat killed enzyme. Heat killed enzyme was obtained by keeping supernatant in

The relative decline is more in PB1 as comparative to that of CSR10. Non-photochemical quenching (qN) increased in response to increasing salt concentration and duration in both of the cultivars. However the relative increase is more in PB1 than CSR10.

Whole chain activity decreased in response to increasing salt concentration in both of the cultivars. However the relative decline in whole chain activity is more in PB1 as comparative to that of CSR10 at any salt concentration. PSI activity is partially affected in response to salt stress in both the cultivars. PSII activity declined in response to increasing salt stress in both of the cultivars. However the relative decline in PSII activity was more in PB1 as comparative to that of CSR10.

Light saturation curve of Photosystem II shows that both initial slope at low light intensity and saturated electron transport were affected during salt stress in both of the cultivars. Percent inhibition of PSII was more in salt sensitive cultivar PB1 as comparative to that of CSR10.

Room temperature spectra shows that relative decrease in PSII fluorescence at 684 was more in PB1 than CSR10 in response to salt stress. To understand the structural organization of thylakoid membranes low temperature spectra were observed in response to salt stress in CSR10 and PB1 cultivars. In the presence of Mg^{2+} LHCII is more close to PSII so the F686/F740 increases in both CSR10 and PB1.

Protein expression of some of the PSII proteins such as D₁, D₂, LHCPII, Lhcb1, Lhcb2, Lhcb4 and OEC33 decreased in response to increasing salt stress in both of the cultivars. However the relative decline in PB1 is higher than CSR10. Cytb559 protein expression decreased in response to salt stress. Photosystem I (PSI) proteins PSI sub III and PSI sub V expression decreased in response to increasing salt stress in both of the cultivars. However the relative decline in their protein expression is higher in PB1 than CSR10. Among the Cytbf complex subunits protein expression of Cytf, Cytb and Rieske Fe-S decreased in response to salt stress whereas protein expression of Subunit IV remained almost unchanged.

Gene expressions of few genes encoding photosynthetic proteins such as PsbA, PsbD decreased in response to salt stress in both of the cultivars. However the relative decline was

ammonical acetone and their Pchlde contents were estimated. The difference between the net amount of Pchlde synthesized in dark and the same remaining after 15 min of light treatment is the amount of Pchlde phototransformed from Pchlde to Chlide.

POR activity was measured as % of phototransformation of Pchlde to Chlide as follows: [(Net amount of Pchlde synthesized in 6h of dark period – pchlde content remaining after 15 min of light exposure) / Net amount of Pchlde synthesized in 6 h of dark period] x 100.

Isolation of total RNA by TRI reagent (Sigma) method

Total RNA was isolated from different tissues by TRI reagent (Sigma) according to manufacturer's instruction. All the glassware and mortar pestles used during RNA isolation was baked for 3 h at 230⁰C, the plastic wares were treated with DEPC and then autoclaved to avoid the possible contamination of RNAase. The gel apparatus used to check the quality of RNA was treated with H₂O₂ for 1-2 h, washed several times with DEPC water.

Tissues (100 mg) were taken and homogenized in liquid nitrogen in mortar and pestle. After the evaporation of liquid nitrogen, 1 ml of TRI reagent was added to powdered tissues and homogenized again. The TRI reagent containing the powdered tissues was transferred to 1.5 ml centrifuge tube and the insoluble material was separated from the homogenate by centrifugation at 11,000 g for 10 min at 4⁰C in a microfuge. The supernatant was transferred into a fresh Eppendorf tube and to this 0.2 ml chloroform was added and mixed vigorously. The sample was centrifuged at 12,000 rpm for 15 min at 4⁰C and the upper aqueous phase was transferred to a fresh Eppendorf tube. The RNA was precipitated from the aqueous phase by mixing with 0.5 ml isopropanol followed by centrifugation at 12,000 rpm for 15 min. The pellet was washed with 75 % ethanol, dried and dissolved in minimal volume of RNase free sterile water.

RNA gel

After isolation of RNA, the quality was checked by running 1.2% formaldehyde denaturing agarose gel. The constituents of the formaldehyde gel:

5X formaldehyde gel running buffer

MOPS	0.1M (pH 7.0)
Sodium acetate	40mM
EDTA	5mM (pH 8.0)
Formaldehyde	2.2M

Ethidium bromide	10mg / ml
Sample buffer	
10X MOPS	1ml
Formaldehyde	1.8ml
Formamide	0.5ml
DEPC-water	2.2ml

RNA gel loading dye:

Glycerol	50%
EDTA	1mM (pH 8.0)
Bromophenol blue	0.25%
Xylene	0.25%

1.2% agarose gel was prepared by dissolving appropriate amount of agarose in water (heating the agarose in water and then cooling it to 60°C). To it, 5X formaldehyde gel-running buffer and formaldehyde were added to give final concentrations of 1X and 2.2 M respectively. 0.25 µg/ml of ethidium bromide was added to the gel. Gel was cast in acrylic tray in chemical hood and allowed to polymerize for 30 min-1 h.

To load RNA, 25µg RNA was taken in appropriate volume. To this 2 volumes of sample buffer was added and this was then incubated at 65°C for 15 min. To this 2µl gel loading dye was added, mixed and centrifuged at 12,000 rpm for 2 min in Beckman microfuge. The RNA was then loaded on the gel.

Before loading the samples, the gel was pre-run at 5 V/cm for 5 min in 1X formaldehyde gel-running buffer. After samples were loaded in different lanes of the gel, the gel was run at 5 V/cm for 2-3 h. After run was complete, the gel was kept on UV-transilluminator to visualize the rRNA bands in the gel.

DNase I treatment of total RNA:

To remove the traces of genomic DNA, 5 unit of RNase free DNase I was added to total RNA in 10 mM Tris-Cl, pH 8.3, 50 mM KCl, 1.5 mM MgCl₂ and incubated for 10 min at 37°C. After this, DNase I was inactivated by heating at 75°C and extracted twice with phenol: chloroform: Isoamyl alcohol (24:24:1). RNA was precipitated from the aqueous phase by sodium

acetate, pH 4.8 and ethanol, washed twice with 75% ethanol, vacuum dried and finally dissolved in DEPC-treated water. The pure RNA was either used immediately or stored at -80°C.

First strand cDNA synthesis:

4µg of RNA was taken and first strand cDNA synthesis was carried out using oligo-dT₍₂₀₎ (1µg), by using first strand cDNA synthesis kit from invitrogen, following manufacturer's protocol. After the first strand synthesis the reaction was terminated by heat inactivation at 70°C for 15 minutes followed by addition of 4 unit of RNase H (Amersham pharmacia) to remove RNA.

Semi-quantitative RT-PCR:

The reaction mixture (20 µl) contained 50 ng DNA template, 150 ng (30 pmoles) of each primer, 8 µl of 1.25 mM dNTPs, 5 µl of 10X Taq buffer and 2.5 units of Taq polymerase. The reaction condition of PCR consisted of denaturation (94°C), annealing (varies from gene to gene) and extension (72°C) for 1 min. per 1 kb pair to be amplified. PCR was performed for 27-30 cycles within a linear range of amplification of *GSAT*, *ChII*, *GluTR*, *Protox*, *PsbA*, *PsbD* and *Actin11*. The number of each cycles and annealing temperatures were optimized for each specific primer pairs. Ten ml of the PCR products were loaded and separated on 1% agarose Tris-acetate EDTA gel and seen by ethidium bromide staining.

Northern hybridization:

Total RNA was fractionated on 1.2% formaldehyde denaturing agarose gel as described above (Sambrook *et al.*, 1989). Gel was electrophoresed for 2-3 h and after completion of the run, the gel was rinsed in DEPC treated water and equilibrated with 5X SSC for 10 min. Nylon membrane (Amersham Hybond NX) and Whatman paper 3 MM equal to the size of gel were cut and were in 5X SSC along with the gel. RNA was transferred to nylon membrane by capillary transfer in 5X SSC for 16 h. 5X SSC was taken in the Borosil tray and a glass plate was placed on it. A wick of Whatman paper 3mm was placed on the glass plate with both of its ends dipped in 5X SSC. On the wick, a piece of Whatman paper was placed followed by gel and nylon membrane. A piece of Whatman paper was then placed on nylon membrane. Air bubbles between the gel and the membrane were removed using a glass rod. A stack of blotting sheets (5-8 cm height) was placed on this followed by a weight of 0.5 kg. RNA was then allowed to

transfer by capillary action for 16 h. Once the transfer was over, wells on membrane were marked and the membrane was washed in 2X SSC to remove any agarose. The membrane was then allowed to dry and cross-linked in UV-cross linker at 0.15 J/sq.cm. Membrane was then stored at 4°C in a plastic bag till further use.

The membrane was pre-hybridized for 6-8 h at 65°C in buffer containing 5 X SSC, 5X Denhardt reagent (0.5% Ficoll, 0.5% PVP, 0.5% BSA), 50mM sodium phosphate (pH 7.2), 2.5mM EDTA, 0.4% SDS and 100 µg/ ml denatured salmon sperm DNA and 5% dextran sulphate. Thereafter, to the prehybridization solution radiolabelled probe (pre- denatured by boiling for 10 min) was added. After 16- 18 h of incubation at 65°C in the hybridization solution, the membrane was washed twice with 2X SSC, 0.1 % SDS at room temperature for 5 min, twice with 0.5X SSC, 0.1% SDS at 65 °C for 15 min and twice with 2X SSC at room temperature for 5 min. The membrane was then exposed for autoradiography.

Preparation of probe by random primer labeling method:

[Megaprime™ DNA labelling system RPN 1605 (Amersham life science)]

Twenty-five ng of DNA (PCR amplified) and 5 µl of primer were taken in an eppendorf. After denaturation by heating to 95–100°C for 5 min, brief spin was given. Then dNTPs (4 µl each) were added without dCTP, which was used as label, 5 µl of reaction buffer, 5 µl of $\alpha^{32}\text{P}$ dCTP and 2 µl of enzyme and appropriate volume of water was added to make total volume of 50 µl. The contents were mixed gently by pipetting up and down and capped the tube. The reaction mixture was incubated at 37 °C for 1 h and stopped by adding of 5 µl of 0.2 M EDTA. Before use in a hybridization reaction the labelled DNA was denatured by heating to 100°C for 5 min and chilled on ice.

Preparation of probe by nick translation method:

[Nick translation kit N 5000 (Amersham life science)]

50 ng of total DNA was taken in an eppendorf and heated to 95-100°C for 5 min and cooled on ice immediately. A brief spin was given and 10 µl of nucleotide buffer, 5 µl ($\alpha^{32}\text{P}$) dCTP, and 5 µl of enzyme solution was added and kept on 15°C for 1 hr, reaction was stopped by adding 5 µl of 0.2 M EDTA pH 8.0. The labeled probe was denatured before using.

Table-2. Primers used in this study

Name	Sequence	T_m
<i>GSAT</i>	F: 5' GGAAACCCTCTAGCTATGACTGC 3'	64.0
	R: 5' CACACATCTCATGTCCAGTTTTC 3'	63.3
<i>GluTR</i>	F: 5' ATCTGCTGGGCTTGACTCTTTGG 3'	69.5
	R: 5' TCAGTTCTGGGACTTCTCCACCTTC 3'	69.5
<i>ALAD</i>	F: 5' TCAGGCCTCTTGACTTGACAA 3'	64.9
	R: 5' CTCCAGCTTTGATCATGGAGTACT 3'	64.4
<i>PBGD</i>	F: 5' CATCTGTATTGTCAGTGGACGAA 3'	63.7
	R: 5' TCTCTTTCACATGCAACAGCTAA 3'	63.6
<i>UROD</i>	F: 5' TGATTTTGAGGAGTTTAGCTTGC 3'	63.2
	R: 5' GCTAACAACATCAACACCTGTCA 3'	63.8
<i>PPXI</i>	F: 5' AGGGCGTGAGGAGTCGGTG 3'	70.1
	R: 5' TCACTTGTAGGCGTACTTGGTCAAGTAGTC 3'	69.3
<i>PORB</i>	F: 5' CAGAAGTACATCACCAAGGGCTA 3'	64.0
	R: 5' GAGTTGTTGTTCCAGCTCCAGTA 3'	64.3
<i>ChlP</i>	F: 5' TCCTACTTGGAGGAACAAGACAA 3'	63.7
	R: 5' CCCTCTTAATCCATCAACATTCA 3'	63.6
<i>hemH</i>	F: 5' CTATGCATCCATTGGTGGTGGTT 3'	68.5
	R: 5' TACGTGGAACAAAGGCAGGATG 3'	67.9
<i>PsbA</i>	F: 5' ATTACTTCCATACCAAGATTAGCACGGTTG 3'	69.3
	R: 5' ATGACTGCAATTTTAGAGAGACGCGA 3'	69.4
<i>PsbD</i>	F: 5' ATGACTATAGCCCTTGGTAGAGTTACTAAAGAAGAAA 3'	68.1
	R: 5' TTAAAGAGCGTTTCCACGTGGTAGAA 3'	68.9
<i>PetD</i>	F: 5' ATGGGAGTAACAAAGAAACCTGACTTAAAC 3'	66.6
	R: 5' AGTTAAGGATTTTCAATGGGTAATGTTG 3'	66.1
<i>SodCc2</i>	F: 5' ATGGTGAAGGCTGTTGCTG 3'	63.9
	R: 5' CTAACCCTGGAGTCCGATGAT 3'	64.0
<i>CatA</i>	F: 5' ATGGATCCTTGCAAGTTCCG 3'	66.1

	R5:’ TCACATGCTTGGCTTCACG 3’	66.2
<i>GRase</i>	F5:’ ATGGCTAGGAAGAGGCTCAAG 3’	62.2
	R5:’ CTACAAGTTTGTCTTTGGCTTGG 3’	63.6
<i>OsAPx2</i>	F5:’ AGGTGAGTTGAGTTGGGGATT 3’	63.6
	R5:’ TCATCCATCAAGGGGAATTC 3’	63.6
<i>OsDREB2</i>	F5:’ GATTGCTCCGTGCAAGTGA 3’	65.2
	R5:’ ACCCATCATCTCCCTCTTGG 3’	65.1
<i>OsCIPK15</i>	F5:’ ATGGAGAGTAGAGGGAAGATTCTAATG 3’	63.6
	R5:’ CTAGGCCAAGACAATGTCCTTC 3’	63.7
<i>OsRab7</i>	F5:’ GACGTCCCTGATGAACCAATAT 3’	63.7
	R5:’ ATTCTTTACAATGCACTGGAAAGC 3’	64.1
<i>ACT11</i>	F: 5’ CAGCCACACTGTCCCCATCTA 3’	62.0
	R: 5’ AGCAAGGTCGAGACGAAGGA 3’	62.0
<i>Oligo dT</i>	5’ TTTTTTTTTTTTTTTTTTTTTTTT 3’	39.1

Table-3. cDNA clones used for Northern which were ordered from RGRC (Rice Genome Resource Centre).

Gene	Clone name	Clone I.D.
<i>PBGD</i>	001-035-G03	103261
<i>UROD</i>	J023065H03	206693
<i>CAO</i>	001-047-B05	105143

Purification of DNA fragments from agarose gel:

PCR amplified product were electrophoresed on 1% agarose gel (Agarose, MB, Pharmacia). The desired fragments were identified using standard molecular weight marker (1 kb ladder or Lambda DNA digested with *Hind* III) and purified using the following technique.

Qiaquick/ GFX gel extraction column

To the excised pieces of agarose gel containing DNA fragment 500 µl of captured buffer (GFX gel extraction kit, Amersham pharmacia, England) was added and dissolved by heating to

55°C for 10 min. The mixture was loaded onto GFX spin column and spun briefly in a microfuge (maximum speed, 30 sec). The flow through was discarded and 500 µl of wash buffer was added to the spun column. The column was again centrifuged at maximum speed for 30 sec. Purified DNA fragment was eluted with 50 µl of 10 mM Tris- Cl, pH 8.0.

Spectrophotometric estimation of nucleic acid

The quantity and quality of the nucleic acid was determined by measuring the absorbance at 260 nm and 280 nm. The amount was calculated taking $1.0 A_{260} = 50 \mu\text{g/ml}$ for DNA and $1.0 A_{260} = 40 \mu\text{g}$ for RNA. The purity of the nucleic acid was determined by calculating the ratio A_{260}/A_{280} for each sample.

Transmission electron microscopy

Leaves samples from control and salt stressed rice plants were taken at different time h and vacuum infiltrated with 2.5% glutaraldehyde solution for 30 minutes. After fixation the seedlings were kept for overnight in the same solution (Graham and Karnovsky, 1965). The fixation solution was discarded and to that 0.1M sodium-phosphate buffer (pH 7.0) was added. Then tissue was kept in secondary fixative containing 1% OsO₄. Fixation was done by immersing the tissue in fixative at 4°C for 2-4 h. Tissue was washed with 0.1M PO₄ buffer, dehydration was done, which involved following steps:

- 1) 30% acetone twice for 15 minutes each time.
- 2) 50% acetone twice for 15 minutes each time.
- 3) 70% acetone twice for 15 minutes each time.
- 4) 80% acetone twice for 15 minutes each time.
- 5) 90% acetone twice for 15 minutes each time.
- 6) 95% acetone twice for 15 minutes each time.
- 7) Dry acetone twice for 15 minutes each time.
- 8) Dry acetone twice for 30 minutes each time.

All these steps were done at room temperature. For clearing tissues of acetone, epoxy propane or xylene was used twice for 30 minutes at room temperature and infiltration was done in a resin containing araldite and toluene in following ratios:

- 1) 1 part of araldite + 3 parts of toluene.
- 2) 2 parts of araldite + 2 parts of toluene.

3) 3 parts of araldite + 1 part of toluene.

For embedding araldite cy212 embedding medium was prepared. After embedding, the liquid araldite was polymerized in a gradual process by keeping blocks at 50°C for 12-24 h and then at 60°C for 24-48 h. After this, sectioning was done using ultramicrotomes. These ultra thin sections were then stained in uranyl acetate. Saturated solution of uranyl acetate was prepared in 50% ethanol. This was mixed vigorously and centrifuged to allow the excess of uranyl acetate to settle down. For staining small amount of uranyl acetate was taken in a clean watch glass. Grid containing section was placed on to the stain. Staining was done in dark for 10-15 min. Each grid was then washed in 50% ethanol twice and distilled water twice with continuous agitation. This was then dried carefully on filter paper. After this sections were viewed in a Transmission Electron Microscope (Phillips CM-10) at the Electron Microscopy Facility, All India Institute of Medical Sciences (AIIMS), New Delhi.

Spectrofluorometry

Fluorescence spectra were recorded in ratio mode in a computer-driven SLM AMINCO 8000 spectrofluorometer having a photon-counting device. Rhodamine B was used in the reference channels as a quantum counter. A tetraphenylbutadiene block was used to adjust the voltage in the sample as well as in the reference channels to 20,000 counts per second at excitation and emission wavelengths of 348 and 422 nm, respectively.

Fluorescence spectra of thylakoids

Room temperature (298 K) and low temperature (77 K) fluorescence emission spectra of thylakoids were recorded in SLM AMINCO 8000 spectrofluorometer having a photon-counting device. The excitation and emission slit widths were 4 nm. For room temperature spectra excitation slit width was 8 nm. Spectra were corrected for instrument response in case of only room temperature spectra and not in low temperature spectra. Plants leaves were ground in HEPES-NaOH buffer pH 7.6 (20 mM HEPES, 10 mM NaCl, 0.4 M sucrose, 0.5 % BSA) and then centrifuged at 5,000 rpm for 7 min, pellet was suspended in 5 mM HEPES-NaOH buffer containing 0 or 4 mM MgCl₂. Room temperature spectra were recorded using thylakoids equivalent to 3 µg / ml Chl at excitation wavelength of 440 nm and emission wavelength of 620-750 nm. For liquid nitrogen spectra thylakoids equivalent to 3 mg/ ml Chl containing 25 %

glycerol was used and spectra were monitored at excitation wavelength of 440 nm and emission wavelength of 620-780 nm.

Fluorescence spectra of leaves for shibata shift

Low temperature spectra of leaves were recorded from etiolated leaves after 48 h of salt stress at excitation wavelength of 440 nm and emission wavelength of 600-740 nm. Spectra were not corrected for photomultiplier tube response. For low temperature spectra. Salt stress was given in dark to five day old rice seedlings. After 48 h of salt stress leaves were excised and put in liquid nitrogen before red flash and after red flash following dark incubation of 0, 30 min and 1 h. Then spectra were recorded.

Chlorophyll a Fluorescence Measurements

All measurements of chlorophyll (Chl) a fluorescence were performed with a portable PAM 2100 fluorometer (Walz, Effeltech, Germany). Before each measurement, the sample leaf was dark-adapted for 20 min (Demmig et al., 1987) in respective salt stress regimes with leaf-clips provided by the Walz Company. The angle and distance from the leaf surface to the end of the optic fiber cable were kept constant during the experiments. Chl a fluorescence was detected by a photodiode (BPY 12; Siemens, Munich, Germany) that was shielded by a long-pass far-red filter (RG9; Southbridge, MA, USA) and a heat filter. To determine the initial fluorescence, F_0 , the weak measuring light was turned on and F_0 was recorded. Then the leaf sample was exposed to a 0.8 s saturation flash of approximately $3000 \mu \text{ moles photons m}^{-2} \text{ s}^{-1}$ to obtain the maximal fluorescence, F_m . Optimum quantum efficiency of PSII was calculated as $F_v/F_m = (F_m - F_0) / F_m$. The quantum yield of PSII was calculated from Chl a fluorescence as $F_v'/F_m' = (F_m' - F) / F_m'$ where F_m' and F are maximum fluorescence yield reached in a pulse of saturating light when the sample is pre-illuminated and measured fluorescence yield at any given time respectively (Genty et al., 1989). Using the values of the quantum yield of PSII, the electron transport rate (ETR), expressed in $\mu \text{ moles electrons m}^{-2} \text{ s}^{-1}$, was estimated using the equation, $\text{ETR} = \text{calculated yield of PSII} \times \text{PAR} \times 0.5 \times 0.84$ where PAR corresponds to the flux density of the incident photosynthetically active radiation, measured in $\mu \text{ moles photons m}^{-2} \text{ s}^{-1}$, 0.5 is based on the assumption that the incident light is equally distributed between PSII and PSI, and 0.84 is for the assumed fractional absorption of light by the leaf. Non-photochemical quenching (qN) was calculated as $1 - [(F' - F_0') / (F_m - F_0)]$. Photochemical quenching (qP) was calculated as $(F_m' -$

$F_t)/(F_m'-F_0')$. All measurements of F_0 were performed with the measuring beam set to a frequency of 0.6 KHz, whereas all measurements of F_m were performed with the saturation flash automatically switching to 20 KHz.

Isolation of thylakoid membranes:

Thylakoid membranes were isolated as described by Chakraborty and Tripathy, 1992. Around 5 g of leaves were homogenised in 40 ml of isolation buffer containing 0.4 M sorbitol, 0.05 M Hepes / KOH (pH 7.3), 1mM $MgCl_2$, and 1mM EDTA at 4°C and in green safe light. Homogenate was passed through 8 layers of cheese cloth and 1 layer of Mira cloth and centrifuged at 4000 rpm for 7 min. Pellet containing crude fraction of thylakoid membranes was suspended in suspension buffer containing sorbitol 0.4 M, tris 0.05 M, $MgCl_2$ 1 mM and EDTA 1 mM. For isolating plastidic membranes pellet was taken and suspended in 1 ml of TE buffer containing 0.01M tris pH 7.5 and 1mM EDTA. This was then kept on ice for 10-15 min and centrifuged at 4000 rpm for 7 min. Pelleted thylakoid membranes were resuspended in suspension buffer.

Polyacrylamide gel electrophoresis of proteins (SDS-PAGE):

SDS-PAGE was carried out according to Laemmli, 1970. The chemicals and solutions used for SDS-PAGE:

Acrylamide (30%):

Acrylamide	58.4g
Bis-acrylamide	1.6g

Distilled water added to make vol. 200 ml

This stock solution was filtered and stored at 4°C in an amber bottle.

Separating gel buffer (4X):

Tris (1.5M)	36.3g
-------------	-------

Final vol. made to 200 ml with distilled water after adjusting pH to 8.8 with HCl. Stored at 4°C.

Stacking gel buffer (4X):

Tris (0.5M)	6.0g
-------------	------

Final vol. made to 100ml with distilled water after adjusting pH to 6.8 with HCl. Stored at 4°C.

SDS (10%):

SDS	10g
-----	-----

Vol. made to 100ml with distilled water and stored at room temperature.

Sample buffer (2X):

Tris Cl (0.125M, pH 6.8)

2.5ml of stacking gel buffer

SDS (4%) 4ml of 10% SDS

β -mercaptoethanol (10%) 1ml

Glycerol (20%) 2ml

Distilled water added to make up the vol. to 10ml.

Tank buffer (4X):

Tris (0.025M) 15g

Glycine (0.192M) 72g

SDS (0.1%) 40ml of 10% SDS

Distilled water added to make up the vol. to 1L.

APS 10%: Always prepared fresh.

TEMED used from stock as such

β -mercaptoethanol used from stock as such

<u>Recipes</u>	<u>12.5% Separating gel</u>	<u>4.5% Stacking gel</u>
Monomer stock solution	10.0ml	1.7ml
Buffer	6.0ml (pH 8.8)	2.5ml (pH 6.8)
SDS (10%)	0.24ml	1.0ml
Water	7.6ml	4.8ml
TEMED	10 μ l	5 μ l
APS (10%)	200 μ l	200 μ l

SDS-PAGE was carried out in a vertical gel electrophoresis apparatus (regular size) (ATTO Corp., Japan) according to Laemmli, 1970. Gels were prepared and electrophoresed under reducing and denaturing conditions in presence of β -ME and SDS. Protein samples (50 μ g) were prepared by mixing with $\frac{1}{2}$ volumes of 2X sample buffer (constituents of sample buffer is mentioned above). The samples were boiled for 3 min in a water bath and centrifuged at 13000 rpm for 2 min at room temperature. The supernatant was loaded on the stacking gel. Gels were

run either at a constant voltage (100V) or a constant current (20 mA). After electrophoresis, the gels were stained with Coomassie blue R 250 (CBB R 250) for visualization of the proteins.

Staining with coomassie brilliant blue R 250 (CBB R 250):

Fixing solution: 40% methanol, 10% acetic acid in double distilled water

Staining solution: CBB (0.05%) in 50% methanol and 5% acetic acid

CBB was dissolved in methanol. Acetic acid was added, followed by Distilled water to make the volume 1L.

Destaining solution: 5% methanol, 7.5% acetic acid in double distilled water.

The gel, after electrophoresis, was incubated in 10 volumes of fixing solution for 20 min on a gyratory shaker. The gel was stained in 5 vol of CBB for 4 h to overnight on the shaker. After staining, stain was removed; gel was rinsed with double distilled water and was then left in 20 vol destaining solution for 2-3 h. The destaining solution was replaced 2-3 times at 1h interval, until the background was clear. The gel was preserved in 7% acetic acid in distilled water.

Western blotting:

Western blot analysis was done according to Towbin *et al.*, 1979. The chemicals and solutions used for western analysis:

TBS (Tris buffered saline):

Tris (25mM) 3.03g (pH 7.4)

NaCl (136mM) 7.95g

KCl 0.2g

Distilled water added to make up the vol. to 1L.

TBST buffer: TBS + 0.05% Tween 20

Blocking solution: TBST + 4% BSA

Transfer buffer:

Tris (0.1M, pH 8.3) 6.05g

Glycine (0.192M) 7.2g

5% Methanol (v/v) 25ml

Distilled water added to make up the vol to 500ml.

Alkaline phosphatase (AP) buffer:

Tris HCl (100mM, pH 9.5)	1.211g
NaCl (100mM)	0.5844g
MgCl ₂ (5mM)	0.10165g

Distilled water added to make up the vol. to 100ml.

AP colour development solution:

AP buffer	10ml
NBT sol	66 μ l
BCIP [®]	33 μ l
Ponceau S:	0.1% (w/v) in 1% acetic acid (v/v)

Transfer of proteins from polyacrylamide gels to nitrocellulose (NC) membranes was carried out in a semi-dry transblot apparatus (ATTO Corp., Japan), as per the manufacturer's instructions. Protein (20 μ g) loaded on SDS-PAGE was run in an ATTO mini gel electrophoresis apparatus as described above. After the run, gel was first equilibrated in transfer buffer for 15 min. NC membrane and Whatman papers (3mm) were also soaked in the transfer buffer. For transfer, 2 pieces of 3mm Whatman paper were placed on the platform of the apparatus, on the top of which membrane was placed followed by gel and 2 layers of Whatman paper. Air bubbles trapped were removed. Constant current equal to twice the area of gel was applied (e.g. if the gel area was 50 sq. cm, 100 mA current was applied) during transfer. Handling of membrane was done wearing gloves. After the transfer was over, gel-facing side of the membrane was marked and the membrane was stained in Ponceau S. Markers were marked with a ballpoint pen and the membrane was destained in water. Membrane was then kept in blocking solution containing 4% BSA in TBST, at room temperature for 2 h. After this the membrane was washed in TBST thrice (5 min each) with constant shaking. The membrane was incubated for 1 h at room temperature with primary antibody at the appropriate dilution. Dilution was made in TBST containing 0.1% BSA. After the incubation, membrane was washed in TBST thrice (5 min each) with constant shaking and then incubated with alkaline phosphatase-conjugated secondary antibody (1:20,000 dilutions) for 1 h at room temperature. Membrane was again washed in TBST thrice (5 min each) with constant shaking. The NC membrane was then stained using substrate for alkaline phosphatase. 16 μ l of 5-bromo-4-chloro-3-indolyl phosphate (BCIP) and 33 μ l of nitroblue

tetrazolium (NBT) were added to 5 ml of AP buffer. Stock solution of BCIP was prepared by dissolving 0.5 g BCIP disodium salt in 10 ml of 100% dimethyl formamide and stored at -20°C and of NBT was prepared by dissolving 0.5 g in 10 ml of 70% dimethylformamide and stored at -20°C. The blot was developed till purple-blue bands appeared at the site of antibody binding (Towbin *et al.*, 1979).

Table1. Antibodies used in this study

Antibodies	Abbreviation	Dilution
Glutamate 1-semialdehyde Aminotransferase (46 kDa)	GSAT	1:1000
Uroporphyrinogen Decarboxylase (39 kDa)	UROD	1:500
Mg-chelatase Subunit I (45 kDa)	CHLI	1:1000
Protochlorophyllide oxidoreductase (36 kDa)	POR	1:500
Protoporphyrinogen oxidase (60 kDa)	PPXI	1:1000
Geranyl-geranyl reductase (47 kDa)	CHLP	1:1000
Oxygen Evolving Complex (33 kDa)	OEC33	1:3000
PSII Reaction Center subunit (32 kDa)	D1	1:3500
PSII Reaction Center subunit (34 kDa)	D2	1:3000
Light Harvesting Chlorophyll Protein (25 kDa)	LHCPII	1:500
Light Harvesting Chlorophyll Protein b1 (25 kDa)	Lhcb1	1:500
Light Harvesting Chlorophyll Protein b2 (25 kDa)	Lhcb2	1:500
Light Harvesting Chlorophyll Protein b4 (29 kDa)	Lhcb4	1:500
Cyt f (34 kDa)	Cytf	1:500
Cyt b (34)	Cyt b	1:500
Subunit IV (17 kDa)	Subunit IV	1:500
Reiske (20 kDa)	Pet C	1:2000
PSI Subunit III (16 kDa)	PS I F	1:3000
PSI Subunit V (17 kDa)	PS I L	1:3000

Superoxide Dismutase:

Leaf samples (0.4–0.8 g) were homogenized in ice-cold extraction buffer (pH 7.5) containing 50 mM HEPES, 0.4 mM EDTA, 5 mM MgCl₂, 10% glycerol, 1% PVP, 2 mM DTT, and 1 mM phenyl methyl sulfonyl fluoride (Gegenheimer, 1990). The homogenate was centrifuged (14,000g) at 4⁰C for 20 min. The supernatant was used for enzyme activity assays and also stored in -80⁰C for further processing. Total protein was determined by the Bradford (1976) method. SOD activity was assayed according to the method of Gupta et al, 2009. The assay mixture contained 50 mM potassium phosphate buffer (pH 7.0), containing 0.2 mM EDTA, 57 μM NBT, 1.13 μM Riboflavin, 0.025% Triton X-100 and enzyme in a total volume of 1 ml. Nitroblutetrazolium (NBT) was the last component to be added. The superoxide formation in next 7 min was recorded at 560 nm in a UV–vis spectrophotometer. One unit of SOD activity is expressed as the amount of enzyme required to cause 50% inhibition of H₂O₂ oxidation under the experimental conditions.

SOD in gel assay:

For native polyacrylamide gel electrophoresis (PAGE) analysis, leaf tissues (1 g) were homogenized in a chilled mortar and pestle maintained in an ice bath, in 10 ml chilled 50 mM potassium phosphate buffer (pH 7.0) containing 1 mM EDTA and 1% polyvinylpyrrolidone. The homogenate was centrifuged at 15,000g for 20 min at 4⁰C and the supernatant was used for analysis. Protein content in the extracts was determined according to Lowry et al. (1951). In-gel analysis of SOD isozyme activity by native PAGE was determined according to the procedure of Beauchamp and Fridovich (1971). In order to identify the different isoforms of SOD, we used 5 mM H₂O₂ (inhibitor of CuZnSOD and FeSOD). In gel assay was carried out at 24 and 72 h of greening in response to 200 mM NaCl stress.

Catalase:

Leaf samples (0.4-0.8 g) were homogenized in ice-cold extraction buffer (pH 7.5) containing 50 mM HEPES, 0.4 mM EDTA, 5 mM MgCl₂, 10% glycerol, 1% PVP, 2 mM DTT, and 1 mM phenyl methyl sulfonyl fluoride (Gegenheimer, 1990). The homogenate was centrifuged (14,000g) at 4⁰C for 20 min. The supernatant was used for enzyme activity assays and also stored in -80⁰C for further processing. Total protein was determined by the Bradford (1976) method. Catalase (CAT) activity was determined spectrophotometrically by measuring

the rate of H₂O₂ disappearance at 240 nm, taking dA/dt at 240 nm as 43.6 mol/L⁻¹cm⁻¹ (Patterson et al. 1984). The reaction mixture contained 50 mM potassium phosphate (pH 7.0), 10.5 mmol/L H₂O₂. The reaction was run at 25^oC for two minute, after adding the enzyme extract containing 20 µg of protein, and the initial rate of decrease in absorbance at 240 nm was used to calculate the activity.

Catalase in gel assay:

A total of 3 g of tissue were homogenized with 50 mM potassium phosphate buffer (pH 7.0), including 1 mM 2-mercaptoethanol, 0.5 mM phenylmethylsulfonyl fluoride, and 1 mM EDTA. The homogenate was centrifuged at 10000g at 4 °C for 20 min. The supernatant was used for the detection of isoenzymes (Wang et al, 2005). The isoenzymes CAT were separated on the discontinuous polyacrylamide gels (stacking gel of 5% and separating gel of 10%) under the nondenaturing conditions. Proteins were electrophoresed at 4 °C and 10 mA in the stacking gel, followed by 15 mA in the separating gel. For the detection of CAT isoenzyme activity, the gel was soaked in deionized water for 15 min. Subsequently, the gel was incubated in 0.03% H₂O₂ for 25 min and then carefully washed with deionized water to remove the residual H₂O₂. After that, the gel was stained in the solution of 1% (w/v) potassium ferricyanide and 1% (w/v) ferric chloride (Woodbury et al, 1971). This caused the gel to turn blue, except at positions exhibiting CAT activity. When maximum contrast was achieved, the reaction was stopped by rinsing the gel with deionized water.

Glutathione Reductase:

Leaf tissues were grounded in 100 mM phosphate buffer (pH 7.6), homogenate were centrifuged at 12000 rpm for 10 min. Supernatant was taken for enzyme assay. Glutathione reductase (GR) (EC 1.6.4.2) activity was determined as described previously (Foyer and Halliwell 1976). The oxidized glutathione (GSSG)-dependent oxidation of NADPH was followed at 340 nm in a 1 ml reaction mixture containing 100 mM sodium phosphate buffer, pH 7.8, 0.5 mM GSSG, 50 µl extract, and 0.1 mM NADPH.

Ascorbate Peroxidase

Leaf tissue was grinded in isolation buffer (50 mM phosphate buffer pH 6.8, 1 mM ascorbate). Extract was centrifuged at 12000 rpm for 10 min. and supernatant was taken.

Reaction mix 3 ml is of 1.5 ml of 0.1 M potassium phosphate buffer pH 6.8, 0.5 ml of 6 mM ascorbate, 0.5 ml of 12 mM H₂O₂ and 0.5 ml of enzyme extract. Change in absorbance was monitored at 290 nm. Extinction coefficient used was 2.8 mmol/L⁻¹cm⁻¹ (Ramel et al, 2009).

HPLC Analysis of tocopherol:

To quantify tocopherol in rice leaves, 200 mg samples of frozen leaves were extracted with methanol. The extracts were filtered (0.45 µm PVDF, 4 mm syringe filters) into autosampler tubes. Tocopherols were separated by isocratic reverse-phase HPLC (58% [v/v] acetonitrile and 42% [v/v] methanol containing 7%-isopropanol) using an injection volume of 20 µl, a flow rate of 1.5 ml min⁻¹, and a run time of 20 min. HPLC analysis was performed on a Phenomenex Luna C18 column (25 cm × 4.6 mm, 5 µm), using a fluorescence detector (Shimadzu, RF-10AXL, Japan). Sample excitation was at 298 nm, and emission was monitored at 328 nm. Peaks of γ- and α-tocopherol were identified by comparing their retention times with commercially available authentic standards. Tocopherol concentration and composition was calculated from standard curves. Extraction and HPLC measurement of tocopherols were done three times, independently.

Determination of Hydrogen Peroxide in Leaf Extracts:

Hydrogen peroxide was determined according to Velikova et al. (2000). Leaf tissues (200 mg) were homogenized in 2 ml of 0.1% (w/v) TCA solution on ice. The homogenate was centrifuged at 12,000g for 15 min, and 0.4 ml of the supernatant was added to 0.4 ml of 10 mM potassium phosphate buffer, pH 7.0, and 0.8 ml of 1 M KI. The absorbance of the supernatant was measured at 390 nm. The content of H₂O₂ was calculated by comparison with a standard calibration curve previously made using different concentrations of H₂O₂.

Estimation of lipid peroxide:

The level of lipid peroxidation products were estimated using 200 mg fresh tissue according to the method of Hodges *et al.*, 1999 and were expressed as thiobarbituric acid reactive substances (TBARS). Plant samples were extracted in 0.25% 2-thiobarbituric acid (TBA) in 10% TCA using a mortar and pestle. Contents were heated at 95⁰C for 30 minutes and the quickly cooled in an ice bath and centrifuged at 12,000 rpm for 10 min. The absorbance of the supernatant was read at 532 nm and correction for unspecific turbidity was done by subtracting the absorbance of the same at 600 nm. The blank was 0.25% TBA in 10% TCA. The

concentration of lipid peroxides together with oxidatively modified proteins were quantified and expressed as total TBARS in terms of n mol g^{-1} fresh weight using an extinction coefficient of $155 \text{ nM}^{-1} \text{ cm}^{-1}$. TBARS are an index of lipid peroxidation.

To increase the accuracy of determining TBA-MDA levels by correcting for compounds other than MDA, which absorb at 532 nm, subtraction of the absorbance at 532 nm of a solution containing plant extract incubated without TBA from an identical solution containing TBA was done. Plant samples were homogenized in (i) -TBA solution comprised of 20.0% (w/v) trichloroacetic acid (-TBA) or (ii) TBA solution containing the above plus 0.25% TBA (+TBA). Samples were then mixed vigorously, heated at 95°C in a water bath for 25 min, cooled, and centrifuged at 12,000 rpm for 10 min. Absorbances were read (Shimadzu, Japan) at 440 nm, 532 nm, and 600 nm. Malondialdehyde equivalents were calculated in the following manner: 1) $[(\text{Abs } 532_{+TBA}) - (\text{Abs } 600_{+TBA}) - (\text{Abs } 532_{-TBA}) - (\text{Abs } 600_{-TBA})] = A$; 2) $[(\text{Abs } 440_{+TBA} - \text{Abs } 600_{+TBA}) \cdot 0.0571] = B$; 3) MDA equivalents (nmol.ml^{-1}) = $(A-B/157\ 000) \cdot 10^6$.

Two-Dimensional Gel Electrophoresis:

Protein Sample preparation for thylakoids:

Plants were grown for five days in dark and treated with salt stress in dark, 12 h after stress in dark plants were transferred to light for greening. Thylakoid membrane protein was isolated as per stated earlier.

Isolation of soluble protein:

Soluble protein was isolated according to Kim et al, 2001. Two grams of plant tissues were placed in liquid nitrogen and then stored at -80°C . The plant tissue was transferred to a prechilled mortar, and ground with a pestle in liquid nitrogen to a fine powder. The powder was homogenized in 10 ml of ice-cold Mg/NP-40 extraction buffer containing 0.5 M Tris-HCl, pH 8.3, 2% v/v NP-40, 20 mM MgCl_2 , 2% v/v β -mercaptoethanol, 1 mM phenylmethylsulfonyl fluoride (PMSF) and 1% w/v polyvinylpyrrolidone (PVPP). After centrifugation at 12 000g for 15 min at 4°C , pellet is discarded and to the supernatant is added a 50 % (w/v) PEG stock solution to final conc. of 10% PEG. The solution is incubated in ice for 15 min. and then centrifuged at 1500g for 15 min. at 4°C (At this point protein pellet constitutes 10% PEG fraction). The supernatant is adjusted to 20 % PEG by adding 50 % (W/V) PEG stock sol. And then incubated and centrifuged as described above. The resulting pellet constitutes 10-20% PEG

proten fraction. The final supernatant is used for 2-D by using PERFECT-FOCUS™ kit from G.Biosciences.

For protein estimation Bradford method of protein estimation was followed (1976). 300 µg of protein was taken from each sample. Then they are precipitated in 90% cold acetone in -20°C for 1 h. After that protein was recovered by pelleting it down in 12,000 rpm for 10 mins. The pellets were air dried and finally dissolved rehydration buffer (6 M urea, 2 M thiourea, 3% CHAPAS, 0.2% ampholyte, 15mM DTT).

Isoelectric focusing:

Protein sample containing 300µg in 300 µl of rehydration buffer was spread equally in one of the lain of rehydration tray. IPG stip of 17 cm (pH 4-7) was laid on the sample from gel side down. Mineral oil was overlaid to prevent evaporation. It was left for rehydration for 16 hour at 20⁰C temperature in isoelectric focusing cell. Paper wicks wet with 8 µl of milli Q water were put on two electrodes of focusing tray. IPG strip was taken from rehydration tray and put on electrode in focusing tray upside down. Focusing tray was adjusted in isoelectric focusing cell. Mineral oil was overlaid and run was carried out according to program given below. After that take out IPG strip and put in equilibration buffer I for 10 min. and then in equilibration buffer II for 10 min.

Equilibration buffer I: 6M urea, 2% SDS, 0.375M Tris-Hcl (pH 8.8), 20% glycerol and 2% (w/v) DTT.

Equilibration buffer II: 6M urea, 2% SDS, 0.375M, Tris-Hcl (pH 8.8), 20% glycerol.

Running Programme for Isoelectric Focusing:

17 cm strip	voltage	time	volt-hours	ramp
Step1	250	20 min.	-	Linear
Step2	10,000	3.30 hr	-	Linear
Step3	10,000	-	40,000 V-hr	Rapid
Total		8 hr	54,000 V-hr	

Then they were used for second dimensional run in 12.5% SDS-PAGE.

Silver staining:

After the completion of 2nd dimensional run gels were soaked in fixer (40% methanol and 10% glacial acetic acid) for atleast for 1h. Then they were given three washings of 30min each. Subsequently gel was treated with 0.02% solution of sodium thiosulphate for 1min, gel was washed with double distilled water for 1 min. Silver nitrate solution (0.2%) was added containing 75 μ l of formaldehyde for 20min. After silver nitrate staining gels were washed for 1min and gels were transferred to 2% sodium carbonate solution. The reaction was stooped in the 5% glacial acetic acid. Gels were stored in milli Q water till further processing. Staining was done with continuous shaking and the timings were maintained very accurately.

MALDI-TOF Analysis of protein bands

Excision of protein bands from polyacrylamide gel: The gel was washed with water for two times, each wash was for ten minutes. Protein band/ spots of interest were excised from the gel and the excised piece of gel was cut into small pieces of approx. 1mm-cubes. The gel pieces were transferred in to a 0.5ml microfuge tube.

Destaining: Approximately 30 μ l of a freshly prepared 1:1(v/v) mixture of the two destaining reagents was added {[$(K_3[Fe(CN)_6]$ conc.30mm/l and $Na_2S_2O_3$ conc.100mm/l dissolve in water)}. The sample was incubated for 30 min at room temperature. After incubation the destaining solution was discarded from the sample.

Washing of gel pieces: The gel particles were washed with water and 50mM NH_4HCO_3 / acetonitrile 1+1(v/v) for 15 min. After washing all remaining liquid from the sample was

removed and then enough amount of acetonitrile added to cover the gel particles, this will make the gel shrink and stick together. The acetonitrile from the gel sample was removed. After removing acetonitrile, the gel particles were dried down in a vacuum centrifuge.

Reduction and alkylation: 10mM dithiothreitol/50mM NH_4HCO_3 freshly prepared solution (a few μl) was taken and applied to the gel particle so that the gel swells. After swelling the gel incubated it for 45 min at 56°C . It was brought to room temperature. The excess liquid was removed and replaced quickly by roughly the same volume as above of freshly prepared 55mM iodoacetamide (light sensitive) in 50mM NH_4HCO_3 . After adding iodoacetamide incubated the sample for 30 min at room temperature in the dark. The iodoacetamide solution was removed from the sample by pipetting out. The gel particles were washed with 50mM NH_4HCO_3 and acetonitrile (1+1; v/v) two times for 15 min each. After that enough amount of acetonitrile was added to cover and shrink the gel particles. The acetonitrile was removed from the sample after total shrinkage of the gel particles. The gel particles were dried down in a vacuum centrifuge.

In gel digestion: Freshly prepared enzyme solution of 25mM NH_4HCO_3 with 5 ng/ μl of trypsin (modified by reductive methylation and treated with TPCK to reduce autolysis and inactivate chymotrypsin respectively) was added into the gel so that it can cover the gel. It was incubated at 37°C for 30 minutes. After incubation excess amount of enzyme solution was removed. 25mM NH_4HCO_3 (approx.2-3 μl) was added so that the gel become wet for overnight. The gel sample was incubated at 37degree C for overnight (Shevchenko et al., 1996).

Extraction of peptides: Extraction buffer [50% acetonitrile, 0.1% Trifluoroacetic acid (TFA)] was added to immerse the gel completely. However, care was taken to avoid addition of excess volume. The extraction yield was improved by ultrasonication for 30 min at room temperature.

Dry droplet method: Saturated matrix (α -cyano-4-hydroxycinnamic acid) solution was prepared freshly by sonication. The solvent used is TA (33% acetonitrile,0.1% TFA).The matrix solution is mixed in equal volumes with the sample solution. The mixture is pipeted on the target (0.5 to 1 ml) and dried at ambient temperature. Then the crystals on the target surface were ready for the laser shot by MALDI.

Data analysis:

Protein identification was performed using the Mascot search engine (<http://www.matrixscience.com>), which uses a probability based scoring system .NCBI non-redundant and SwissProt databases were selected as the primary databases to be searched.

Results

RESULTS

Plants growth:

Two cultivars of Rice (*Oryza sativa* L) i.e. a salt resistant genotype CSR10 and a salt sensitive variety Pusa Basmati (PB1) were taken for study. Five-day-old etiolated rice seedlings of these two cultivars were treated with 0 mM NaCl (half-strength MS salt solution), or 100 mM NaCl (half-strength MS salt solution + 100 mM NaCl) or 150 mM NaCl (half-strength MS salt solution + 150 mM NaCl) or 200 mM NaCl (half-strength MS salt solution + 200 mM NaCl) 12 h prior to the transfer to cool white fluorescent+incandescent light ($100 \mu\text{moles photons m}^{-2} \text{ s}^{-1}$), at 28°C at 75% relative humidity maintained by a Conviron plant growth chamber. CSR10 seedlings (Fig 1A) looked greener than those of PB1 (Fig 1B). Growth of seedlings was reduced due to increase in the concentration of NaCl from 0 to 200 mM NaCl in both the varieties (Fig 1). Seedlings shown in figure.1 are after 72 h of greening in the absence or presence of different concentrations of NaCl.

Chlorophyll and Carotenoids Contents:

Five-day-old etiolated control and salt-stressed rice seedlings of two cultivars were treated with 100 mM, 150 mM and 200 mM NaCl 12 h prior to the transfer to cool white fluorescent+incandescent light ($100 \mu\text{moles photons m}^{-2} \text{ s}^{-1}$), at 28°C at 75% relative humidity. Leaves were harvested after 12, 24, 48, 72 h of greening and their Chl and carotenoids contents were estimated.

Total Chlorophyll

Total chlorophyll contents of CSR10 and PB1 are shown in Fig.2 (A) and (B) respectively. Fig.2 (C) shows the Chl as % of control after 24, 48 and 72 h of salt stress. CSR10 cultivar had maximum Chl contents within 48 h of greening and there was almost no further increase in Chl contents till 72 h. In PB1 genotype chlorophyll biosynthesis continued upto 72 h of greening. The total chlorophyll content was more in CSR10 than that in PB1. As compared to their respective controls, the chlorophyll contents (corrected for the loss of moisture during salt stress) decreased in response to salt stress in both the cultivars. However, as compared to the

salt sensitive PB1 genotype, CSR10 had a reduced relative decrease of Chl content in response to different concentrations of salt. For example as shown in the fig.2 C, in response to 150 mM NaCl CSR 10 had only 25% decline in chlorophyll content whereas in PB1, the loss of Chl was nearly 50%. Chl a/b ratio increases in response to 200 mM NaCl stress after 24 h and 72 h of greening as shown in Fig. 2 (D).

Carotenoids

Carotenoid contents of CSR10 and PB1 are shown in Fig.3 (A) and (B) respectively. Carotenoid contents of both the cultivars decreased in response to salt stress. However, the decline of carotenoid contents of CSR10 was lower than that of PB1 (Fig.3 C).

Protein

Protein content of CSR10 and PB1 measured after 72 h of salt stress shown in Fig.4. In both the cultivars protein content decreased in response to salt stress. Decline in protein content was higher in PB1 than that in CSR10 especially in response to 100mM and 150 mM NaCl.

Element Analysis:

To understand if the differential responses of PB1 and CSR10 to salt stress is due to differential uptake and / or transport of sodium and other salts, their sodium, potassium and calcium contents were estimated in root and shoot tissues after 72 h of greening. Five-day-old etiolated rice seedlings of CSR10 and PB1 were treated with 0 mM, 100 mM and 200 mM NaCl 12 h prior to the transfer to cool white fluorescent+incandescent light ($100 \mu\text{moles photons m}^{-2} \text{ s}^{-1}$), at 28°C at 75% relative humidity maintained by a Conviron plant growth chamber. Element analysis was done after 72 hours of greening as described in materials and methods.

Sodium contents:

Sodium contents in root were enhanced with increase in NaCl concentration. Under non-stressed condition CSR10 plants accumulates more NaCl than PB1. After 200 mM NaCl the sodium contents were increased by 66.49 % and 56.8 % in CSR10 and PB1 respectively as compared to that of control rice seedlings (Fig.5 A).

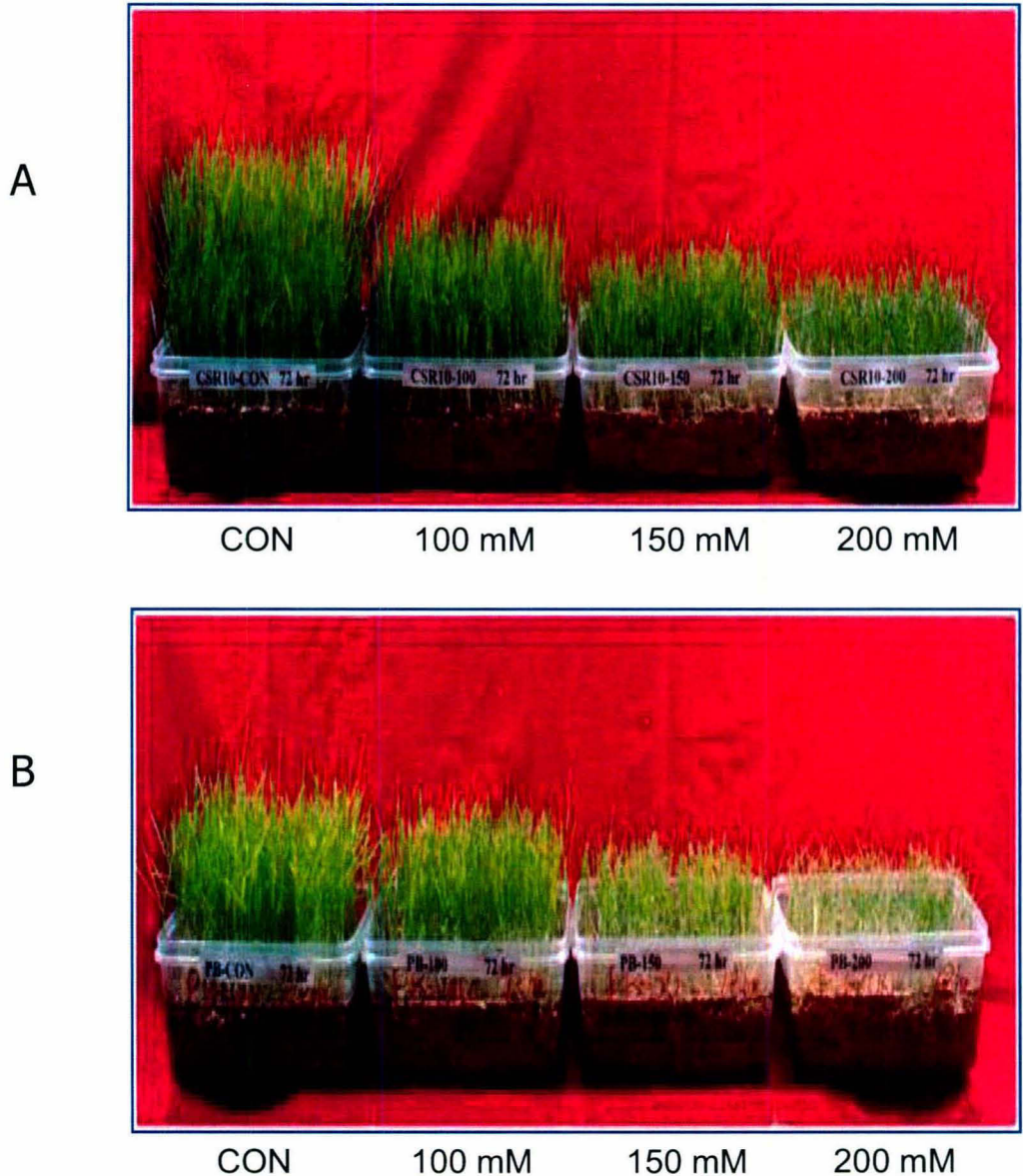


Fig 1: Control and salt-stressed rice seedlings of (A) CSR10 and (B) PB1. Five-day-old etiolated seedlings were treated with 0 mM, 100 mM, 150 mM and 200 mM NaCl 12 h prior to the transfer to cool white fluorescent+incandescent light ($100 \mu\text{moles photons m}^{-2} \text{s}^{-1}$), at 28°C at 75% relative humidity maintained by a Conviron plant growth chamber. Seedlings shown here are 72 h of greening.

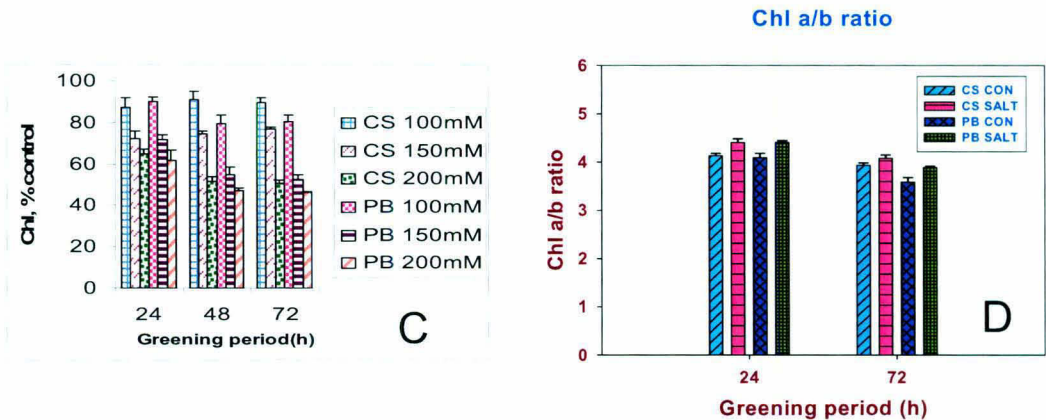
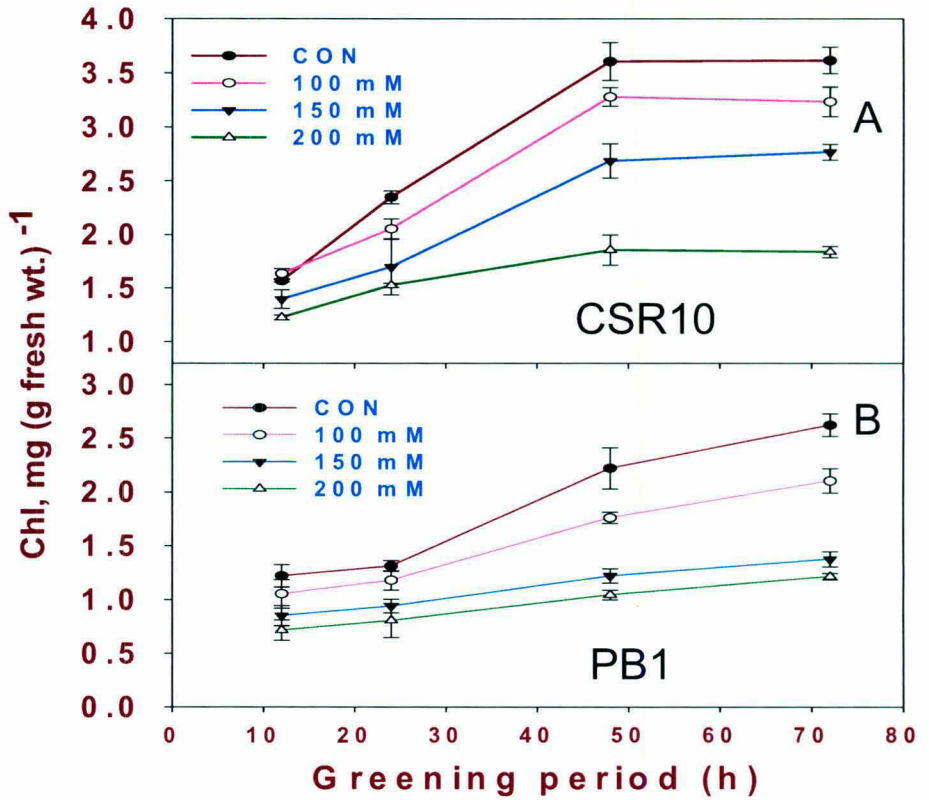


Fig 2: Total Chl contents of control and salt-stressed rice seedlings of (A) CSR10 and (B) PB1 (C) chlorophyll contents as percentage of control of CSR10 and PB1 (D) Chl a/b ratio after 24h and 72h of greening in response to 200 mM NaCl stress. seedlings. Five-d-old etiolated seedlings were treated with 0 mM, 100 mM, 150 mM and 200 mM NaCl 12 h prior to the transfer to cool white fluorescent+incandescent light ($100 \mu\text{moles photons m}^{-2} \text{s}^{-1}$), at 28°C at 75% relative humidity. Leaf samples were harvested at desired time points and their chlorophyll contents were measured as described in materials and methods. Each data point is the average of three replicates. The *error bar* represents SD.

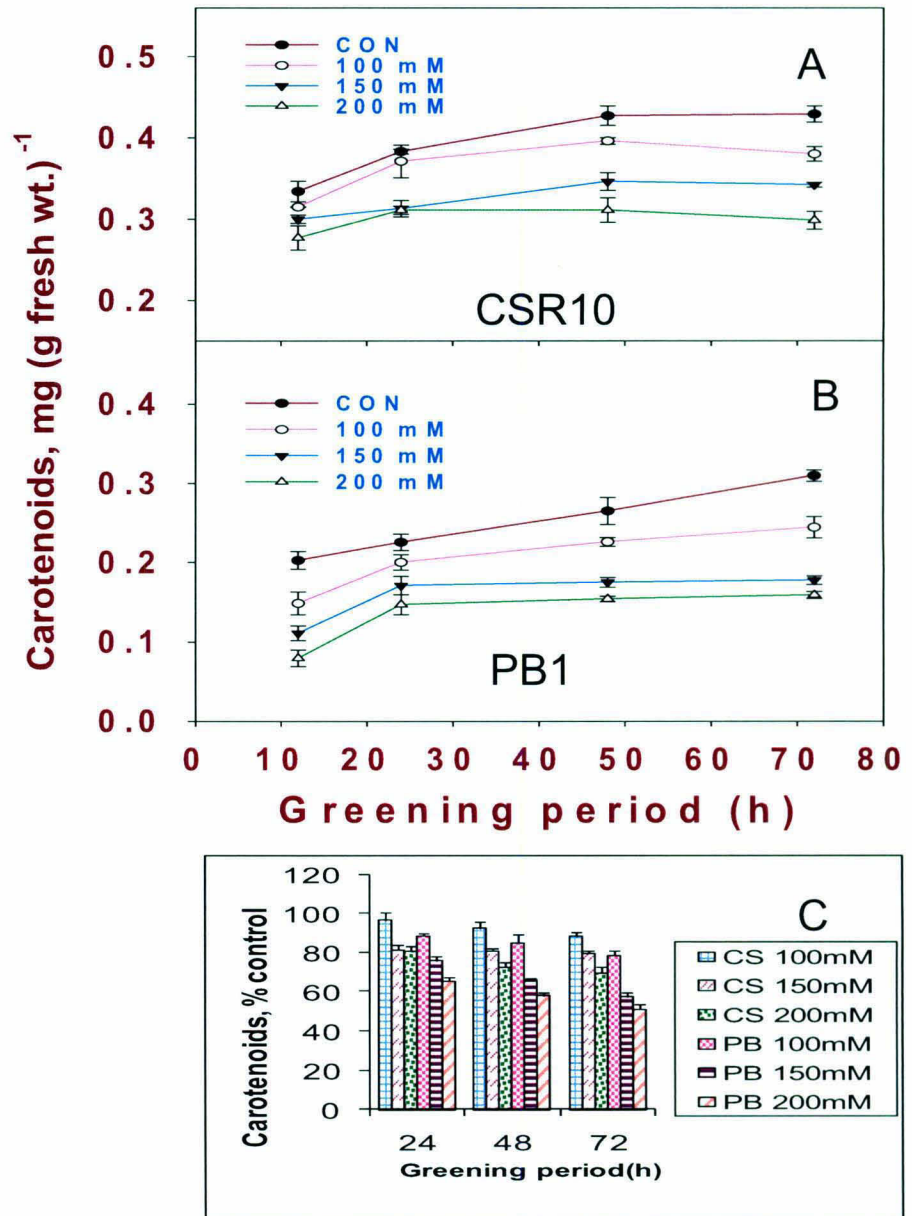


Fig 3: Carotenoids contents of control and salt-stressed rice seedlings of (A) CSR10 and (B) PB1 (C) carotenoids contents as percentage of control of CSR10 and PB1 seedlings. Five-d-old etiolated seedlings were treated with 0 mM, 100 mM, 150 mM and 200 mM NaCl 12 h prior to the transfer to cool white fluorescent+incandescent light ($100 \mu\text{moles photons m}^{-2} \text{s}^{-1}$), at 28°C at 75% relative humidity. Leaf samples were harvested at desired time points and their carotenoids contents were measured as described in materials and methods. Each data point is the average of three replicates. The *error bar* represents SD.

CSR10 and PB1

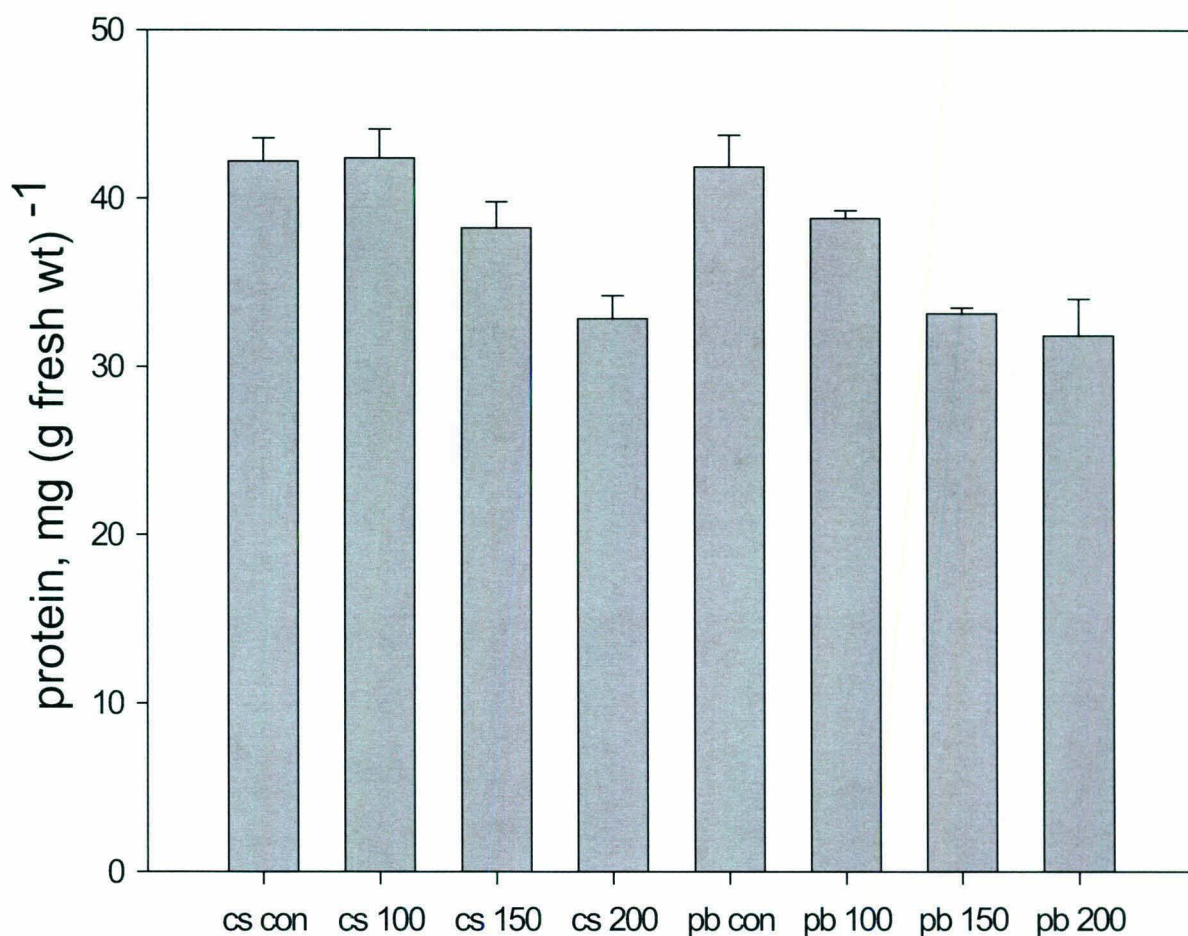


Fig 4: Total protein contents of control and salt-stressed rice seedlings of CSR10 and PB1. Five-d-old etiolated seedlings were treated with 0 mM, 100 mM, 150 mM and 200 mM NaCl 12 h prior to the transfer to cool white fluorescent+incandescent light ($100 \mu\text{moles m}^{-2} \text{s}^{-1}$), at 28°C at 75% relative humidity. Leaf samples were harvested at 72 h of greening and their protein contents were measured as described in materials and methods. Each data point is the average of three replicates. The *error bar* represents SD.

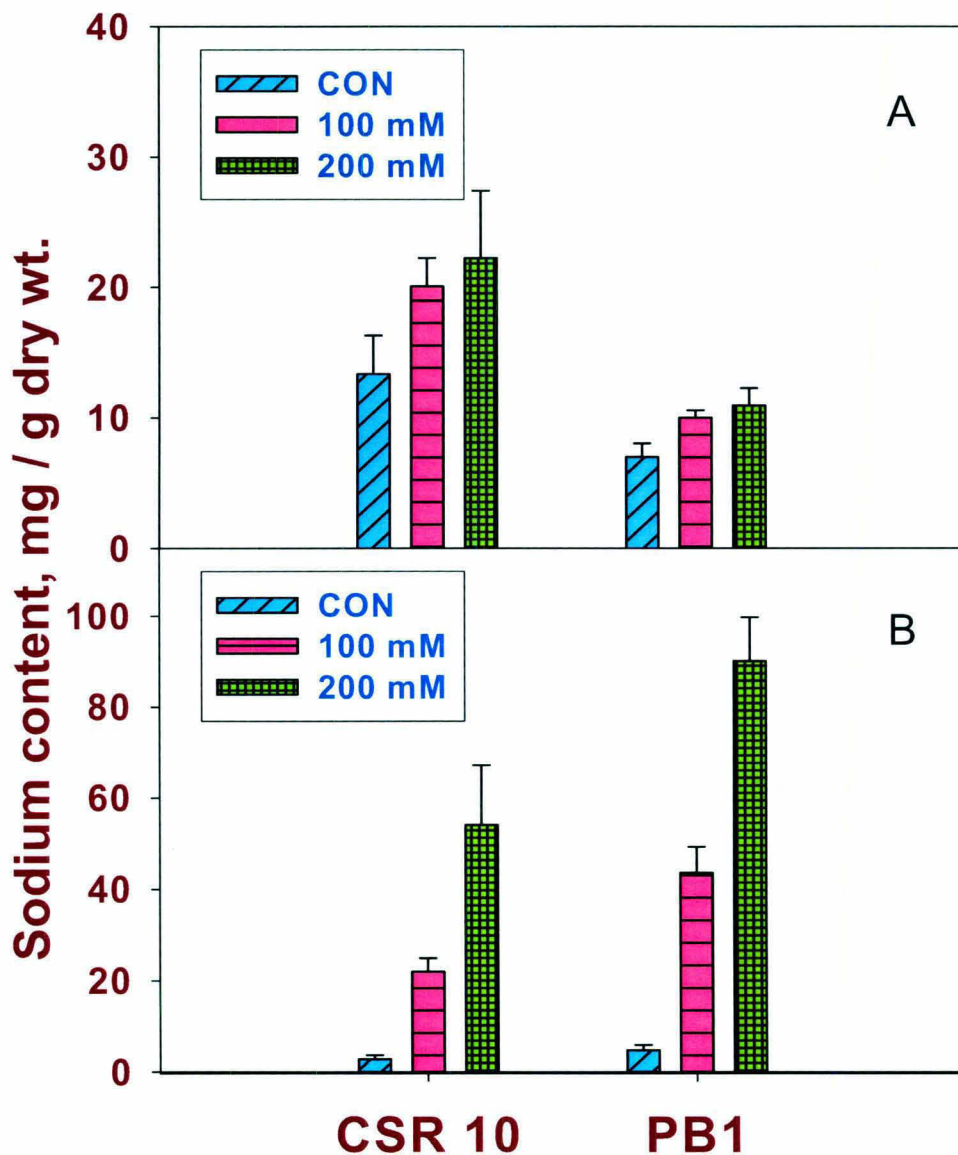


Fig 5: Sodium contents of rice seedlings in (A) root and (B) shoot. Five-day-old etiolated rice seedlings of CSR10 and PB1 were treated with 0 mM, 100 mM and 200 mM NaCl 12 h prior to the transfer to cool white fluorescent+incandescent light ($100 \mu\text{moles photons m}^{-2} \text{s}^{-1}$), at 28°C at 75% relative humidity. Sodium contents of roots and shoots were measured after 72 h of salt stress by inductively coupled plasma atomic emission spectrophotometry (ICP-AES) as described in materials and methods. Each data point is the average of three replicates. The *error bar* represents SD.

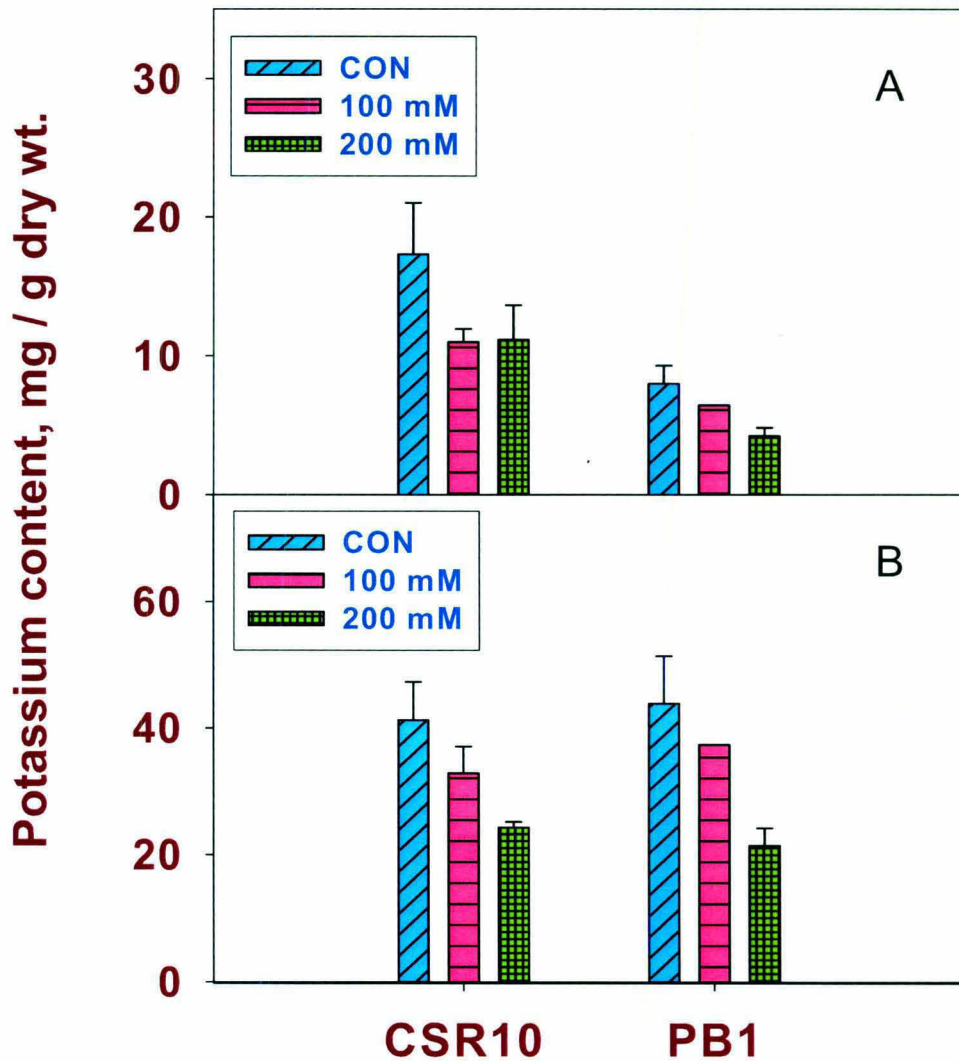


Fig 6: Potassium contents of rice seedlings in (A) root and (B) shoot. Five-day-old etiolated rice seedlings of CSR10 and PB1 were treated with 0 mM, 100 mM and 200 mM NaCl 12 h prior to the transfer to cool white fluorescent+incandescent light ($100 \mu\text{moles photons m}^{-2} \text{s}^{-1}$), at 28°C at 75% relative humidity. Potassium contents of roots and shoots were measured after 72 h of salt stress by inductively coupled plasma atomic emission spectrophotometry (ICP-AES) as described in materials and methods. Each data point is the average of three replicates. The *error bar* represents SD.

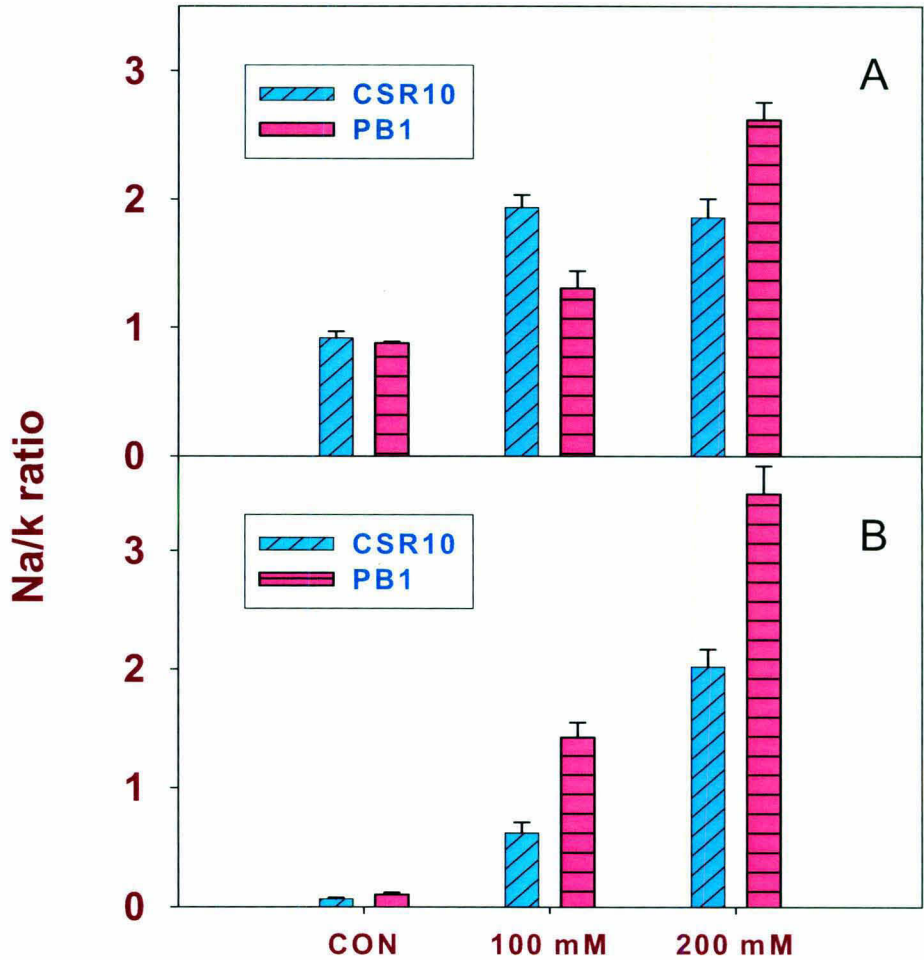


Fig 7: Sodium-potassium ratio in (A) root and (B) shoot of rice seedlings. Five-day-old etiolated rice seedlings of CSR10 and PB1 were treated with 0 mM, 100 mM and 200 mM NaCl 12 h prior to the transfer to cool white fluorescent+incandescent light ($100 \mu\text{mol photons m}^{-2} \text{s}^{-1}$), at 28°C at 75% relative humidity. Sodium and potassium contents of roots and shoots were measured after 72 h of salt stress by inductively coupled plasma atomic emission spectrophotometry (ICP-AES) as described in materials and methods. Each data point is the average of three replicates. The *error bar* represents SD.

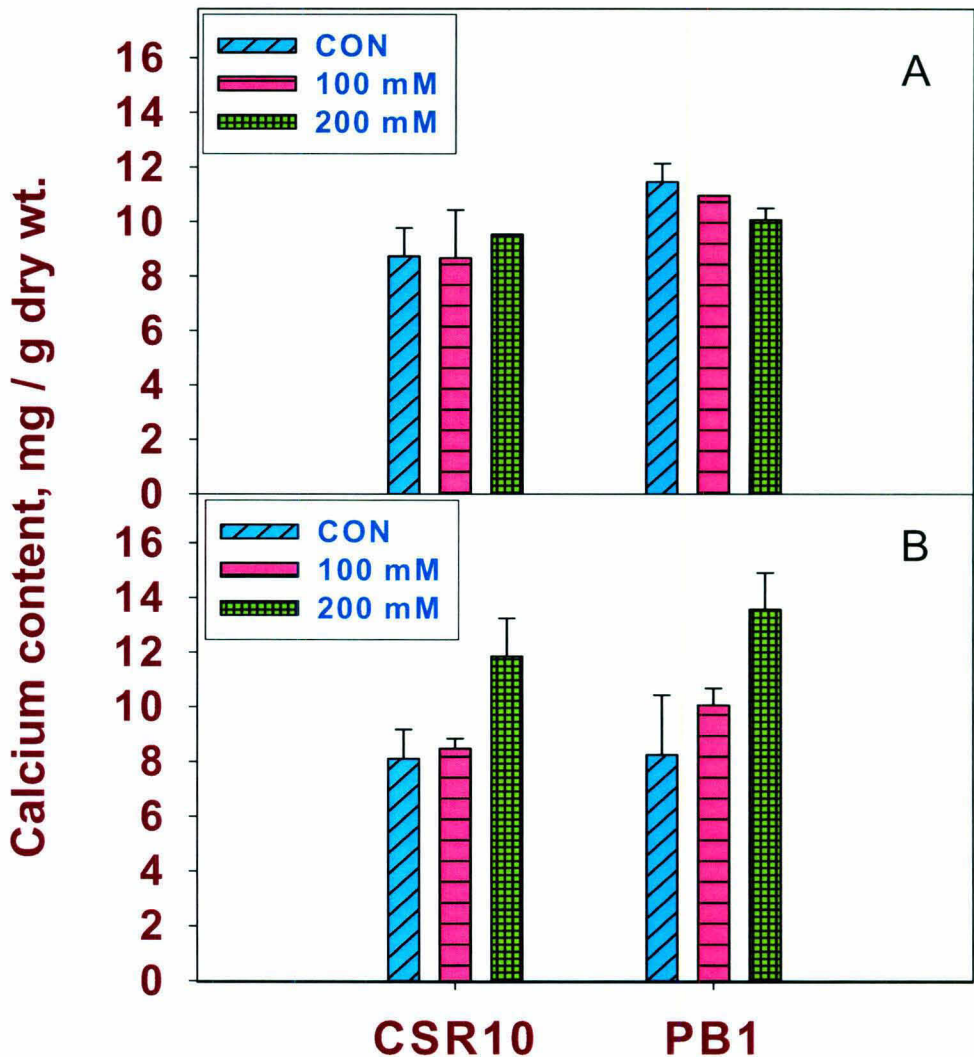


Fig 8: Calcium contents of rice seedlings in (A) root and (B) shoot. Five-day-old etiolated rice seedlings of CSR10 and PB1 were treated with 0 mM, 100 mM and 200 mM NaCl 12 h prior to the transfer to cool white fluorescent+incandescent light ($100 \mu\text{moles photons m}^{-2} \text{s}^{-1}$), at 28°C at 75% relative humidity. Calcium contents of roots and shoots were measured after 72 h of salt stress by inductively coupled plasma atomic emission spectrophotometry (ICP-AES) as described in materials and methods. Each data point is the average of three replicates. The *error bar* represents SD.

Sodium contents in shoots were also enhanced with increase in NaCl concentration. Under non-stressed condition PB1 plants accumulates relatively more sodium than CSR10 (Fig.5 B). After 200 Mm NaCl stress there was 18.55 fold increase in sodium content in CSR10 and 17.97 fold in PB1 respectively as compared to that of control rice seedlings.

Potassium contents:

Potassium contents in root declined with increase in NaCl stress level. In stressed seedlings PB1 accumulated 50 % less potassium than that of CSR10. After 200 mM NaCl the potassium ion contents were decreased by 35.6 % and 47.1 % in CSR10 and PB1 respectively as compared to that of control seedlings (Fig.6 A).

Potassium contents in shoot were also declined with increase in NaCl concentration. In response to 200 mM NaCl treatment, the potassium contents were reduced by 41 % and 51 % in CSR10 and PB1 respectively as compared to that of control seedlings. (Fig.6 B).

Na⁺/K⁺ Ratio:

Na⁺/K⁺ ratio in roots increased when NaCl concentration was enhanced from 100 mM to 200 mM. However in CSR10 Na⁺/K⁺ ratio increased only upto 150 mM salt (Fig.7 A).

Na⁺/K⁺ ratio increased in shoot due to NaCl application to the roots. However increase of Na⁺/K⁺ ratio in shoot was higher in PB1 than that in CSR10 (Fig.7 B).

Calcium contents:

In roots no remarkable changes in calcium concentration were observed in both the cultivars in stressed or non-stressed rice seedlings. (Fig.8 A).

Calcium contents in shoot enhanced with increase in NaCl stress. After 200 mM NaCl stress calcium contents declined by 31.5 % and 39.17 % in CSR10 in PB1 respectively as compared to control seedlings (Fig.8 B).

Effect of salt stress on chlorophyll biosynthesis.

As shown in Fig. 1-2. chlorophyll accumulation was impaired in salt stressed seedlings. To understand the mechanistic details of salt stress induced down regulation of Chl biosynthesis and greening process, steady state accumulation of Chl biosynthetic intermediates and activities of certain enzymes involved were studied.

Glutamate -1-semialdehyde (GSA) accumulation:

GSA is the precursor of ALA in chlorophyll biosynthesis. GSA accumulation decreased in response to salt stress in the presence of gabaculine which is an ALA biosynthesis inhibitor. After 72 h of greening in the presence of 200 mM NaCl stress, GSA accumulation declined by 21.2% and 47% in CSR10 and PB1 respectively. This demonstrates reduced susceptibility of CSR10 to salt stress (Fig. 9).

ALA contents:

The next early intermediate of chlorophyll biosynthesis after GSA is ALA. Net accumulation of ALA was measured in the presence of Levulinic acid an inhibitor of ALA dehydratase as it is a structural analog of ALA. ALA accumulation decreased in response to increased length of greening and NaCl stress. In response to salt stress ALA contents of both the cultivars declined. However the sensitive cultivar PB1 had a severe decrease. As compared to control after 72 h of greening, ALA contents decreased by 36.9% and 77.1 % in CSR10 and PB1 respectively (Fig. 10).

Pchlide contents:

ALA is further metabolized to pchlide during greening process. Pchlide contents were measured after 72 h of continuous light exposure. Pchlide contents of both the cultivars declined in response to salt stress. Pchlide contents declined by 56.4% and 52.4% in CSR10 and PB1 respectively (Fig. 11).

Chlorophyll biosynthetic enzymes:

To understand the mechanism of impairment of biosynthesis of Chl and that of Chl biosynthetic intermediates due to salt stress, the effect of 200 mM NaCl on different enzymes

GSA ACCUMULATION

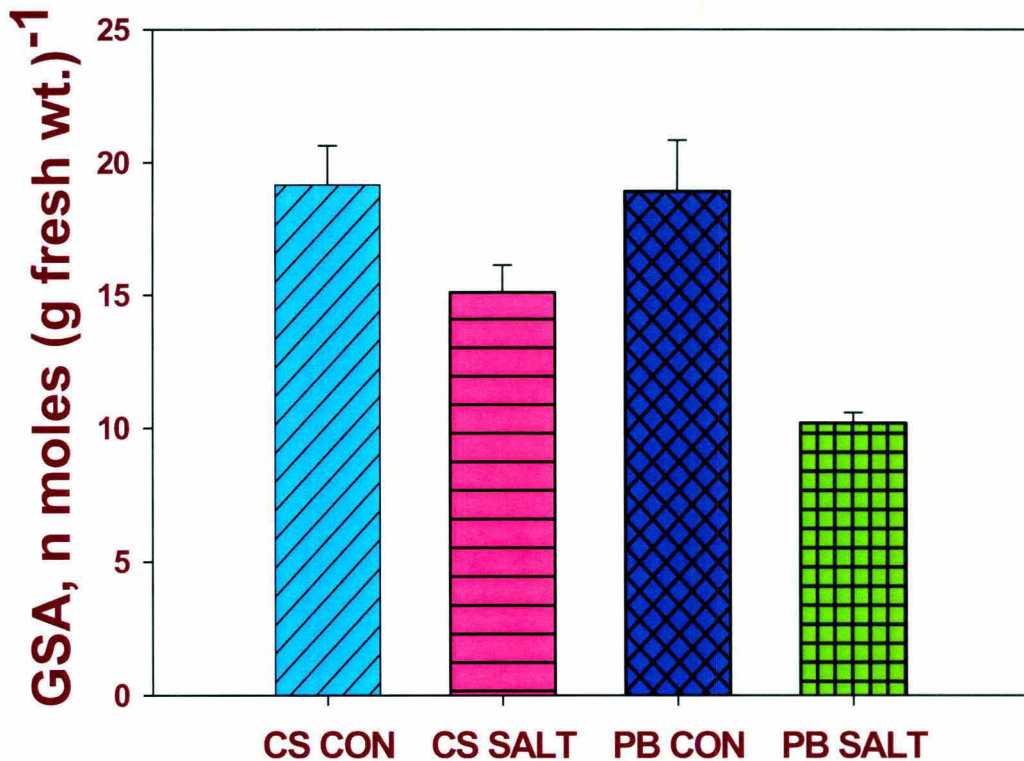


Fig 9: GSA contents in rice seedlings. Five-day-old etiolated rice seedlings of CSR10 and PB1 were treated 0 and 200 mM NaCl 12 h prior to the transfer to cool white fluorescent+incandescent light ($100 \mu\text{moles photons m}^{-2} \text{s}^{-1}$), at 28°C at 75% relative humidity. Net accumulation of GSA was monitored in response to salt stress in rice leaves in the presence of $500 \mu\text{M}$ gabaculine after 72 h of greening as described in materials and methods. Each data point is the average of three replicates. The *error bar* represents SD.

ALA accumulation

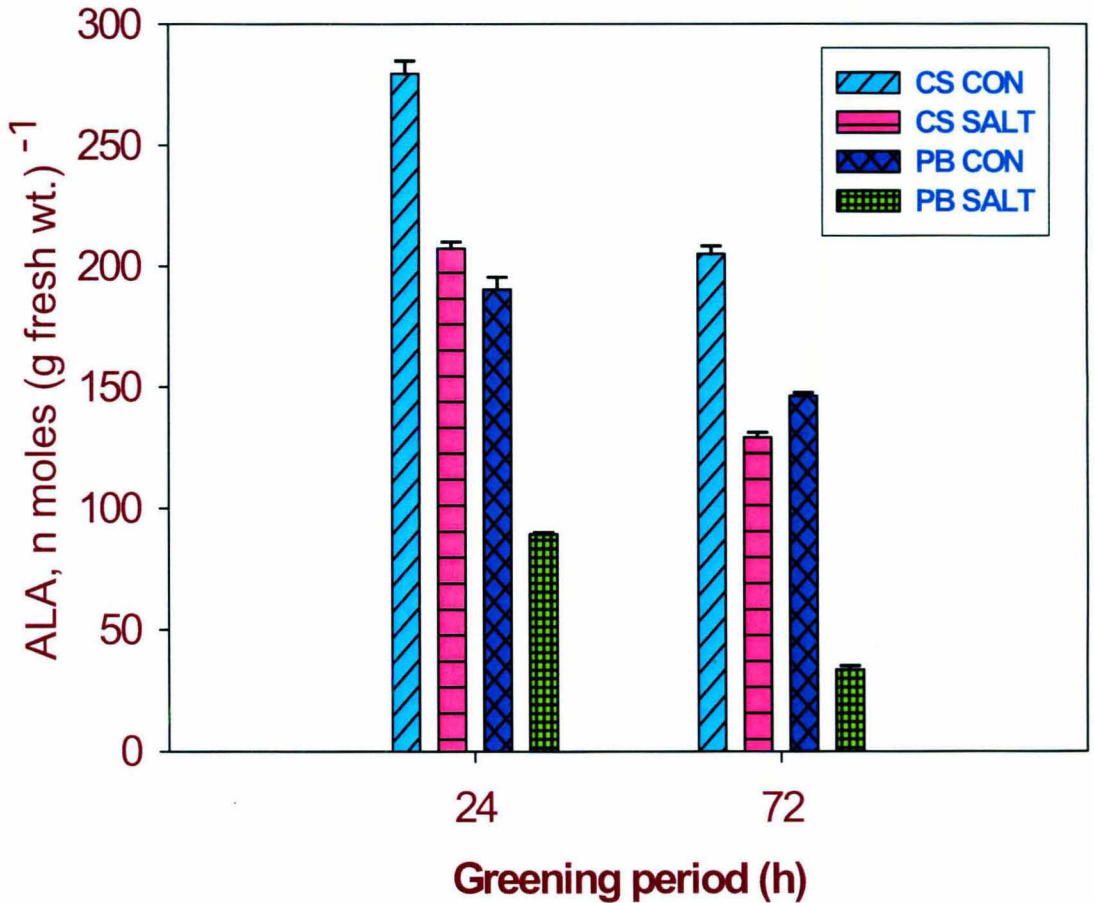


Fig10: ALA contents in rice seedlings. Five-day-old etiolated rice seedlings of CSR10 and PB1 were treated 0 and 200 mM NaCl 12 h prior to the transfer to cool white fluorescent+incandescent light ($100 \mu\text{moles photons m}^{-2} \text{s}^{-1}$), at 28°C at 75% relative humidity. Net accumulation of ALA was monitored in response to salt stress in rice leaves in the presence of 60 mM levulinic acid after 24 and 72 h of greening as described in materials and methods. Each data point is the average of three replicates. The *error bar* represents SD.

Pchlide content

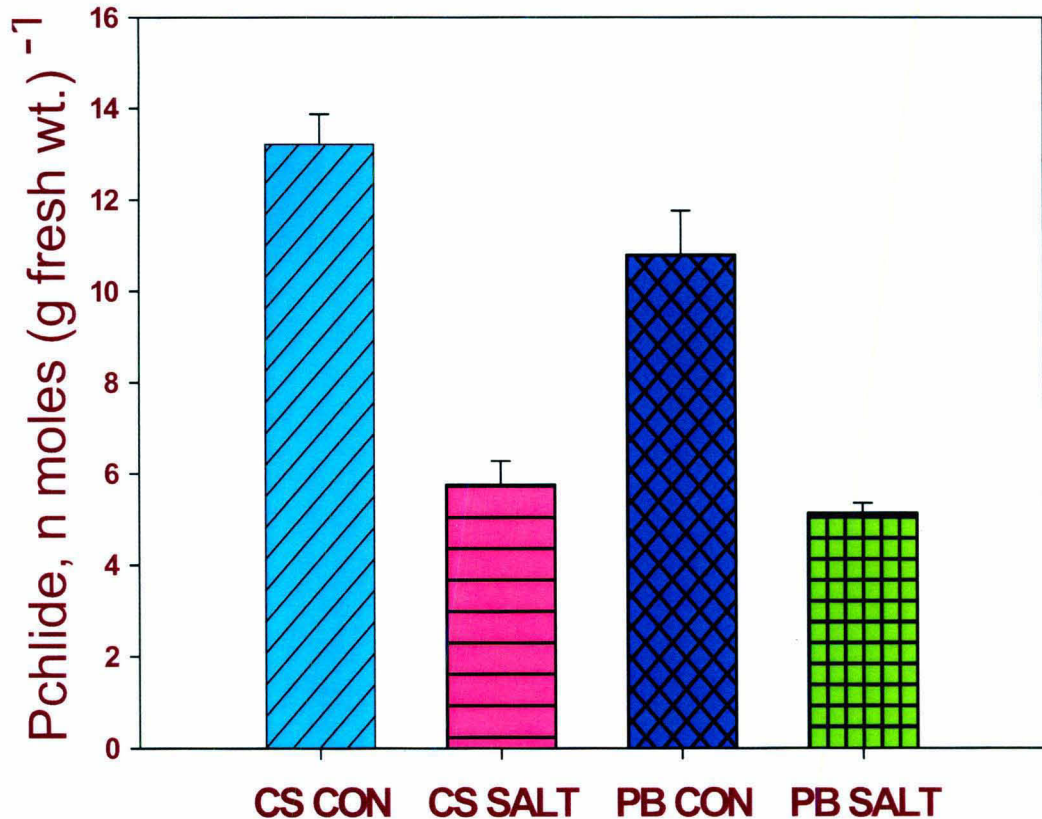


Fig 11: Pchlide contents in rice seedlings. Five-day-old etiolated rice seedlings of CSR10 and PB1 were treated with 0 and 200 mM NaCl 12 h prior to the transfer to cool white fluorescent+incandescent light ($100 \mu\text{moles photons m}^{-2} \text{ s}^{-1}$), at 28°C at 75% relative humidity. Pchlide contents were monitored in response to salt stress at 72 h of greening as described in materials and methods. Each data point is the average of three replicates. The *error bar* represents SD.

involved in Chl biosynthesis was studied. Five-day-old etiolated rice seedlings of CSR10 and PB1 were treated with 0 mM or 200 mM NaCl 12 h prior to the transfer to cool white fluorescent+incandescent light ($100 \mu\text{mol photons m}^{-2} \text{ s}^{-1}$), at 28°C at 75% relative humidity maintained by a Conviron plant growth chamber. Enzyme activity was determined at different hours greening.

ALA dehydratase:

The enzymatic activity of ALAD that synthesizes PBG from two molecules of ALA was determined in rice seedlings after 24, 48 and 72 h of greening in response to 200 mM NaCl stress. The ALAD activity decreased in response to salt stress with h of greening. After 72 h of salt stress the ALAD activity declined by 7.18 % and 51.6 % in CSR10 and PB1 respectively as compared to control seedlings (Fig.12).

Porphobilinogen deaminase (PBGD):

The next step in the Chl biosynthesis is the conversion of four molecules of porphobilinogen to uroporphyrinogen, which is catalysed by PBGD. The enzyme activity was estimated by measuring the amount of porphyrin synthesis from PBG at 24, 48 and 72 hours of greening in response to 200 mM NaCl stress. After 72 h of greening the PBGD activity declined due to salt treatment by 20.3 and 23.01 % in CSR10 and PB1 (Fig 13).

Coproporphyrinogen III oxidase:

This enzyme catalyzes the conversion of coproporphyrinogen III to protoporphyrinogen IX. Its activity was estimated by measuring the amount of proto IX formed from coproporphyrinogen III after 24 h of greening. In response to salt stress the enzymatic activity was reduced by 32.68 and 47.6 % in CSR10 and PB1 respectively (Fig.14).

Protoporphyrinogen IX oxidase:

Protox catalyzes the conversion of protoporphyrinogen IX to protoporphyrin IX. Its activity was estimated by measuring the amount of protoporphyrin IX formed from protoporphyrinogen IX after 24 h of greening. As compared to their respective controls, the

enzymatic activity reduced by 16.9 % and 25.16 % in CSR10 and PB1 in response to 200 mM salt stress (Fig.15).

Mg- chelatase:

Mg-chelatase is the first enzyme in the Mg branch of the Chl biosynthetic pathway that inserts Mg into Proto IX to form Mg-Proto IX. In this experiment Proto IX was used as a substrate and Mg-chelatase activity was measured as the amount of Mg-Proto IX and its monoester synthesized in the plastids isolated from control and salt stressed rice seedlings. Enzyme activity was estimated at 24 hours of greening in response to 200 mM NaCl stress. As compared to controls, in salt stressed samples, its activity reduced 45.05 and 81.8% in CSR10 and PB1 respectively (Fig.16).

Protochlorophyllide oxidoreductase:

Pchlde accumulates in dark as conversion of Pchlde to Chlide is catalysed in the angiosperms by the light dependent enzyme protochlorophyllide oxidoreductase (POR). The POR activity was estimated by measuring the photo transformation of pchlde to chlide. Five-day-old etiolated rice seedlings of CSR10 and PB1 were treated 0 and 200 mM NaCl 12 h prior to the transfer to cool white fluorescent+incandescent light ($100 \mu\text{moles photons m}^{-2} \text{s}^{-1}$), at 28°C at 75% relative humidity. After 72 h of greening seedlings were transferred to dark for 6h, a few of their leaves were harvested and homogenized in dark. Subsequently, seedlings were transferred to light ($100 \mu\text{moles photons m}^{-2} \text{s}^{-1}$) for 15 min and their leaves were harvested and homogenized. Pchlde contents of dark incubated and 15 min- light-exposed seedlings were estimated as described in materials and methods (Fig.17 A). POR activity was calculated as percent transformation of pchlde. In response to salt stress, the enzymatic activity marginally affected in CSR10 and decreased 58.06 % in PB1 respectively (Fig.17 B).

Immunoblot analysis of chlorophyll biosynthetic enzymes:

To correlate enzymatic activities with that of protein abundance, in response to salt stress Western blot analysis of certain enzymes involved in chl biosynthesis was studied. Equal loading (30 μg) of thylakoids protein is shown in Fig. 18 (B)

ALAD activity

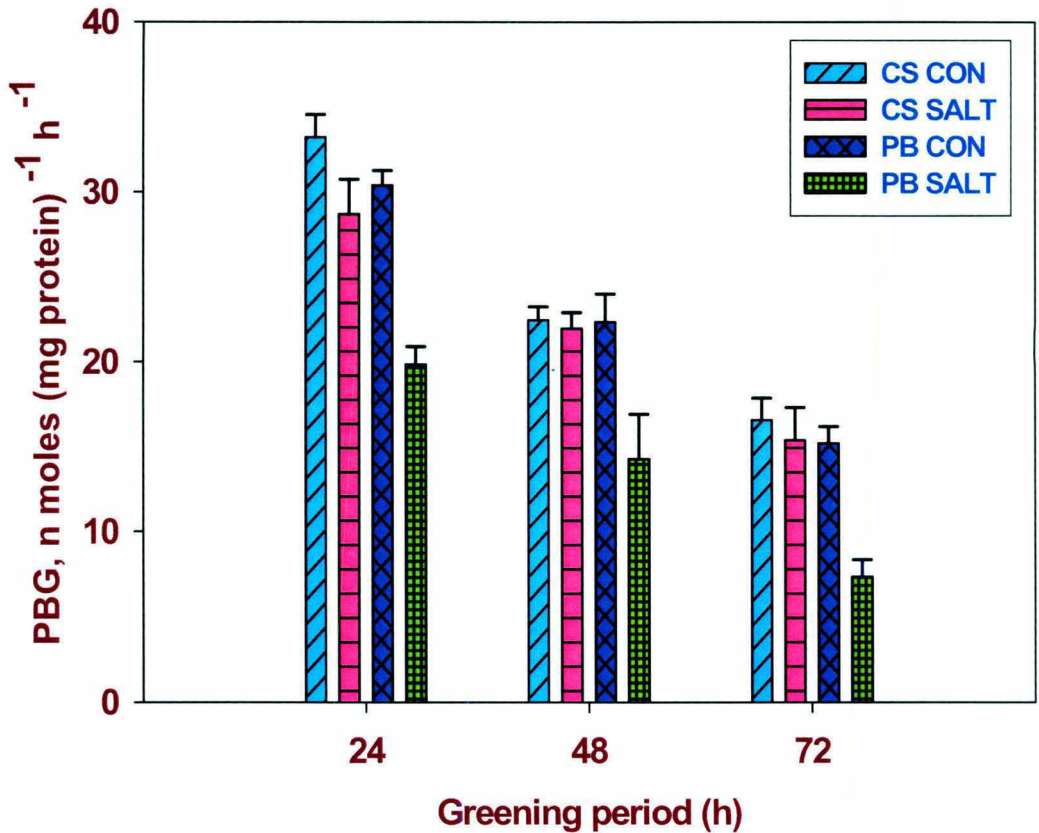


Fig 12: ALA dehydratase activity in rice seedlings. Five-day-old etiolated rice seedlings of CSR10 and PB1 were treated with 0 and 200 mM NaCl 12 h prior to the transfer to cool white fluorescent+incandescent light ($100 \mu\text{moles photons m}^{-2} \text{s}^{-1}$), at 28°C at 75% relative humidity. ALAD activity was measured in response to salt stress after 24, 48, 72 h of greening as described in materials and methods. Each data point is the average of three replicates. The *error bar* represents SD.

PBG Deaminase activity

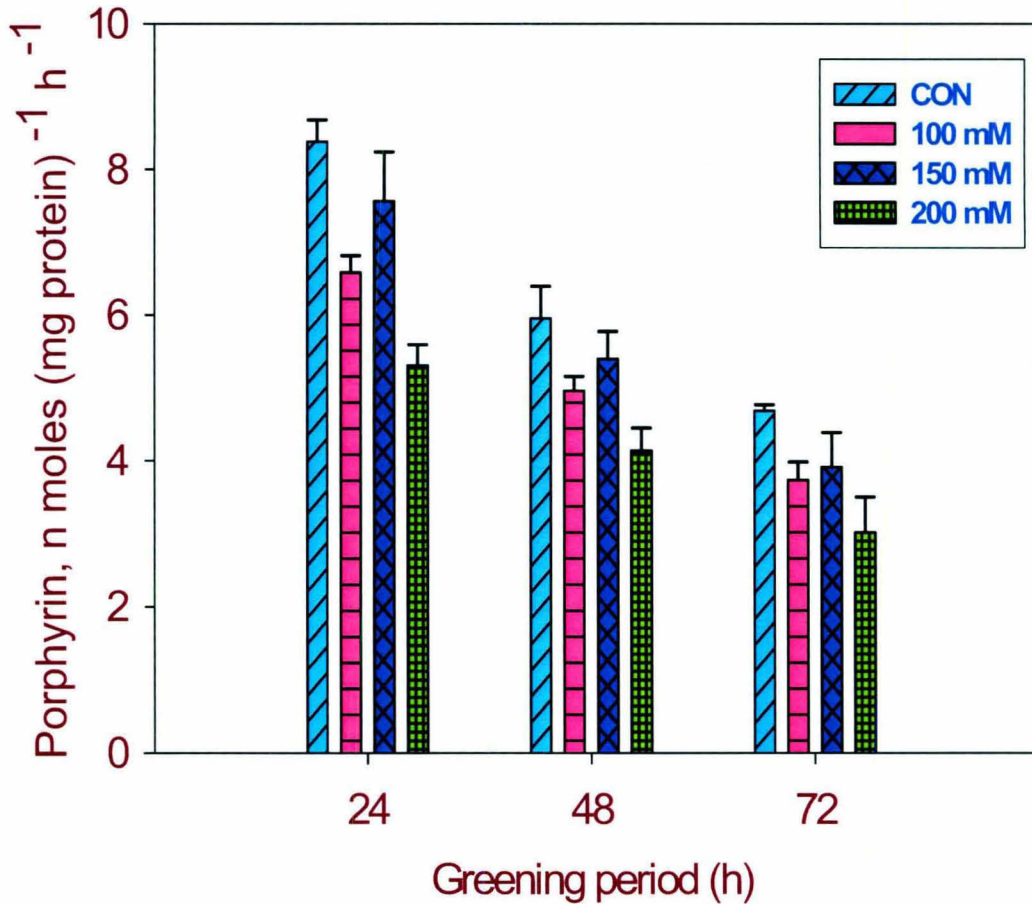


Fig 13: PBG deaminase activity in rice seedlings. Five-day-old etiolated rice seedlings of CSR10 and PB1 were treated with 0 and 200 mM NaCl 12 h prior to the transfer to cool white fluorescent+incandescent light ($100 \mu\text{moles photons m}^{-2} \text{s}^{-1}$), at 28°C at 75% relative humidity. PBGD activity was measured in response to salt stress after 24, 48, 72 h of greening as described in materials and methods. Each data point is the average of three replicates. The *error bar* represents SD.

Coprogen oxidase

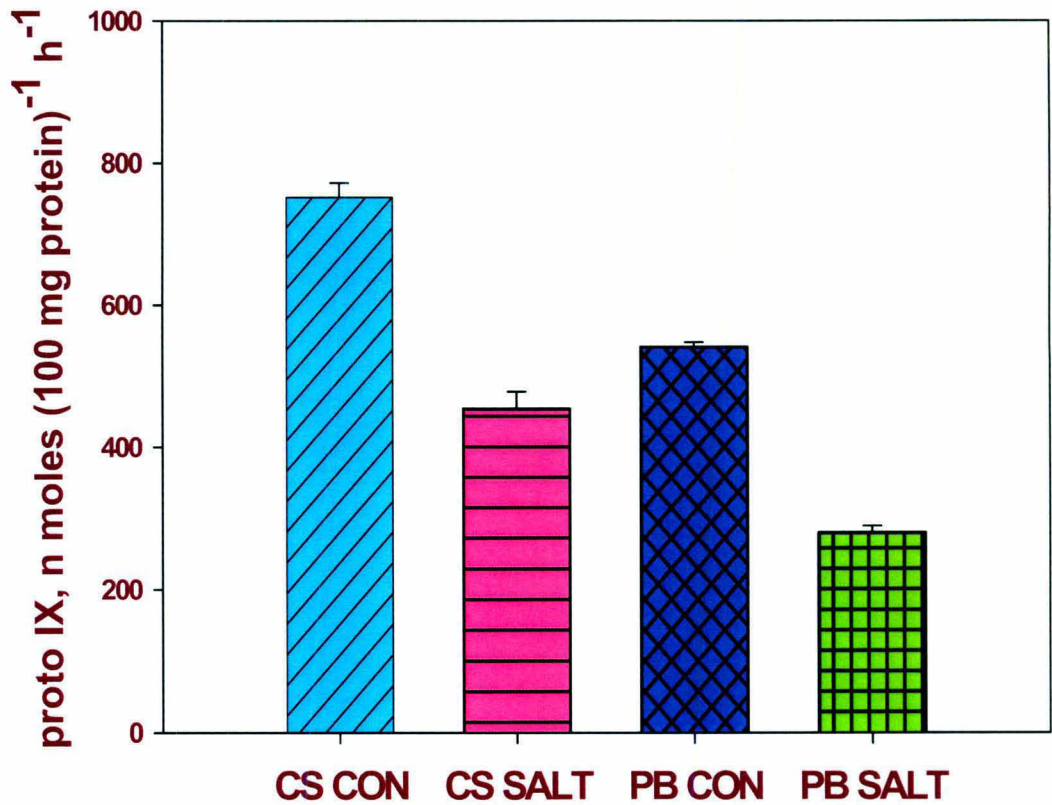


Fig 14: Coprogen oxidase activity in rice seedlings. Five-day-old etiolated rice seedlings of CSR10 and PB1 were treated with 0 and 200 mM NaCl 12 h prior to the transfer to cool white fluorescent+incandescent light ($100 \mu\text{moles photons m}^{-2} \text{s}^{-1}$), at 28°C at 75% relative humidity. Coprogen oxidase activity was monitored in response to salt stress after 24 h of greening as described in materials and methods. Each data point is the average of three replicates. The *error bar* represents SD.

Protox activity

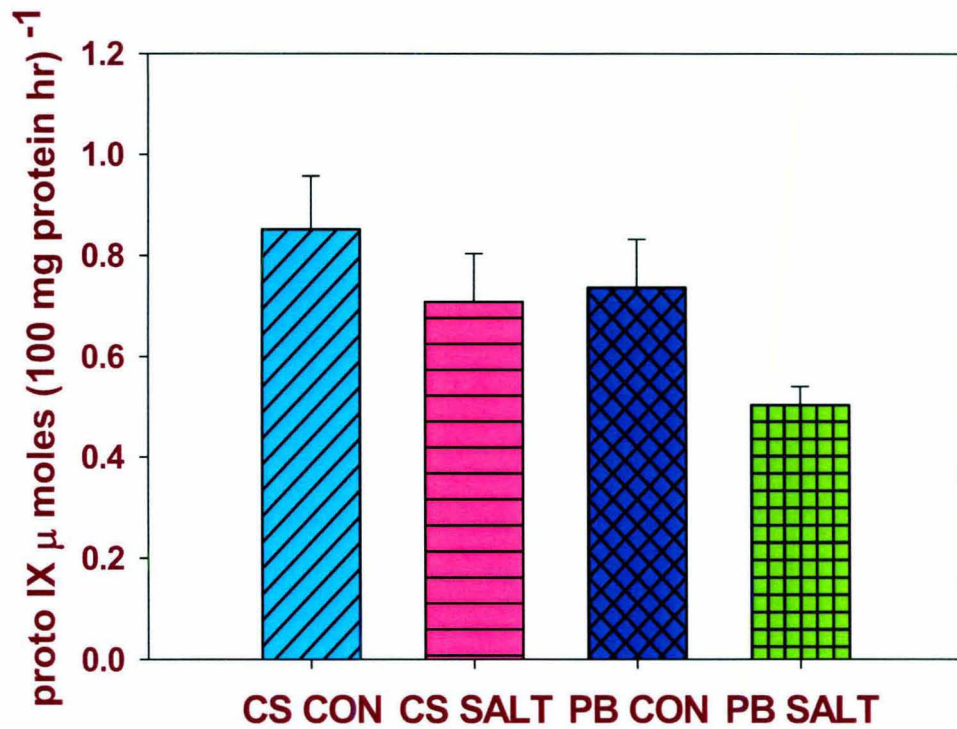


Fig 15: Protox activity in rice seedlings. Five-day-old etiolated rice seedlings of CSR10 and PB1 were treated with 0 and 200 mM NaCl 12 h prior to the transfer to cool white fluorescent+incandescent light (100 μmoles photons m⁻² s⁻¹), at 28°C at 75% relative humidity. Protox activity was monitored in response to salt stress after 24 h of greening as described in materials and methods. Each data point is the average of three replicates. The *error bar* represents SD.

Mg-chelatase activity

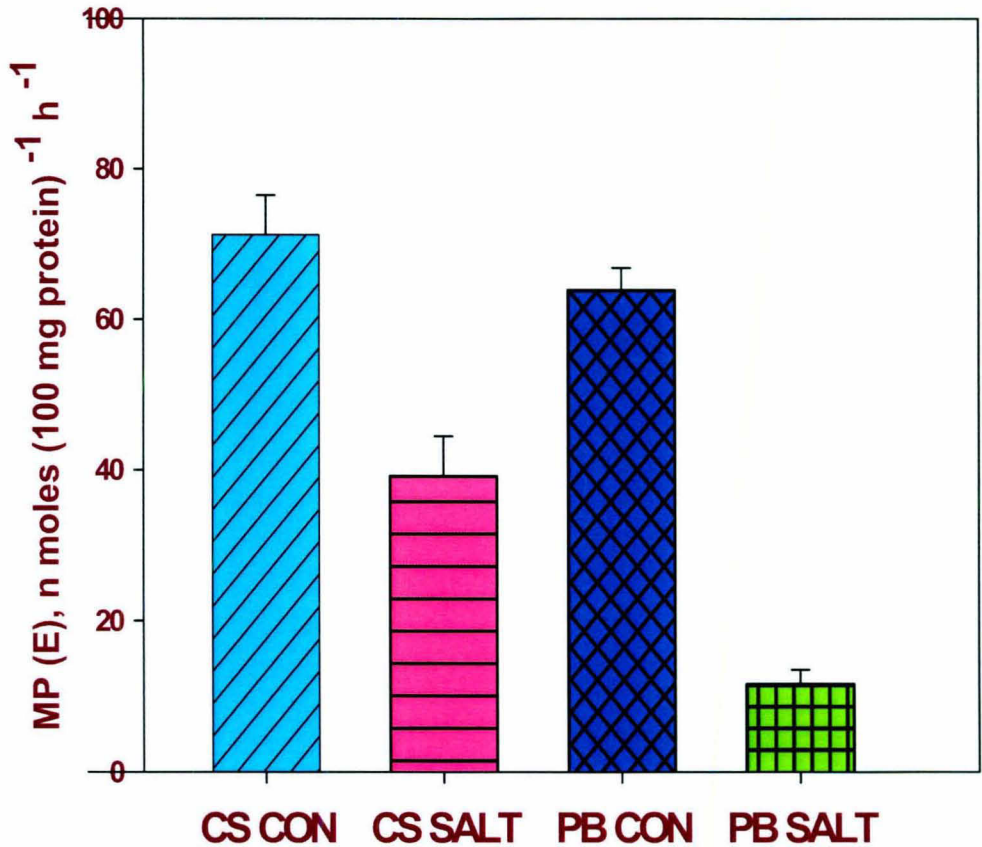


Fig 16: Mg-chelatase activity in rice seedlings. Five-day-old etiolated rice seedlings of CSR10 and PB1 were treated with 0 and 200 mM NaCl 12 h prior to the transfer to cool white fluorescent+incandescent light (100 μ moles photons m^{-2} s^{-1}), at 28^oC at 75% relative humidity. Mg-chelatase activity was monitored in response to salt stress after 24 h of greening as described in materials and methods. Each data point is the average of three replicates. The *error bar* represents SD.

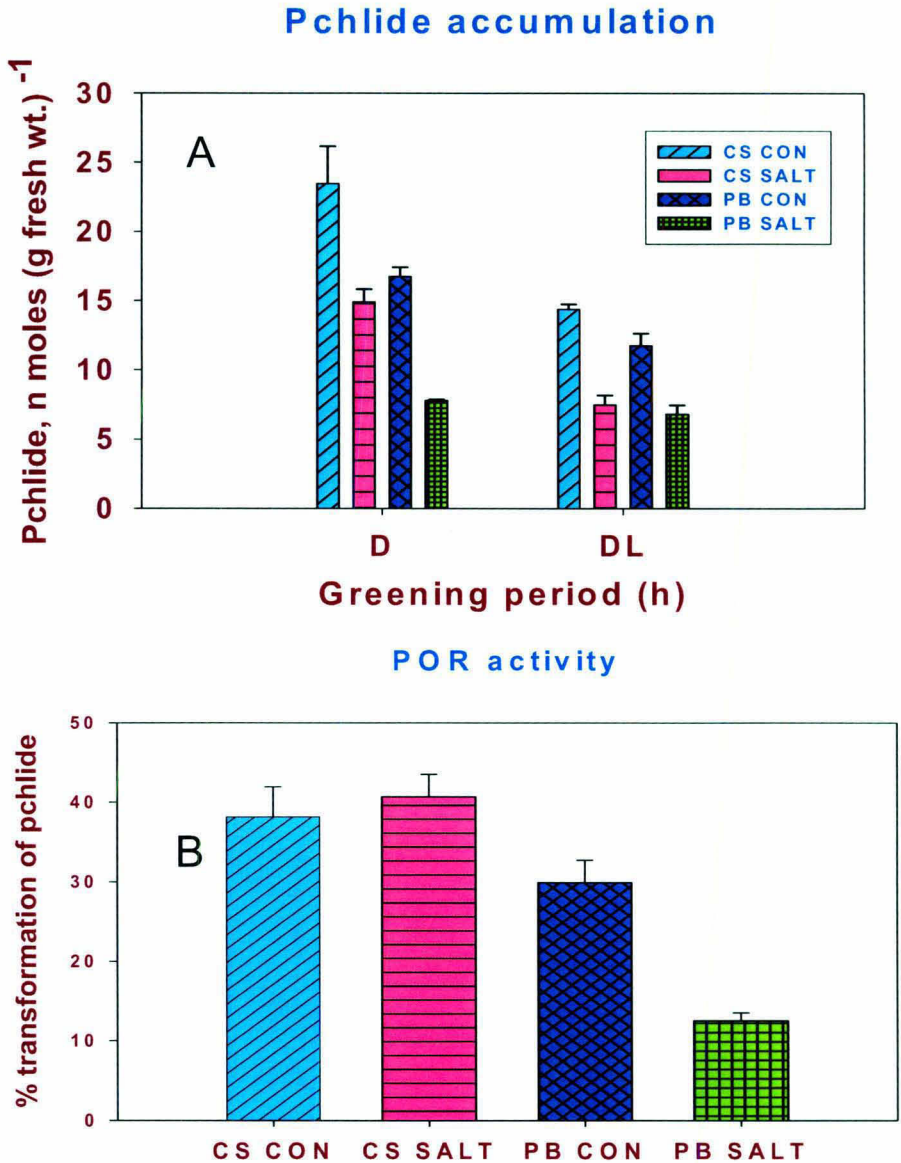


Fig 17: (A) Pchl_a content in rice seedlings and (B) POR activity. Five-day-old etiolated rice seedlings of CSR10 and PB1 were treated with 0 and 200 mM NaCl 12 h prior to the transfer to cool white fluorescent+incandescent light ($100 \mu\text{moles photons m}^{-2} \text{s}^{-1}$), at 28°C at 75% relative humidity. After 72 h of greening, seedlings were transferred to dark for 6h, their leaves were harvested and homogenized in dark and then seedlings were transferred to light ($100 \mu\text{moles photons m}^{-2} \text{s}^{-1}$) for 15 min and their leaves were harvested and homogenized. Pchl_a contents of dark incubated and 15 min light exposed seedlings were estimated as described in materials and methods. POR activity was calculated as percent transformation of pchl_a. Each data point is the average of three replicates. The *error bar* represents SD.

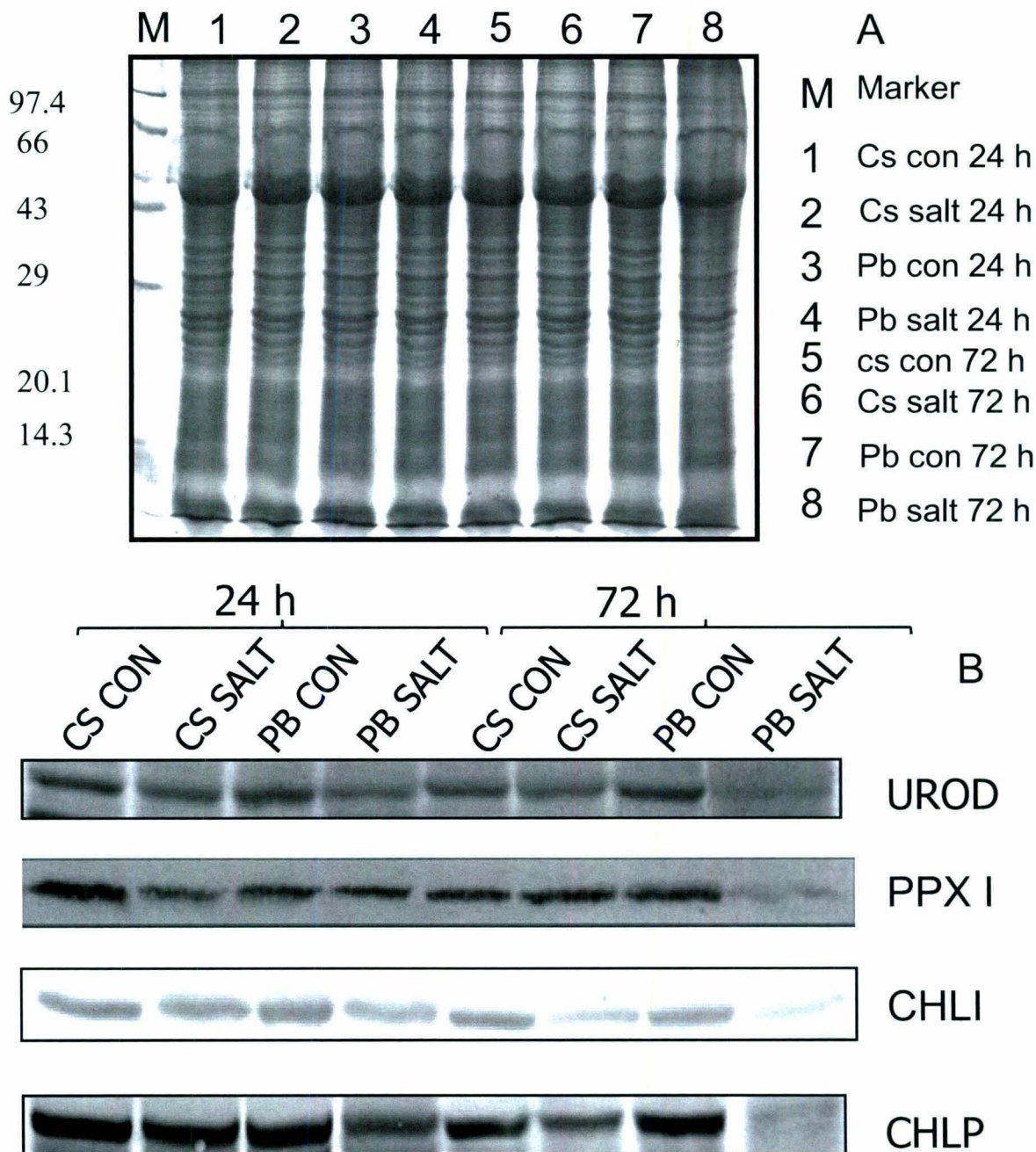


Fig 18: (A) Equal loading (30 μ g) of thylakoids proteins is shown as Coomassie Brilliant Blue stained in 12.5 % SDS-PAGE. (B) Immunoblot analysis of chlorophyll biosynthetic enzymes. Five-day-old etiolated rice seedlings of CSR10 and PB1 were treated with 0 and 200 mM NaCl 12 h prior to the transfer to cool white fluorescent+incandescent light (100 μ moles photons $m^{-2} s^{-1}$), at 28 $^{\circ}$ C at 75% relative humidity. Thylakoid membranes were isolated from control and salt stressed rice seedlings after 24 and 72 h of greening. Western blot was performed as described in materials and methods. Equal amounts of protein (30 μ g) were loaded on each lane.

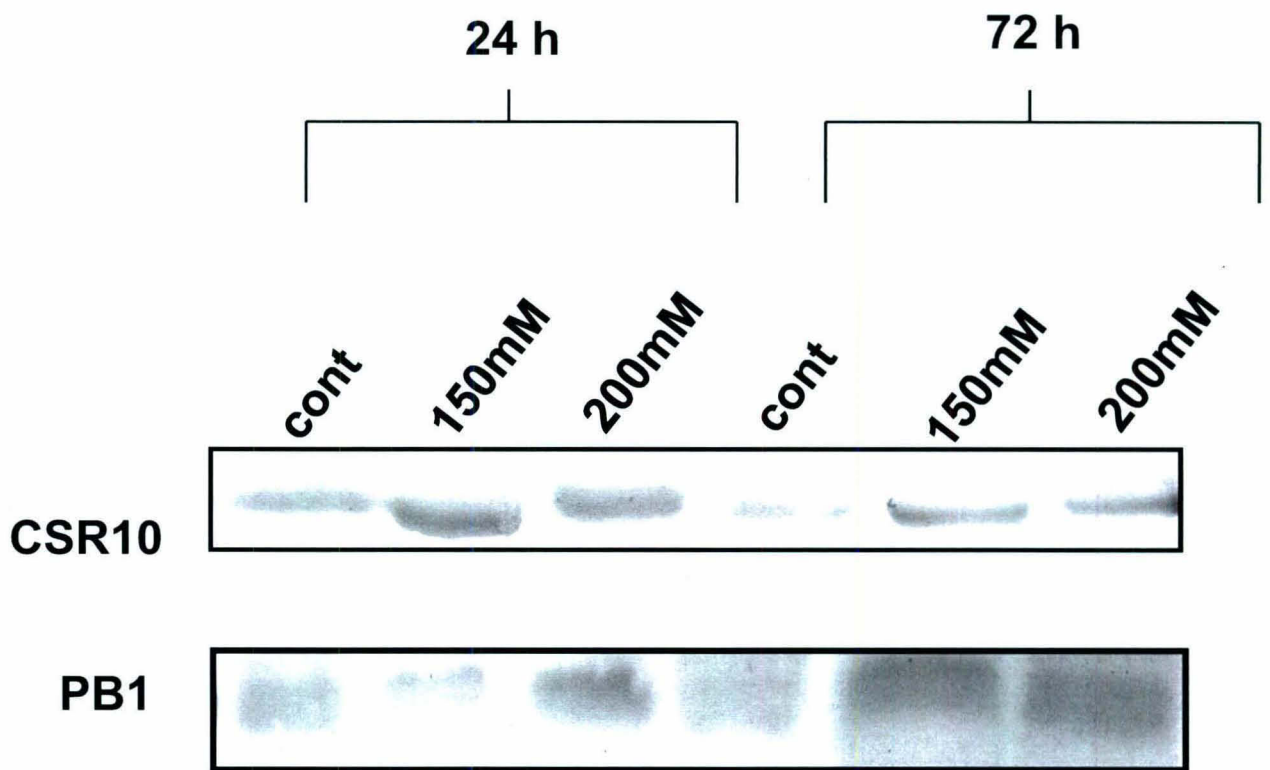


Fig 19: Immunoblot analysis of Protochlorophyllide oxidoreductase (POR). Five-day-old etiolated rice seedlings of CSR10 and PB1 were treated with 0, 150 and 200 mM NaCl 12 h prior to the transfer to cool white fluorescent+incandescent light ($100 \mu\text{moles photons m}^{-2} \text{s}^{-1}$), at 28°C at 75% relative humidity. Thylakoids membranes were isolated from control and salt stressed rice seedlings after 24 and 72 h of greening. Western blot was performed as described in materials and methods. Equal amounts of protein (30 μg) were loaded on each lane.

Urogen Decarboxylase (UROD): Expression of *UROD* that catalyses the conversion of uroporphyrinogen III to coproporphyrinogen III decreased in both the cultivars in response to salinity stress. However, the decrease was higher in PB1 as compared to that in CSR10 (Fig.18. A).

Protoporphyrinogen oxidase: The protein abundance of plastidic protoporphyrinogen oxidase I (PPX1), that catalyzes the conversion of proto-porphyrinogen IX to protoporphyrin IX, decreased with increasing salinity stress in both CSR10 and PB1. Relative decrease was much higher in PB1 as compared to that in salt tolerant CSR10 (Fig.18. A).

Magnesium chelatase subunit I (Chl I): In response to salt-stress the relative decline in protein expression of ChlI was quite severe in PB1 as compared to that in CSR10 (Fig.18. A).

Geranyl-geranyl reductase (chlP): Due to salt treatment, the protein abundance of *CHLP* declined severely in PB1 as compared to that in CSR10 (Fig.18. A).

Protochlorophyllide oxidoreductase (POR): POR protein abundance increased in both the cultivars in response to salt stress. The POR abundance severely declined in control seedlings after 72 h of greening. However, its abundance increased due to 150 mM and 200 mM NaCl treatment after 24 h and 72 h of greening (Fig.19).

Gene expression of chlorophyll biosynthetic enzymes:

To correlate the protein abundance of Chl biosynthetic enzymes with that of their message levels Northern blot / RT-PCR analysis was done at 24 and 72 h of greening in response to 200 mM NaCl stress (Fig.20, 21).

The gene *GluTR* encodes Glutamyl-t-RNA reductase enzyme that catalyses conversion of Glutamyl-t-RNA into Glutamate-1-semialdehyde (GSA) in chlorophyll biosynthetic pathway. *GluTR* expression increased with salt stress in both the cultivars.

The gene expression of *GSAT* increased in CSR10 and declined in PB1 in response to salt stress.

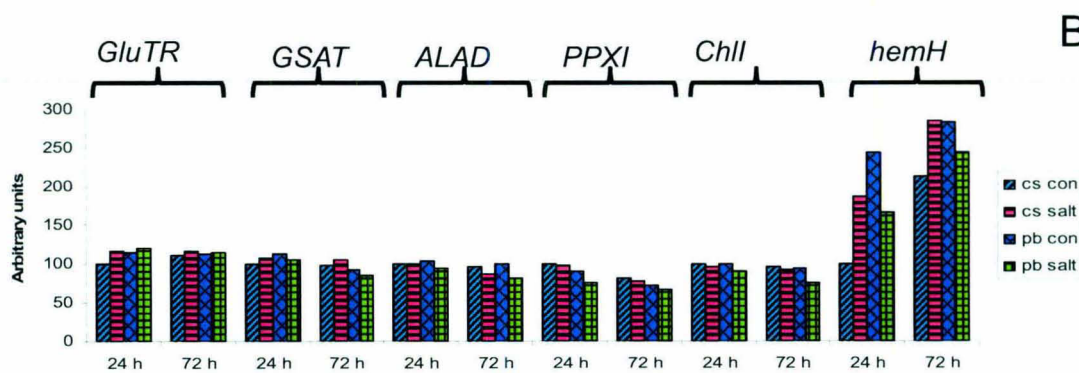
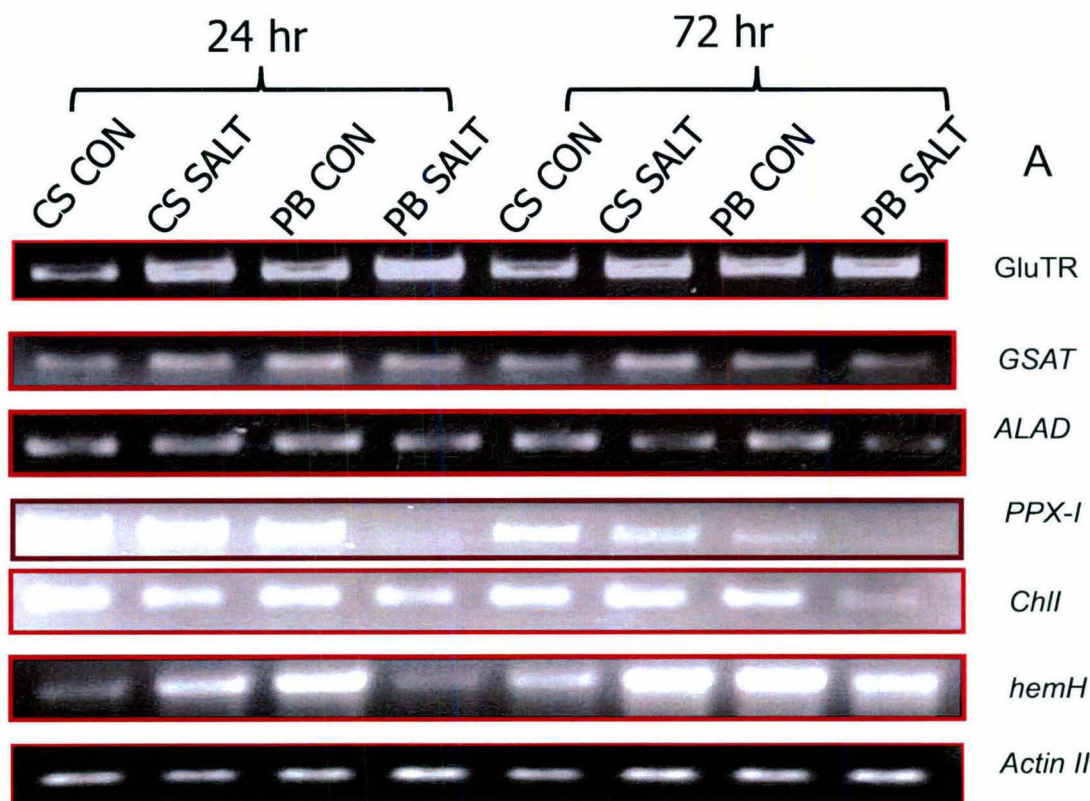


Fig 21: (A) Gene expression of chlorophyll biosynthetic enzymes. Five-day-old etiolated rice seedlings of CSR10 and PB1 were treated with 0 and 200 mM NaCl 12 h prior to the transfer to cool white fluorescent+incandescent light ($100 \mu\text{moles photons m}^{-2} \text{s}^{-1}$), at 28°C at 75% relative humidity. Semi quantitative RT-PCR was performed as in materials and methods. Total RNA was extracted from control and salt stressed leaves of rice seedlings after 24 and 72 h of greening and cDNA was made from $2 \mu\text{g}$ of total RNA as described in materials and methods. (B) Bar diagram of gene expression (%)

The message abundance of *ALAD* that encodes for 5-amino levulinic acid dehydratase declined in response to salt stress and greening period in both of the cultivars. However the relative decline is more in PB1 than CSR10.

The *PBGD* encodes PBG deaminase enzyme that converts PBG to hydroxymethylbilane in porphyrin biosynthetic pathway. The *PBGD* expression decreased with increasing length of greening in the absence or presence of 200 mM NaCl. However the decrease was more severe in salt-sensitive PB1.

The message abundance of *UroD* declined in response to salt stress in both the cultivars. Its expression reduced with increase in the length of the greening period. The relative decline was more in salt sensitive PB1.

The gene expression of *PPX-I* that encodes for Protoporphyrinogen oxidase-I declined in response to salt stress and greening period in both the cultivars. However the decline in transcripts abundance of this enzyme was more severe in PB1 as comparative to that of CSR10.

The transcripts level of gene *ChlI*, which encodes for I subunit of Mg-chelatase was down regulated in response to salt stress in both the cultivars at 72 h of salt stress. After 24 h of salt stress Chl I expression increased partially in CSR10 whereas its expression declined in PB1.

The expression of *hemH* that encodes for ferrochelatase, at branch point in chlorophyll and heme biosynthetic pathway and shares substrate (Protoporphyrin IX) with Mg-chelatase, increased in CSR10 in response to salt stress whereas its expression decreased in PB1. Its expression is higher in PB1 than CSR10 under non-stressed control conditions.

The *CAO* encodes chlorophyll a oxygenase enzyme that converts Chl a to Chl b in chlorophyll biosynthesis pathway. Its transcripts level declined in response to salt stress in both the cultivars. The gene expression reduced with increasing length of time. There was severe decrease in its transcripts abundance in PB1 as compared to CSR10 after 72 h of salt stress.

Shibata shift:

To monitor Shibata shift leaves were taken from control and salt stressed etiolated seedlings of CSR10 and PB1. They were illuminated by a pulse of red light (1500 μ moles

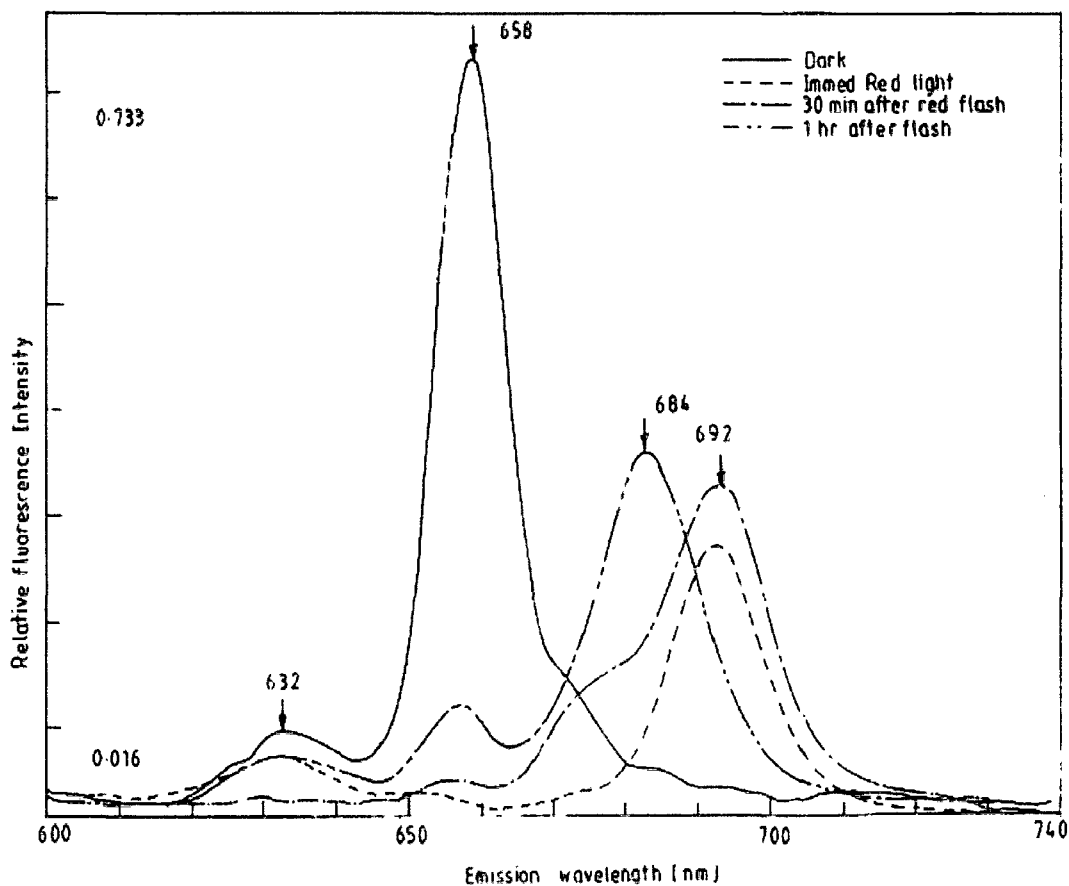


Fig22: Low temperature (77K) fluorescence emission spectra (E440) of leaves showing Shibata-shift. Five-day-old etiolated rice seedlings of CSR10 were treated with 0 mM NaCl 12 h prior to the transfer to cool white fluorescent+incandescent light ($100 \mu\text{moles photons m}^{-2} \text{s}^{-1}$) for 72 h of greening, at 28°C at 75% relative humidity. Fluorescence emission spectra of leaves were recorded in ratio mode in a photon counting SLM-AMINCO 8000 spectrofluorometer having excitation and emission slit width of 4 nm. Spectra were not corrected for the instrument response.

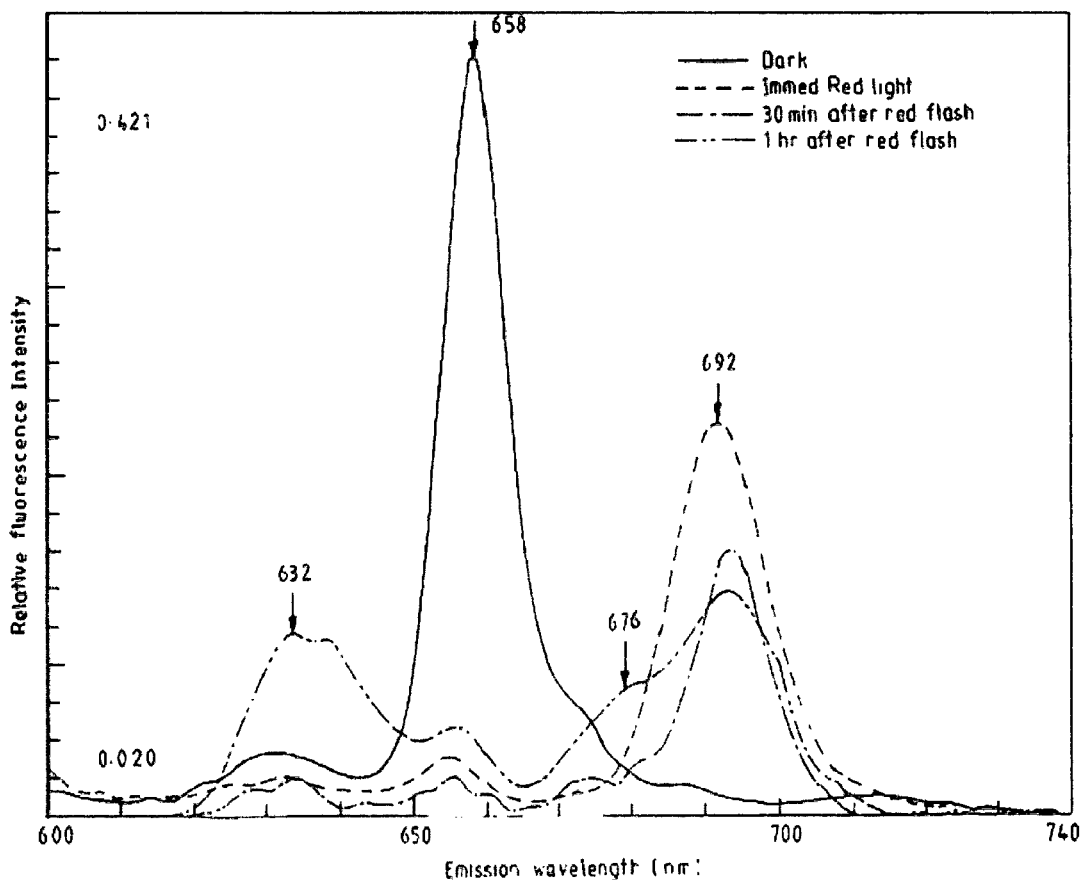


Fig 23: Low temperature (77K) fluorescence emission spectra (E440) of leaves showing Shibata-shift. Five-day-old etiolated rice seedlings of CSR10 were treated with 200 mM NaCl 12 h prior to the transfer to cool white fluorescent+incandescent light ($100 \mu\text{moles photons m}^{-2} \text{s}^{-1}$) for 72 h of greening, at 28°C at 75% relative humidity. Fluorescence emission spectra of leaves were recorded in ratio mode in a photon counting SLM-AMINCO 8000 spectrofluorometer having excitation and emission slit width of 4 nm. Spectra were not corrected for the instrument response.

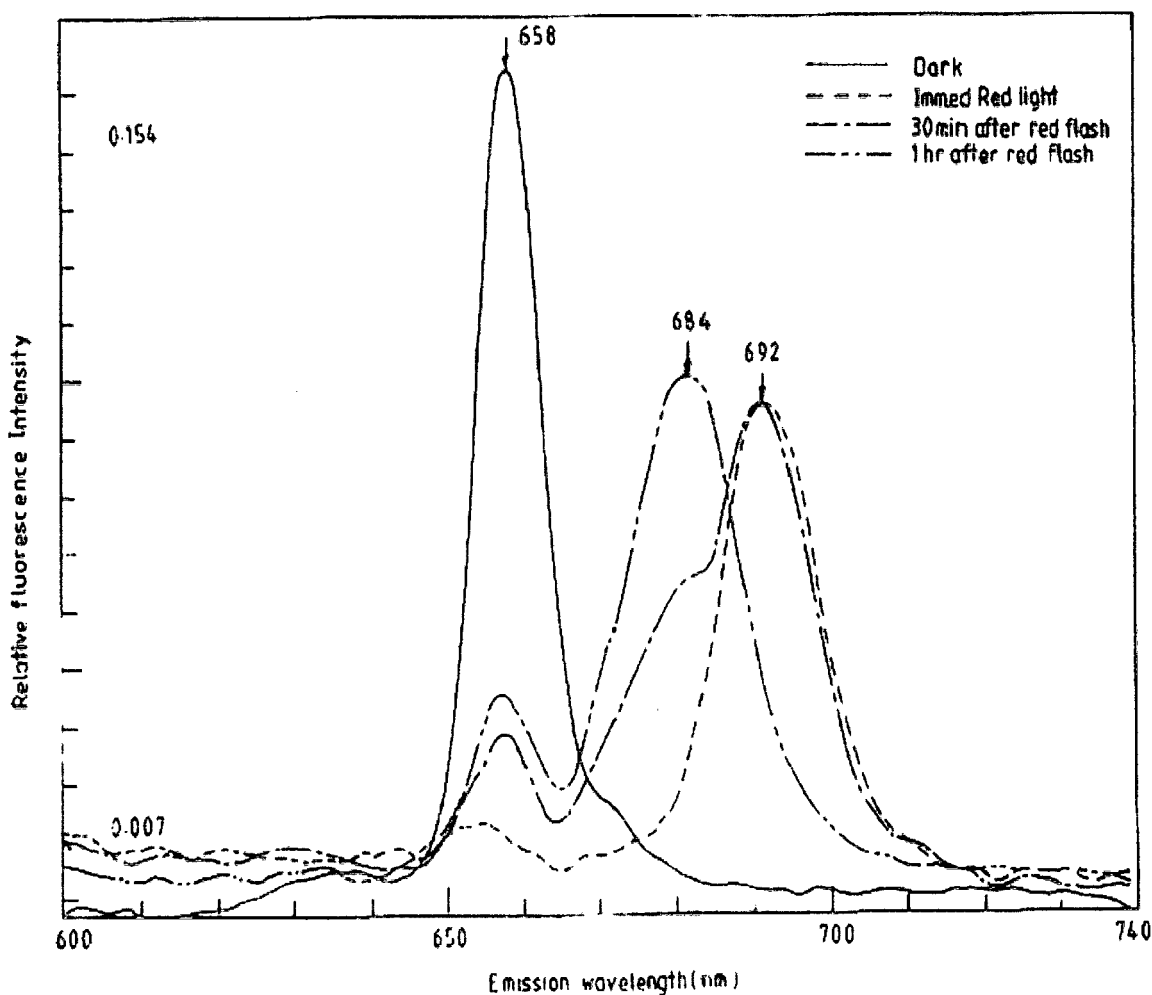


Fig 24: Low temperature (77K) fluorescence emission spectra (E440) of leaves showing Shibata-shift. Five-day-old etiolated rice seedlings of PB1 were treated with 0 mM NaCl 12 h prior to the transfer to cool white fluorescent+incandescent light ($100 \mu\text{moles photons m}^{-2} \text{s}^{-1}$) for 72 h of greening, at 28°C at 75% relative humidity. Fluorescence emission spectra of leaves were recorded in ratio mode in a photon counting SLM-AMINCO 8000 spectrofluorometer having excitation and emission slit width of 4 nm. Spectra were not corrected for the instrument response.

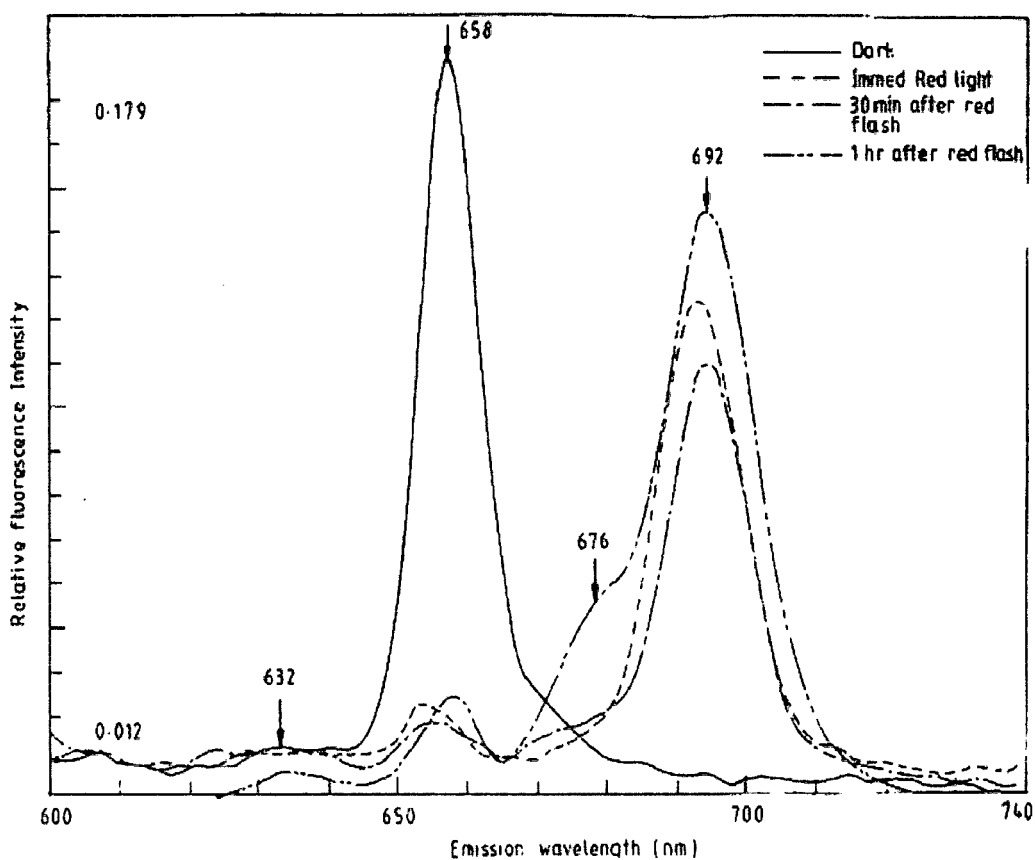


Fig 25: Low temperature (77K) fluorescence emission spectra (E440) of leaves showing Shibata-shift. Five-day-old etiolated rice seedlings of PB1 were treated with 200 mM NaCl 12 h prior to the transfer to cool white fluorescent+incandescent light ($100 \mu\text{moles photons m}^{-2} \text{s}^{-1}$) for 72 h of greening, at 28°C at 75% relative humidity. Fluorescence emission spectra of leaves were recorded in ratio mode in a photon counting SLM-AMINCO 8000 spectrofluorometer having excitation and emission slit width of 4 nm. Spectra were not corrected for the instrument response.

$\text{m}^{-2} \text{s}^{-1}$) of 0.2 seconds and were frozen in liquid nitrogen either immediately after red flash or after 30 min or 1 h of dark incubation subsequent to flash illumination. Fluorescence emission spectra (E440) of leaves were recorded before as well as after red flashes. Immediately after flash illumination, leaves from control seedlings of CSR10 exhibited a peak at 692 nm with a concomitant decrease of photo-transformable peak at 658 nm (Fig 22). After 30 min. of flash illumination, a small hump at 684 nm appeared. After 1 h of dark incubation following red flash, the peak at 692 nm disappeared with a concomitant increase of peak at 684 nm (Fig 22).

In salt stressed seedlings of CSR10 following flash illumination, the 657 nm peak declined due to photo-transformable Pchl_a with simultaneous appearance of peak at 692 nm. After 30 min. of dark incubation, unlike their control counterpart, the hump at 684 nm was not observed. After 1 h of flash incubation a small hump at 684 nm was observed (Fig 23).

One h after salt treatment immediately after flash illumination, leaves from control seedlings of PB1 exhibited a peak at 692 nm with a concomitant decrease of photo-transformable peak at 658 nm (Fig 24). After 30 min. of flash illumination, a small hump at 684 nm appeared. After 1 h of dark incubation following red flash, the peak at 692 nm disappeared with a concomitant increase of peak at 684 nm (Fig 24).

In salt stressed seedlings of PB1 following flash illumination, the 658 nm peak declined due to photo-transformable Pchl_a with simultaneous appearance of peak at 692 nm. After 30 min. of dark incubation, unlike their control counterpart, the hump at 684 nm was not observed. However after 1 h of flash a small hump at 684 nm appeared (Fig 25). Control seedlings of both the cultivars show similar pattern. However in salt stressed seedlings after 1 h of flash illumination hump regenerated at 684 nm was partially smaller than that of CSR10.

Photosynthetic response of plants to salt stress:

Chl a fluorescence

F_0 , F_m , F_v/F_m , Electron transport rate (etr), quantum yield of photosystemII (ϕ PSII), photochemical quenching (qP) and non-photochemical quenching (qN) were measured by PAM fluorometer (PAM 2100). Five-d-old etiolated control and salt-stressed rice seedlings of salt sensitive PB1 and salt tolerant CSR10 were treated with 0 mM, 100 mM, 150 mM or 200 mM

NaCl 12 h prior to the transfer to cool white fluorescent+incandescent light ($100 \mu\text{moles photons m}^{-2} \text{ s}^{-1}$), at 28°C at 75% relative humidity maintained by a Conviron plant growth chamber as described before. Measurements were done after 24, 48, and 72 hours of greening in the absence and the presence of different concentrations of NaCl.

F₀, F_m and F_v/F_m: - After application of 200 mM NaCl for 24 h F₀ fluorescence was not affected in the salt resistant genotype CSR10 however under identical conditions F₀ declined in salt sensitive PB1 cultivar. After 48h and 72 h of greening, F₀ of both the cultivars declined (Fig.26 A). The decrease in F₀ was higher in PB1 than that of CSR10. This was probably due to reduced presence of Chl in PB1 as compared to that in CSR10.

After 24 h of greening in the response of 200 mM NaCl, due to marginal changes in the F_m, the F_v/F_m was not affected in both the cultivars. After 48 h of stress treatment the F_v/F_m of CSR10 was not affected. However the F_v/F_m declined in salt sensitive PB1. Longer stress treatment (72 h) resulted in decrease of F_v/F_m in both cultivars although the decline F_v/F_m was higher in PB1 as compared to that in CSR10 (Fig.26 C).

Electron transport rate (etr):- The estimated electron transport rate of CSR10 and PB1 at 24, 48 and 72 hours of greening are shown in Fig 27, 28 and 29 (A and B) respectively. Fig 27, 28 and 29 (C) show the etr as % of control at maximum light intensity. Electron transport rate of both the varieties increased in response to increase in the light intensity. The etr of both the cultivars decreased as compared to control with increase in salt stress as well as the greening period. The maximum decline in etr was observed in both the genotypes after 72 h of greening in 200 mM NaCl stress. However, the decline of etr of PB1 was higher than that of CSR10. After 72 h of greening in 200 mM NaCl the etr declined by 40% in CSR10 and by 75% in PB1.

Quantum yield of photosystemII (PSII):- Quantum yield of photosystemII of CSR10 and PB1 at 24, 48 and 72 hours of greening are shown in Fig 30, 31 and 32 respectively. Part C of the figures show yield as % of control at maximum light intensity. Quantum yield of photosystemII of CSR10 and PB1 decreased with increase in the light intensity. As compared to respective controls, the yield decreased in both the cultivars with increase in salt concentration, hours of

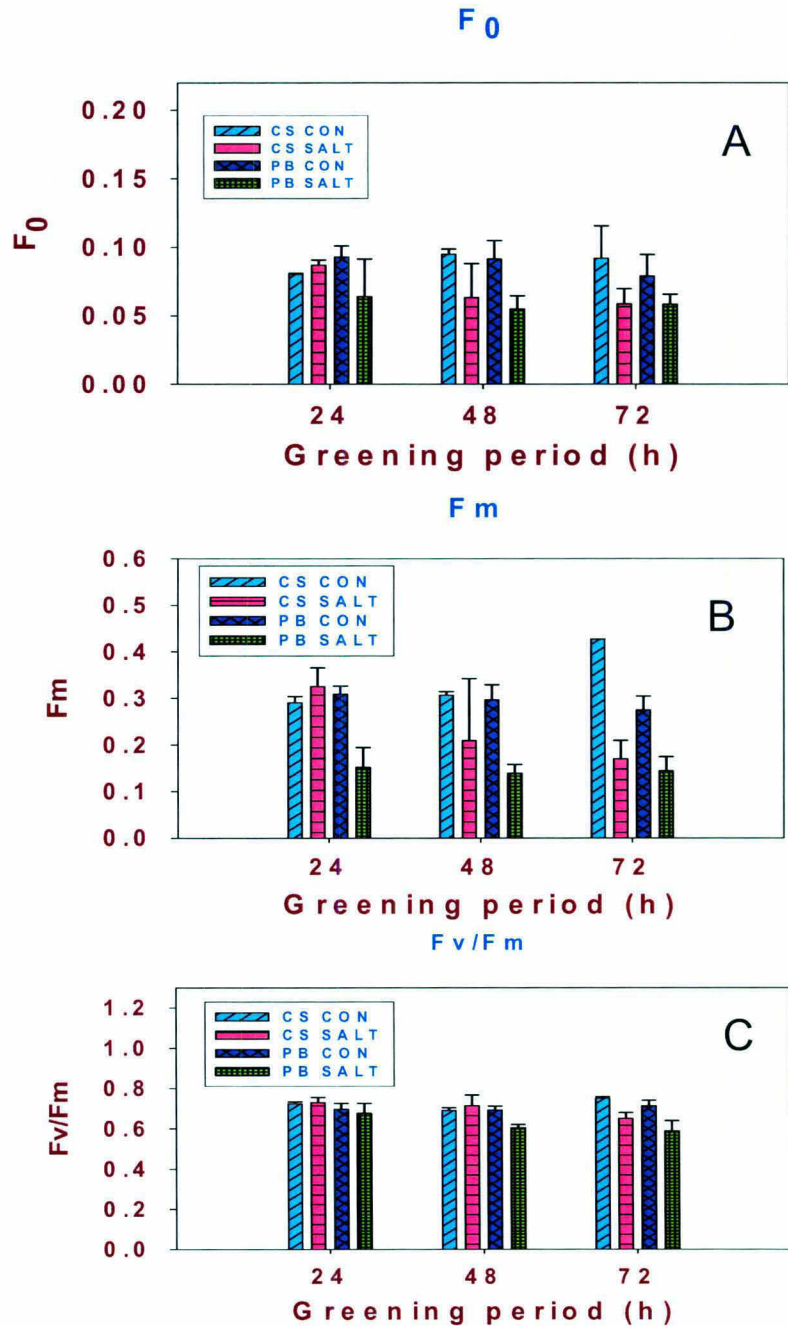


Fig 26: F_0 , F_m and F_v/F_m . Five-day-old etiolated rice seedlings of CSR10 and PB1 were treated with 0 mM and 200 mM NaCl 12 h prior to the transfer to cool white fluorescent+incandescent light ($100 \mu\text{moles photons m}^{-2} \text{s}^{-1}$), at 28°C at 75% relative humidity. (A) F_0 , (B) F_m and (C) F_v/F_m were measured from control and salt stressed seedlings after 24, 48 and 72 h of greening by PAM-2100 fluorometer as described in materials and methods. Each data point is the average of three replicates. The error bar represents SD.

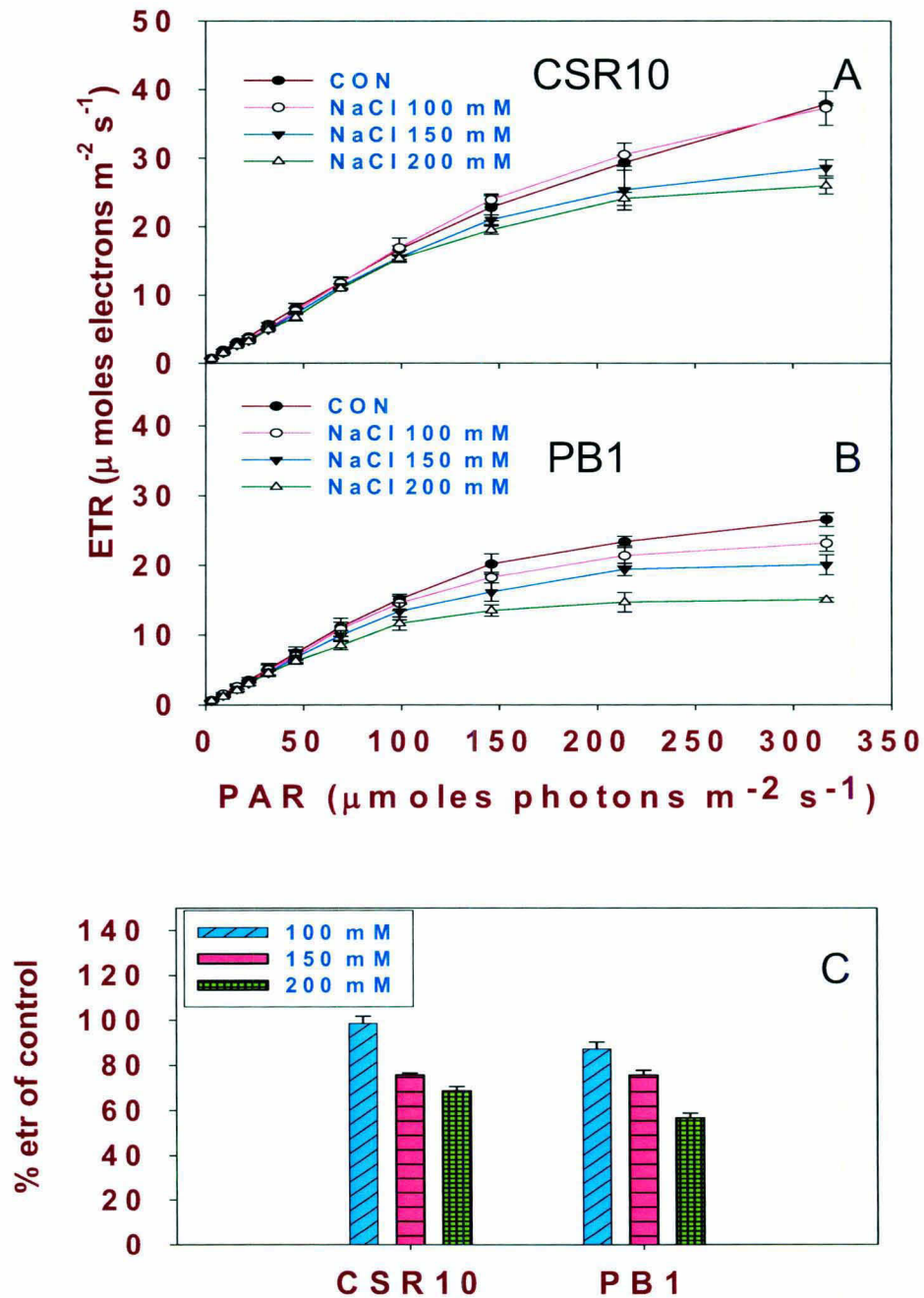


Fig 27: Electron transport rate (etr) of photosystem II (PSII) of control and salt-stressed rice seedlings of (A) CSR10 and (B) PB1. Five-d-old etiolated seedlings were treated with 0 mM, 100 mM, 150 mM and 200 mM NaCl 12 h prior to the transfer to cool white fluorescent+incandescent light ($100 \mu\text{moles photons m}^{-2} \text{s}^{-1}$), at 28°C at 75% relative humidity. Electron transport rate was measured after 24 h of greening as described in materials and methods. Percent of control is shown in fig.C. Each data point is the average of three replicates. The *error bar* represents SD.

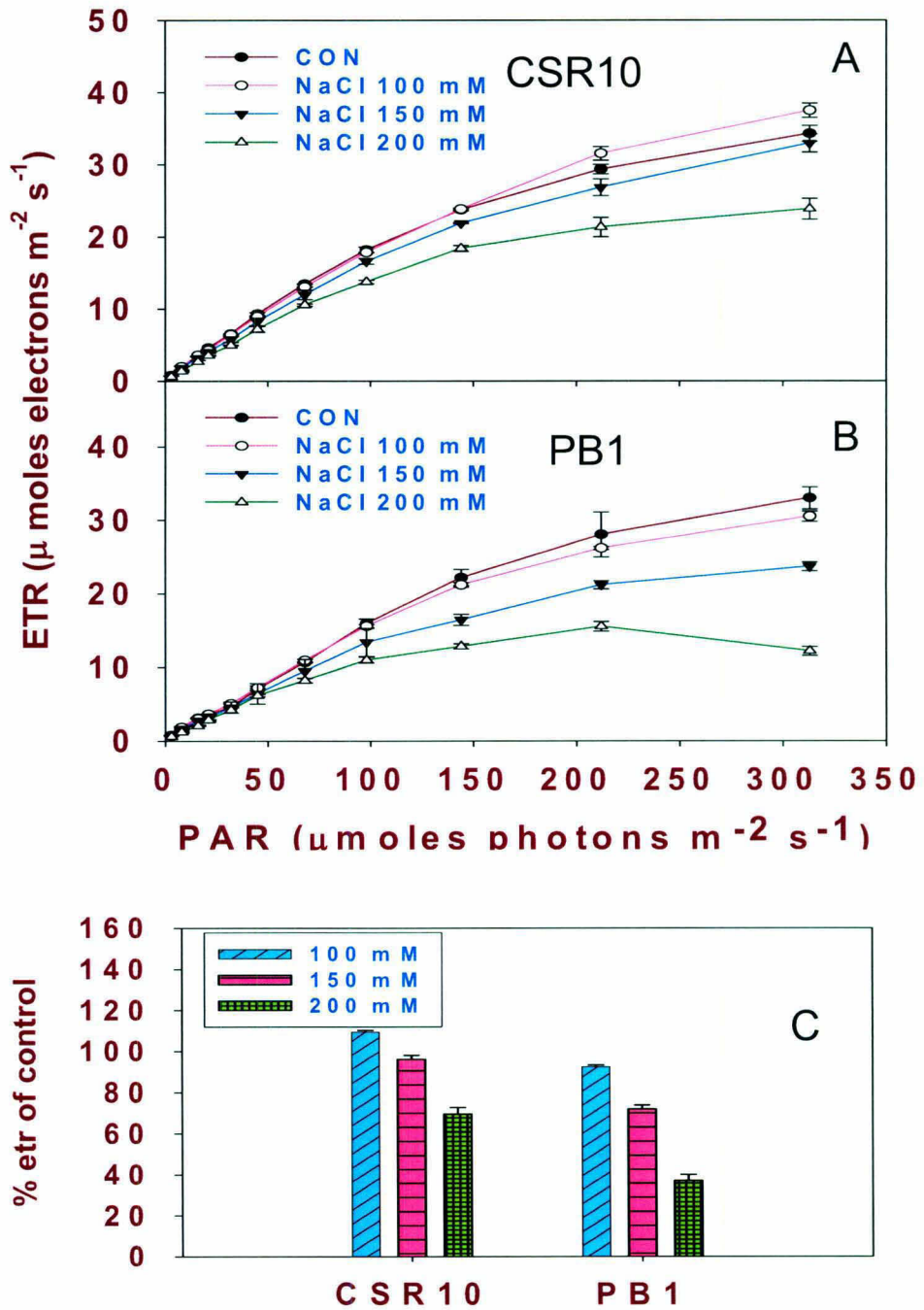


Fig 28: Electron transport rate (etr) of photosystem II (PSII) of control and salt-stressed rice seedlings of (A) CSR10 and (B) PB1. Five-d-old etiolated seedlings were treated with 0 mM, 100 mM, 150 mM and 200 mM NaCl 12 h prior to the transfer to cool white fluorescent+incandescent light ($100 \mu\text{moles photons m}^{-2} \text{s}^{-1}$), at 28°C at 75% relative humidity. Electron transport rate was measured after 48 h of greening as described in materials and methods. Percent of control is shown in fig.C. Each data point is the average of three replicates. The *error bar* represents SD.

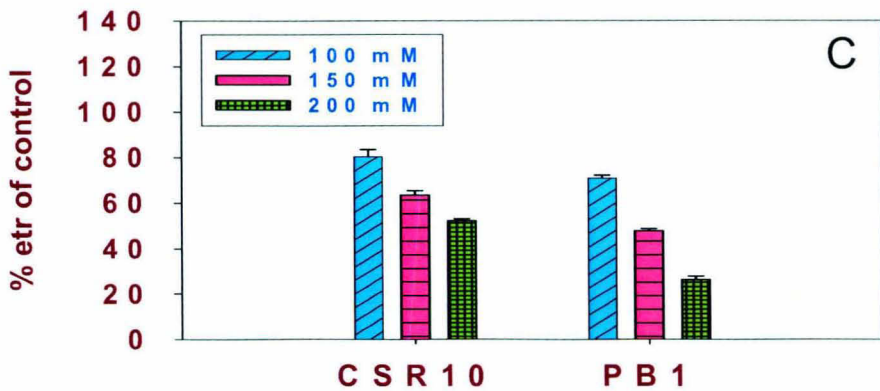
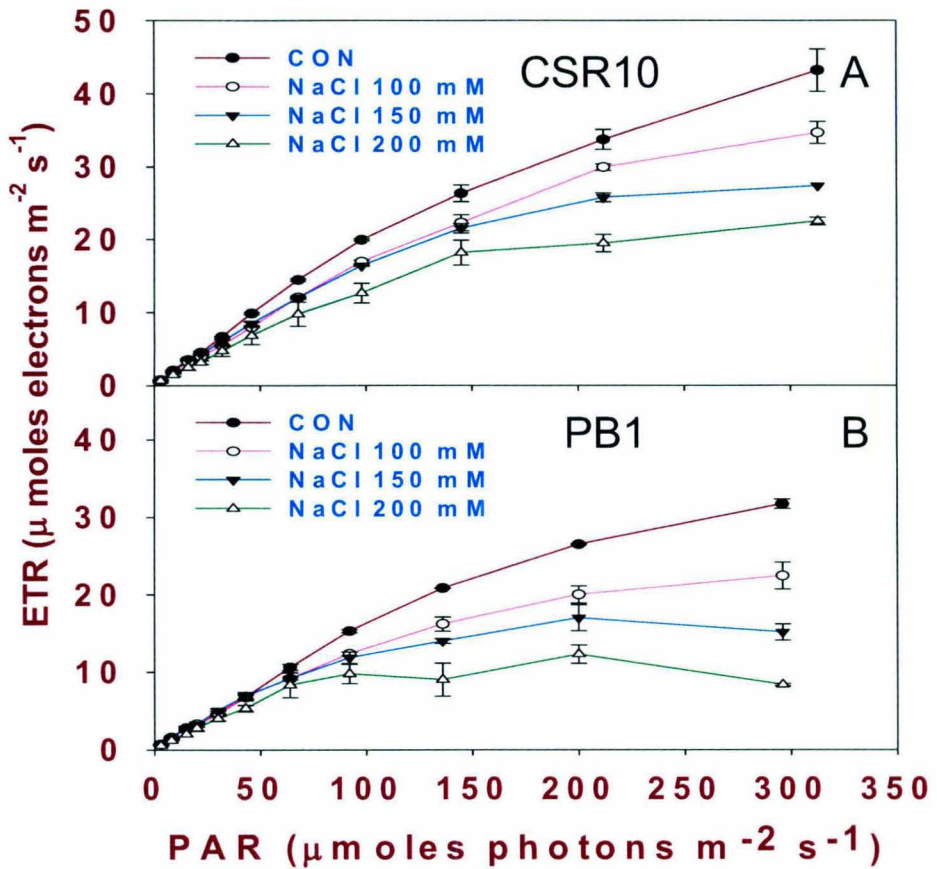


Fig 29: Electron transport rate (etr) of photosystem II (PSII) of control and salt-stressed rice seedlings of (A) CSR10 and (B) PB1. Five-d-old etiolated seedlings were treated with 0 mM, 100 mM, 150 mM and 200 mM NaCl 12 h prior to the transfer to cool white fluorescent+incandescent light ($100 \mu\text{moles photons m}^{-2} \text{s}^{-1}$), at 28°C at 75% relative humidity. Electron transport rate was measured after 72 h of greening as described in materials and methods. Percent of control is shown in fig.C. Each data point is the average of three replicates. The *error bar* represents SD.

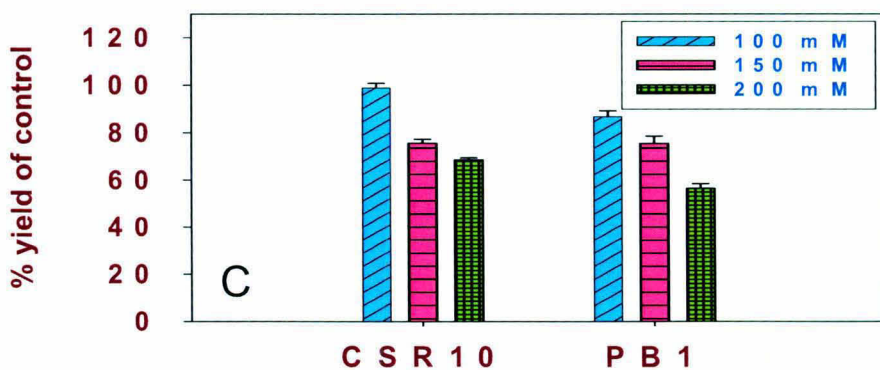
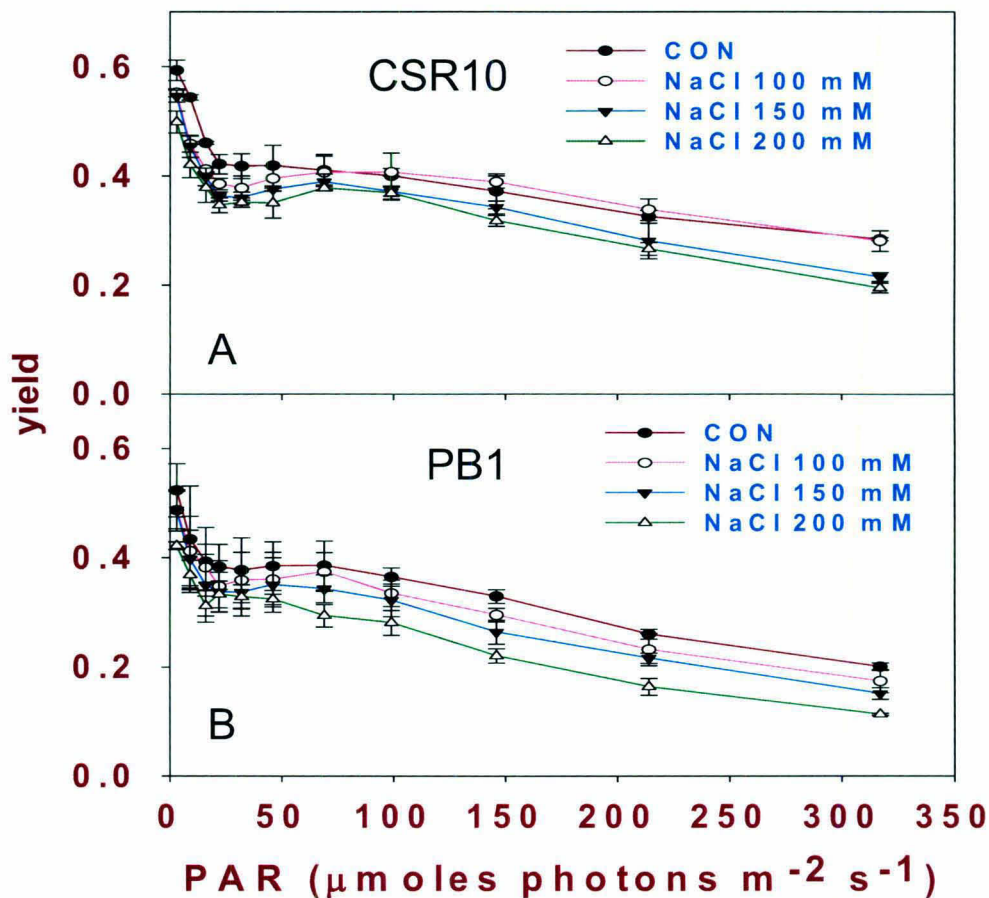


Fig 30: Quantum yield of photosystem II (PSII) of control and salt-stressed rice seedlings of (A) CSR10 and (B) PB1. Five-d-old etiolated seedlings were treated with 0 mM, 100 mM, 150 mM and 200 mM NaCl 12 h prior to the transfer to cool white fluorescent+incandescent light ($100 \mu\text{moles photons m}^{-2} \text{s}^{-1}$), at 28°C at 75% relative humidity. Quantum yield was measured after 24 h of greening as described in materials and methods. Percent of control is shown in fig.C. Each data point is the average of three replicates. The *error bar* represents SD.

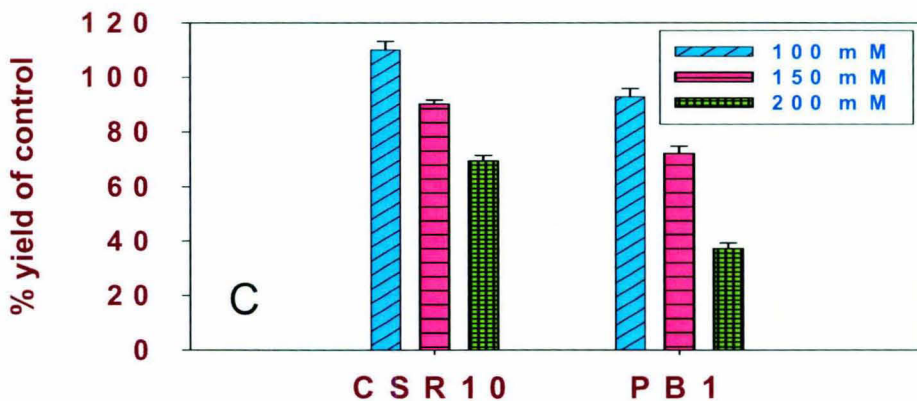
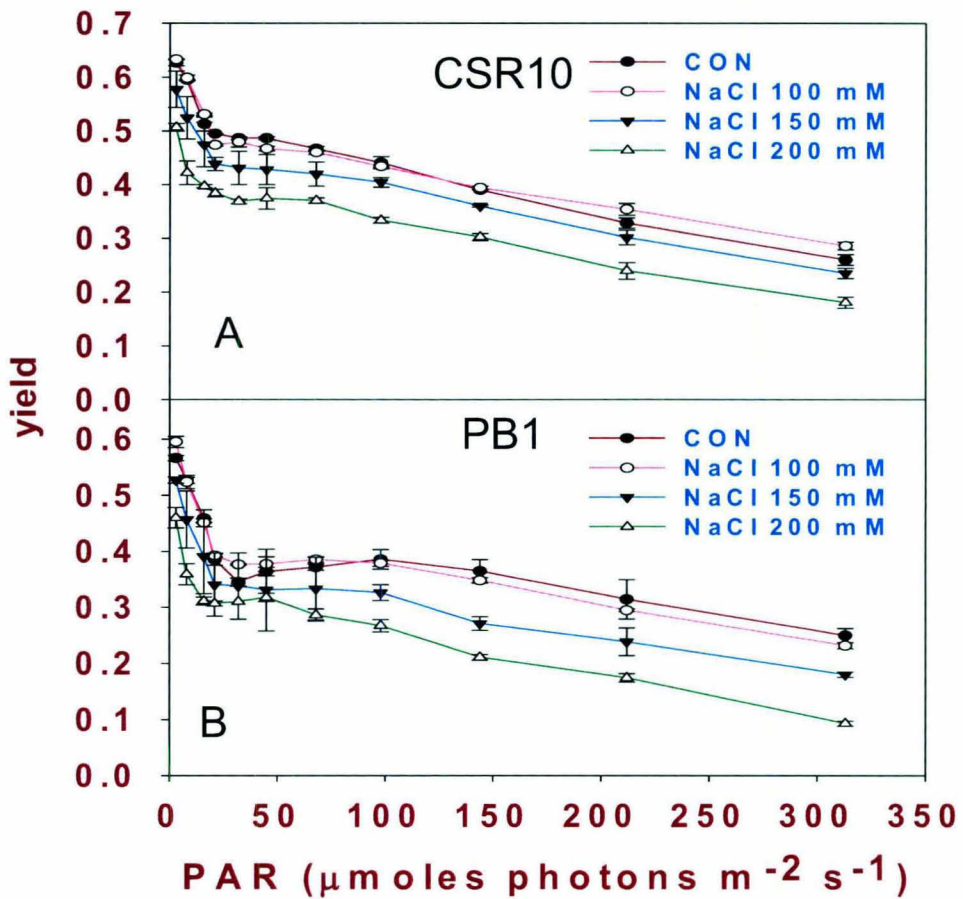


Fig 31: Quantum yield of photosystem II (PSII) of control and salt-stressed rice seedlings of (A) CSR10 and (B) PB1. Five-d-old etiolated seedlings were treated with 0 mM, 100 mM, 150 mM and 200 mM NaCl 12 h prior to the transfer to cool white fluorescent+incandescent light ($100 \mu\text{moles photons m}^{-2} \text{s}^{-1}$), at 28°C at 75% relative humidity. Quantum yield was measured after 48 h of greening as described in materials and methods. Percent of control is shown in fig.C. Each data point is the average of three replicates. The *error bar* represents SD.

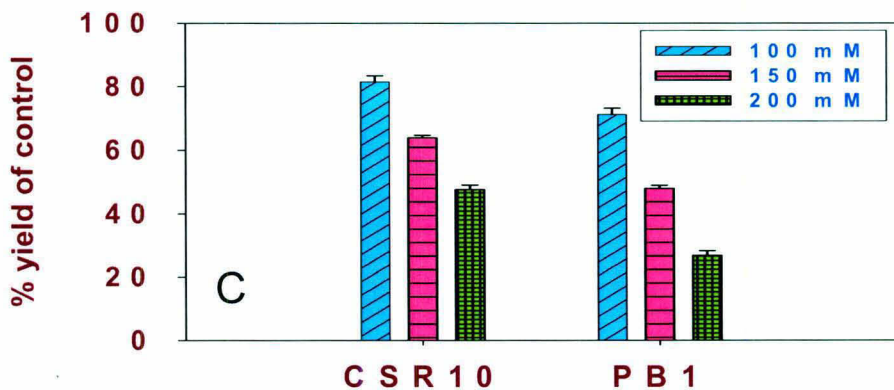
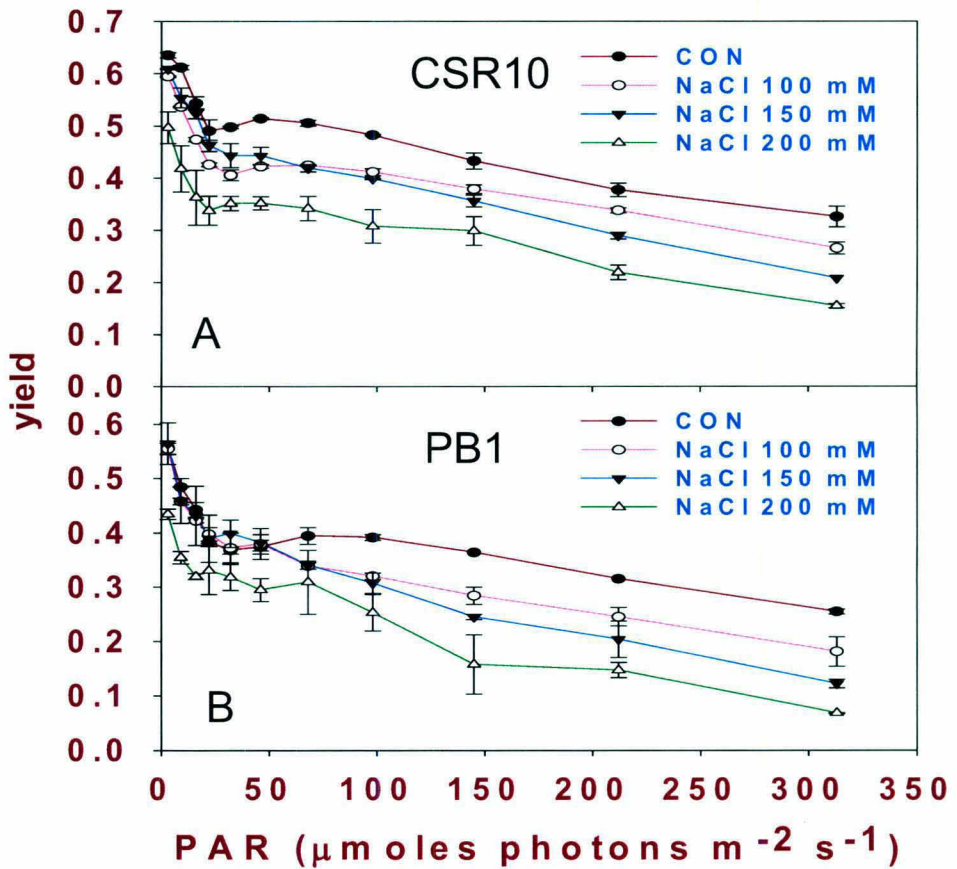


Fig 32: Quantum yield of photosystem II (PSII) of control and salt-stressed rice seedlings of (A) CSR10 and (B) PB1. Five-d-old etiolated seedlings were treated with 0 mM, 100 mM, 150 mM and 200 mM NaCl 12 h prior to the transfer to cool white fluorescent+incandescent light ($100 \mu\text{moles photons m}^{-2} \text{s}^{-1}$), at 28°C at 75% relative humidity. Quantum yield was measured after 72 h of greening as described in materials and methods. Percent of control is shown in fig.C. Each data point is the average of three replicates. The *error bar* represents SD.

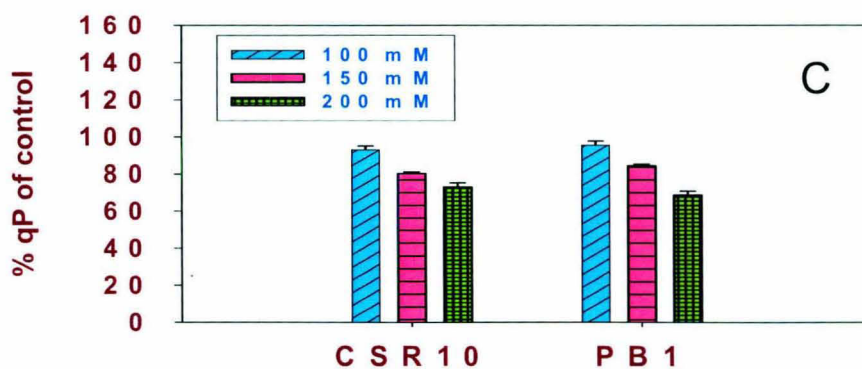
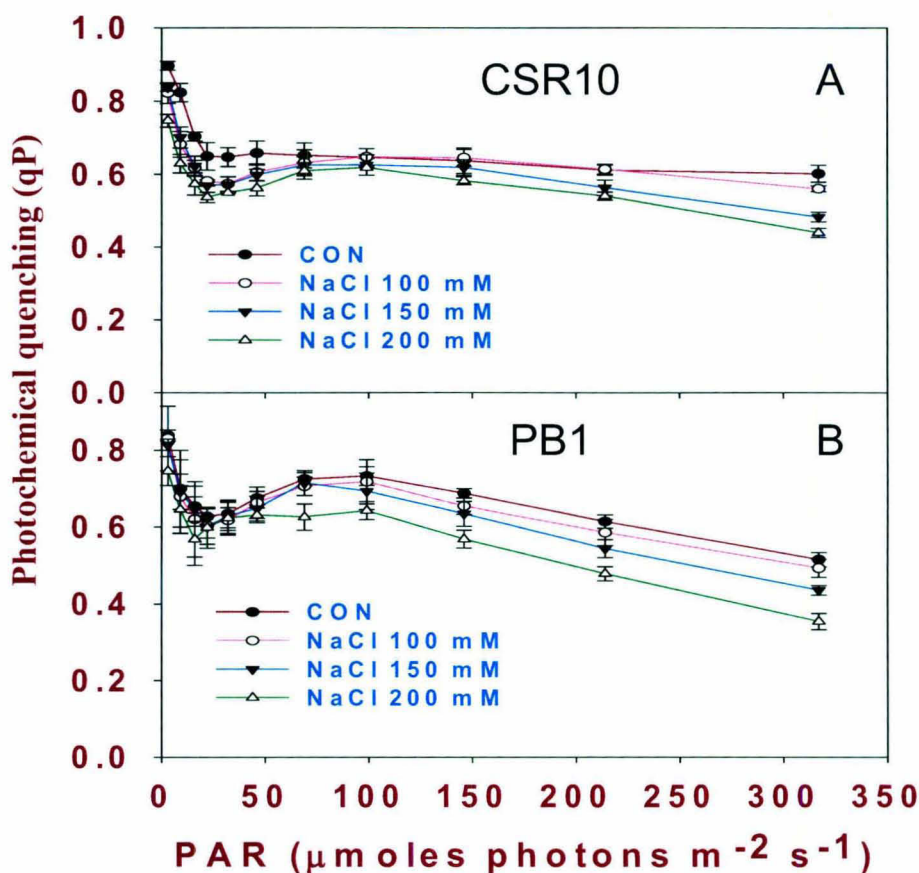


Fig 33: Photochemical quenching (qP) of control and salt-stressed rice seedlings of (A) CSR10 and (B) PB1. Five-d-old etiolated seedlings were treated with 0 mM, 100 mM, 150 mM and 200 mM NaCl 12 h prior to the transfer to cool white fluorescent+incandescent light ($100 \mu\text{moles photons m}^{-2} \text{s}^{-1}$), at 28°C at 75% relative humidity. Photochemical quenching (qP) was measured after 24 h of greening as described in materials and methods. Percent of control is shown in fig. C. Each data point is the average of three replicates. The *error bar* represents SD.

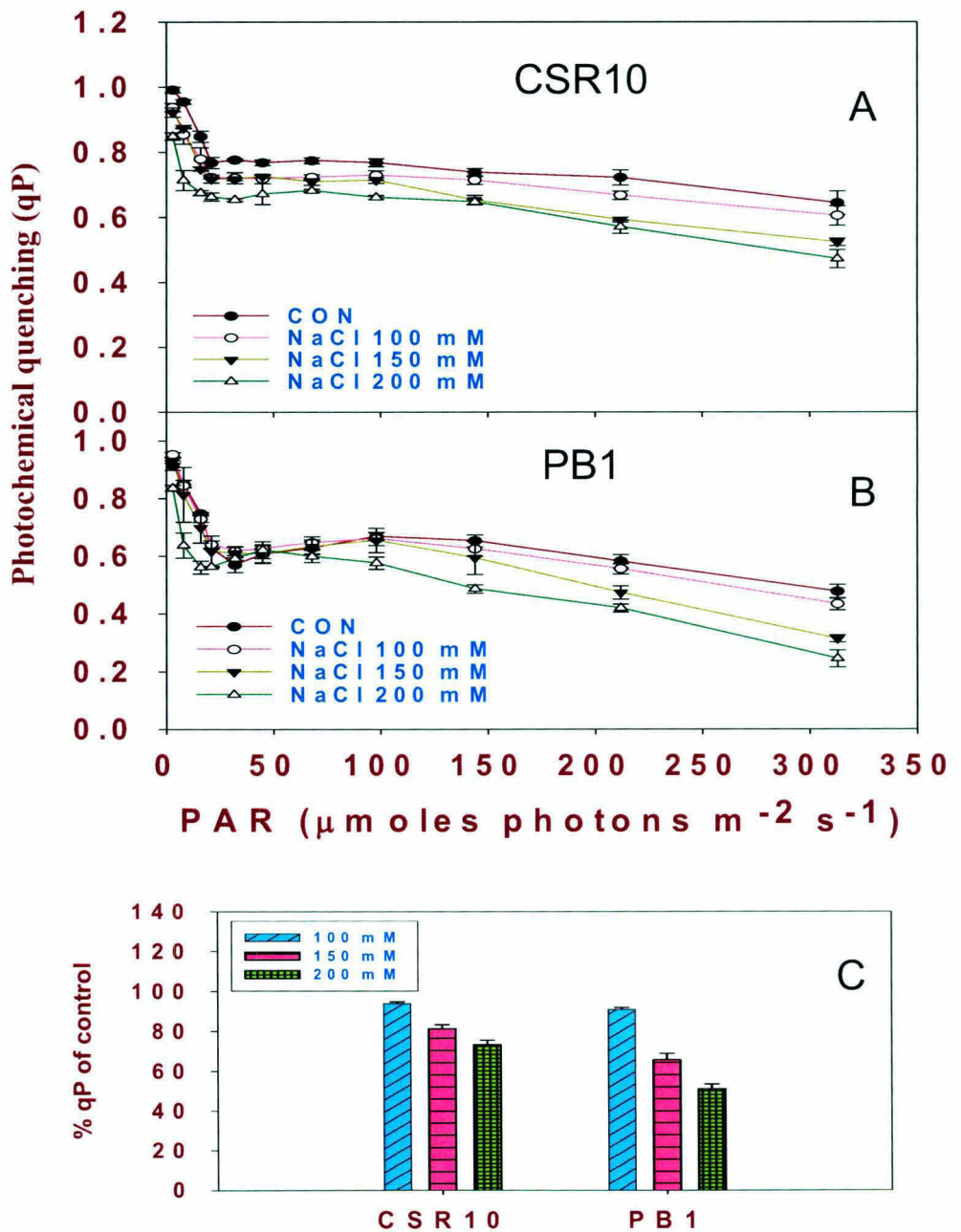


Fig 34: Photochemical quenching (qP) of control and salt-stressed rice seedlings of (A) CSR10 and (B) PB1. Five-d-old etiolated seedlings were treated with 0 mM, 100 mM, 150 mM and 200 mM NaCl 12 h prior to the transfer to cool white fluorescent+incandescent light ($100 \mu\text{moles photons m}^{-2} \text{s}^{-1}$), at 28°C at 75% relative humidity. Photochemical quenching (qP) was measured after 48 h of greening as described in materials and methods. Percent of control is shown in fig. C. Each data point is the average of three replicates. The error bar represents SD.

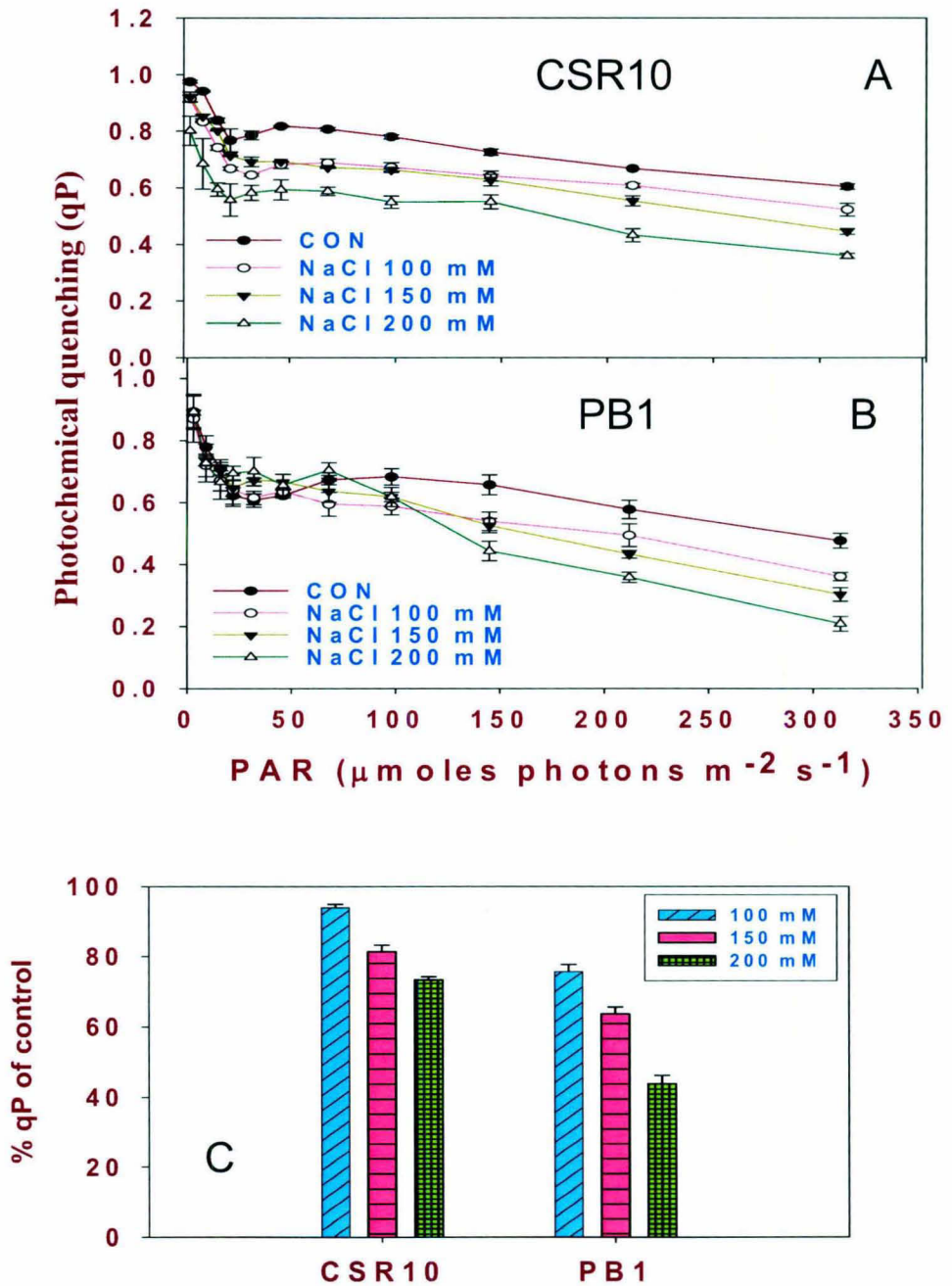


Fig 35: Photochemical quenching (qP) of control and salt-stressed rice seedlings of (A) CSR10 and (B) PB1. Five-d-old etiolated seedlings were treated with 0 mM, 100 mM, 150 mM and 200 mM NaCl 12 h prior to the transfer to cool white fluorescent+incandescent light ($100 \mu\text{moles photons m}^{-2} \text{s}^{-1}$), at 28°C at 75% relative humidity. Photochemical quenching (qP) was measured after 72 h of greening as described in materials and methods. Percent of control is shown in fig. C. Each data point is the average of three replicates. The *error bar* represents SD.

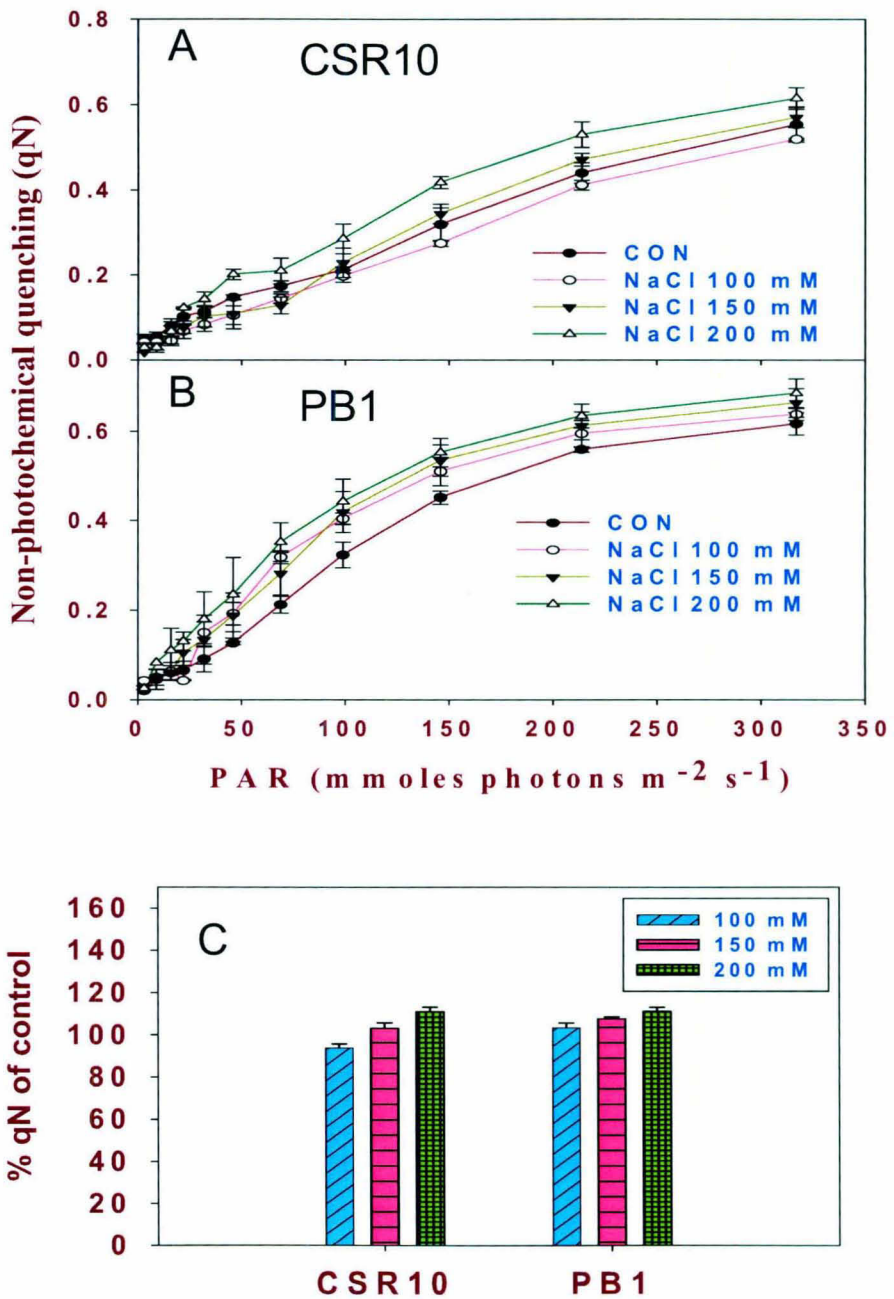


Fig 36: Non-photochemical quenching (qN) of control and salt-stressed rice seedlings of (A) CSR10 and (B) PB1. Five-d-old etiolated seedlings were treated with 0 mM, 100 mM, 150 mM and 200 mM NaCl 12 h prior to the transfer to cool white fluorescent+incandescent light (100 $\mu\text{moles m}^{-2} \text{s}^{-1}$), at 28°C at 75% relative humidity. Non-photochemical quenching (qN) was measured after 24 h of greening as described in materials and methods. Percent of control is shown in fig. C. Each data point is the average of three replicates. The *error bar* represents SD.

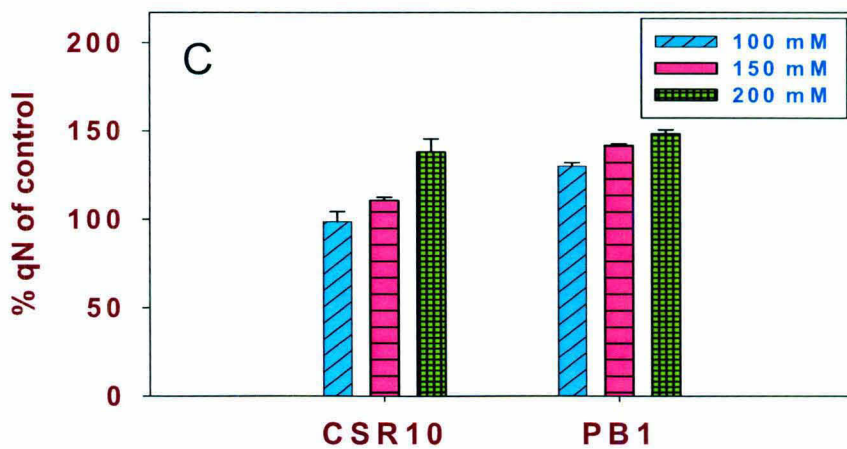
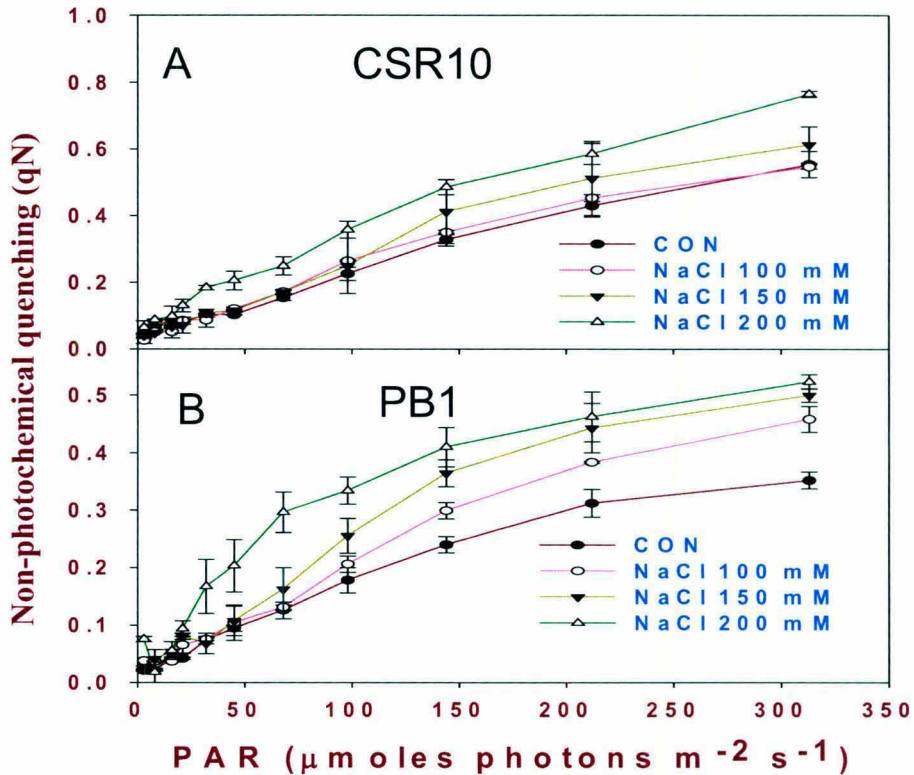


Fig 37: Non-photochemical quenching (qN) of control and salt-stressed rice seedlings of (A) CSR10 and (B) PB1. Five-d-old etiolated seedlings were treated with 0 mM, 100 mM, 150 mM and 200 mM NaCl 12 h prior to the transfer to cool white fluorescent+incandescent light ($100 \mu\text{moles photons m}^{-2} \text{s}^{-1}$), at 28°C at 75% relative humidity. Non-photochemical quenching (qN) was measured after 48 h of greening as described in materials and methods. Percent of control is shown in fig. C. Each data point is the average of three replicates. The *error bar* represents SD.

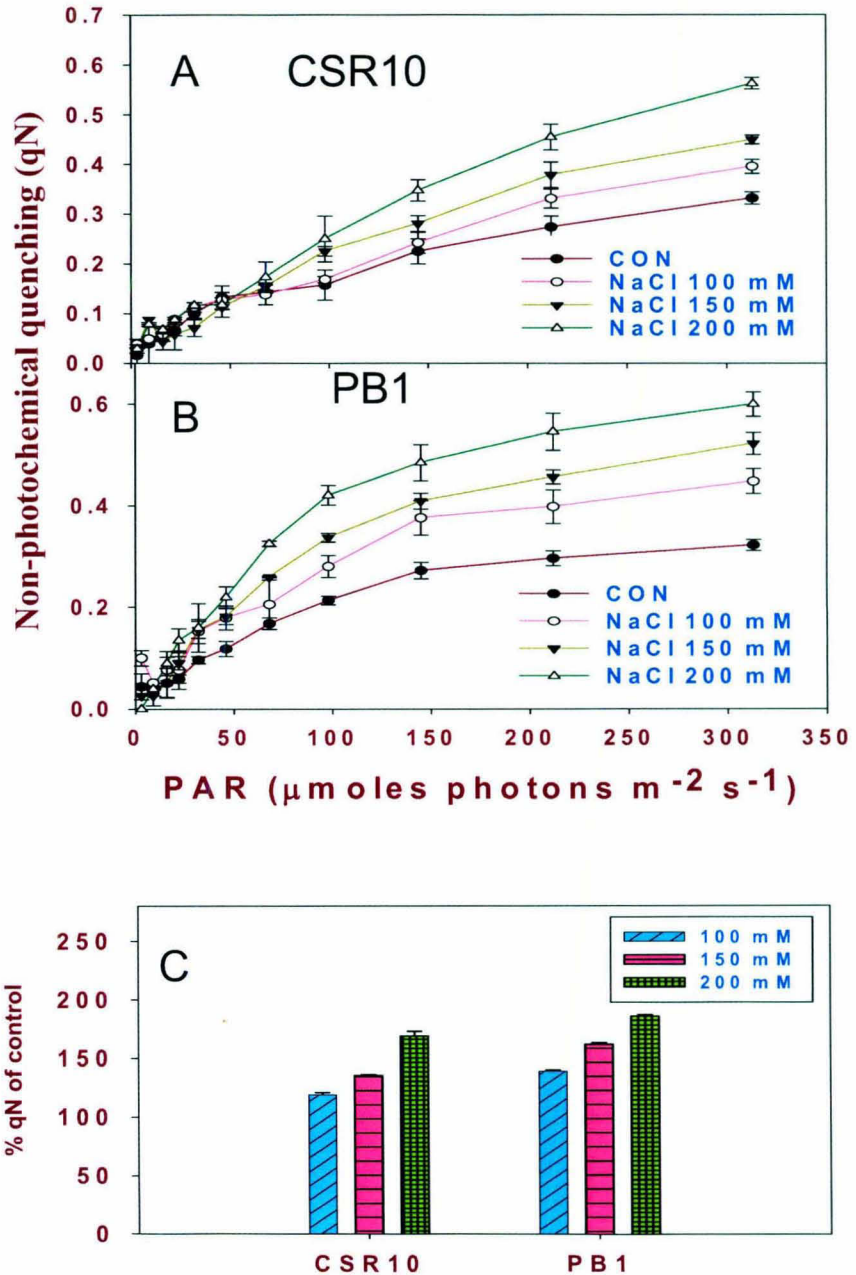


Fig 38: Non-photochemical quenching (qN) of control and salt-stressed rice seedlings of (A) CSR10 and (B) PB1. Five-d-old etiolated seedlings were treated with 0 mM, 100 mM, 150 mM and 200 mM NaCl 12 h prior to the transfer to cool white fluorescent+incandescent light ($100 \mu\text{moles photons m}^{-2} \text{s}^{-1}$), at 28°C at 75% relative humidity. Non-photochemical quenching (qN) was measured after 72 h of greening as described in materials and methods. Percent of control is shown in fig. C. Each data point is the average of three replicates. The *error bar* represents SD.

greening and light intensity. Relative decrease in PSII yield in response to salt was more in PB1. After 72 h of greening in 200 mM NaCl yield declined by 45.5% in CSR10 and in 73 % in PB1.

Photochemical quenching: - Photochemical quenching (qP) of CSR10 and PB1 at 24, 48, and 72 h of greening are shown in Fig 33, 34 and 35 respectively. Part C of each figure shows the qP as % of control at maximum light intensity. Photochemical quenching of CSR10 and PB1 decreased in response to increase in the light intensity. The photochemical quenching (qP) of both the cultivars decreased in response to NaCl salt stress as comparative to control. The relative decline in qP was more in PB1 than in CSR10. For example, after 72h of greening in 200 mM NaCl, qP declined by 28% in CSR10 and 60% in PB1.

Non-photochemical quenching: - The non-photochemical quenching (qN) of CSR10 and PB1 after 24, 48, and 72 hours of greening are shown in Fig 36, 37 and 38 respectively. Parts C of each figure show the qN as % of control at maximum light intensity. In control the non-photochemical quenching (qN) of both the genotypes increased in response to increase in the light intensity. In both the genotypes qN also increased in response to salt stress. The increase in qN was more pronounced after longer stress treatment i.e. after 72 h of greening. Increase in qN in the presence of 200 mM NaCl was higher in PB1 than that in CSR10.

The photosynthetic electron transport reactions:

Whole chain, PSII, and PSI reactions of controls samples were higher in CSR10 than that in PB1.

Whole chain reaction: - The electron transport through the whole chain of photosynthesis, i.e. from H₂O to MV (O₂ uptake) was measured polarographically. The whole chain reaction was measured in 150 mM and 200 mM NaCl stress at 72 hours of greening. The whole chain reaction was reduced by 35.58 % and 41 % in 150 mM and 200 mM NaCl respectively in CSR10 at 72 hours of greening. Higher loss of photosynthetic electron transport reaction was recorded for the salt sensitive PB1 cultivar by 46.37 % and 50.9 % in response to 150 mM and 200 mM salt stress respectively (Fig.39).

PSI reaction: - The partial electron transport chain through PSI from the artificial electron donor DCIP/ascorbate to MV was measured polarographically as O₂ uptake. PSI activity was

Whole chain activity

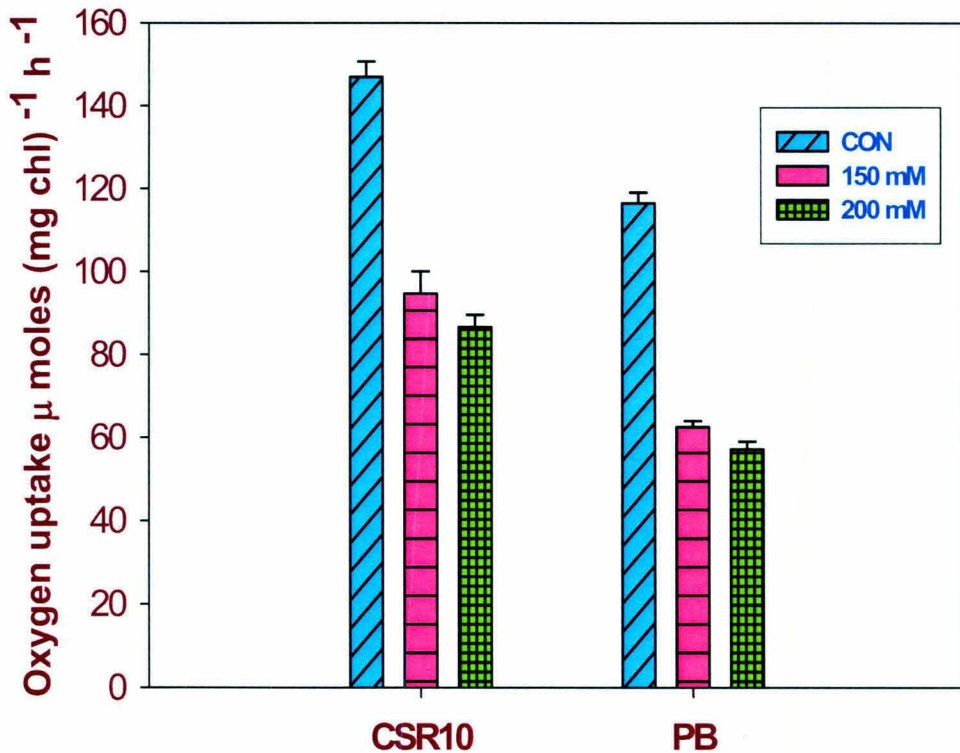


Fig 39: Whole chain reaction. Five-day-old etiolated rice seedlings of CSR10 and PB1 were treated with 0, 150 and 200 mM NaCl 12 h prior to the transfer to cool white fluorescent+incandescent light ($100 \mu\text{ moles photons m}^{-2} \text{ s}^{-1}$), at 28°C at 75% relative humidity maintained by a Conviron plant growth chamber. Oxygen uptake was measured by Oxy Lab Hansatech as described in materials and methods. Thylakoid were isolated from control and salt stressed seedlings after 72 h of greening and equivalent to $20 \mu\text{g}$ of Chl were used for each reaction. Each data point is the average of three replicates. The error bar represents SD.

PSI activity

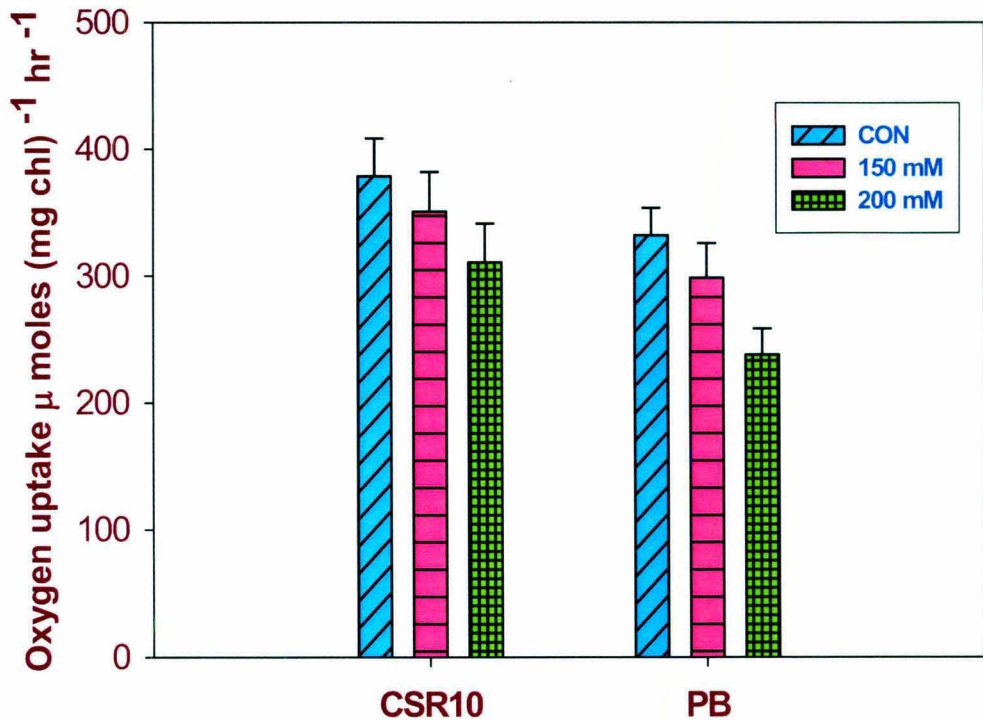


Fig 40: PSI reaction. Five-day-old etiolated rice seedlings of CSR10 and PB1 were treated with 0, 150 and 200 mM NaCl 12 h prior to the transfer to cool white fluorescent+incandescent light ($100 \mu\text{ moles photons m}^{-2} \text{ s}^{-1}$), at 28°C at 75% relative humidity maintained by a Conviron plant growth chamber. Oxygen uptake was measured by Oxy Lab Hansatech as described as in materials and methods. Thylakoids were isolated from control and salt stressed seedlings after 72 h of greening and equivalent to $20 \mu\text{g}$ of Chl were used for each reaction. Each data point is the average of three replicates. The *error bar* represents SD.

PSII activity

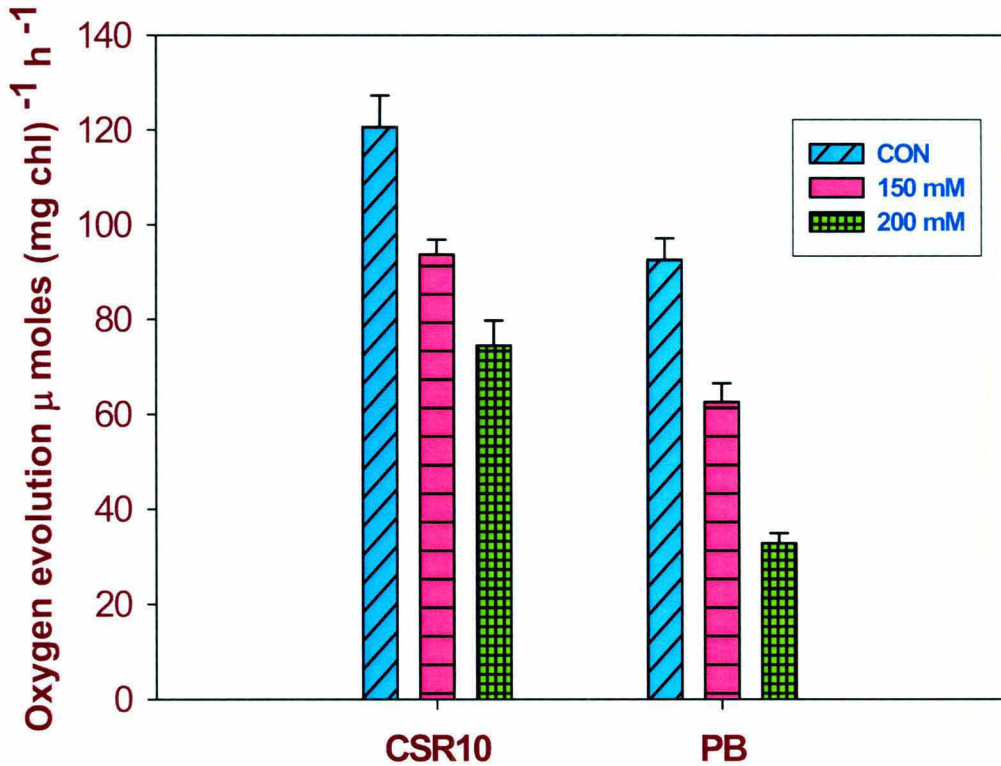


Fig 41: PSII reaction. Five-day-old etiolated rice seedlings of CSR10 and PB1 were treated with 0, 150 and 200 mM NaCl 12 h prior to the transfer to cool white fluorescent+incandescent light ($100 \mu\text{moles photons m}^{-2} \text{s}^{-1}$), at 28°C at 75% relative humidity maintained by a Conviron plant growth chamber. Oxygen evolution was measured by Oxy Lab Hansatech as described as in materials and methods. Thylakoids were isolated from control and salt stressed seedlings after 72 h of greening and equivalent to $20 \mu\text{g}$ of Chl were used for each reaction. Each data point is the average of three replicates. The *error bar* represents SD.

monitored in response to 150 mM and 200 mM NaCl stress after 72 h of greening. PSI activity was marginally decreased in CSR10 in response to salt stress whereas it reduced substantially in PB1 (Fig 40). After 200 mM PSI reaction decreased by 18 % in CSR10 and by 28.6 % in PB1.

PSII reaction: - PD-supported PSII-dependent O₂ evolution was monitored polarographically. PSII activity was reduced in response to salt stress in both the cultivars. However the extent of inhibition of PSII reaction was less in CSR10 as compared to that in PB1. PSII reaction was reduced by 22.33 % and 38.34 % respectively in response to 150 mM and 200 mM NaCl salt stress in CSR10. Inhibition of PSII reaction in PB1 was by 32.43 % and 64.58 % in response to 150 mM and 200 mM NaCl salt stress respectively (Fig. 41).

Light saturation curve of PSII:

To further ascertain if the inhibition of photosystem II photochemical reaction was due to reduction in the quantum yield of photosystem II or in the light saturated electron transport rate or both, the rate of PSII reaction as a function of light intensity was measured in thylakoid membranes isolated from control and salt treated rice seedlings after 72 h of greening (Fig. 42 and 43). Dependence of PSII activity on light intensity showed typical saturation kinetics. Both the the initial slope at limiting light intensities as well as light saturated electron transport were affected in salt treated seedlings. The maximum light intensity at 100% saturation was 1500 μ moles photons $m^{-2} s^{-1}$, obtained from a tungsten light source. The varying low light intensities were obtained using neutral density filters (Blazers). Both the initial slope at limiting light intensities as well as well as light saturated electron transport rates were affected in salt treated seedlings of CSR10 cultivar. As compared to control, the percent inhibition of PSII reaction in salt-treated thylakoids was almost constant (nearly 45 %) at all the light intensities used (Fig.42). The Eadie plot (i.e., the rate of oxygen evolution versus rate/light intensity i.e. % saturation) for control and salt treated (inset Fig.42) reveals a marked drop in the quantum efficiency of PSII reaction (intercept on the abscissa) and a substantial reduction of V_{max} (intercept on the ordinate) due to salt stress. Both V_{max} and quantum efficiency of PSII were reduced almost by 45 %. This suggests that inhibition of V_{max} and quantum efficiency of PSII was due to damage to the reaction centre.

CSR10 PSII light saturation curve

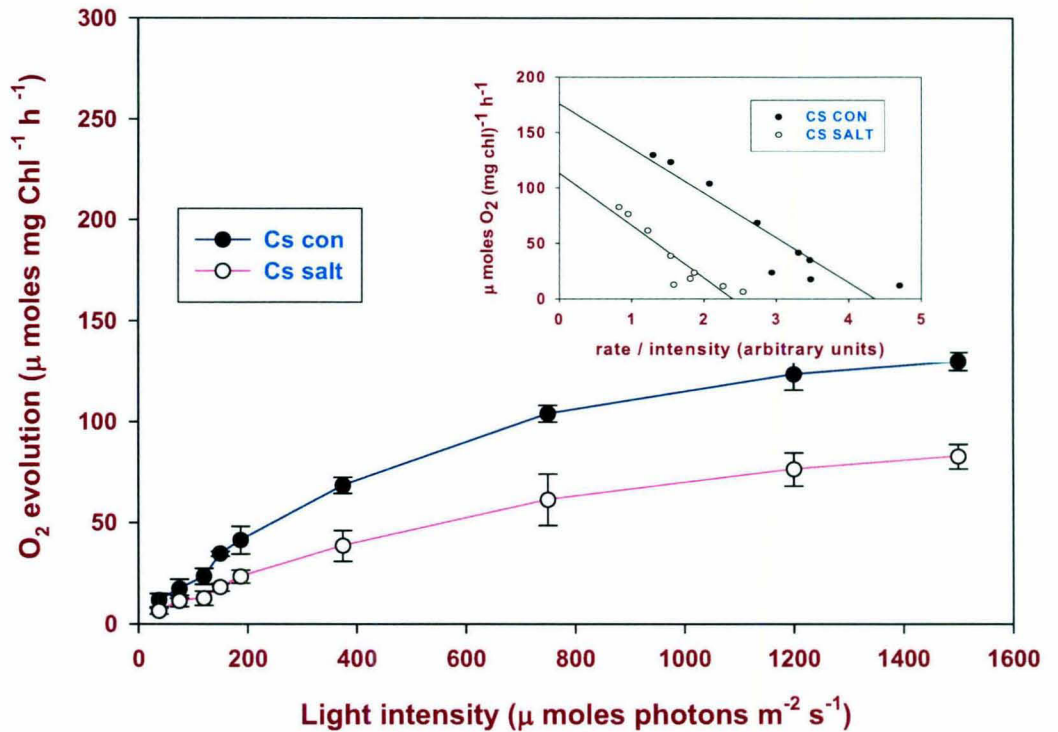


Fig 42: PSII light saturation curve of CSR10. Five-day-old etiolated seedlings of CSR10 were treated with 0 and 200 mM NaCl 12 h prior to the transfer to cool white fluorescent+incandescent light ($100\ \mu\text{ moles photons m}^{-2}\text{ s}^{-1}$), at 28°C at 75% relative humidity. Oxygen evolution was measured by Oxy Lab Hansatech at different light intensities as described in materials and methods. Maximum light intensity used was $1500\ \mu\text{ moles m}^{-2}\text{ s}^{-1}$. Thylakoids were isolated from control and salt stressed seedlings after 72 h of greening and equivalent to $20\ \mu\text{g}$ of Chl were used for each reaction. Each data point is the average of three replicates. The *error bar* represents SD. Missing error bars indicate that they are smaller than the symbols.

PB1 PSII light saturation curve

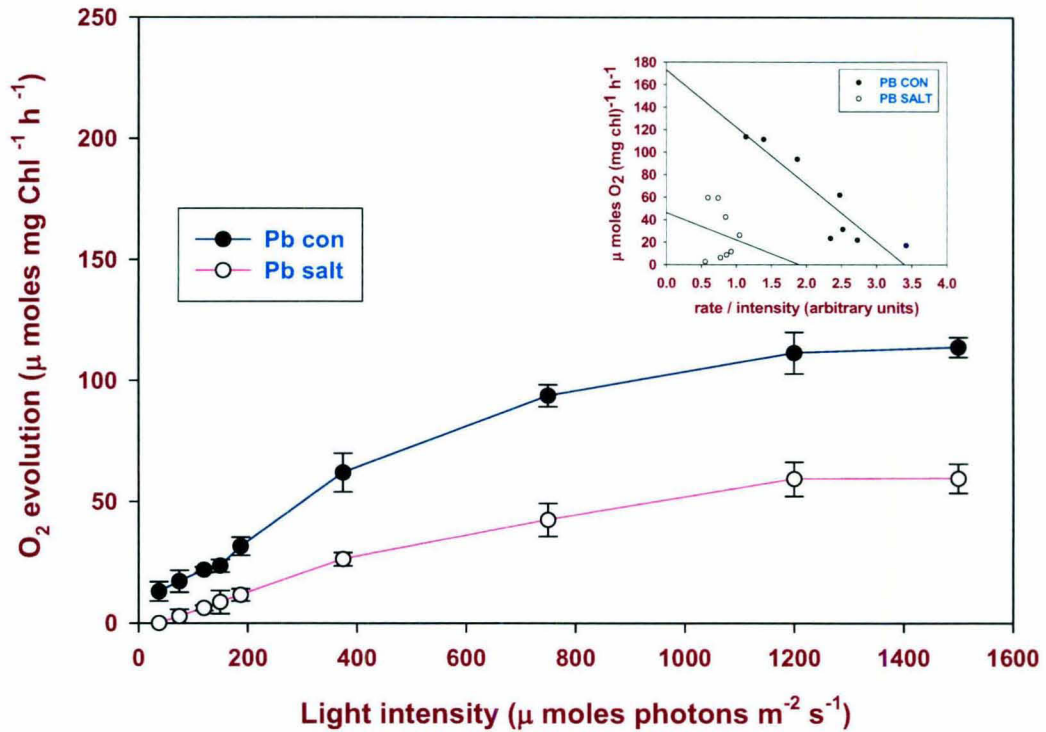


Fig 43: PSII light saturation curve of PB1. Five-day-old etiolated rice seedlings of PB1 were treated with 0 and 200 mM NaCl 12 h prior to the transfer to cool white fluorescent+incandescent light ($100\ \mu\text{ moles photons m}^{-2}\text{ s}^{-1}$), at 28°C at 75% relative humidity. Oxygen evolution was measured by Oxy Lab Hansatech at different light intensities as described in materials and methods. Maximum light intensity used was $1500\ \mu\text{ moles m}^{-2}\text{ s}^{-1}$. Thylakoids were isolated from control and salt stressed seedlings after 72 h of greening and equivalent to $20\ \mu\text{g}$ of Chl were used for each reaction. Each data point is the average of three replicates. The *error bar* represents SD.

In Pusa Basmati 1 (PB1) dependence of PSII activity on light intensity also showed typical saturation kinetics (Fig.43). Both the initial slope at limiting light intensities as well as well as light saturated electron transport rates were affected in salt treated seedlings of PB1 cultivar. As compared to control, the percent inhibition of PSII in salt stressed thylakoids was almost 50 % at higher intensity and was more pronounced at lower intensities (≥ 60 %). The Eadie plot (i.e., the rate of oxygen evolution versus rate/light intensity i.e. % saturation) for control and salt treated (inset Fig.43) reveals a marked drop in the quantum efficiency of PSII reaction (intercept on the abscissa) and a substantial reduction of V_{\max} (intercept on the ordinate) due to salt-stress. The quantum efficiency of PSII was reduced by almost 50 % and V_{\max} by almost 75 %. This suggests that inhibition of V_{\max} and quantum efficiency of PSII was due to both, damage to the reaction centre as well as antenna complex.

Room temperature chl a fluorescence:

Room temperature chl a fluorescence was observed at 440 nm excitation and at 620-750 nm emission in the presence of Mg^{2+} . Fluorescence emission of PSII at 684 nm declined in response to salt stress in both the cultivars, 38.04% in CSR10 and 51.32% in salt sensitive PB1 (Fig.44).

Low temperature spectra:

To understand if the structural organization of thylakoid membranes were affected by salt stress the low temperature (77K) fluorescence spectra was monitored in thylakoids membranes isolated from rice seedlings treated with 200 mM NaCl after 72 h of greening (Fig.45, 46). For the measurement of 77K chlorophyll a fluorescence emission spectra, samples were excited at 440 nm and the emission was observed at 620 -780 nm in the absence and presence of Mg^{2+} . The fluorescence emission spectra were normalized at 686 nm emanating from PSII to see changes in PSI fluorescence.

As shown in Fig.45 in control sample of CSR10 the F686/ F740 ratio is 1.1467 in the absence of Mg^{2+} . In the presence of Mg^{2+} F686/ F740 ratio (1.973) increases due to efficient stacking of thylakoid membranes resulting in increased energy transfer from LHCII to PSII. In salt stress F686/ F740 ratio in CSR10 seedlings is 1.372 in the absence of Mg^{2+} however in

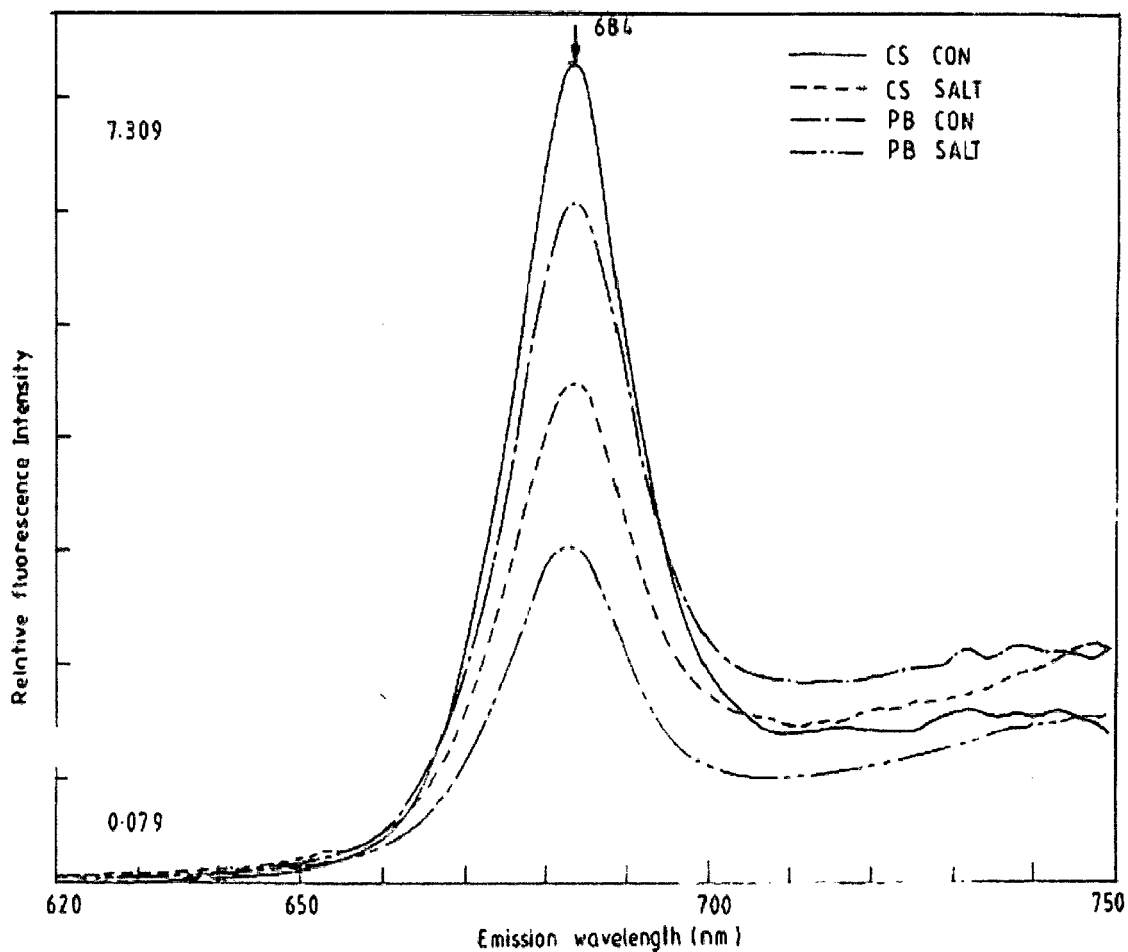


Fig 44: Room temperature (298 K) fluorescence emission spectra (E 440) of thylakoid membranes in the presence of Mg. Five-day-old etiolated rice seedlings of CSR10 and PB1 were treated 0 and 200 mM NaCl 12 h prior to the transfer to cool white fluorescent+incandescent light ($100 \mu\text{moles photons m}^{-2} \text{s}^{-1}$) for 72 h of greening, at 28°C at 75% relative humidity. Fluorescence emission spectra of isolated thylakoid membranes suspended at a concentration of $3 \mu\text{g Chl/ml}$ were recorded in ratio mode in a photon counting SLM-AMINCO 8000 spectrofluorometer having excitation slit width of 8 nm and emission slit width of 4 nm. Spectra were corrected for the instrument response.

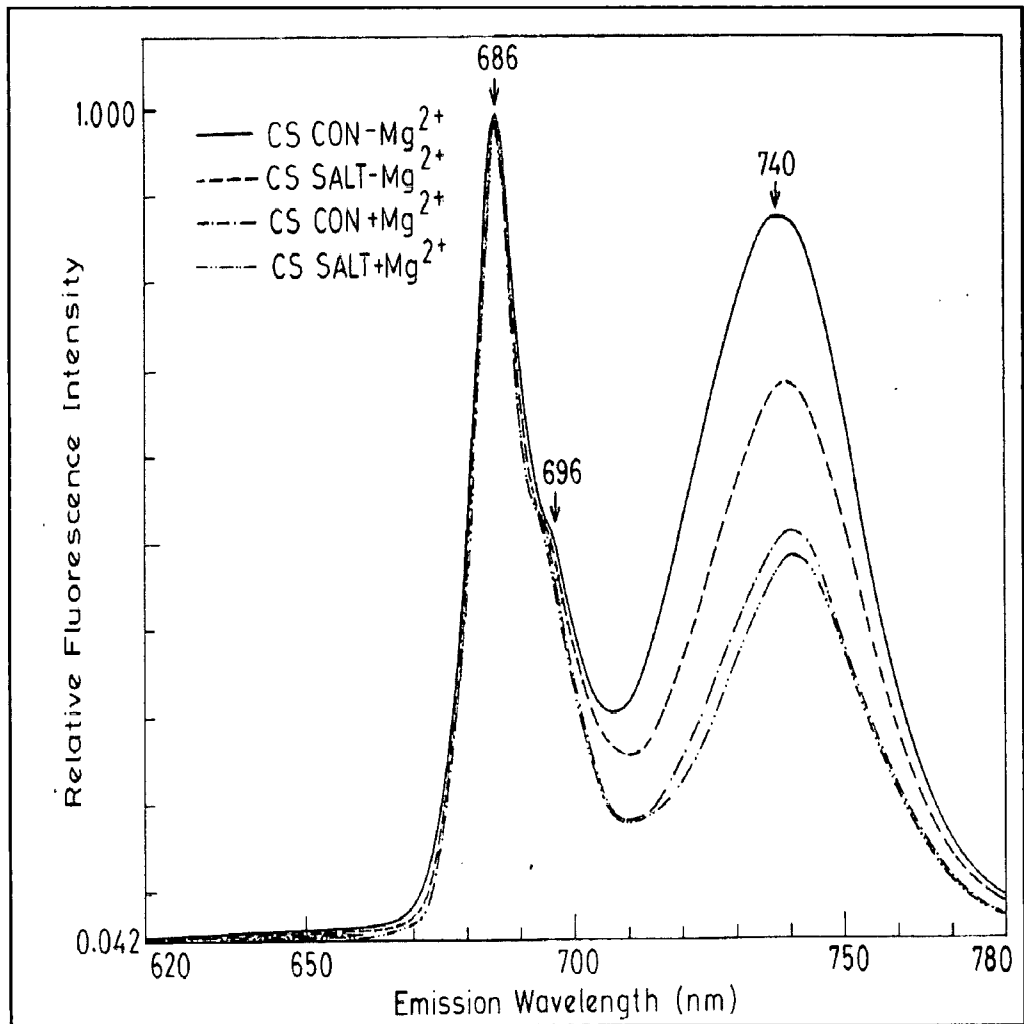


Fig 45: Low temperature (77K) fluorescence emission spectra (E 440) of thylakoid membranes in the presence or absence of Mg. Five-day-old etiolated rice seedlings of CSR10 were treated 0 and 200 mM NaCl 12 h prior to the transfer to cool white fluorescent+incandescent light (100 $\mu\text{moles photons m}^{-2} \text{ s}^{-1}$) for 72 h of greening, at 28^oC at 75% relative humidity. Fluorescence emission spectra of isolated thylakoid membranes suspended at a concentration of 3 $\mu\text{g Chl/ml}$ were recorded in ratio mode in a photon counting SLM-AMINCO 8000 spectrofluorometer having excitation and emission slit width of 4 nm. Spectra were not corrected for the instrument response.

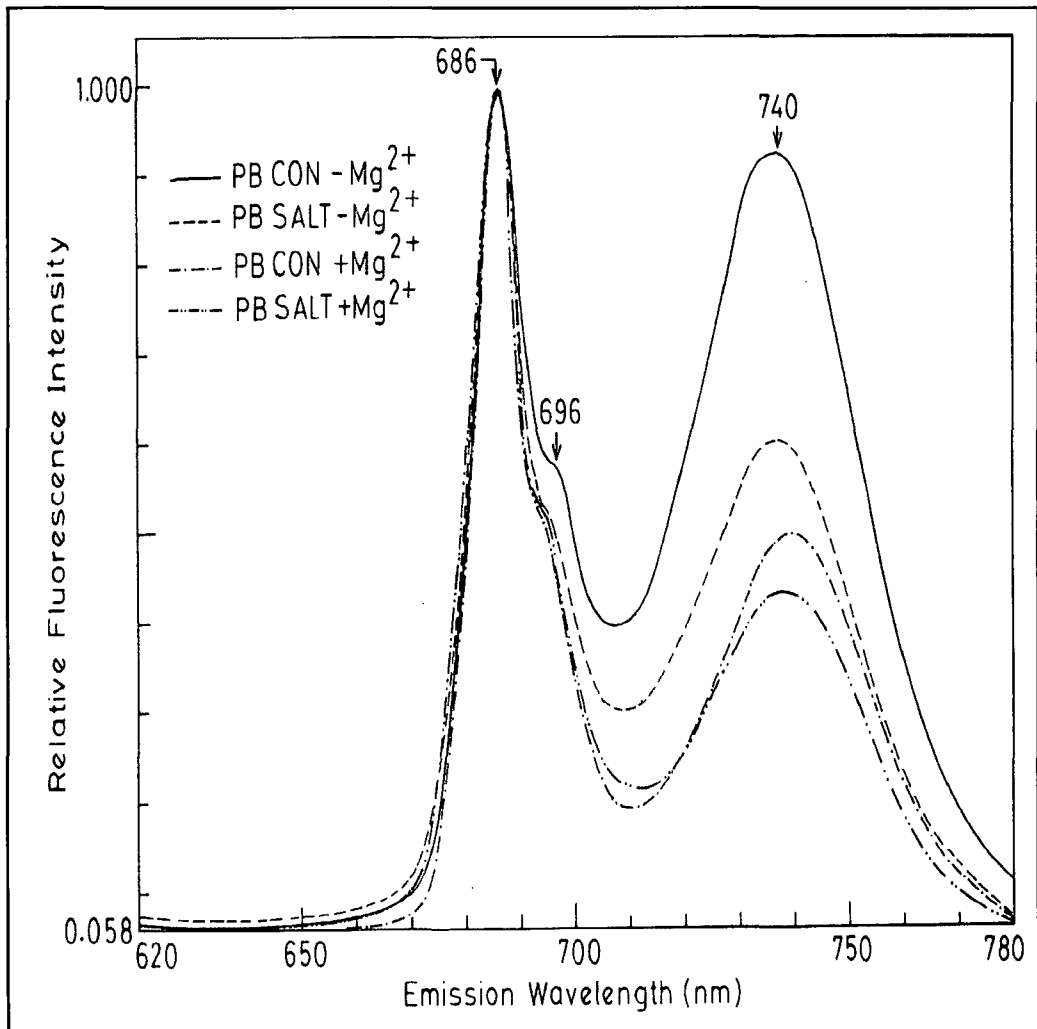


Fig 46: Low temperature (77K) fluorescence emission spectra (E 440) of thylakoid membranes in the presence or absence of Mg. Five-day-old etiolated rice seedlings of PB1 were treated 0 and 200 mM NaCl 12 h prior to the transfer to cool white fluorescent+incandescent light (100 $\mu\text{moles photons m}^{-2} \text{s}^{-1}$) for 72 h of greening, at 28°C at 75% relative humidity. Fluorescence emission spectra of isolated thylakoid membranes suspended at a concentration of 3 $\mu\text{g Chl/ml}$ were recorded in ratio mode in a photon counting SLM-AMINCO 8000 spectrofluorometer having excitation and emission slit width of 4 nm. Spectra were corrected for the instrument response.

presence of Mg^{2+} F686/ F740 ratio (2.083) increases. But % increase in F686/ F740 ratio in control and salt stress were 72 % and 51.8 % respectively.

In salt sensitive PB1 also F686/ F740 ratio increases in the presence of Mg^{2+} in both control and salt stressed seedlings. The % increase in F686/ F740 ratio in control and salt stressed seedlings were 81.1% and 50.4 % respectively (Fig.46). There was relatively less increase in F686/ F740 ratio in salt stress in both the cultivars from - Mg^{2+} to + Mg^{2+} condition. The relative less increase in F686/ F740 ratio during salt stress from - Mg^{2+} to + Mg^{2+} condition as compared to control was more in PB1 (salt sensitive) 37.85% as compared to CSR10 (salt tolerant) i.e. 28.05%.

Immunoblot analysis of photosynthetic proteins:

To understand the molecular basis of the loss of photosynthetic functions, the abundance of various photosynthetic proteins due to salt stress was studied by immunoblot analysis. Thylakoids proteins (30 μ g) were loaded on each lane and separated on 12.5% SDS-PAGE stained with Commassie Brilliant Blue (R250) are shown in Fig. 47 (A) at different salt concentrations and Fig. 47 (B) at different time period of greening.

PSII proteins:

PSII reaction centre proteins (D1 and D2): The chloroplast encoded D1 protein expression was decreased in response to NaCl stress in both CSR10 and PB1. The relative decrease was higher in PB1 as compared to that in CSR10. The abundance of D2 also decreased due to salt stress in both the cultivars. However, its expression was more stable in CSR10 as compared to that in PB1. (Fig.48 A).

Cytb 559: The abundance of cyt b 559, an intrinsic membrane protein intimately associated with reaction center, declined due to salt-stress in both the cultivars. Decline was highest after 72 h of greening. Relative decline in protein abundance was higher in salt sensitive PB1 as compared to that in CSR10 (Fig.48 B).

Light harvesting chlorophyll binding proteins: The protein abundance of chlorophyll proteins (LHCPII, Lhcb1, Lhcb2, and Lhcb4) decreased due to salt stress in both the cultivars. The

expression of these proteins was severely affected in salt sensitive PB1 as compared to that in salt tolerant genotype CSR10 (Fig.48 A).

Oxygen evolving complex protein (OEC33): Protein expression of OEC 33 was reduced under increasing NaCl stress. Its abundance was drastically reduced in salt sensitive PB1 genotype (Fig.48 A).

PSI proteins:

PSI subunits III and V): The protein abundance of the subunit III (16 kD) of PSI decreased due to salt stress, its abundance was highly reduced in salt sensitive PB1 cultivar. The protein abundance of subunit V (17 kD) was also highly reduced in salt-sensitive cultivar PB1 as compared to that in CSR10 (Fig. 49).

Cytochrome b f complex:

Cyt f:

The protein abundance of cyt f decreased in response to salt-stress in both the cultivars. However the decline was higher in salt-sensitive cultivar PB1 as compared to salt tolerant CSR10 (Fig.50 A).

Subunit IV:

There was no significant change in protein abundance of subunit IV of cyt bf complex in response to salt stress (Fig.50 A).

Cyt b:

Protein expression of cyt b decreased in response to salt stress in both the cultivars. However the decline was higher in salt sensitive cultivar PB1 (Fig.50 B).

Rieske Fe-S protein:

The abundance of Riske protein declined drastically in response to salt stress in both the cultivars, however the extent of decrease was higher in salt sensitive PB1 (Fig.50 B).

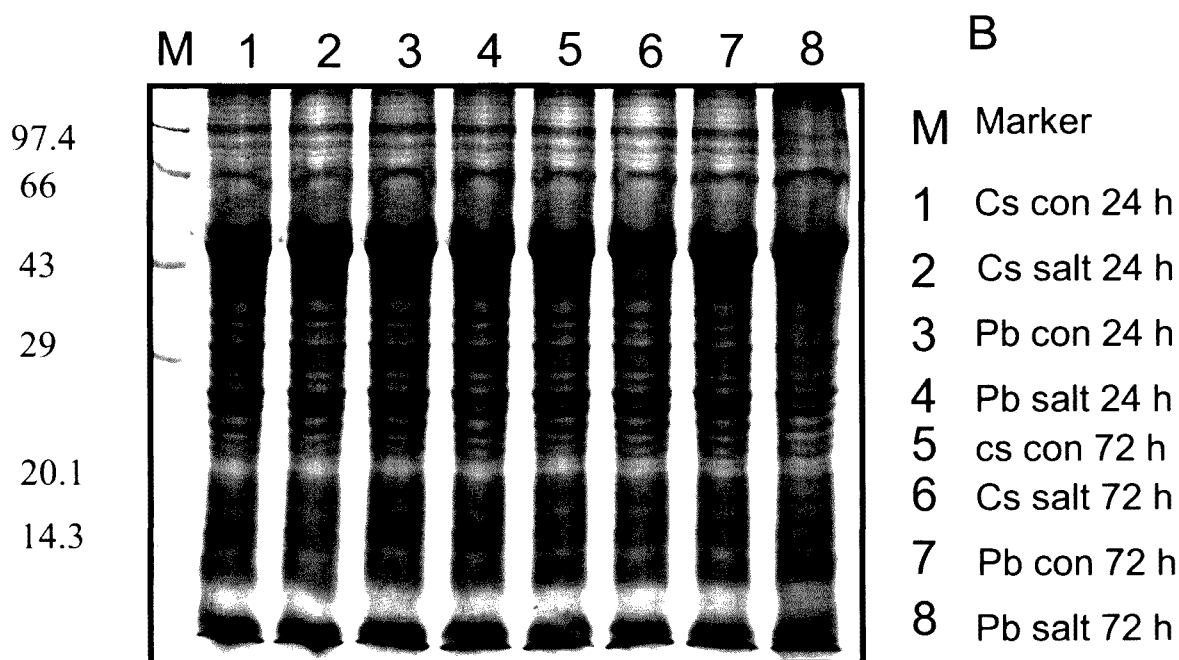
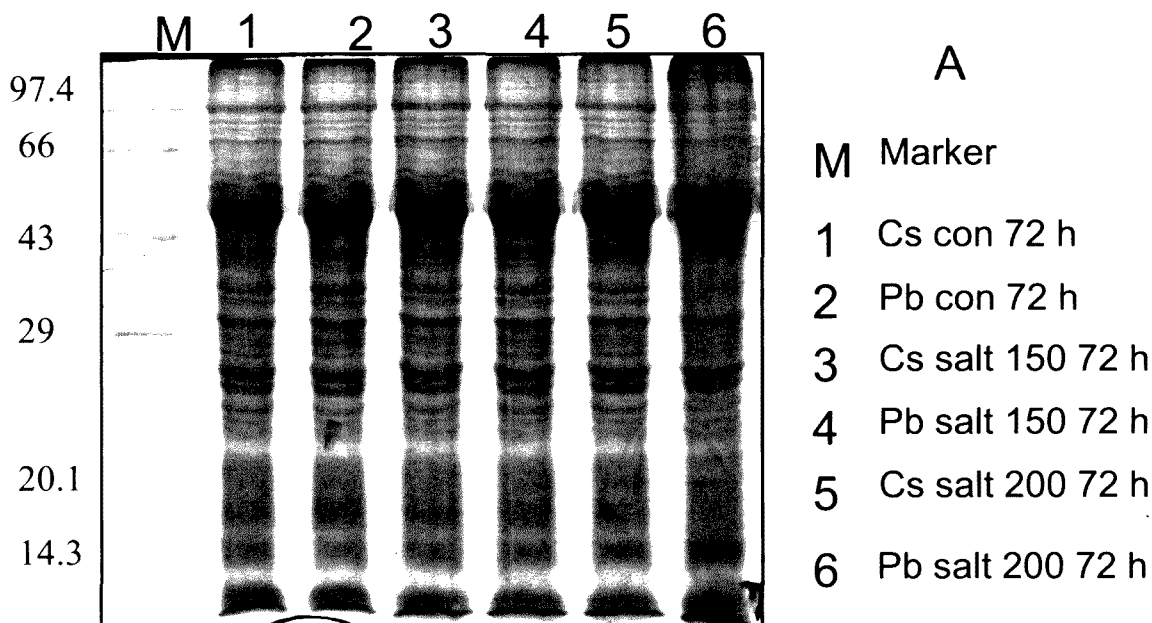


Fig 47: Coomassie Brilliant Blue (R 250) stained SDS-gels of thylakoids proteins. Five-day-old etiolated rice seedlings of CSR10 and PB1 were treated with 0, 150 and 200 mM NaCl 12 h prior to the transfer to cool white fluorescent+incandescent light ($100 \mu\text{moles photons m}^{-2} \text{s}^{-1}$), at 28°C at 75% relative humidity. Thylakoids proteins were isolated and resolved on 12.5 % SDS-PAGE. Equal amounts of proteins ($30\mu\text{g}$) were loaded on each lane. (A) SDS-PAGE of thylakoids proteins after 72 h of 150 mM and 200 mM salt stress. (B) SDS-PAGE of thylakoids proteins after 24h and 72h of 200 mM salt stress.

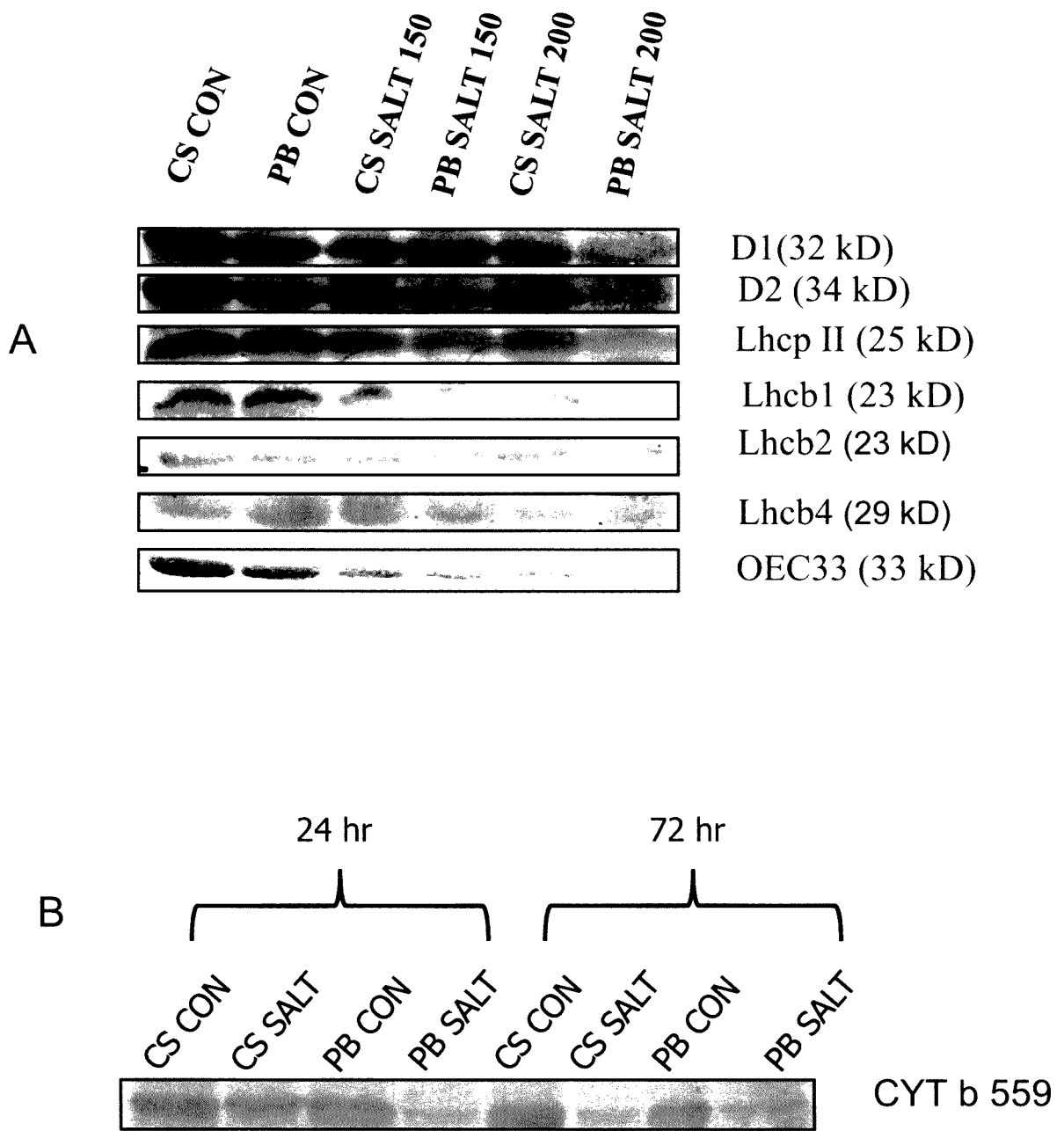


Fig 48: (A) Immunoblot analysis of photosynthetic (PSII) proteins. Five-day-old etiolated rice seedlings of CSR10 and PB1 were treated with 0, 150 and 200 mM NaCl 12 h prior to the transfer to cool white fluorescent+incandescent light ($100 \mu\text{moles photons m}^{-2} \text{s}^{-1}$), at 28°C at 75% relative humidity. Western blot was performed as described in materials and methods. Thylakoids were isolated from control and salt stressed seedlings after 72 h of greening. (B) Cyt b 559 expression was studied at 24 h and 72 h of greening in response to 200 mM NaCl stress. Equal amounts of protein (30 mg) were loaded on each lane.

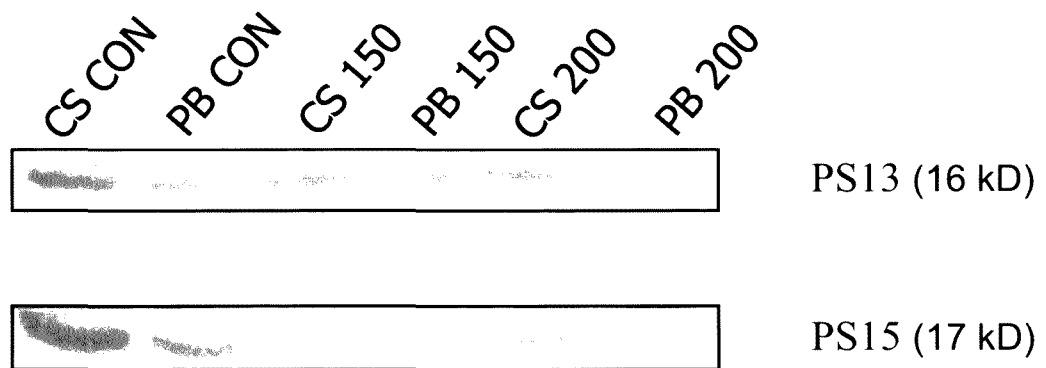


Fig 49: Immunoblot analysis of photosynthetic (PSI) proteins. Five-day-old etiolated rice seedlings of CSR10 and PB1 were treated with 0, 150 and 200 mM NaCl 12 h prior to the transfer to cool white fluorescent+incandescent light ($100 \mu\text{moles photons m}^{-2} \text{s}^{-1}$), at 28°C at 75% relative humidity. Western blot was performed as described in materials and methods. Thylakoids were isolated from control and salt stressed seedlings after 72 h of greening. Equal amounts of protein ($30 \mu\text{g}$) were loaded on each lane.

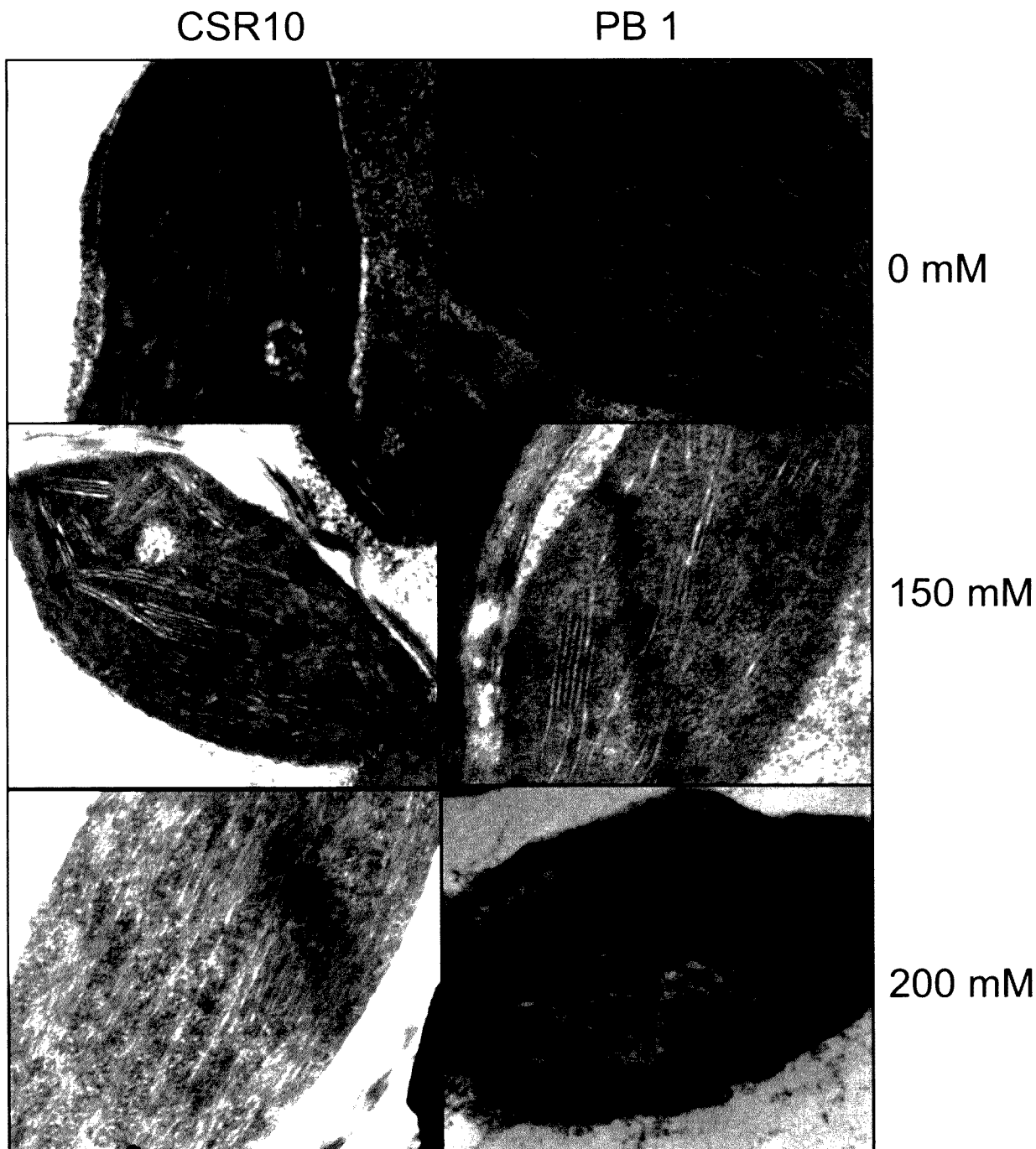


Fig 52: Ultrastructure of chloroplast in rice seedlings. Five-day-old etiolated rice seedlings of CSR10 and PB1 were treated with 0 mM, 150 mM and 200 mM NaCl 12 h prior to the transfer to cool white fluorescent+incandescent light ($100 \mu\text{moles photons m}^{-2} \text{s}^{-1}$), at 28°C at 75% relative humidity. Transmission electron micrograph depicting the ultrastructure of chloroplast (20,000 X) was performed as described in materials and methods after 24 h of greening.

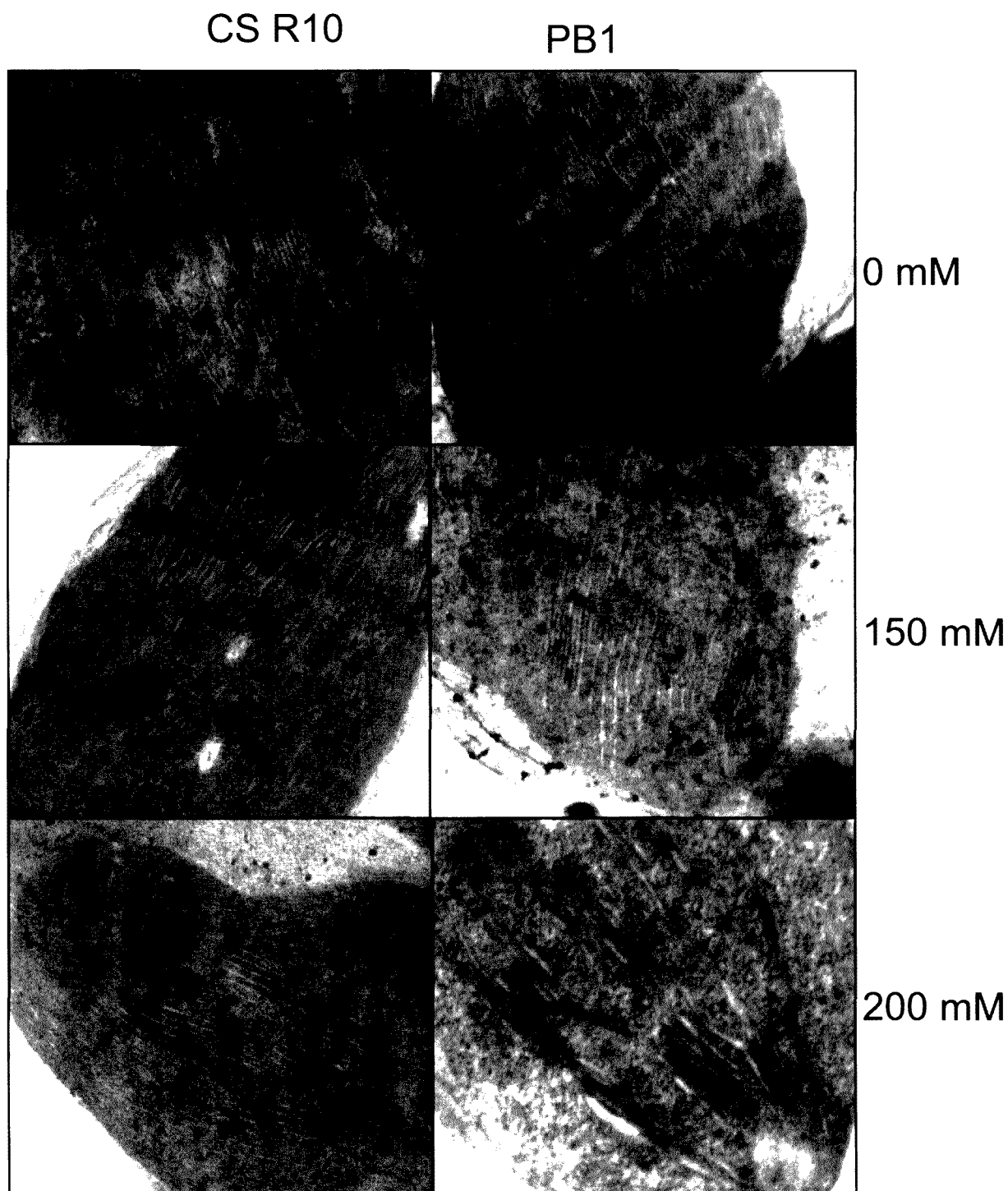


Fig 53: Ultrastructure of chloroplast in rice seedlings. Five-day-old etiolated rice seedlings of CSR10 and PB1 were treated with 0 mM, 150 mM and 200 mM NaCl 12 h prior to the transfer to cool white fluorescent+incandescent light ($100 \mu\text{moles photons m}^{-2} \text{s}^{-1}$), at 28°C at 75% relative humidity maintained by a Conviron plant growth chamber. Transmission electron micrograph depicting the ultrastructure of chloroplast (20,000 X) was performed as described in materials and methods after 72 h of greening.

Gene expression of few PSII proteins:

To correlate protein expression of photosynthetic proteins with that of their gene expression RT-PCR was performed for a few PSII genes (Fig. 51. A).

The gene expression of PsbA that encodes for PSII reaction centre protein D1 was down-regulated in response to salt stress in both the cultivars. Gene expression decreased with the increased duration of stress exposure. However relative decline in expression was higher in PB1 than that in CSR10.

The transcripts abundance of PsbD that encodes for PSII reaction centre protein D2 reduced with increasing period of salt stress in both the cultivars. However PB1 shows more severe decline in gene expression in response to salt stress than that in CSR10.

The gene PetD encodes for cytb/f complex subunit IV. Transcripts level of PetD remains almost unaltered during salt stress in both the cultivars. However, gene expression slightly decreased in PB1 after 72 h of salt stress.

Ultrastructure of Chloroplast Thylakoids:

To understand the effect of salinity stress on chloroplast biogenesis it was essential to study ultrastructure of chloroplast and development of thylakoids. So ultrastructure of chloroplast was studied in both CSR10 and PB1 at different NaCl stress (0, 150 and 200 mM) after different hours of greening (24 h and 72 h). In control seedlings of CSR10 and PB1, thylakoids were well developed. In response to salt stress granal stacking was distorted and effect was more pronounced in salt sensitive cultivar PB1 (Fig. 52 and 53).

Antioxidative enzymes:

Superoxide dismutase: It catalyzes the dismutation of superoxide radicals to H₂O₂. Its activity was measured after 24 h and 72 h of greening in response to 200 mM NaCl stress. SOD activity continuously declined till 72 h of stress in control samples. In response to stress its activity increased in both the cultivars (Fig. 54). However, the increase in SOD activity was higher in the salt-sensitive genotype PB1.

In order to discern between different forms of SOD, its in gel assay was performed. The SOD had three distinct bands for Mn-SOD, Fe-SOD and Cu-Zn SOD (Fig. 55) which was identified by inhibition studies using H₂O₂. Mn-SOD and Fe-SOD remained unchanged in response to salt-stress. However, the Cu-Zn-SOD activity increased in response to salt stress in both the cultivars, suggesting that increase in SOD activity in response to salt stress was due to increase in chloroplastic Cu-Zn-SOD.

Ascorbate peroxidase:

Ascorbate peroxidases are enzymes that detoxify peroxides such as hydrogen peroxide using ascorbate as a substrate. The reaction they catalyse is the transfer of electrons from ascorbate to peroxide, producing dehydroascorbate and water as products. Ascorbate peroxidase (cytosolic) activity was estimated by measuring the decrease in absorbance at 290 nm at 24 and 72 hours of greening as described in materials and methods. After 72 h of light exposure, catalase activity declined. In response to salt treatment ascorbate peroxidase activity increased in both the cultivars. However ascorbate peroxidase activity was always higher in CSR10 as compared to salt sensitive PB1 in control seedlings. In response to salt treatment ascorbate peroxidase activity increased in both the cultivars. However, the increase in ascorbate peroxidase activity was much higher in the salt-sensitive genotype PB1 to a greater extent in PB1 (Fig. 56).

Glutathione reductase:

Total Glutathione reductase (GR) activity was measured spectrophotometrically by monitoring the decline in absorbance at 340 nm due to oxidation of NADPH. GR activity was measured at 24 h of greening. In response to salt stress the GR activity increased partially in both the cultivars (Fig.57).

Catalase:

Catalase is one of the most potent catalysts known. Catalase also catalyses conversion of hydrogen peroxide, a powerful and potentially harmful oxidizing agent, to water and molecular oxygen. Catalase also uses Hydrogen Peroxide to oxidise toxins including Phenols, Formic Acid, Formaldehyde and Alcohols. Cytosolic catalase activity was estimated by measuring decrease in

SOD activity

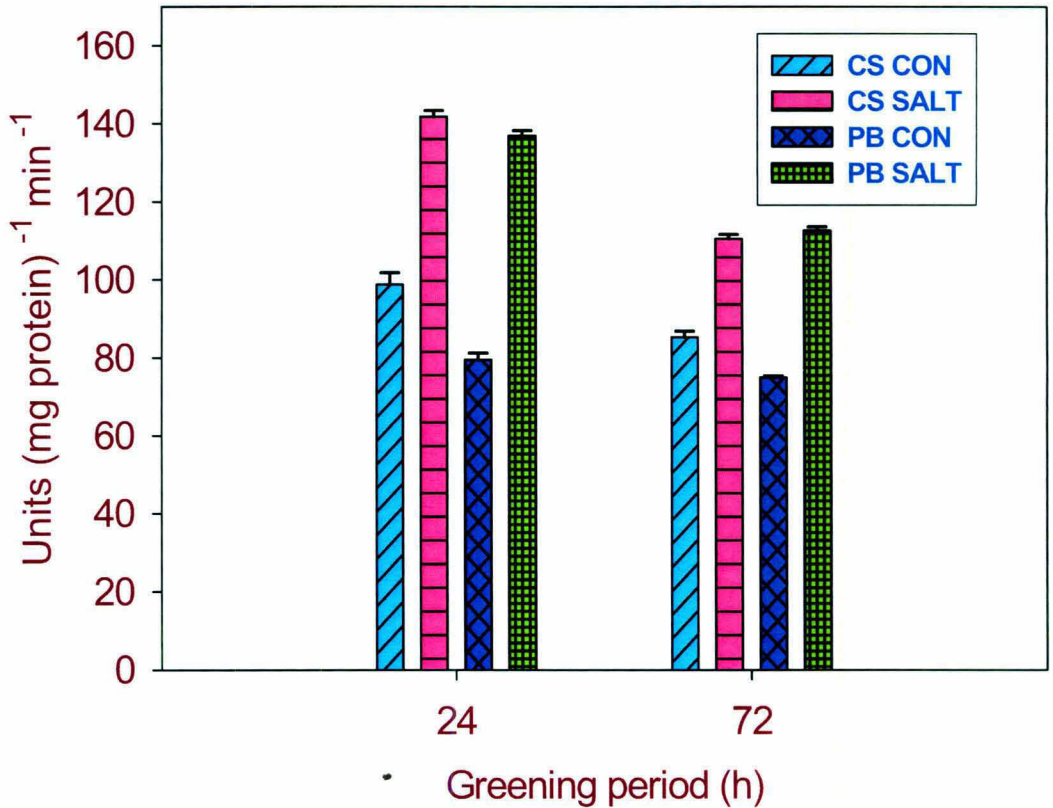


Fig 54: Superoxide dismutase activity in rice seedlings. Five-day-old etiolated rice seedlings of CSR10 and PB1 were treated with 0 and 200 mM NaCl 12 h prior to the transfer to cool white fluorescent+incandescent light ($100 \mu\text{moles photons m}^{-2} \text{s}^{-1}$), at 28°C at 75% relative humidity. Enzyme activity was measured as described in materials and methods after 24 and 72 h of greening. Each data point is the average of three replicates. The *error bar* represents SD.

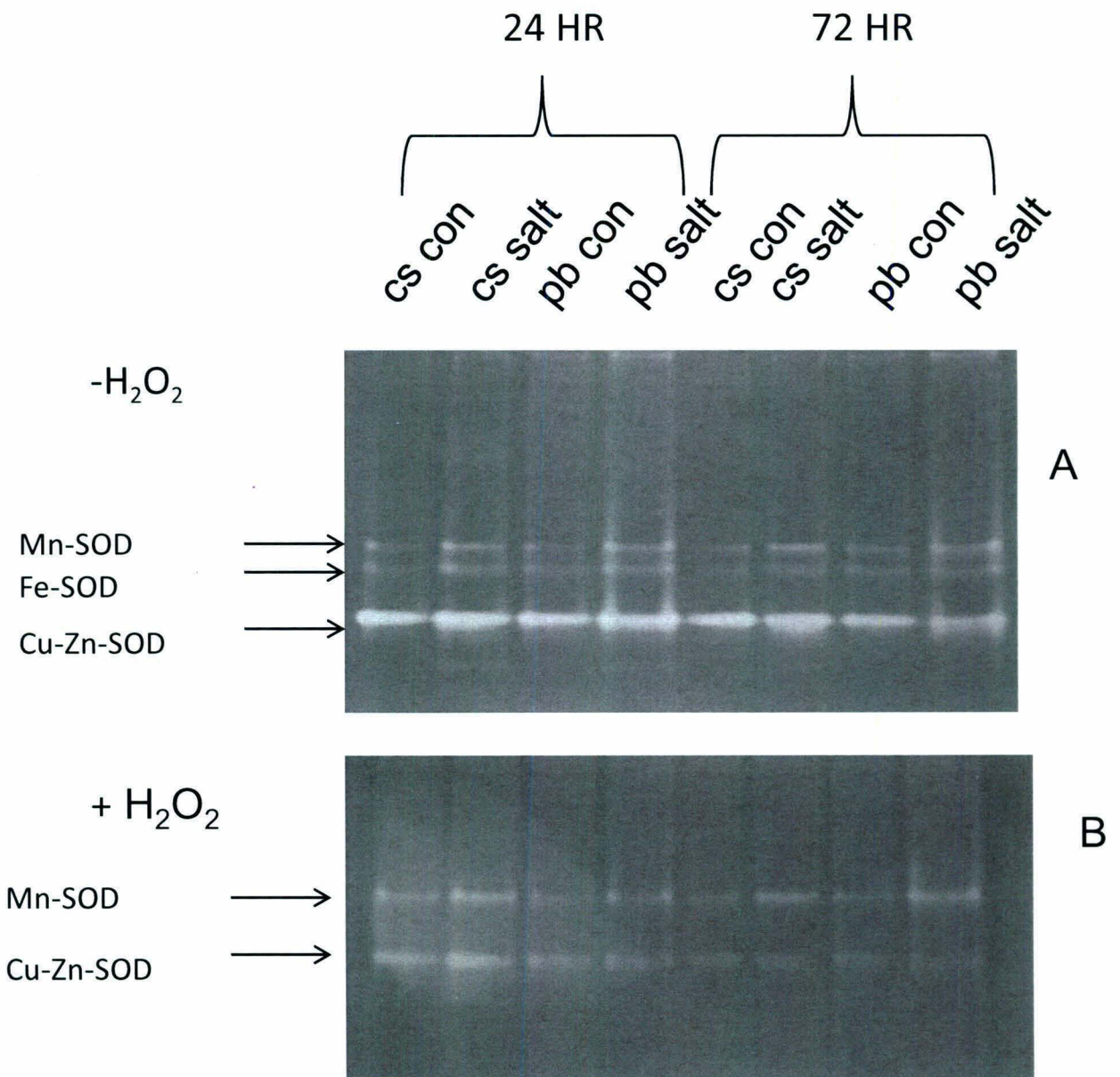


Fig 55: In gel assay of superoxide-dismutase in rice seedlings. Five-day-old etiolated rice seedlings of CSR10 and PB1 were treated with 0 and 200 mM NaCl 12 h prior to the transfer to cool white fluorescent+incandescent light ($100 \mu\text{moles photons m}^{-2} \text{s}^{-1}$), at 28°C at 75% relative humidity. In gel assay was carried out as described in materials and methods after 24 and 72 h of greening in the (A) absence and (B) presence of H_2O_2 .

Ascorbate peroxidase activity

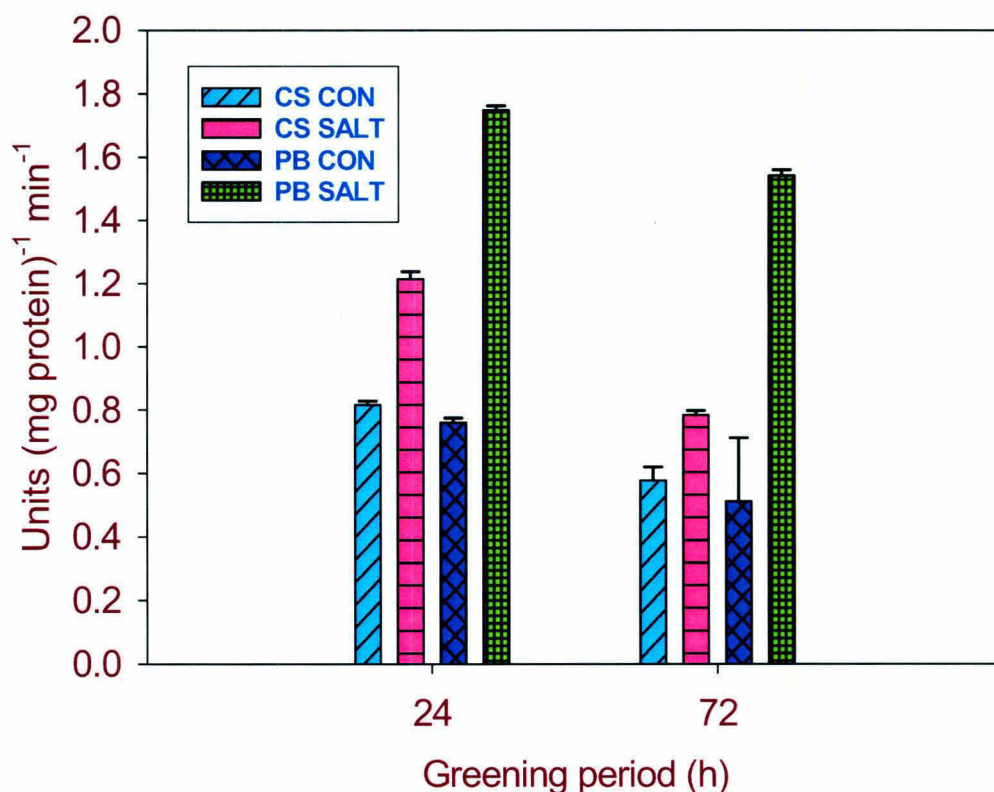


Fig 56: Ascorbate peroxidase activity in rice seedlings. Five-day-old etiolated rice seedlings of CSR10 and PB1 were treated with 0 and 200 mM NaCl 12 h prior to the transfer to cool white fluorescent+incandescent light ($100 \mu\text{moles photons m}^{-2} \text{s}^{-1}$), at 28°C at 75% relative humidity. Ascorbate peroxidase activity was measured as described in materials and methods after 24 and 72 h of transfer to light. Each data point is the average of three replicates. The *error bar* represents SD.

Glutathione reductase activity

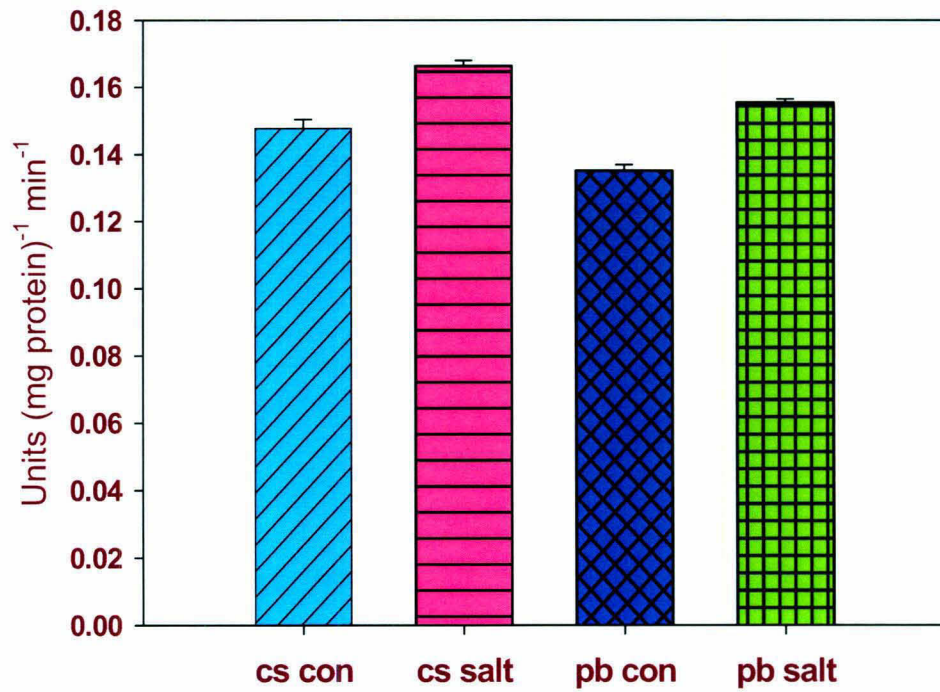


Fig 57: Glutathione reductase activity in rice seedlings. Five-day-old etiolated rice seedlings of CSR10 and PB1 were treated with 0 and 200 mM NaCl 12 h prior to the transfer to cool white fluorescent+incandescent light ($100 \mu\text{moles photons m}^{-2} \text{s}^{-1}$), at 28°C at 75% relative humidity. Glutathione reductase activity was measured as described in materials and methods after 24 h of greening. Each data point is the average of three replicates. The *error bar* represents SD.

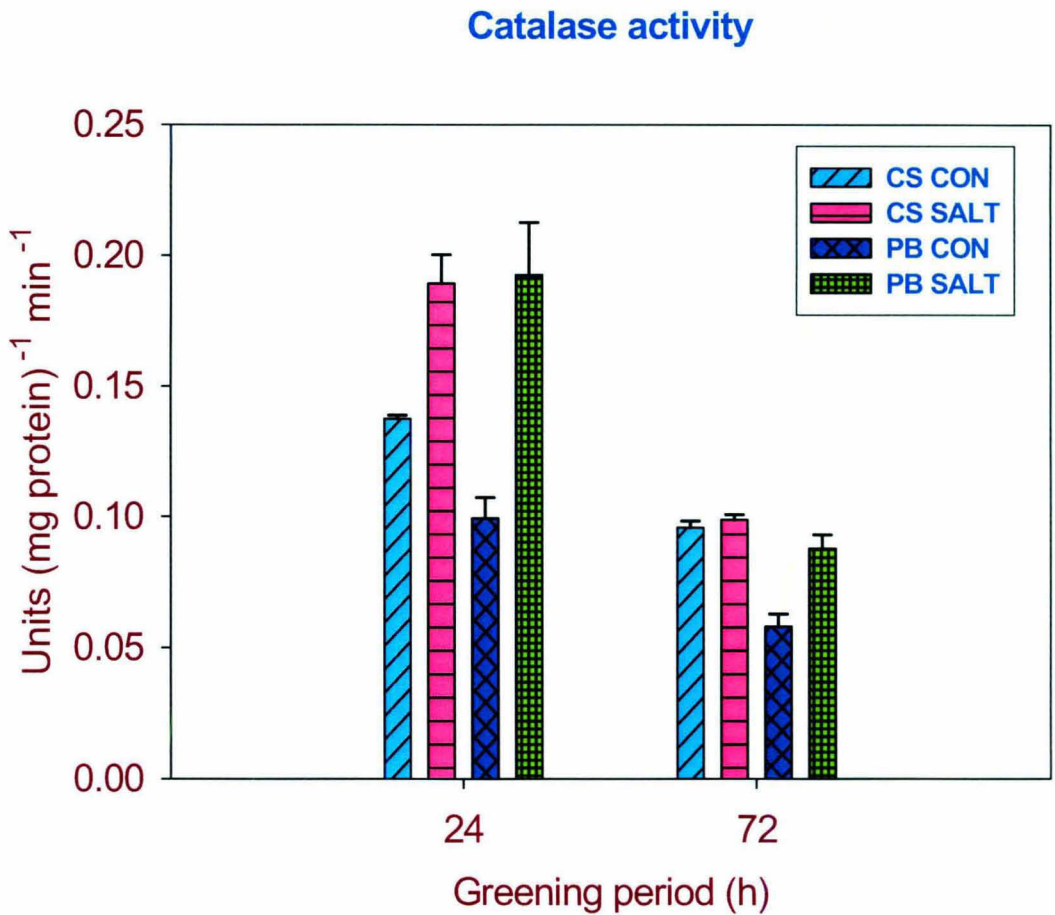


Fig 58: Catalase activity in rice seedlings. Five-day-old etiolated rice seedlings of CSR10 and PB1 were treated with 0 and 200 mM NaCl 12 h prior to the transfer to cool white fluorescent+incandescent light ($100 \mu\text{moles photons m}^{-2} \text{s}^{-1}$), at 28°C at 75% relative humidity. Catalase activity was measured as described in materials and methods after 24 and 72 h of greening. Each data point is the average of three replicates. The *error bar* represents SD.

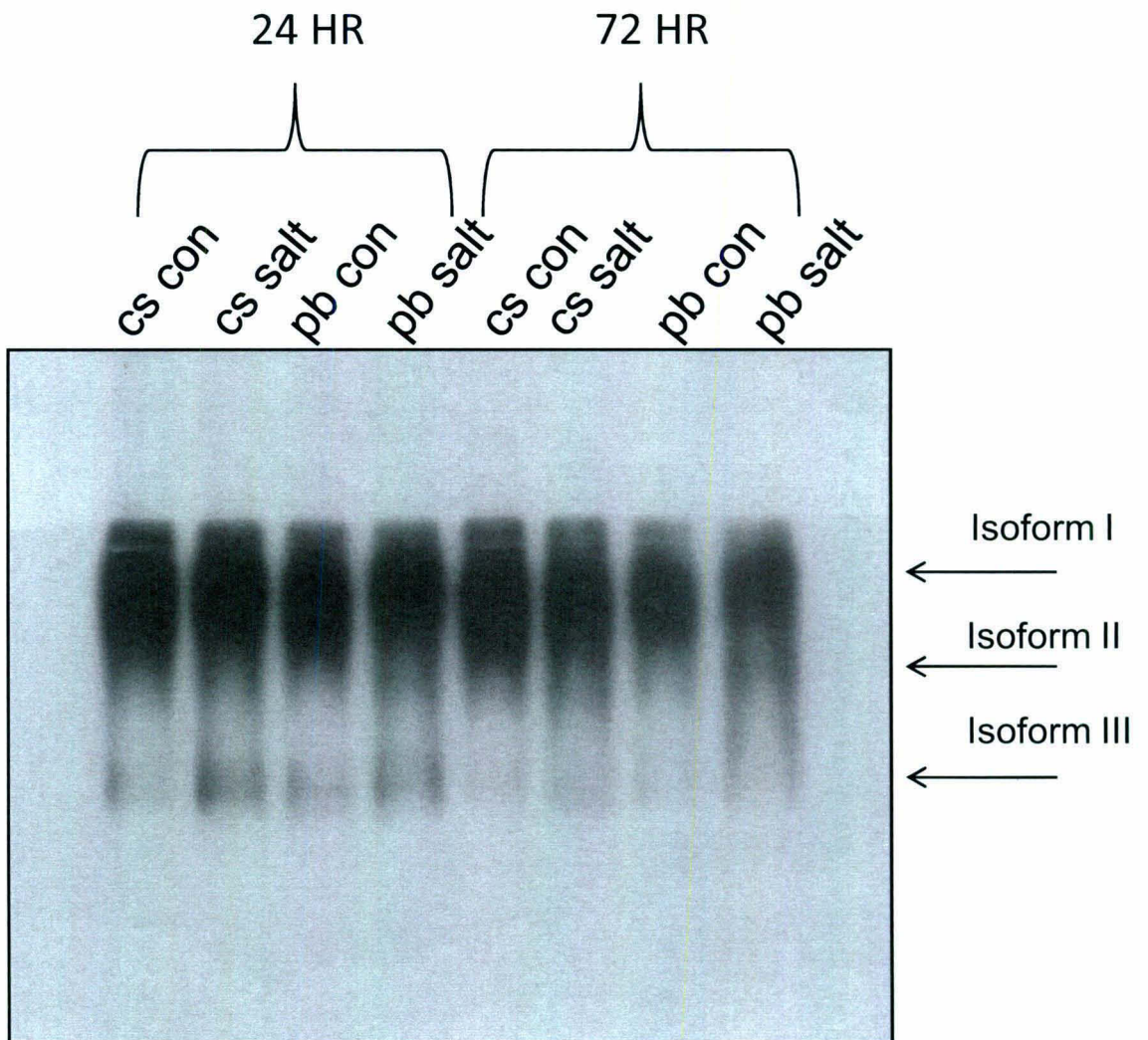


Fig 59: In gel assay of catalase in rice seedlings. Five-day-old etiolated rice seedlings of CSR10 and PB1 were treated with 0 and 200 mM NaCl 12 h prior to the transfer to cool white fluorescent+incandescent light ($100 \mu\text{moles photons m}^{-2} \text{s}^{-1}$), at 28°C at 75% relative humidity. In gel assay was carried out as described in materials and methods after 24 and 72 h of greening.

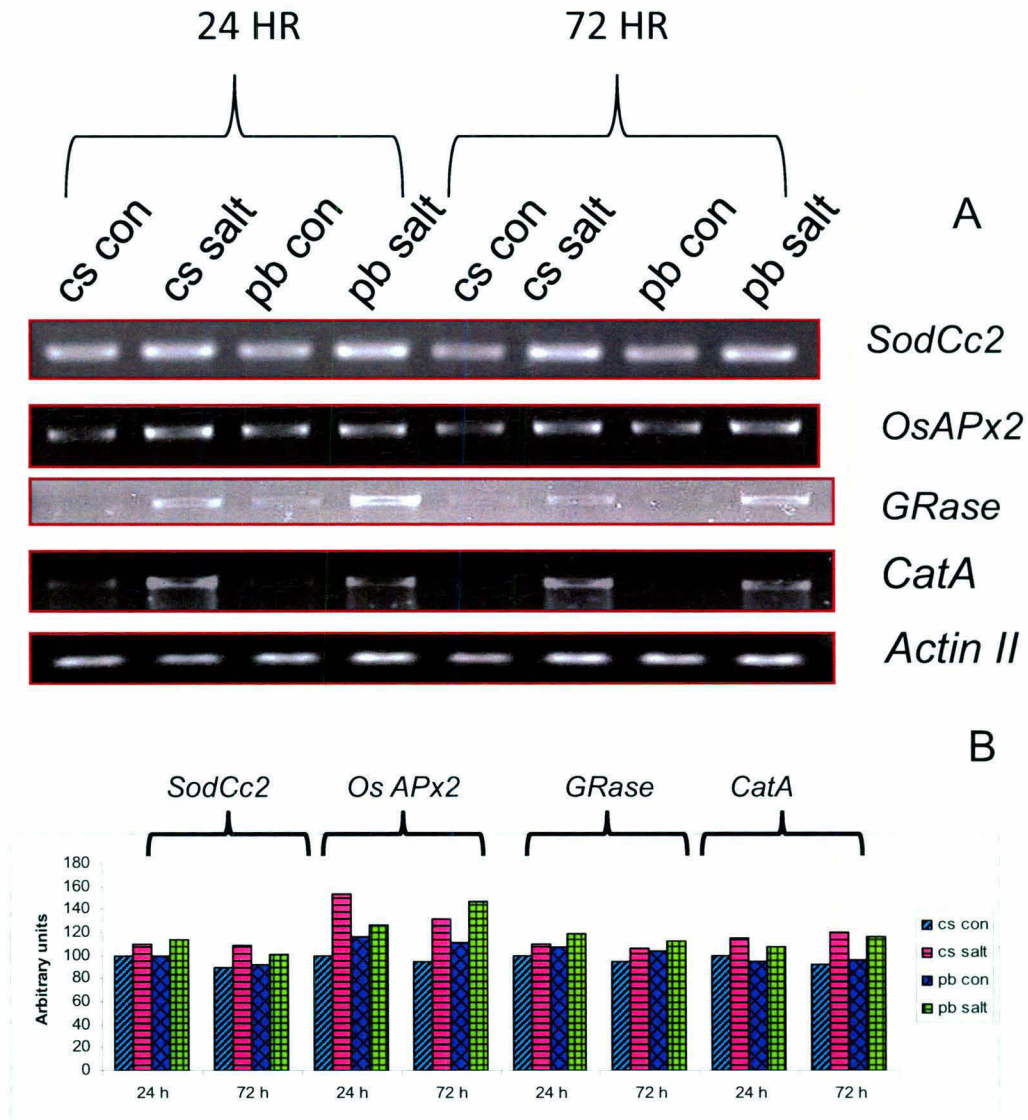


Fig 60: (A) Gene expression of antioxidative enzymes. Five-day-old etiolated rice seedlings of CSR10 and PB1 were treated with 0 and 200 mM NaCl 12 h prior to the transfer to cool white fluorescent+incandescent light ($100 \mu\text{moles photons m}^{-2} \text{s}^{-1}$), at 28°C at 75% relative humidity. Semi quantitative PCR was performed as in materials and methods. Total RNA was extracted from control and salt stressed leaves of rice seedlings after 24 and 72 h of greening and cDNA was made from $2 \mu\text{g}$ of total RNA as described in materials and methods. Each data point is average of three replicates. (B) Bar diagram of gene expression (%)

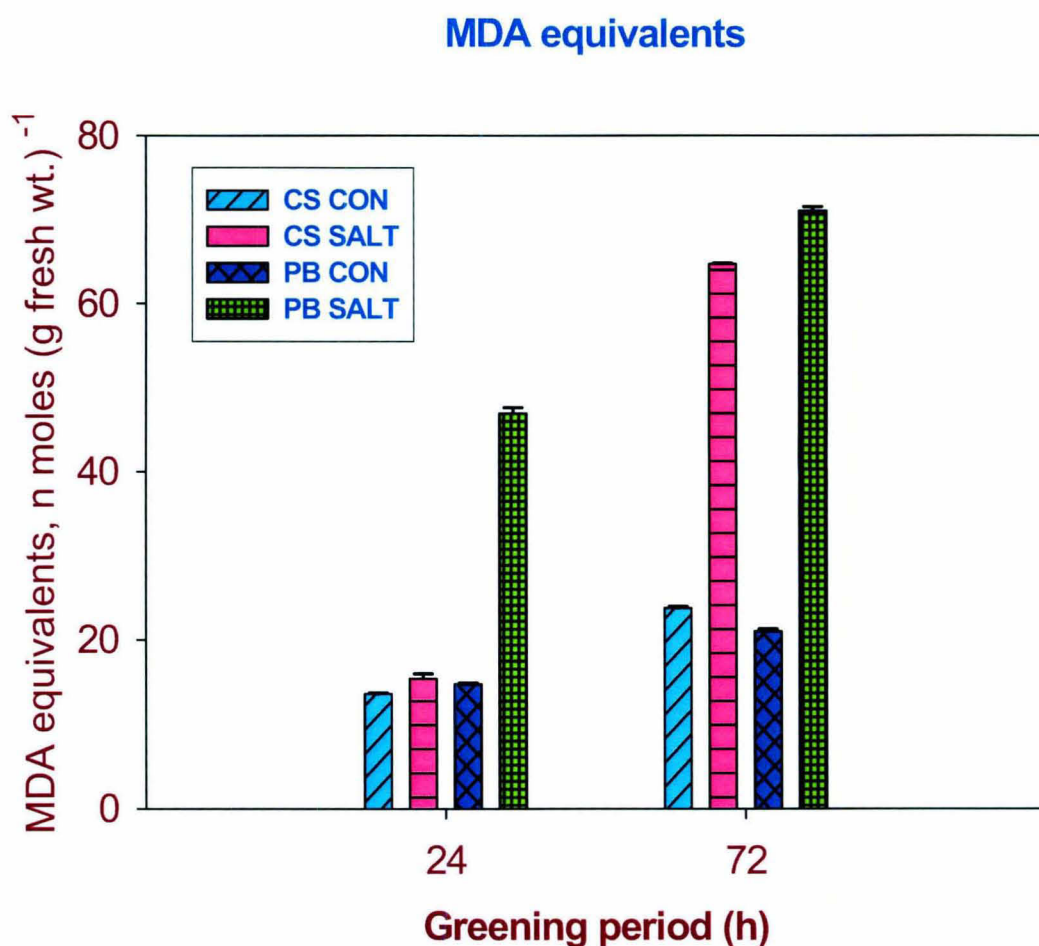


Fig 61: MDA content in rice seedlings. Five-day-old etiolated rice seedlings of CSR10 and PB1 were treated with 0 and 200 mM NaCl 12 h prior to the transfer to cool white fluorescent+incandescent light ($100 \mu\text{moles photons m}^{-2} \text{s}^{-1}$), at 28°C at 75% relative humidity. MDA Equivalents were measured as described in materials and methods after 24 and 72 h of greening. Each data point is the average of three replicates. The *error bar* represents SD.

H₂O₂ content

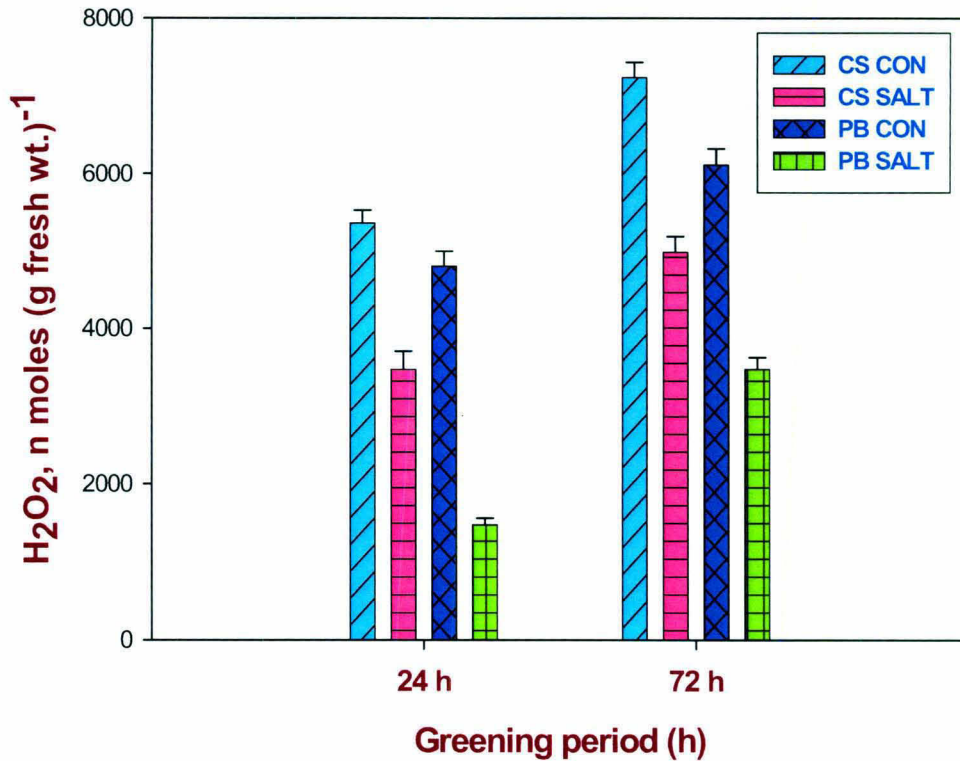


Fig 62: H₂O₂ contents in rice seedlings. Five-day-old etiolated rice seedlings of CSR10 and PB1 were treated with 0 and 200 mM NaCl 12 h prior to the transfer to cool white fluorescent+incandescent light (100 μ moles photons m^{-2} s^{-1}), at 28°C at 75% relative humidity. H₂O₂ contents were measured as described in materials and methods after 24 and 72 h of transfer to light. Each data point is the average of three replicates. The *error bar* represents SD.

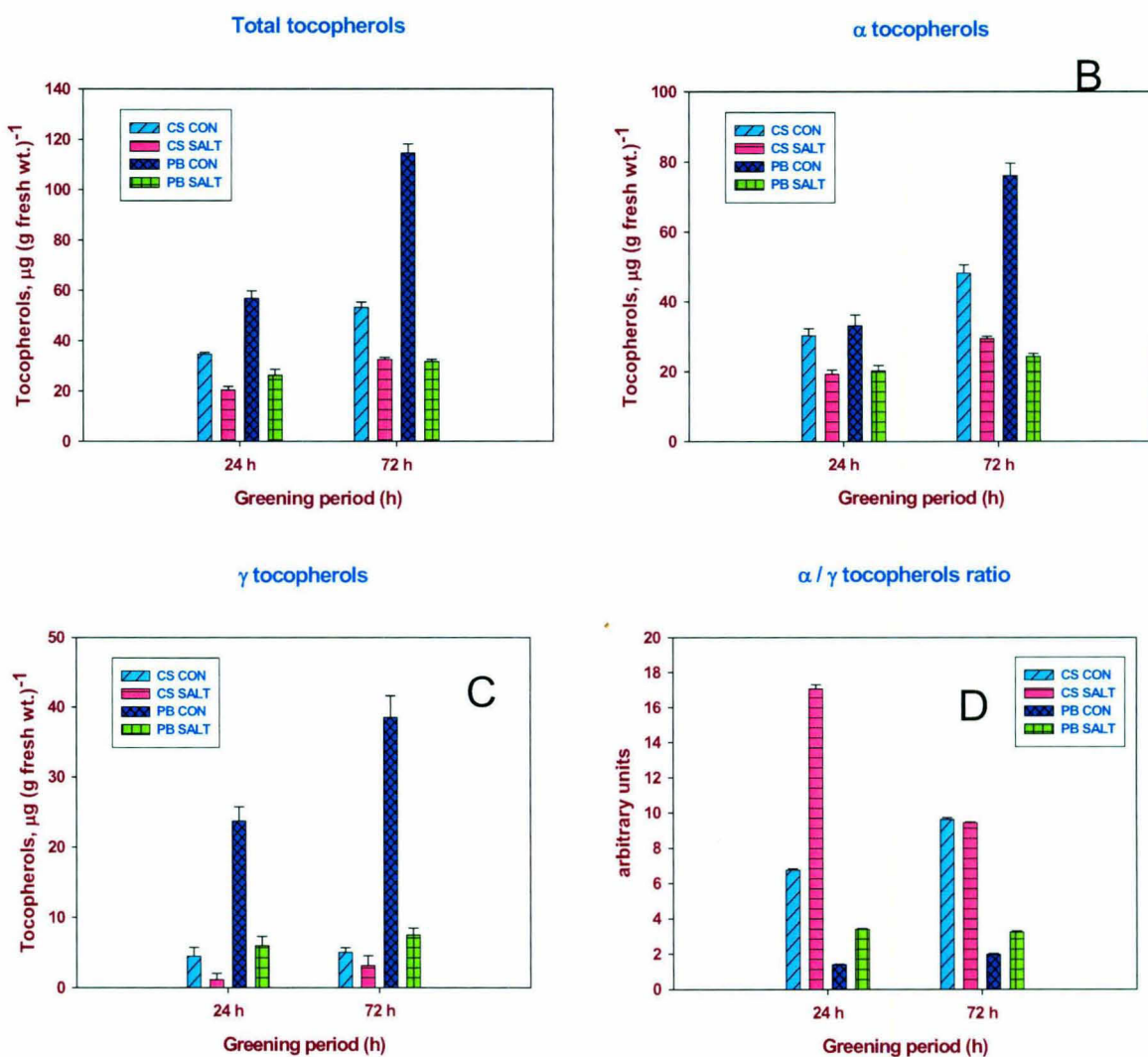


Fig 63: Tocopherols contents in leaves of rice seedlings (A) total ($\alpha+\gamma$) tocopherols. (B) α -tocopherols. (C) γ -tocopherols. (D) α / γ tocopherols ratio. Five-day-old etiolated rice seedlings of CSR10 and PB1 were treated with 0 mM and 200 mM NaCl 12 h prior to the transfer to cool white fluorescent+incandescent light ($100 \mu\text{moles photons m}^{-2} \text{s}^{-1}$), at 28°C at 75% relative humidity. Tocopherols contents were measured by HPLC as described in materials and methods after 24 and 72 h of greening. Each data point is the average of three replicates. The *error bar* represents SD.

absorbance at 240 nm after 24 and 72 hours of greening. The activity declined after 72 h of greening. In response to salt treatment catalase activity increased in both the cultivars. However, catalase activity after salt treatment was always higher in CSR10 as compared to salt sensitive PB1 genotype. In response to salt treatment the catalase activity increased to a greater extent in PB1 (Fig.58).

Catalase in gel assay:

Three isoforms of catalase were seen in the gel. Most of the activity of catalase was due to isoform I. After stress treatment isoform II was more pronounced in PB1. After 72 h of salt-stress isoform III was substantially reduced (Fig. 59).

Gene expression of Antioxidative enzymes:

To correlate the enzymatic activity to that of gene expression, the RT-PCR of certain genes involved in anti-oxidant activities was carried out. Transcript abundance of genes *SodCc2*, *CatA*, *OsAPx2*, *GRase* coding for Cu/Zn-SOD, catalase, ascorbate peroxidase and glutathione reductase respectively increased in response to salt stress in both of the cultivars (Fig. 60).

MDA content:

MDA production is an index of membrane lipids peroxidation. MDA contents were measured at 24 h and 72 h of greening in response to 200 mM NaCl. The MDA level highly increased in response to salt stress in salt-sensitive cultivar PB1 after 24 h of greening. Under identical conditions the MDA contents did not increase in salt resistant CSR10 cultivar. However after 72 h of greening MDA level of both the cultivar substantially increased although the increase in MDA content of PB1 was higher than that of CSR10 (Fig. 61).

H₂O₂ content:

H₂O₂ content were measured after 24 h and 72 h of greening in response to 200 mM NaCl stress as described in materials and methods. The H₂O₂ content partially declined in both the cultivars after 24 h and 72 h of greening. Under stress conditions H₂O₂ content declined probably due to increase in SOD, ascorbate peroxidase and catalase activities (Fig.62).

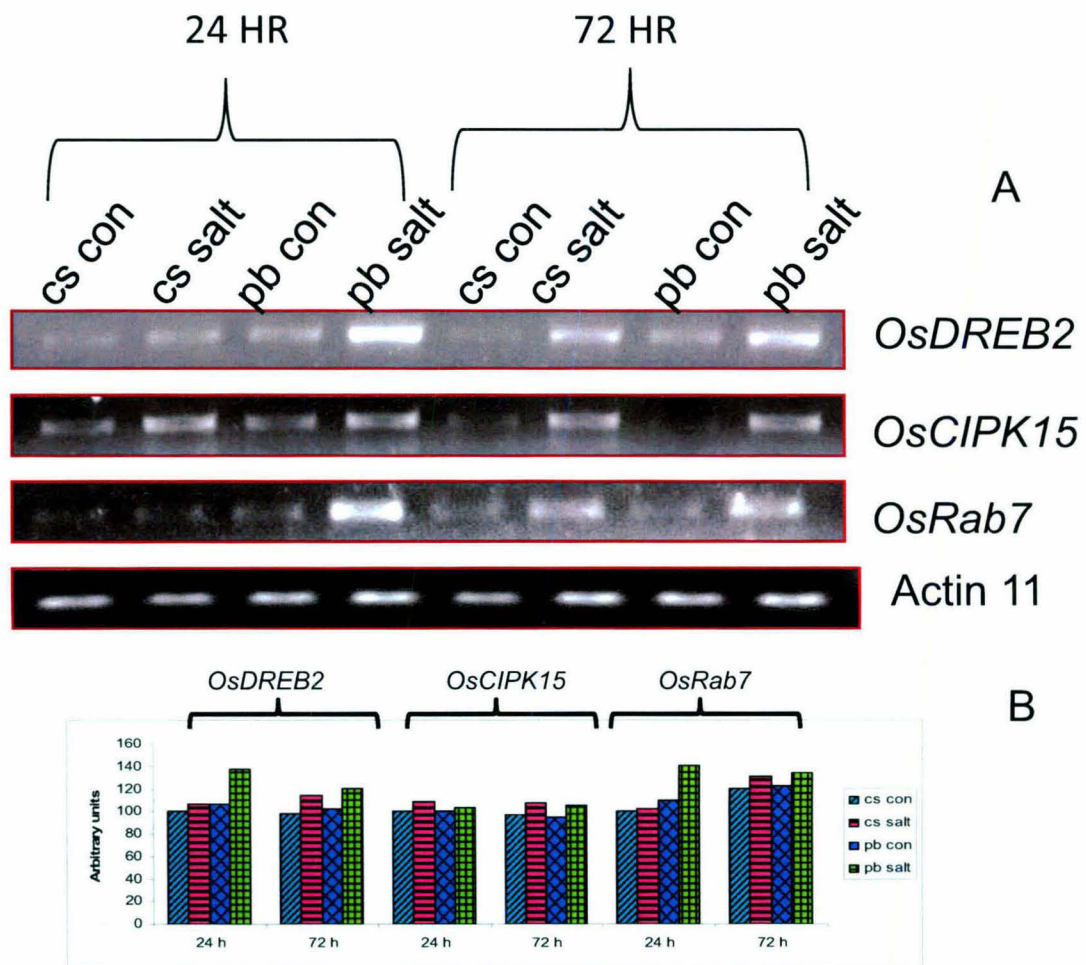


Fig 64: (A) Gene expression of salt stress related proteins. Five-day-old etiolated rice seedlings of CSR10 and PB1 were treated with 0 and 200 mM NaCl 12 h prior to the transfer to cool white fluorescent+incandescent light ($100 \mu\text{moles photons m}^{-2} \text{s}^{-1}$), at 28°C at 75% relative humidity. Semi quantitative PCR was performed as in materials and methods. Total RNA was extracted from control and salt stressed leaves of rice seedlings after 24 and 72 h of greening and cDNA was made from $2 \mu\text{g}$ of total RNA as described in materials and methods. Each data point is average of three replicates. (B) Bar diagram of gene expression (%)

Tocopherol content:

Tocopherol contents were measured in CSR10 and PB1 seedlings after 24 h and 72 h of greening in response to 200 mM NaCl stress (Fig. 63). In control samples both α and γ tocopherols increased as the seedlings became greener. However, their contents declined in response to salt-stress in both the cultivars. Ratio of α/γ is higher in CSR10 than PB1 and it further increased two fold in response to salt stress in both the cultivars after 24 h of salt stress. After 72 h of salt stress α/γ ratio is almost same in CSR10 whereas in PB1 it is still higher than control seedlings.

Gene expression of salt stress related genes:

To see expression of some stress inducible genes RT-PCR was performed (Fig. 64)

***OsDREB2*:** The gene codes for a stress inducible *Oryza sativa* transcription factor which causes salt tolerance after overexpression showed increased expression during salt stress especially in the salt-sensitive genotype PB1.

***OsCIPK15*:** The gene codes for one of the rice calcineurin B-like protein-interacting protein kinases which are induced by salt stress and causes salt tolerance when overexpressed, was induced by salt stress in both the cultivars.

***OsRab7*:** The gene codes for a stress inducible protein which is involved in vesicular transport, is induced by salt stress in both the cultivars. However its transcripts are higher in PB1 at early h of greening in the presence of salt than that in CSR10.

2-DE analysis of thylakoid proteins

For IEF run 300 μ g of thylakoid proteins were taken. After silver staining the protein profiles were analyzed to identify the differentially expressed protein in CSR10 seedlings grown in 200 mM NaCl stress (Fig.65 and 66). Differentially expressed protein were picked, in-gel digested with trypsin and their peptide mass finger printing (PMF) analysis was done through matrix assisted laser desorption ionization technique (MALDI-TOF-TOF). Some of the differentially expressed thylakoids proteins identified by MALDI-TOF-TOF are listed in Table 1.

pH 3 10

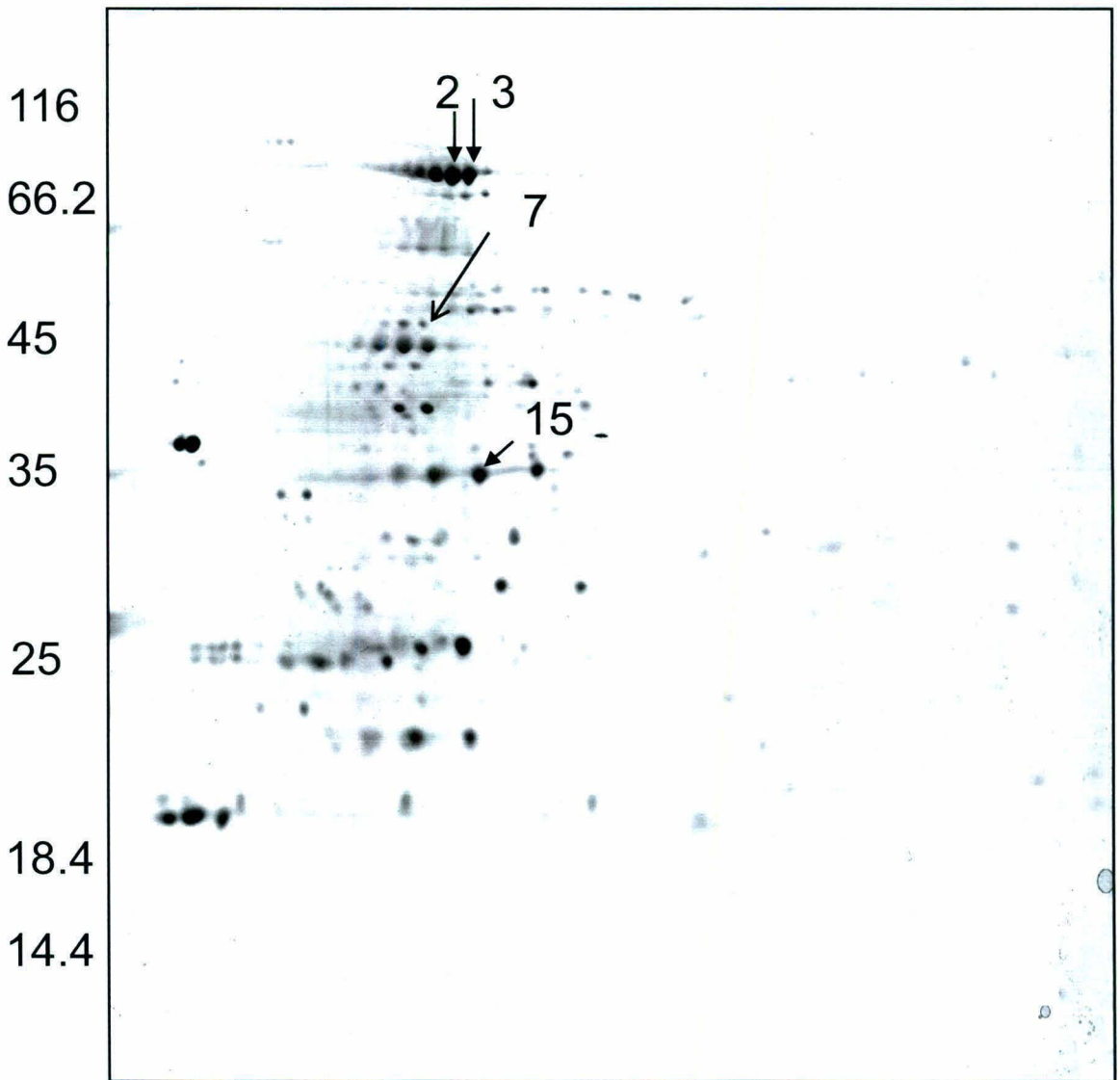


Fig 65 2-Dimensional-gel electrophoresis of thylakoids proteins from control seedlings of rice. Five-day-old etiolated rice seedlings of CSR10 were treated with 0 mM NaCl 12 h prior to the transfer to cool white fluorescent+incandescent light ($100 \mu\text{moles photons m}^{-2} \text{s}^{-1}$), at 28°C at 75% relative humidity. 2-Dimensional-gel electrophoresis was performed for thylakoids proteins isolated after 72 h of greening and silver stained.

pH 3 \longrightarrow 10

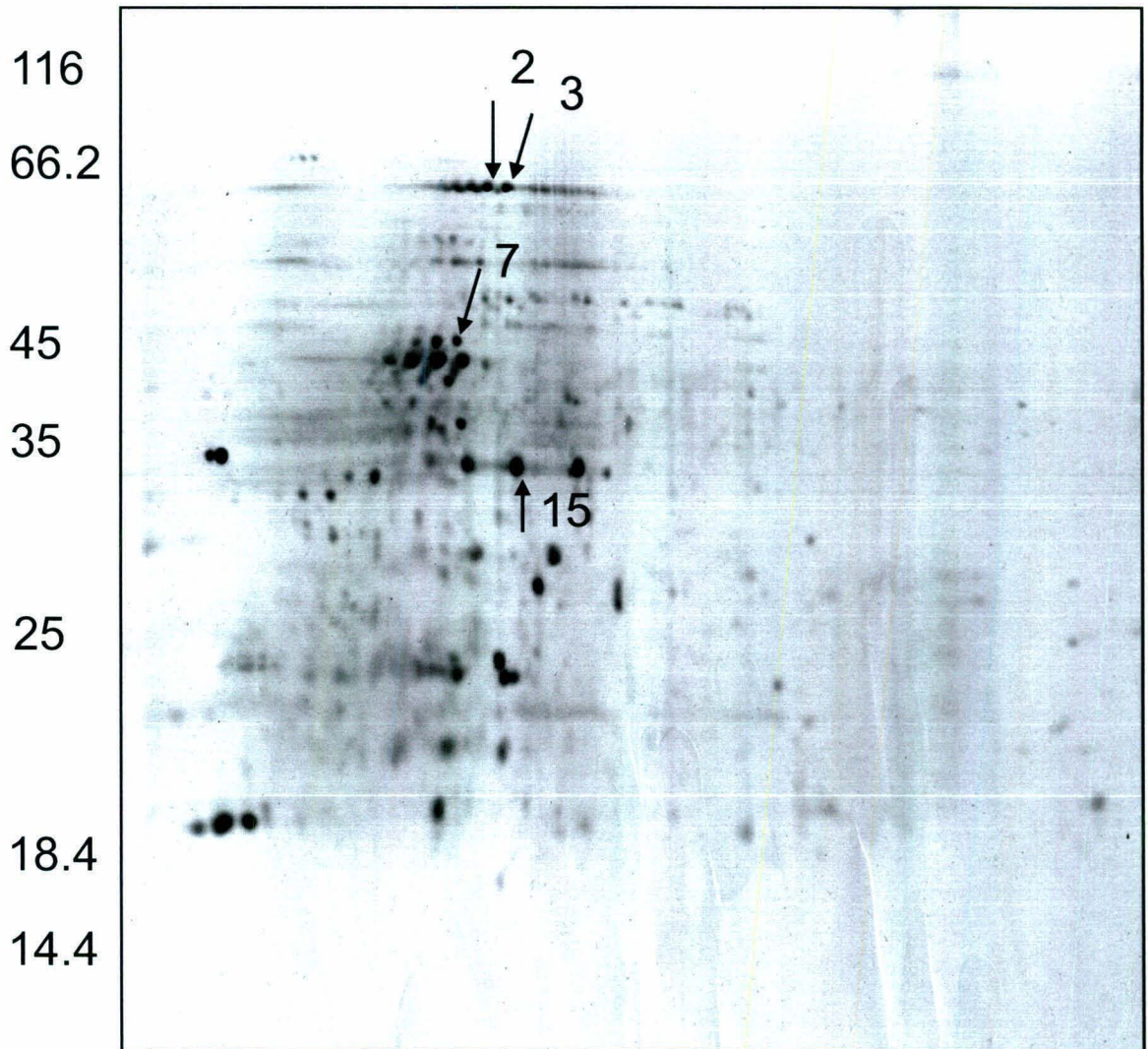


Fig 66: 2-Dimensional-gel electrophoresis of thylakoids proteins from salt stressed seedlings of rice. Five-day-old etiolated rice seedlings of CSR10 were treated with 200 mM NaCl 12 h prior to the transfer to cool white fluorescent+incandescent light ($100 \mu\text{moles m}^{-2} \text{s}^{-1}$), at 28°C at 75% relative humidity. 2-Dimensional-gel electrophoresis was performed for thylakoids proteins isolated after 72 h of greening and silver stained.

SPOT NO	Sequence name	Acession	Mass	Sequence coverage	pI	Score	Expression
2	ATP synthase CF1 beta subunit	gi 50233978	53.9	59.4	5.2	309	Down
3	ATP synthase CF1 beta subunit	gi 11466794	54.7	58.6%	5.3	297	Down
7	putative ATP synthase beta chain	gi 46391135	43.78	27.1%	5.6	86.4	Up
15	probable photosystem II oxygen-evolving complex protein 2 precursor	T02873	27.94	25.6%	9.4	69.9	Up

Table 1: Differentially expressed thylakoids proteins of CSR10 seedlings. Five-day-old etiolated rice seedlings of CSR10 were treated with 0 and 200 mM NaCl 12 h prior to the transfer to cool white fluorescent+incandescent light (100 μ moles photons $m^{-2} s^{-1}$), at 28°C at 75% relative humidity. 2-Dimensional-gel electrophoresis was performed after 72 h of greening, silver stained and spots were identified by MALDI TOF-TOF.

The proteins that were up-regulated in 200 mM NaCl stress at 72 hours of greening are Putative ATP synthase beta chain, probable photosystem II oxygen-evolving complex protein 2 precursor whereas down regulated are ATP synthase CF1 beta subunits (Table. 1).

2-DE analysis of PEG fractionated soluble proteins:

To know the differential expression of soluble proteins in response to salt stress 2-DE was carried out in CSR10 and PB1 after 72 h of greening (Fig. 67-70). Differentially expressed proteins were picked, in-gel digested with trypsin and their peptide mass finger printing (PMF) analysis was done through matrix assisted laser desorption ionization technique (MALDI-TOF-TOF). Some of the differentially expressed proteins identified by MALDI-TOF-TOF are listed in Table. 2, 3 and 4.

There were many proteins which were differentially regulated in response to salt stress in both CSR10 and PB1. Proteins identified by MALDI-TOF TOF are given in table 2, 3, and 4. In CSR10 cultivar the up-regulated proteins were amine oxidase putative, dehydration-responsive protein-like, putative indole-3-acetic acid-regulated protein, putative cytochrome P 450, mitogen-activated protein kinase 4, Formin-like protein 2, Fructose-bisphosphate aldolase, chloroplast precursor. The down-regulated proteins were homeobox protein knotted-1-like 13 OS, Retrotransposon protein putative, putative GTP-binding protein, mitogen-activated kinase kinase alpha putative expressed, Cytochrome c oxidase subunit 6b-1 (Cytochrome c oxidase subunit 6b), Putative malate dehydrogenase (Putative mitochondrial malate dehydrogenase), Ankyrin repeat domain protein 2 putative expressed. Putative probable transcription repressor HOTR was the newly protein synthesized (Table.2 & Table. 3).

In PB1 upregulated proteins are homeobox protein knotted-1-like 13 OS, Ribulose bisphosphate carboxylase large chain, putative, Calcineurin B-like protein 5, Probable glutathione S-transferase GSTF2. Proteins that were down-regulated are dehydroascorbate reductase, hypothetical protein OSJNBa0048A13.20. There is one newly synthesized protein named hypothetical protein OsI_16284.

Proteomic responses of different kind were observed in two cultivars CSR10 and PB1. There were proteins which were upregulated in both the cultivars such as spots number assigned (203, 218, 307, 308), only induced in CSR10 such as spot number (201,202, 212, 214, 215, 216,

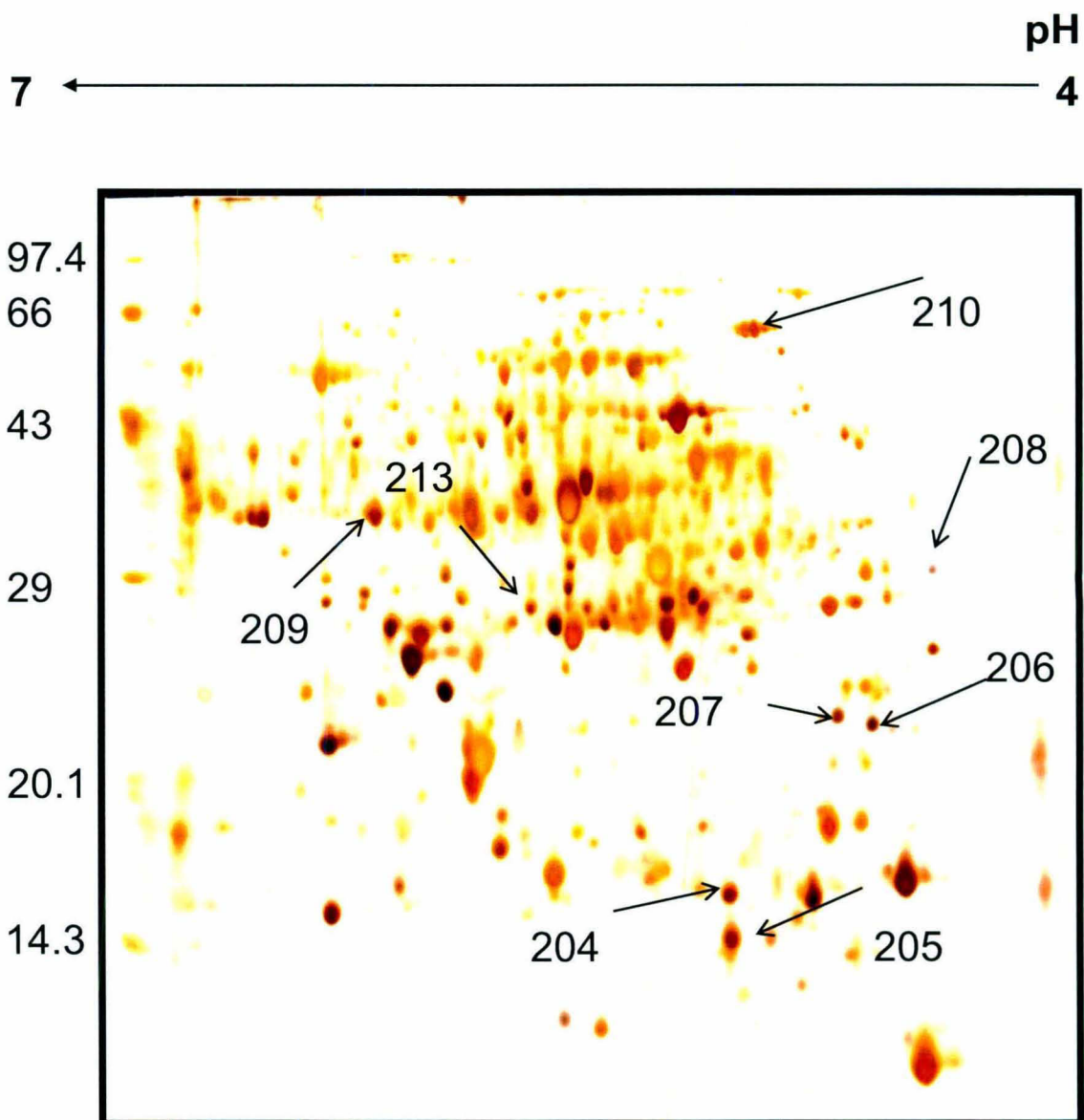


Fig 67: 2-Dimensional-gel electrophoresis of PEG fractionated soluble proteins of rice seedlings. Five-day-old etiolated rice seedlings of CSR10 were treated with 0 mM NaCl 12 h prior to the transfer to cool white fluorescent+incandescent light ($100 \mu\text{moles photons m}^{-2} \text{s}^{-1}$), at 28°C at 75% relative humidity. 2-Dimensional-gel electrophoresis was performed for soluble PEG fractionated proteins isolated from leaves after 72 h of salt stress and silver stained.

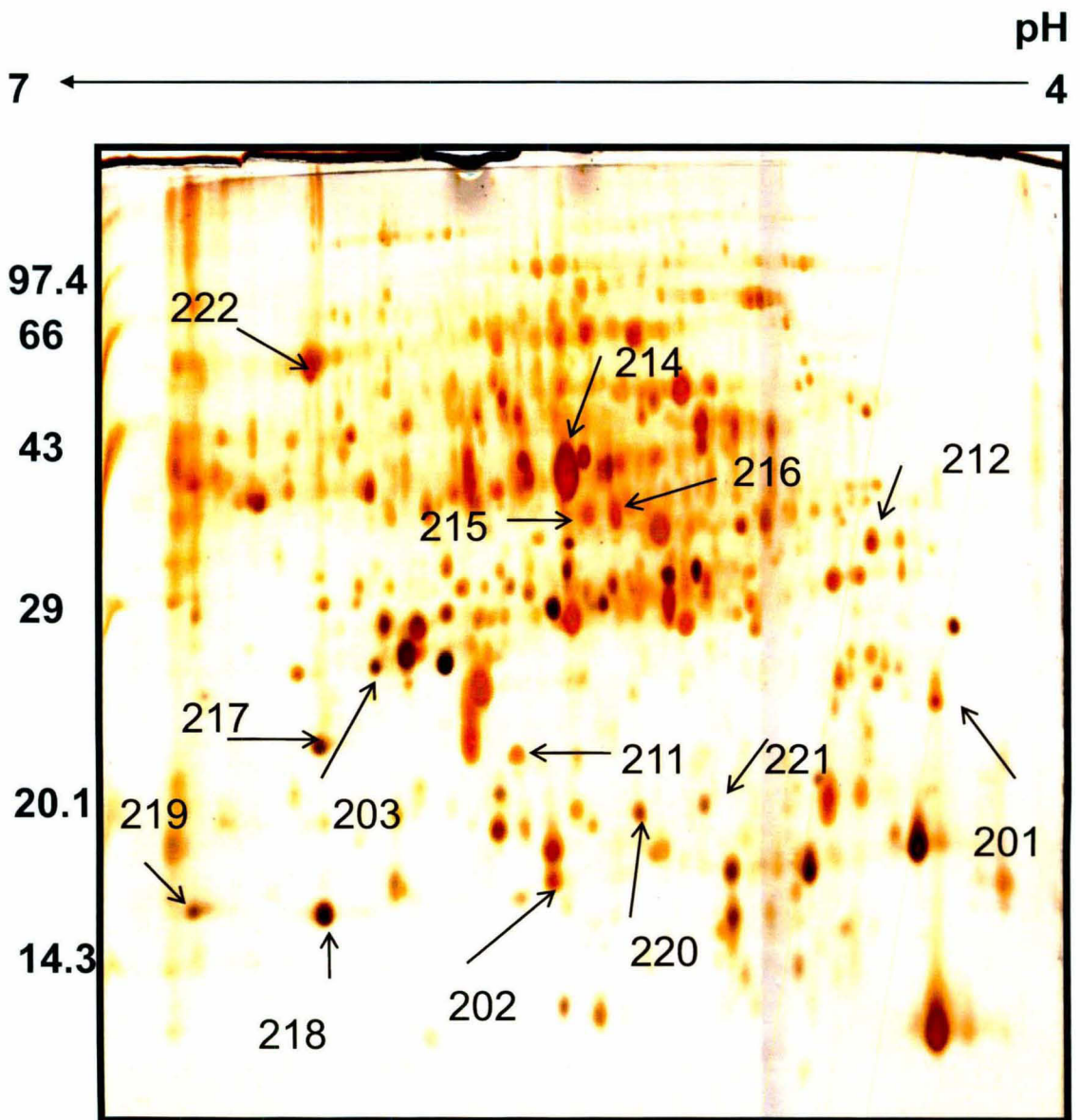


Fig 68: 2-Dimensional-gel electrophoresis of soluble PEG fractionated soluble proteins of rice seedlings. Five-day-old etiolated rice seedlings of CSR10 were treated with 200 mM NaCl 12 h prior to the transfer to cool white fluorescent+incandescent light ($100 \mu\text{moles photons m}^{-2} \text{s}^{-1}$), at 28°C at 75% relative humidity. 2-Dimensional-gel electrophoresis was performed for soluble PEG fractionated proteins isolated from leaves after 72 h of salt stress and silver stained.

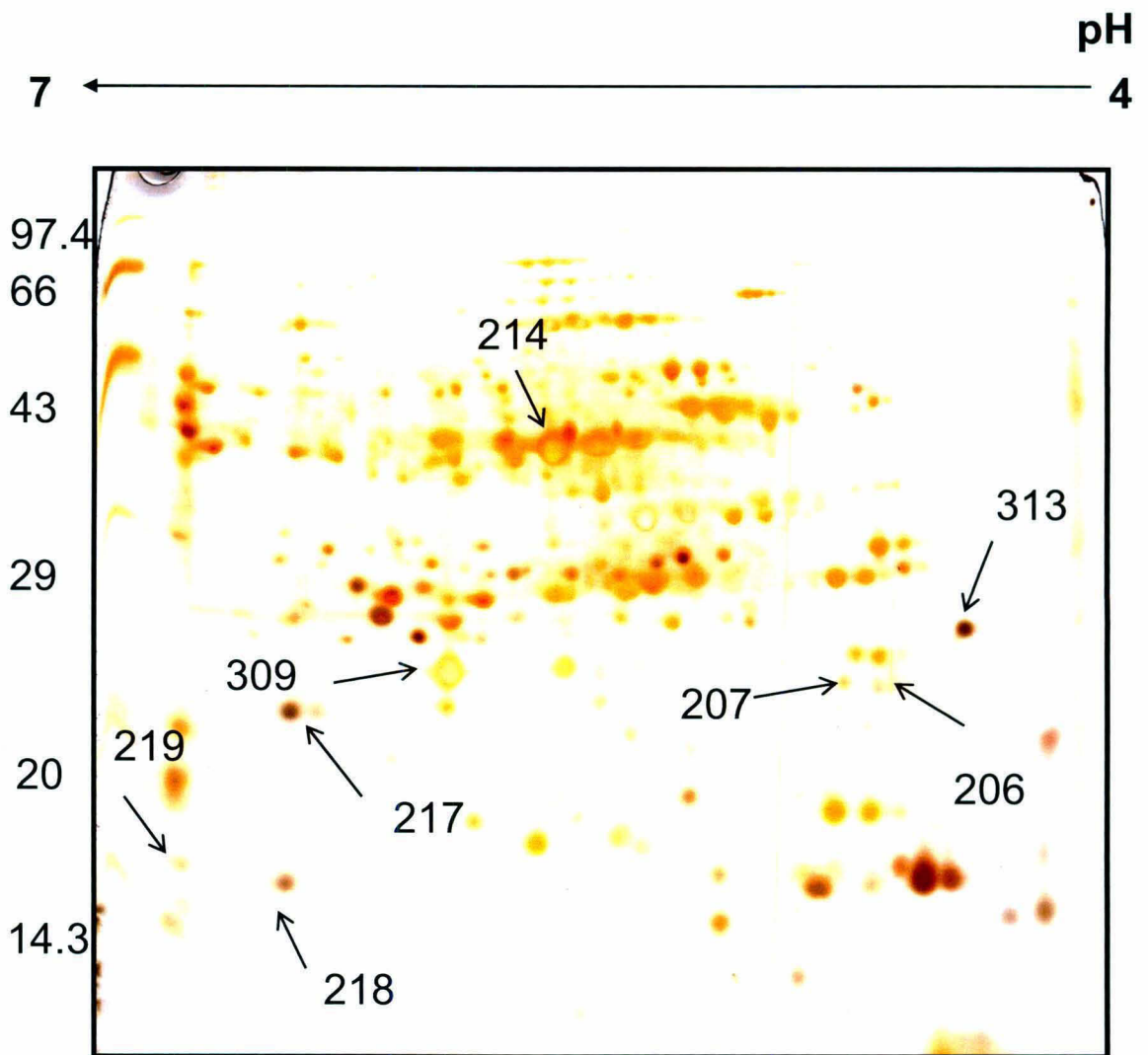


Fig 69: 2-Dimensional-gel electrophoresis of soluble PEG fractionated soluble proteins of rice seedlings. Five-day-old etiolated rice seedlings of PB1 were treated with 0 mM NaCl 12 h prior to the transfer to cool white fluorescent+incandescent light ($100 \mu\text{moles photons m}^{-2} \text{s}^{-1}$), at 28°C at 75% relative humidity. 2-Dimensional-gel electrophoresis was performed for soluble PEG fractionated proteins isolated from leaves after 72 h of salt stress and silver stained.

Spot No.	Sequence name	Acession	Mass	Sequence coverage	pI	Score	Expression
201	DP000009 NID	ABF94888	48.9	17.8%	10.0	58.100000	Up
202	mitogen-activated protein kinase 4	gi 222430540	41.3	21.8%	6.4	55.400000	Up
203	Formin-like protein 2	A2XUA1	91.63	11.0	9.6	34.200000	Up
204	Homeobox protein knotted-1-like 13 OS	GI:221272018	41.1	22.5%	5.4	45.000000	Down
205	Retrotransposon protein, putative	ABA97821	42.13	15.9%	4.5	30.900000,	Down
206	putative GTP-binding protein	AAL58207	67.2	16.4%	9.0	41.800000	Down
207	mitogen-activated kinase kinase kinase alpha, putative, expressed	gi 108864120	42	19.1%	9.7	41.70000	Down
208	Cytochrome c oxidase subunit 6b-1 (Cytochrome c oxidase subunit 6b)	NP_001050275	18.59	30.8%	4.1	57.500000	Down
209	Putative malate dehydrogenase (Putative mitochondrial malate dehydrogenase)	NP_001043717	37.4	22.1%	9.5	52.6000	Down
210	Os02g0764100	gi 115448867	27.8	39.9%	12.0	62.800000	Down
211	Putative probable transcription repressor HOTR	NP_001060131	68.4	31.8%	10.2	47.60000	new

Table 2. Five-day-old etiolated rice seedlings of CSR10 were treated 0 mM and 200 mM NaCl 12 h prior to the transfer to cool white fluorescent+incandescent light ($100 \mu\text{mol m}^{-2} \text{s}^{-1}$), at 28°C at 75% relative humidity maintained by a Conviron plant growth chamber. Soluble proteins were isolated from leaves sample and 2-Dimensional gel electrophoresis was performed. Gels were silver stained and spots were identified by MALDI TOF-TOF.

Spot no	Sequence name	Acession	Mass	Sequence coverage	pI	Score	Expression
212	Os02g0328300	gi 115445869	31.57	48.8%	5.3	97.1	Up
213	Ankyrin repeat domain protein 2 putative	gi 108712139	38.39	26.4%	4.5	55.1	Down
214	Fructose-bisphosphate aldolase, chloroplast precursor putative	gi 108864048	42.24	32%	6.0	105.0	Up
215	Os06g0479100	gi 115468092	20.24	37.5%	12.4	51.3	Up
216	Putative protein kinase	gi 22773239	38.5	32.3%	6.4	50.4	Up
217	Ternary complex factor MIP1-like	ABA41566	49.94	17.8%	5.7	42.3	Down
218	amine oxidase, putative, expressed	gi 108711419	28.05	18.4%	9.4	49.9	Up
219	dehydration-responsive protein-like	gi 55296764	69.4	25.2%	9.5	53.5	Up
220	putative indole-3-acetic acid-regulated protein	gi 15144310	11.99	36.7%	7.0	45.6	Up
221	putative cytochrome P450	gi 50511461	51.59	25.6%	9.5	59.4	Up
222	Os06g0598500	gi 115468792	47.96	36.0%	7.2	144.0	Up

Table 3. Five-day-old etiolated rice seedlings of CSR10 were treated 0 mM and 200 mM NaCl 12 h prior to the transfer to cool white fluorescent+incandescent light ($100 \mu\text{mol m}^{-2} \text{s}^{-1}$), at 28°C at 75% relative humidity. Soluble proteins were isolated from leaves sample and 2-Dimensional gel electrophoresis was performed. Gels were silver stained and spots were identified by MALDI TOF-TOF.

SPOT NO	Sequence name	Acession	Mass	Sequence coverage	pI	Score	Expression
301	Hypothetical protein	gi 15624054	19.58	36.5%	11.3	32.8	Up
302	Os11g0139500	gi 115484087	28.71	23.4%	10.2	45.3	Up
303	hypothetical protein OsI_15018	gi 125547390	45.87	23.5%	6.4	63.7	Up
304	Homeobox protein knotted-1-like 13 OS	Q851L5_ORYSA	45.87	33.3%	5.4	69.9	Up
305	Hypothetical protein OSJNBa0025H18.7	Q6K388_ORYSA	7.0	100%	9.8	61.9	Up
306	AE016959 NID	AAP53794	20.2	42.4%	4.9	60	Up
307	Ribulose biphosphate carboxylase large chain, putative	Q2QW49_ORYSA	54	16.1%	9.7	73.8	Up
308	Ribulose biphosphate carboxylase large chain	Q5K3B1_ORYSA	53.2	19.1%	6.2	110	Up
309	Calcineurin B-like protein 5	CNBL5_ORYSJ	23.98	18.3%	4.6	24.5	Up
310	Probable glutathione S-transferase GSTF2	GSTF2_ORYSJ	23.65	10.7%	5.7	32.4	Up
311	Dehydroascorbate reductase	Q84UH5_ORYSA	23.43	36.6%	5.8	52.2	Down
312	hypothetical protein OsI_16284	gi 218195036	23.43	41.8%	7.0	59.5	New
313	Hypothetical protein OSJNBa0048A13.20	Q6H589_ORYSA	26.5	17.0%	5.6	46.6	Down

Table 4. Five-day-old etiolated Rice seedlings of CSR10 were treated 0 mM and 200 mM NaCl 12 h prior to the transfer to cool white fluorescent+incandescent light ($100 \mu\text{mol m}^{-2} \text{s}^{-1}$), at 28°C at 75% relative humidity maintained by a Conviron plant growth chamber. Soluble proteins were isolated from leaves sample and 2-Dimensional gel electrophoresis was performed. Gels were silver stained and spots were identified by MALDI TOF-TOF.

220, 221), and only upregulates in PB1 such as spot number (205, 206, 210, 217, 219). For example-retrotransposon protein putative at spot 205 is down regulated in CSR10 however its expression increased in PB1 in response to salt stress. Similarly protein Os02g0328300 identified from spot 212 upregulated in CSR10 whereas its expression is downregulated in PB1 in response to salt stress.

Discussion

DISCUSSION

Plants are frequently exposed to a plethora of stress conditions such as low temperature, salt, drought, flooding, heat, oxidative stress and heavy metal toxicity. Salinity is a major environmental stress and is a substantial constraint to crop production. Plant growth is drastically reduced under increasing salt stress (for recent reviews see Hasegawa et al, 2000; Munns and Tester, 2008).

Chlorophyll plays an important role in harnessing solar energy for its utilization in photosynthesis. Chloroplast biogenesis is regulated by chlorophyll biosynthesis that is adversely affected by salt stress. As shown in Fig.1 salt sensitive cultivar PB1 (Fig.1 B) was more affected by salt stress than relatively resistant cultivar CSR10 (Fig.1 A). Chlorophyll and carotenoids contents were also reduced in response to increased NaCl stress in both the cultivars (Figs. 2 and 3), although the relative decrease in Chl and carotenoids contents were more in salt sensitive PB1 as compared to that of salt-tolerant CSR10. Chl a/b ratio increased in response to salt stress possibly due to less synthesis of Chlb (Fig. 2 D). Pérez-Tornero et al, 2009 have reported decrease in total chlorophyll in *Citrus macrophylla* in response to salt stress. In wheat chlorophyll contents decrease due to NaCl stress (Shafi et al, 2009). Chl and carotenoids contents decreased in halophyte *Cakile maritime* at extreme salt concentration (Debez et al, 2008).

Impact of salt-stress on ion homeostasis

To understand the molecular mechanism of resistance of CSR-10 to salt stress, concentrations of different salts in roots and shoot were analysed. Sodium contents increased in shoot as well as root in response to salt stress in both the cultivars (Fig.5). However, in salt-sensitive PB1, the shoots accumulated more Na⁺ than that in CSR10 (Fig.5 B). However, CSR10 roots accumulated more sodium as compared to that in PB1 (Fig.5 A). This shows that CSR10 sequesters Na⁺ in roots. The K⁺ content decreased due to stress in both the cultivars in shoot as well as root (Fig. 6) and the Ca²⁺ increased in the shoot (Fig.8 B). In salt-stressed rice Sengupta and Majumdar, 2009 observed reduced accumulation of Na⁺ in shoots of salt-resistant rice cultivar and Jia et al, (2008) observed a decrease in K⁺ contents of leaf and root tissues in response to salt stress in plant species from *Elemyus* genus.

Na^+ disequilibrium is a primary consequence of salt stress and leads to catastrophic pathologies affecting cell survival, division, and growth (Hasegawa et al., 2000; Tester and Davenport, 2003; Zhu, 2003). Another consequence of Na^+ disequilibrium that is caused by salt stress is the detrimental effect of Na^+ on K^+ acquisition and nutrition. K^+ has essential functions in plant metabolism (e.g. charge balance, osmotic adjustment, and enzyme catalysis) and in growth and development (Maathuis and Sanders, 1996; Rigas et al., 2001; Elumalai et al., 2002). Na^+ in the soil solution disturbs K^+ homeostasis in plants presumably because the cytotoxic ion competes for binding sites in transport systems that mediate K^+ uptake (Epstein, 1961; Rains and Epstein, 1965; Niu et al., 1995; Hasegawa et al., 2000).

Effect of temperature stress on chlorophyll biosynthesis and the greening process

Inhibition of Chl biosynthesis by salinity stress was due to reduced synthesis of ALA (Fig. 10), the committed precursor of Chl. Unlike bacterial and animal systems, in plants ALA is synthesized from a five carbon compound glutamate. Accumulation of Glutamate -1-semialdehyde (GSA), an intermediate leading to ALA synthesis, was higher in salt-resistant CSR10 as compared to that in salt-sensitive PB1 cultivar (Fig. 9). The increased synthesis of GSA in CSR10 may be due to increased gene expression of *GluTR*, encoding Glutamyl-t-RNA reductase that converts Glutamyl-t-RNA to GSA. *GluTR* expression also increased in PB1 due to salt stress although the extent of increase was smaller than that in CSR10 (Fig. 21 A).

GSA is converted to ALA by Glutamate-1-semialdehyde aminotransferase coded by *GSAT*. Its expression also increased in CSR10 in response to salt stress leading to higher ALA synthesis (Fig. 21 A). In salt sensitive genotype PB1, its expression partially downregulated in response to salt stress. Results demonstrate that the maintenance of ALA biosynthesis in salt stressed condition is extremely important and plants upregulate the gene expression of ALA biosynthetic enzymes. The gene and protein expression of *GSAT* also increases in heat-stressed wheat and cucumber seedlings (Mohanty et al, 2006).

ALA is metabolized to protoporphyrin IX by a set of enzymes named ALA dehydratase (ALAD) that converts ALA into porphobilinogen (PBG), Porphobilinogen deaminase (PBGD), Uroporphyrinogen decarboxylase (UROD), Coproporphyrinogen oxidase (CPO) and Protoporphyrinogen oxidase (Protox) acting in series. The activity of ALAD that converts ALA to porphobilinogen was reduced in PB1 by salt stress whereas in CSR10 it was not substantially

affected (Fig. 12). Similarly, its gene expression was downregulated in PB1 although it was partially affected in CSR10 (Fig. 21 A). Similar to salt-stress, the ALAD activity and *ALAD* expression decrease in response to heat and chill stress in *cucumber* seedlings (Tiwari and Tripathy, 1998).

The PBGD activity declined due to salt stress in both the cultivars (Fig. 13). Salt-induced decline in its activity well correlates with the reduced gene expression of *PBGD* (Fig. 20 A). In temperature-stressed *cucumber* seedlings the PBGD activity is also reduced (Tiwari and Tripathy, 1998).

The UroD, the next enzyme in Chl biosynthetic pathway, decarboxylates uroporphyrinogen III to coproporphyrinogen III and its gene expression and protein abundance were downregulated in CSR10 and to a larger extent in PB1 (Fig. 18 B and 20 A). The next enzyme in the series is Coproporphyrinogen oxidase (Coprox) that converts coproporphyrinogen III to protoporphyrinogen IX. Its activity was downregulated both in CSR10 and PB1 cultivars (Fig. 14). In the same vein activity of Protoporphyrinogen oxidase (Protox) that remove six electrons from macrocycle is also downregulated in both of the cultivars in response of salt (Fig.15). Decreased Protox activity is due to its transcriptional and translational downregulation (Fig. 18 B and 21 A). Decline in enzymatic activities of coprox and protox was observed in *cucumber* seedlings in response to chill-stress by Tiwari and Tripathy, 1998. In heat stress coprox activity was not affected although protox activity increased (Tiwari and Tripathy, 1998).

Mg is inserted to the protoporphyrin ring by an ATP dependent reaction of Mg-chelatase. The latter consists of three subunits namely ChIH, ChID and ChII. In response to salt stress as compared to CSR10, the Mg-chelatase activity was severely down regulated in PB1 (Fig. 16). This was due to severe downregulation of gene expression and protein abundance of ChII in PB1 cultivar (Fig. 18 B and 21 A). Similar decline in Mg-chelatase activity and ChII expression was previously observed in *cucumber* and *wheat* in response to temperature-stress (Tiwari and Tripathy, 1998, Mohanty et al., 2006).

Protochlorophyllide (Pchlde) is converted to chlorophyllide (Chlide) by protochlorophyllide oxidoreductase (POR). The POR abundance substantially increased in response to salt stress in the salt resistant CSR10 cultivar and only partially increased in PB1 (Fig. 19). Due to higher POR abundance the POR activity, measured as percent

phototransformation of Pchl_{id}e to Chl_{id}e, was not substantially affected in CSR10 due to salt stress. However the POR activity was substantially declined in PB1 (Fig. 17). The *ChlP* that codes geranyl-geranyl reductase is responsible for phytol synthesis. It was partially downregulated in CSR10 and more severely in PB1 due to salt stress treatment (Fig.18 B).

Chlorophyll a oxygenase (CAO) converts Chl a to Chl b, and its gene expression was severely downregulated in PB1 seedlings due to salt-stress (Fig. 20 A). The decreased CAO could reduce Chl b biosynthesis leading to increased Chl a/b ratio in both the cultivars (Fig. 2 D).

Shibata shift: Leaves of dark grown rice seedlings has a smaller emission fluorescence peak (77K) at 632 nm due to non-phototransformable Pchl_{id}e and a larger peak at 658 nm due to phototransformable Pchl_{id}e. The non-phototransformable Pchl_{id}e emitting at 632 nm is due to monomeric Pchl_{id}e complex or esterified Pchl_{id}e i.e. Protochlorophyll (Lindsten et al. 1988), which spontaneously dimerizes to form (POR-Pchl_{id}e-NADPH)₂. The short-wavelength, monomeric Pchl_{id}e is not flash-photoactive; instead it regenerates the long wavelength Pchl_{id}e forms (Schoefs and Franck 1993; He et al. 1994; Schoefs et al. 1994, 2000a, 2000b). The dimer has the absorption maximum at 638 nm and emission maximum at 645 nm (Ouazzani Chahdi et al. 1998; Lebedev and Timko 1999). The dimeric POR-Pchl_{id}e- NADPH complex further polymerizes to form 16-mer or larger aggregates of POR-Pchl_{id}e- NADPH complex i.e., (POR-Pchl_{id}e-NADPH)_n having absorption maximum at 650 nm and emission maximum at 658 nm (Böddi et al. 1989; Wiktorsson et al. 1993) and is flash photoactive (Böddi et al., 1991). However, long-term illumination i.e., greater than minute usually converts non-active Pchl_{id}e to photo-active Pchl_{id}e.

Results demonstrate that results demonstrate that in etiolated rice seedlings, the phototransformable peak is substantially higher than the non-phototransformable peak demonstrating the presence of large aggregate of POR-Pchl_{id}e-NADPH ternary complexes.

The flash-induced photo-transformation and Shibata shift leading to chloroplast biogenesis is substantially affected in salt-stressed samples. Upon flash illumination (0.2 sec) of leaves from control seedlings the phototransformable Pchl_{id}e peak at 658 nm emanating from large aggregates of polymeric POR-Pchl_{id}e-NADPH complexes almost disappeared due to photo-reduction of Pchl_{id}e to Chl_{id}e and a new peak appeared at 692 nm . Transformation of Pchl_{id}e₆₅₈ into Chl_{id}e₆₉₂ was previously observed by exposing the leaf primordia of common ash (*Fraxinus*

excelsior L.) and Hungarian ash (*Fraxinus angustifolia* Vahl.) (Solymosi and Böddi 2006) and that of Horse chestnut (*Aesculus hippocastanum*) (Solymosi et al. 2006) to white light flash of 10 sec.

After half an h of dark incubation following flash illumination of etiolated rice seedlings (Five day old), a hump at 676 nm appears (shibata shift). However in present experimental conditions a complete blue shift to 676 nm was not observed and major peak remained at 692 nm. After 1h dark incubation after flash treatment lead to a complete blue shift at 684 nm (Fig.22). This 684 peak could be due to Chlorophyllide₆₈₄. After 1 h of dark incubation some amount of phototransformation pchlde (F658) were regenerated. Salt stress impairs shibata shift even after 30 min (Fig. 23). of dark incubation following flash illumination there was no blue shift was observed. Only after 1 h of dark incubation following flash illumination a small hump at 676 nm appeared and the major peak remained at 692 nm demonstrating the arrest of shibata shift by salt stress in CSR10 cultivar. During this 1 h of dark incubation following flash illumination protochlorophyllide which was regenerated accumulated in POR-Pchlde-NADPH monomeric form leading to the formation of non-phototransformable pchlde having fluorescence maximum at 632 nm. Similarly in PB1 after half an h of dark incubation following flash illumination of etiolated rice seedlings (Five day old), a hump at 676 nm appears and major peak remained at 692 nm. After 1h dark incubation after flash treatment lead to a complete blue shift at 684 nm (Fig.24). Salt stress impairs shibata shift also in PB1 cultivar, after 30 min. of dark incubation following flash illumination there was no blue shift was observed (Fig.25). Only after 1 h of dark incubation following flash illumination a small hump at 676 nm appeared and the major peak remained at 692 nm demonstrating the arrest of shibata shift by salt stress. As in PB1 after 1 h of dark incubation following flash illumination hump appeared was not as prominent as it was in CSR10 so this suggests there is more arrest of shibata shift in PB1 due to salt stress than that in CSR10. There is no substantial regeneration of non-phototransformable Pchlde in PB1 as comparative to that in CSR10 after 1 h of dark incubation following red flash.

Overall, in response to salt-stress rice seedlings down-regulated Chl biosynthesis by regulating biochemical reactions, protein abundance and gene expression of several enzymes involved in tetrapyrrole synthesis. In the presence of salt, the salt-tolerant CSR-10 cultivar accumulated more Chl than that of salt-sensitive genotype PB1 by upregulating the gene expression and protein abundance of several Chl biosynthetic enzymes.

Impact of salt stress on photosynthesis

Chl a fluorescence is used as a signature to understand the interrelationship of structure and function of photosynthetic apparatus (Govindjee, 1995, 2004). Although the F_0 was not affected in CSR10 after 24 h of greening, it declined in PB1. However after 24 h and 72 h of greening in the presence of salt the F_0 value significantly declined in both the cultivars due to their reduced Chl contents (Fig. 26 A). The ratio of F_v/F_m is a measure of the functional status of PSII. It was not significantly declined after 24 h of greening in the presence of salt. After 48 h of greening in presence of salt, it declined in PB1 and was not affected in CSR10. However 72 h of greening it decreased in both of the cultivars suggesting that salt stress impairs quantum efficiency of PSII (Fig 26 C).

Electron transport rate (etr), photochemical quenching (qP) and quantum yield of PSII (Φ PSII) decreased with increasing salt stress and duration of salt stress exposure (Figs. 27-35). However, the rate of decline with duration and intensity of salt stress was more in salt-sensitive PB1 than salt-tolerant cultivar CSR10. Decline in etr in both the cultivars was observed both at low and high light intensities suggesting damage to the light harvesting complex as well as reaction centre.

Non-photochemical quenching (qN) increased in response to salt stress in both of the cultivars although it was higher in salt sensitive PB1 (Figs. 36-38). The major component of qN is due to a regulatory mechanism, called qE, which results in thermal dissipation of excess absorbed light energy in the light-harvesting antenna of PSII. qE is induced by low pH of thylakoid lumen that is generated by photosynthetic electron transport in excess light. Low thylakoid lumen pH that induces qE has two roles. One is the pH dependent activation of a lumen localized violaxanthin de-epoxidase (VDE) that catalyzes conversion of violaxanthin to zeaxanthin via the intermediate antheraxanthine (Demmig-Adams and Adams, 1996). Zeaxanthin is necessary for qE in plants. In limiting light intensity zeaxanthin epoxidase (ZE) converts zeaxanthin back to violaxanthin. This light dependent interconversion is known as xanthophylls cycle (Yamamoto et al, 1999). The second role of low lumen pH is driving protonation of one or more PSII protein involved in qE (Horton and Ruban, 1992). The characterization of *Arabidopsis thaliana* mutant that lack qE has revealed that qE requires PsbS in addition to low lumen pH. The *npq1* and *npq2* mutants were defective in VDE and ZE respectively (Niyogi et al, 1998) whereas *npq4* mutants which lack qE and delta-A535 have

normal xanthophylls cycle. The *npq4* mutation was mapped to chromosome 1 and ultimately have shown to affect the gene encoding PsbS (Li *et al*, 2000). Although the mechanism of qE remains unresolved, increase in qN suggests increased operation of xanthophyll cycle leading to excess qE quenching and loss of excitation energy as heat to protect the membrane from photodamage.

Increased qN in PB1 in response to salt-stress suggests that it is not able to dissipate the pH gradient created across the thylakoid membrane probably due to the damage to the photophosphorylation apparatus (CF_0 and CF_1). The proteomics data clearly suggest the down-regulation of ATP synthase CF_1 beta subunit. Low thylakoid lumen pH would activate VDE converting violaxanthine to zeaxanthine responsible for increased qE or qN quenching

In Sorghum, maximum quantum yield of photosystem II (Fv/Fm), photochemical quenching coefficient (qP) and electron transport rate (ETR) significantly decreased, but non-photochemical quenching (qN) increased substantially under saline conditions (Netondo *et al.*, 2004). In *Spirulina platensis* cells salinity stress induced a decrease in oxygen evolution activity, which correlated with the decrease in the quantum yield of PSII electron transport (Φ PSII) and induced an increase in non-photochemical quenching (qN) and a decrease in photochemical quenching (qP) (Lu & Vonshak, 2002). Similar decrease in *etr* and increase in non-photochemical quenching was shown by Moradi and Ismail, 2007 in salt tolerant rice cultivars IR651 and IR632 and in salt sensitive cultivar IR29.

Due to salt stress whole chain electron transport rate (H_2O to MV) (Fig. 39) and PD supported partial electron transport of PSII (H_2O to PD) (Fig. 41) were severely impaired in both CSR10 and PB1 cultivars. However, the CSR10 had reduced loss of electron transport activity as compared to that of PB1. PSI was only partially affected by salt stress (Fig.40).

Salt stress is known to inhibit PSII and/or PSI activities in cyanobacteria (Allakhverdiev and Murata, 2008), *Spirulina platensis* (Lu & Vonshak, 2002), *Arabidopsis thaliana* (Stepien and Johnson, 2009), and several other plants (Bongi and Loreto, 1989; Mishra *et al.*, 1991; Masojidek & Hall, 1992; Baelkhodja *et al.*, 1994; Everard *et al.*, 1994). The results of salinity stress on PSII photochemistry are conflicting. Some studies have indicated that salt stress has no effects on PSII (Robinson *et al.*, 1983; Brugnoli and Bjorkman, 1992; Morales *et al.*, 1992; Abdia *et al.*, 1999).

To ascertain if the inhibition of PSII reaction was due to reduction in quantum yield of PSII or in the light saturated electron transport rate or both, the rate of PSII reaction as a function of light intensity was measured in thylakoid membranes isolated from control and salt treated rice seedlings after 72 h of greening (Fig. 42 and 43). Dependence of PSII activity on light intensity showed typical saturation kinetics. Both the initial slope at limiting light intensities as well as light saturated electron transport was affected in salt treated seedlings of CSR10 cultivars (Fig. 42). As compared to control, the percent inhibition of PSII reaction in salt-treated thylakoids was almost constant (nearly 45 %) at all the light intensities used (Fig.42). Both V_{max} and quantum efficiency of PSII were reduced almost by 45 %, suggesting that inhibition of V_{max} and quantum efficiency of PSII was predominantly due to damage to the reaction centre.

In Pusa Basmati 1 (PB1) both the initial slope at limiting light intensities as well as well as light saturated electron transport rates were affected in salt treated seedlings (Fig.43). As compared to control, the percent inhibition of PSII in salt stressed thylakoids was almost 50 % at higher intensity and was more pronounced at lower intensities (≥ 60 %). The quantum efficiency of PSII was reduced by almost 50 % and V_{max} by almost 75 %. This suggests that inhibition of V_{max} and quantum efficiency of PSII was due to both, damage to the reaction centre as well as antenna complex. The estimated ETR measured from the leaves of salt-stressed rice seedlings was also affected both at low and high light intensities.

These conclusions are further supported from immunoblot analysis where the reaction centre proteins D_1 and D_2 and oxygen evolving protein 33 (OEC33) and antenna protein LHCPII were highly degraded in PB1 whereas in CSR10 they were partially affected (Fig 48 A). This also explains the reason why the damage to PSII is higher in PB1 than CSR10 at saturating as well as limiting light intensities. Whole chain electron transport was also affected more in PB1 as comparative to CSR10. This could be due to higher loss of other components of electron transport chain such as cyt b, cyt f, Rieske iron-sulfur centre protein and subunit IV of cytb_f complex, PSI subunits III and V (Fig. 49 and 50). In the same vein gene expression of *PsbA* and *PsbD* and *PetD* coding for D_1 and D_2 reaction centre proteins and subunit IV respectively were also severely affected in PB1 as compared to that in CSR10 (Fig. 51).

Electron micrograph reveals a larger disorganization of grana stacking of thylakoid membranes in PB1 as comparative to that of CSR10. Starch granules completely disappeared due to 200 mM NaCl stress treatment in chloroplast suggesting loss of carbohydrate accumulation due to inhibition of photosynthesis (Fig. 52 and 53).

Room temperature emission fluorescence spectrum of thylakoids membrane have a peak at 684 nm due to PSII while excited at 440 nm having 8 nm slit width that produce a actinic illumination. Thylakoids membrane isolated from CSR10 and PB1 had a reduced fluorescence emission at 684 nm originating from PSII due to the loss of variable fluorescence (Fig. 44). Gross perturbation of thylakoid membranes usually induces a difference in fluorescence spectral properties at low temperature (77K). The low temperature fluorescence spectra have a peak at 685 nm (F_{685}) and at 695 nm (F_{695}) emissions which mostly originates from PSII CP43 and CP47 respectively (Govindjee, 1995, 2004) and a large F_{735} peak that originates from mostly from PSI (Mullet et al, 1980). If LHCP1 is removed from PSI by detergent treatment the inner antenna of reaction centre I (RCI) fluoresces at 722 nm (Kung et al, 1984)). Isolated LHCI fluoresces at around 735-740 nm (Haworth et al, 1983). Thus it is apparent that inner antenna of RCI emits F_{722} and LHC emits F_{735} (Briantais et al, 1986). In the absence of Mg^{2+} thylakoid membranes isolated from control samples of CSR10 had a F_{686}/F_{740} ratio of 1.14 (Fig. 45). Due to salt stress the F_{686}/F_{740} ratio increased to 1.37 due to decrease of PSI fluorescence. Similarly, in PB1 in the absence of Mg^{2+} the F_{686}/F_{740} ratio is 1.095 (Fig. 46) and due to salt-stress the ratio increases to 1.5 due to decline in PSI fluorescence. This demonstrates degradation of PSI due to salt stress was much higher in salt sensitive cultivar PB1 as compared to that of salt resistant CSR10. This was further supported by PSI activity measurement where the PSI activity was reduced in more in PB1 as compared to CSR10.

In the presence of Mg^{2+} due to grana stacking LHCP1I migrates closer to PSII and preferentially gives energy to PSII. Therefore, fluorescence due to PSII increases and that due to PSI decreases leading to increase in ratio of PSII/PSI fluorescence. In control samples of CSR10 in the presence of Mg^{2+} the F_{686}/F_{740} ratio increased to 1.9 from 1.147 (in the absence of Mg^{2+}). In salt stressed samples in the presence of Mg^{2+} F_{686}/F_{740} ratio increased from 1.37 (in the absence of Mg^{2+}) to 2.083. This clearly demonstrates that grana stacking is substantially reduced in salt stressed samples due to loss of LHCP1I. Similarly in in PB1 in the presence of Mg^{2+} in control samples F_{686}/F_{740} ratio increased to 2.006 from 1.095 (in the absence of Mg^{2+}).

In salt stressed samples in the presence of Mg^{2+} F686/F740 ratio increased from 1.4703 (in the absence of Mg^{2+}) to 2.211. This suggests more reduced grana stacking in PB1 due to loss of LHCPII. Reduced grana stacking are further supported by larger decrease of LHCPII protein in salt-sensitive PB1 as compared to salt tolerant CSR10 (Fig 48 A).

Salt-stress and reactive oxygen species

Oxidative stress is one of the various influences caused by salt-stress (Ashraf, 2009; Noreen et al., 2009; Sekmen et al, 2007). It has been well established that to counter-act salt-induced oxidative stress, plants generate different types of enzymatic and non-enzymatic antioxidants (Gupta et al., 2005). Commonly known enzymatic antioxidative enzymes are superoxide dismutase (SOD), catalase (CAT), ascorbate peroxidase and glutathione reductase (GR), whereas non-enzymatic antioxidants are glutathione (GSH), ascorbate (AsA), carotenoids and tocopherols (Gupta et al., 2005). In the present investigation cellular superoxide dismutase (SOD) enzymatic activity increased in response to salt stress in both the cultivars (Fig. 54). However, the relative increase in SOD enzymatic activity with respect to control was more in PB1 than CSR10 (Fig.54). This is correlated with increased gene expression of SOD in response to salt stress in both the cultivars (Fig. 60). Activity of different isoforms of SOD was seen by native in-gel assay. As shown in Fig. 55, three SOD isoforms were observed clearly which were identified by H_2O_2 inhibition studies. H_2O_2 completely inhibits Fe-SOD and partially Cu-Zn-SOD (Asada et al, 1974; Seng et al, 2004). In in-gel assay Mn-SOD, Fe-SOD and Cu-Zn-SOD and all the three isoforms upregulated in salt stress. Cu-Zn-SOD was responsible for most of the enzymatic activity. Takemura et al, 2002 have shown an increase in Cu-Zn-SOD transcripts level in *Brugiera gymnorrhiza* in response to salinity stress. Wang et al, 2004 have shown an increase in Mn-SOD and Fe-SOD isoforms in native gel assay in *Suaeda salsa* in response to salinity stress.

Ascorbate peroxides (APX) detoxifies H_2O_2 using ascorbate as electron donor (Nakano and Asada, 1981). Ascorbate peroxidase activity also increased in response to salt stress in both of the cultivars. At higher salt stress relative increase in activity was higher in PB1 (Fig.56). Gene expression of *OsAPx2* coding for one of the cytosolic form of ascorbate peroxidase in rice increased in both of the cultivars (Fig. 60). Parida *et al.* 2004 have shown an increase in ascorbate peroxidase activity in *Brugiera gymnorrhiza* in response to salinity stress.

Glutathione reductase is one of the enzyme operating in Haliwel-Asada pathway of detoxification of superoxide and is needed for regeneration of glutathione. Its activity was partially increased by salt stress in both of the cultivars after 24 h of greening (Fig.57). Gene expression of *GRase*, coding for glutathione reductase increased in response to salt stress (Fig.60). Similar increase in enzymatic activity was observed by Wang *et al*, 2008 in *Philatus popularis* in response to salt stress.

Catalase is a heme-containing enzyme that detoxifies H₂O₂ by catalyzing its conversion into water and molecular oxygen. Catalase activity increased in response to salt stress in both the cultivars (Fig. 58). Similar increase in catalase activity was observed by Takemura *et al*. 2000 in *Brugiera gymnorrhiza* in response to salinity stress. However the relative increases with respect to control was more in PB1. Catalase activity decreased with time of light exposure. Transcript level of gene *CatA* encoding cytosolic isoform increased in rice seedlings in response to salt stress in both the cultivars (Fig 60). Antioxidative response of catalase to salt stress was confirmed by native in gel assays as shown in Fig.59. All the three isoform observed in in-gel assays were upregulated in response to salt stress. Isoform I was responsible for most of catalase enzymatic activities. Increase of antioxidative enzymes activities in response to salt stress as seen by spectrophotometric as well as in gel assays are well correlated (Kim *et al.*, 2005).

MDA is an index of membrane lipid peroxidation (Mandhania *et al*. 2006; Xiao *et al*, 2009). MDA production increased in response to salinity as well as time of stress (light exposure) in both the cultivars (Fig.61). However the relative production of MDA is higher in PB1 as comparative to CSR10 in response to salt stress. Higher MDA production in PB1 than CSR10 during salt stress are correlated with increased degradation of photosynthetic proteins and loss of photosynthetic functions (Fig. 61). Similar increase in MDA production was shown by Moradi and Ismail, 2007 in salt tolerant rice cultivars IR651 and IR632 and in salt sensitive cultivar IR29 in response to salt stress. Increase in MDA contents were also reported by Siegal *et al*, 1982 in *Cucumis*, *Brassica* and other seedlings in response to salinity stress.

H₂O₂ contents decreases in response to salt stress in both of the cultivars (Fig. 62). Decrease in H₂O₂ is probably due to increased activities of antioxidative enzymes such as catalase, ascorbate peroxidase, glutathione reductase in response to salt stress. (Noreen and Ashraf, 2009; Kim *et al*, 2005).

Tocopherols, known collectively as vitamin E, are lipid soluble antioxidants synthesized by plants and other photosynthetic organisms (Grusak, 1999; Traber and Sies, 1996). Tocopherols are thought to have a number of important functions in higher plants, including protection of chloroplasts from photooxidative damage (Eenennaam et al., 2003). α -tocopherols are known to reduce reactive oxygen species (ROS) levels (mainly $^1\text{O}_2$ and OH^\cdot) in photosynthetic membranes and limit the extent of lipid peroxidation by reducing lipid peroxy radicals to their corresponding hydroperoxides (Maeda et al. 2005, Havaux et al. 2005). In the present study both α and γ tocopherols contents decreased in response to salt stress. Ratio of α to γ increased in response to salt stress (Fig. 63). Decrease in tocopherols levels may induce cell signaling response by producing phytohormones to protect plants from stress (Munne-Bosch et al, 2007).

OsDREB2 encodes for a transcription factor which binds and causes drought tolerance when overexpressed in rice (Chen et al, 2008, Dubouzet et al, 2003). OsCIPK15 a calcineurin B-like protein-interacting protein kinases which is induced by salt stress and causes salt tolerance when overexpressed (Xiang et al, 2007). OsRab7 encodes for protein involved in vesicular transport and is differentially regulated by various stress like salt, drought and cold (Nahm et al, 2003). Gene expression of all above genes induced by salt stress in both of the cultivars (Fig. 64). This suggests their role in regulating salt tolerance and plant defence from salt stress.

Salt-induced changes in soluble and thylakoid proteome of rice

Owing to their inherent genetic make-up, the response of the halophytes to environmental stress is expected to be different in comparison to the glycophytes. A meaningful comparison of the two types requires an assessment of the factors responsible for such differential response at the physiological and proteome level. Such consideration has earlier prompted comparative studies between *Arabidopsis* and *Thellungiella*, its halophytic counterpart (M'rah et al. 2007; Kant et al. 2006; Ghars et al. 2008; Volkov et al. 2004).

Partially salt tolerant CSR10 can be used as model for understanding the response of abiotic stress tolerance of rice. Keeping this in view, the present study was undertaken in salt tolerant genotype CSR10 and salt sensitive genotype PB1 for knowing comparative proteomic responses of two cultivars to salt stress. In response to salt stress many proteins were

differentially expressed. Proteomic studies were done for differential expression of thylakoids proteins and PEG fractionated soluble proteins from leaves of rice seedlings in response to salt stress.

Thylakoids proteins:

As seen from 2-Dimensional gel-electrophoresis pattern of thylakoid protein, most of the expressed proteins were distributed in acid area. Few differentially expressed proteins from thylakoids proteins were identified. Proteome analysis of thylakoids proteins shows that many proteins are differentially regulated due to salt stress in CSR10 (Fig. 69 and 70) such as upregulation of ATP synthase CF₁ beta subunit in response to salt stress suggests its role in energy regulation and stress tolerance (Table.1).

Soluble proteins:

Total 35 proteins spots were given for MALDI-TOF/TOF analysis. Out of 35, 17 proteins were identified and assigned functions remaining protein were either hypothetical or unknown proteins (Figs 67-70 and Table 2. 3. 4). Proteins identified in such attempt have the potential to serve as important salt-tolerance factors and their expression alteration may contribute in the stress-biology of *Oryza sativa* L. The interpretations of the regulation pattern observed for some proteins upregulated or downregulated under salinity stress are discussed as follows:

Malate dehydrogenase: Identified from spot no 209, it was down regulated in CSR10 owing to salt-stress. It has a NAD binding domain. Malate dehydrogenases (MDH) is glycosomal and mitochondrial; member of the family of NAD-dependent 2-hydroxycarboxylate dehydrogenases. MDH is one of the key enzymes in the citric acid cycle, facilitating both the conversion of malate to oxaloacetate and replenishing levels of oxalacetate by reductive carboxylation of pyruvate. Members of this family are localized to the glycosome and mitochondria.

Dehydration responsive protein: The protein was identified from spot no. 219 and upregulated due to salt-stress in both the cultivars. However, it was highly upregulated in CSR10 than that in PB1. There are various types of dehydration responsive proteins in plants. The DREB/CBF family of proteins contains two subclasses, DREB1/CBF and DREB2, which are induced by cold and dehydration, respectively, to express various genes involved in stress tolerance (Shinozaki and Yamaguchi- Shinozaki 2000). Upregulation of this protein suggests its role in stress

tolerance. Proteins of this family share a Rossmann-fold NAD(P)H/NAD(P)⁽⁺⁾ binding (NADB) domain. The NADB domain is found in numerous dehydrogenases of metabolic pathways such as glycolysis, and many other redox enzymes.

Homeobox protein: This protein was identified by spot no 204 and down regulated in salt stress. This protein is nuclear encoded and functions in transcriptional regulation. It has homeodomain; DNA binding domains involved in the transcriptional regulation of key eukaryotic developmental processes; may bind to DNA as monomers or as homo- and/or heterodimers, in a sequence-specific manner. This may be involved in salt stress induced transcriptional inhibition.

Mitogen activated protein kinase: The protein identified from spot no. 202 and upregulated in response to salt stress. Member of this family have Serine/Threonine protein kinases, catalytic domain. This is a phosphotransferases of the serine or threonine-specific kinase subfamily. The enzymatic activity of these protein kinases is controlled by phosphorylation of specific residues in the activation segment of the catalytic domain, sometimes combined with reversible conformational changes in the C-terminal autoregulatory tail. Upregulation of this protein suggests its role in regulating salt stress response. Mutants in *Fusarium proliferatum* of Fphog1, an orthologue of the *Saccharomyces cerevisiae* hog1 MAPK gene showed increased sensitivity towards different abiotic stressors including UV-irradiation, heat, salt, osmotic and hydrogen peroxide treatments (Adam et al., 2008).

Putative protein kinase: It was identified from spot no. 216 and is upregulated by salt-stress. This protein belongs to PTKc: Protein Tyrosine Kinase (PTK) family, catalytic domain. This PTKc family is part of a larger superfamily that includes the catalytic domains of protein serine/threonine kinases, RIO kinases, aminoglycoside phosphotransferase, choline kinase, and phosphoinositide 3-kinase (PI3K). PTKs catalyze the transfer of the gamma-phosphoryl group from ATP to tyrosine (tyr) residues in protein substrates. They can be classified into receptor and non-receptor tyr kinases. PTKs play important roles in many cellular processes including, lymphocyte activation, epithelium growth and maintenance, metabolism control, organogenesis regulation, survival, proliferation, differentiation, migration, adhesion, motility, and morphogenesis. Receptor tyr kinases (RTKs) are integral membrane proteins which contain an

extracellular ligand-binding region, a transmembrane segment, and an intracellular tyr kinase domain.

Fructose bisphosphate aldolase chloroplast precursor: This protein was identified from spot no. 214 and upregulated in response to salt stress. It has a functional role in metabolism. Fructose-1,6-bisphosphate aldolase. The enzyme catalyzes the cleavage of fructose 1, 6-bisphosphate to glyceraldehyde 3-phosphate and dihydroxyacetone phosphate (DHAP). This protein upregulation in salt stress suggests its role in carbohydrate synthesis which to compensate loss to salt stress by plants.

Calcinurin B like proein 5: This protein was identified from spot no. 309 and its expression induced by salt stress in PB1. It is a Ca^{2+} -binding protein (EF-Hand superfamily) and have role in Signal transduction mechanisms / Cytoskeleton / Cell division and chromosome partitioning. This protein is possibly involved in Ca^{2+} mediated signaling in response to salt stress.

Cytochrome c oxidase subunit 6b-1: This protein was identified from spot no 208 and downregulated under salt stress. Cytochrome c oxidase (CcO), the terminal oxidase in the respiratory chains of eukaryotes and most bacteria, is a multi-chain transmembrane protein located in the inner membrane of mitochondria and the cell membrane of prokaryotes. It catalyzes the reduction of O_2 and simultaneously pumps protons across the membrane. The number of subunits varies from three to five in bacteria and up to 13 in mammalian mitochondria. Subunits I, II, and III of mammalian CcO are encoded within the mitochondrial genome and the remaining 10 subunits are encoded within the nuclear genome. Found only in eukaryotes, subunit VIb is one of three mammalian subunits that lacks a transmembrane region. It is located on the cytosolic side of the membrane and helps form the dimer interface with the corresponding subunit on the other monomer complex. This protein involved in energy regulation and regulating proton gradient across the membrane.

Ankyrin repeat domain protein: This protein was identified from spot no. 213 and down regulated under salt stress. This protein has ankyrin repeats; ankyrin repeats mediate protein-protein interactions in very diverse families of proteins. The number of ANK repeats in a protein can range from 2 to over 20 (ankyrins, for example). ANK repeats may occur in combinations with other types of domains. The structural repeat unit contains two antiparallel helices and a

beta-hairpin, repeats are stacked in a superhelical arrangement; this alignment contains 4 consecutive repeats.

Putative amine oxidase: This protein was identified from spot no. 218 and upregulated in salt stress. This protein is NAD/FAD dependent oxidoreductase. It is involved in oxidation reactions.

As salt stress affects whole cellular mechanism of plants and also differentially expressed proteins lie in acid area, while global pattern of proteins largely remained unaltered. Proteome analysis of PEG-fractionated soluble proteins shows differential regulation of proteins involved in many cellular processes like cell signaling, metabolism, energy balance, antioxidative defence, structural organization and stress tolerance. Upregulation of putative mitogen activated kinase kinase alpha, putative protein kinase, putative indole 3 acetic acid regulated protein, calcineurin B like protein in salt stress suggests their role in cell signaling during salt stress. Upregulation of formin like protein 2 suggests its role in regulating structural organization during salt stress. Upregulation of fructose bisphosphate aldolase, amine oxidase, putative cytochrome p 450, ribulose bisphosphate carboxylase suggests their role in energy and carbon metabolism. A new protein synthesized in response to salt-stress is the putative transcription repressor HOTR. It may have a role in stress-induced transcriptional regulation. It is interesting to note that a putative retrtransposon-like protein identified from spot 205 from soluble protein is down regulated in CSR10 and upregulated in PB1 during salt stress (Table 2, 3, 4). Differential regulation of proteins in the salt-sensitive and salt-tolerant genotypes suggest that plants adjust their protein concentrations to combat salt stress.

Summary

SUMMARY

Plants are subjected to various types of abiotic stresses during their life time such as temperature, drought, water-logging, metal, oxidative and salinity stress. Salinity stress is among most damaging stresses which reduces crop yield and restricts the use of land. This is most severe in hot temperate regions in irrigated land. Photosynthesis is the most vital process carried out by plants. Salinity stress affects photosynthesis negatively reducing plant growth and yield. Chloroplast biogenesis is a complex process which is regulated by light. As chloroplast biogenesis and photosynthesis are interrelated process hence it is of utmost importance to see impact of salinity stress on chloroplast biogenesis. As rice is the most important staple food for a large part of the world's human population including India, the present study was carried out to understand the importance of salinity stress on chloroplast biogenesis in rice.

Two cultivars of rice (*Oryza sativa* L) i.e. a salt resistant genotype CSR10 and a salt sensitive variety Pusa Basmati (PB1) were taken for study. Five-day-old etiolated rice seedlings of these two cultivars were treated with 0 mM NaCl (half-strength Murashige & Skoog salt solution [vitamin and agar free]), or 100 mM NaCl (half-strength Murashige & Skoog salt solution [vitamin and agar free] + 100 mM NaCl) or 150 mM NaCl (half-strength Murashige & Skoog salt solution [vitamin and agar free] + 150 mM NaCl) or 200 mM NaCl (half-strength Murashige & Skoog salt solution [vitamin and agar free] + 200 mM NaCl) 12 h prior to the transfer to cool white fluorescent+incandescent light ($100 \mu\text{mol m}^{-2} \text{s}^{-1}$), at 28°C at 75% relative humidity maintained by a Conviron plant growth chamber. Chlorophyll and carotenoids contents decreased in response to increasing salinity stress but increased with greening period in both the cultivars CSR0 and PB1. However the relative decrease in their contents at any stress point is higher in PB1 than CSR10. Protein contents also declined in response to increasing salinity stress in both of the cultivars. At moderate stress there was more decline in protein contents in PB1 as compared to CSR10.

Ion homeostasis:

In response to increasing salinity stress there was more accumulation of sodium in shoot in PB1 as comparative to that of CSR10. However sodium accumulation in root was more in CSR10

than PB1. This suggests that CSR10 cultivar does not allow translocation of accumulated sodium in root to shoot. Potassium contents decreased in response to increasing salinity stress in both the cultivars in shoot as well as root. Sodium to potassium ratio increased in both the cultivars in response to salt stress. However the relative increase was higher in PB1 seedlings than CSR10. However in shoots Ca^{2+} increased at higher salt stress.

Chlorophyll biosynthesis:

Chl biosynthetic intermediates were measured in response to salt stress. Net accumulation of Glutamate-1-semialdehyde contents decreased in response to salt stress in both the cultivars. However the decline was higher in PB1 as comparative to that of CSR10. Net accumulation of 5-aminolevulinic (ALA) acid decreased in response to salt stress in both the cultivars. However the decline was severe in PB1 than CSR10.

Chlorophyll biosynthetic enzyme activity was measured in response to 200 mM NaCl. ALA dehydratase (ALAD) activity was decreased in both CSR10 and PB1. Enzymatic activity drastically decreased in PB1 whereas in CSR10 its activity remained almost unchanged. Porphobilinogen deaminase (PBGD) activity decreased with h of greening and in response to salt stress in both of the cultivars. Activity declined by almost 23 % in both CSR10 and PB1. Coprogen oxidase enzymatic activity declined by 32% and 47% in response to salt stress in CSR10 and PB1 respectively. Protoporphyrinogen oxidase (protox) activity decreased in both the cultivars in response to salt stress. Mg-chelatase inserts Mg into protoporphyrin IX, its enzymatic activity reduced by 45% and 80% in CSR10 and PB1 in response to salt stress respectively. Protochlorophyllide oxidoreductase (POR) activity almost remained unchanged in CSR10 in response to salt stress whereas it decreased by 58% in salt sensitive genotype PB1.

Protein abundance of some of the enzymes of Chl biosynthetic enzymes was studied in response to salt stress after 24 h and 72 h of greening. Protoporphyrinogen oxidase protein abundance decreased after 24 h of salt stress in both of the cultivars. After 72 h of salt stress protein abundance of protox remains almost unaltered in CSR10. However in PB1 its expression decreased under identical conditions. Uroporphyrinogen oxidase (UROD), Magnesium-chelatase subunit I (ChII) and Geranyl-geranyl reductase (ChlP) protein abundance decreased in response to salt stress and h of salt stress in both of the cultivars. However the relative decline was higher

in PB1 as comparative to that of CSR10. Protochlorophyllide oxidoreductase (POR) protein abundance increased in response to salt stress especially in CSR10.

Gene's expression of *PBGD*, *CAO* and *UROD* as seen from Northern blot, declined in response to salt stress and greening period in both of the cultivars. However the relative decline is higher in PB1 as comparative to that of CSR10.

The gene expression of GluTR increased in response to salt stress after 24 h and 72 h of greening in both of the cultivars. Transcripts analysis of GSAT increased in CSR10 after 24h and 72 h of salt stress whereas its expression decreased in PB1. Gene expression of ALAD remains almost unchanged in CSR10 after 24 h of salt stress whereas its expression decreased in PB1. After 72 h of salt stress ALAD gene expression decreased in both of the cultivars. However the decline was higher in PB1 than CSR10. Gene expression of protox remained almost unchanged in CSR10 after 24 h of salt stress whereas in PB1 its expression decreased. After 72 h of salt stress transcripts abundance of protox decreased in both CSR10 and PB1. However the decline was higher in PB1 than CSR10. Gene expression of ChII decreased in response to salt stress and the relative decline was also higher in PB1 than CSR10. Transcripts level of Ferrochelatase increased in CSR10 in response to salt stress whereas its expression decreased in PB1 under identical conditions.

Shibata shift: POR-NADPH-Pchl_a complex in etiolated seedlings has been studied by shibata shift and it shows that salt stress causes arrest in shibata shift and the extent of arrest in shibata shift is more in PB1 than CSR10.

Photosynthesis:

Chl a fluorescence was used to measure photosynthetic parameters. F_0 remains almost unaltered after 24 h in both of the cultivars. However it declined after 48 h and 72 h in both the cultivars in response to salt stress due to decrease in Chl contents. F_v/F_m remains almost unchanged after 24 of greening in both the cultivars. After 48 h of greening F_v/F_m was not affected much in CSR10 whereas in PB1 it declined. After 72 h of greening F_v/F_m declined in both of the cultivars. Electron transport rate (etr), Photochemical quenching (qP), Quantum yield of PSII (ϕ PSII) declined in both the cultivars in response to increasing salt concentration and greening period.

The relative decline is more in PB1 as comparative to that of CSR10. Non-photochemical quenching (qN) increased in response to increasing salt concentration and duration in both of the cultivars. However the relative increase is more in PB1 than CSR10.

Whole chain activity decreased in response to increasing salt concentration in both of the cultivars. However the relative decline in whole chain activity is more in PB1 as comparative to that of CSR10 at any salt concentration. PSI activity is partially affected in response to salt stress in both the cultivars. PSII activity declined in response to increasing salt stress in both of the cultivars. However the relative decline in PSII activity was more in PB1 as comparative to that of CSR10.

Light saturation curve of Photosystem II shows that both initial slope at low light intensity and saturated electron transport were affected during salt stress in both of the cultivars. Percent inhibition of PSII was more in salt sensitive cultivar PB1 as comparative to that of CSR10.

Room temperature spectra shows that relative decrease in PSII fluorescence at 684 was more in PB1 than CSR10 in response to salt stress. To understand the structural organization of thylakoid membranes low temperature spectra were observed in response to salt stress in CSR10 and PB1 cultivars. In the presence of Mg^{2+} LHCII is more close to PSII so the F686/F740 increases in both CSR10 and PB1.

Protein expression of some of the PSII proteins such as D₁, D₂, LHCPII, Lhcb1, Lhcb2, Lhcb4 and OEC33 decreased in response to increasing salt stress in both of the cultivars. However the relative decline in PB1 is higher than CSR10. Cytb559 protein expression decreased in response to salt stress. Photosystem I (PSI) proteins PSI sub III and PSI sub V expression decreased in response to increasing salt stress in both of the cultivars. However the relative decline in their protein expression is higher in PB1 than CSR10. Among the Cytbf complex subunits protein expression of Cytf, Cytb and Rieske Fe-S decreased in response to salt stress whereas protein expression of Subunit IV remained almost unchanged.

Gene expressions of few genes encoding photosynthetic proteins such as PsbA, PsbD decreased in response to salt stress in both of the cultivars. However the relative decline was

higher in salt sensitive PB1 as compared to that in CSR10. PetD gene expression remained almost unchanged in CSR10. However in PB1 its expression declined at higher salt stress.

Electron micrograph showed that thylakoids structure was distorted by increasing salt stress in both of the cultivars. However the PB1 shows more distorted grana stacking in the presence of salt as comparative to that of CSR10.

Reactive oxygen species:

Superoxide dismutase, Ascorbate peroxidase and Catalase activity increased in response to salt stress in both of the cultivars. However the relative increase in activity was higher in PB1 as compared to that of CSR10. Different isoforms of SOD and Catalase are also overexpressed in response to salt stress as seen from native gel assay. Glutathione reductase activity partially increased after 24 h of salt stress.

Gene expression of all the antioxidative enzymes genes such as Cu-Zn-SOD, APX, GTR and Catalase increased in response to salt stress in both of the cultivars. Some of the genes encoding for proteins involved in stress tolerance such as OsCIPK15, OsDREB2 and OsRAB7 are induced in response to salt stress.

Tocopherols contents α as well as γ decreased in response to salt stress in both of the cultivars. Decrease in tocopherols contents may induce a signal to protect plants from salt stress. Ratio of α to γ increases during salt stress.

MDA production is increased in response to salt stress in both the cultivars. There was partial increase in MDA contents in CSR10 after 24 h of salt stress. After 72 h of salt stress MDA production increased in both of the cultivars although there was more increase in PB1 as comparative to that in CSR10. H_2O_2 production decreased in both of the cultivars in response to salt stress.

Proteomics:

After 2-DE gel electrophoresis of thylakoids proteins there were many proteins which were differentially expressed in response to salt stress. Few proteins such as putative ATP synthase

beta chain upregulated in response to salt stress and ATP synthase CF₁ beta subunits downregulated.

2-Dimensional gel electrophoresis of PEG fractionated soluble proteins showed that many proteins were differentially regulated in response to salt stress. Among the identified proteins upregulated proteins are putative amine oxidase, dehydration-responsive protein, putative indole-3-acetic acid-regulated protein, putative cytochrome P 450, mitogen-activated protein kinase 4, Formin-like protein 2, Fructose-bisphosphate aldolase and few proteins which were downregulated Homeobox protein knotted-1-like 13 OS, putative retrotransposon protein, putative GTP-binding protein, putative mitogen-activated kinase, Cytochrome c oxidase subunit 6b-1 (Cytochrome c oxidase subunit 6b), Putative malate dehydrogenase (Putative mitochondrial malate dehydrogenase), putative ankyrin repeat domain protein 2 and some of proteins which are newly expressed such as probable transcription repressor HOPR. Differential regulation of proteins in the salt-sensitive and salt-tolerant genotypes suggest that plants adjust their protein concentrations to combat salt stress.

References

REFERENCES

- Abadia A, Belkhdja R, Morales F and Abadia J.** (1999) Effects of salinity on the photosynthetic pigment composition of barley (*Hordeum vulgare* L.) grown under a triple-line source sprinkler system in the field. *Journal of Plant Physiology* 154, 392-400.
- Abdelkader AF, Aronsson H, Solymosi K, Böddi B, Sundqvist C.** (2008) High salt stress induces swollen prothylakoids in dark-grown wheat and alters both prolamellar body transformation and reformation after irradiation. *J Exp Bot.*; 58(10):2553-64.
- Abebe T, Guenzi AC, Martin B, Cushman JC.** 2003. Tolerance of mannitol-accumulating transgenic wheat to water stress and salinity. *Plant Physiol.* 131:1748–55
- Adám AL, Kohut G, Hornok L.** (2008) Fphog1, a HOG-type MAP kinase gene, is involved in multistress response in *Fusarium proliferatum*. *J Basic Microbiol.* Jun;48(3):151-9.
- Adams P, Nelson DE, Yamada S, Chmara W and Jensen RG** (1998). Growth and development of *Mesembryanthemum crystallinum* (Aizoaceae). *New Phytol.*138: 170-90.
- Adams P, Thomas J.C., Vernon D.M., Bohnert H.J., and Jensen R.G.** (1992) Distinct cellular and organic response to salt stress. *Plant Cell Physiol.* 33(8): 1215-1223.
- Addlesee HA, Gibson LC, Jensen PE and Hunter CN.** (1996) Cloning, sequencing and functional assignment of the chlorophyll biosynthesis gene, chlP, of *Synechocystis* sp. PCC 6803. *FEBS Lett.* 389: 126-130.
- Akhtar M.** (1994) The modification of acetate and propionate side chains during biosynthesis of Heme and chlorophylls: Mechanistic and stereochemical studies. In *Biosynthesis of the tetrapyrrole pigments*. D. J. Chadwick, K.A. ckrill, eds, John Willey and sons, Chicchester, UK, pp. 135-1554.
- Alawady AE and Grimm B.** (2005) Tobacco Mg protoporphyrin IX methyltransferase is involved in inverse activation of Mg-porphyrin and proto heme synthesis. *Plant J.* 41: 282-290.
- Allakhverdiev S.I., Kinoshita M, Inaba M, Suzuki I, and Murata N.** (2001) Unsaturated fatty acids in membrane lipids protect the photosynthetic machinery against salt-induced damage in *Synechococcus*. *Plant Physiology.* 125, 1842-1853.

- Allakhverdiev S.I., Sakamoto A., Nishiyama Y, Inaba M, and Murata N.** (2000) Ionic and osmotic effects of NaCl-induced inactivation of photosystem I and photosystem II in *synechococcus* sp. *Plant Physiology* 123, 1047-1056.
- Allakhverdiev SI, Murata N. (2008)** Salt stress inhibits photosystems II and I in cyanobacteria. *Photosynth Res.* Oct-Dec; 98(1-3):529-39.
- Allakhverdiev SI, Nishiyama Y, Miyairi S, Yamamoto H, Inagaki N, Kanasaki Y and Murata N** (2002) Salt stress inhibits the repair of photodamaged photosystem II by suppressing the transcription and translation of *psbA* genes in *synechocystis*. *Plant Physiol.* 130(3): 1443-53.
- Allan AC and Fluhr R.** (1997) Two distinct sources of elicited reactive oxygen species in tobacco epidermal cells. *Plant Cell.* 9: 1559–1572.
- Amtmann,A. and Sanders,D.** (1999) Mechanism of Na⁺ uptake by plant cells. In:eds) *Advances in Botanical Research.Academic Press*, pp.76-114.
- Amzallag GN, Lerner HR and Poljakoff-Mayber.** (1990) Induction of increased salt tolerance in *sorghum bicolor* by NaCl pretreatment. *J.Exp.Bot.*41: 29-34.
- Anthony RG, Henriques R, Helfer A, Meszaros T, Rios G, Testerink C, Munnik T, Deak M, Koncz C and Bogre L.** (2004) A protein kinase target of a PDK1 signalling pathway is involved in root hair growth in *Arabidopsis*. *EMBO J.* 23: 572–581.
- Apel K and Hirt H.** (2004) Reactive oxygen species: metabolism, oxidative stress, and signal transduction. *Annu. Rev. Plant Biol.* 55: 373–399.
- Apel K, Santel HJ, Redlinger TE and Falk H.** (1980) The protochlorophyllide holochrome of barley (*Hordeum vulgare* L.). Isolation and characterization of the NADPH: protochlorophyllide oxidoreductase. *Eur J Biochem.* 111: 251-258.
- Apel K.** (1981) The protochlorophyllide holochrome of barley (*Hordeum vulgare* L.). Phytochrome-induced decrease of translatable mRNA coding for the NADPH: protochlorophyllide oxidoreductase. *Eur J Biochem.* 120: 89–93.
- Apse MP, Aharon GS, Snedden WA and Blumwald E.** (1999). Salt tolerance conferred by overexpression of a vacuolar Na⁺/H⁺ antiport in *Aabidopsis*, *Science* 285:1256-58.
- Armstrong GA, Apel K and Rüdiger W** (2000) Does a lightharvesting protochlorophyllide *a/b*-binding protein complex exist? *Trends Plant Sci.* 5: 40–44.

- Armstrong GA, Runge S, Frick G, Sperling U and Apel K.** (1995) Identification of NADPH: protochlorophyllide oxidoreductase A and B: a branched pathway for light-dependent chlorophyll biosynthesis in *Arabidopsis thaliana*. *Plant Physiol.* 108: 1505-1517.
- Arnould S and Camadro JM.** (1998) The domain structure of protoporphyrinogen oxidase, the molecular target of diphenyl ether-type herbicides. *Proc Natl Acad Sci USA.* 95: 10553-10558.
- Aro E-M, Virgin I and Andersson B.** (1993) Photoinhibition of photosystem II. Inactivation, protein damage and turnover. *Biochim. Biophys. Acta.* 1143: 113–134.
- Aronsson H, Sohrt K and Soll J** (2000) NADPH:protochlorophyllide oxidoreductase uses the general import route into chloroplasts. *Biol Chem.* 381: 1263–1267.
- Aronsson H, Sundqvist C and Dahlin C** (2003a) POR – import and membrane association of a key element in chloroplast development. *Physiol Plant.* 118: 1–9.
- Aronsson H, Sundqvist C, Timko MP and Dahlin C** (2001a) The importance of the C-terminal region and Cys residues for the membrane association of the NADPH:protochlorophyllide oxidoreductase in pea. *FEBS Lett.* 502: 11–15.
- Aronsson H, Sundqvist C, Timko MP and Dahlin C** (2001b) Characterization of the assembly pathway of the pea NADPH:protochlorophyllide (Pchl) oxidoreductase (POR), with emphasis on the role of its substrate, Pchl. *Physiol Plant.* 111: 239–244.
- Asada K, Takahashi M, Nagate M** (1974) Assay and inhibitors of spinach superoxide dismutase. *Agric Biol Chem* 38:471-473
- Asada, K. and Takahashi, M.** (1987) Production and scavenging of active oxygen in photosynthesis. In *Photoinhibition* (Kyle, D.J. *et al.*, eds), pp. 227–287, Elsevier.
- Ashraf M.** (2009) Biotechnological approach of improving plant salt tolerance using antioxidants as markers. *Biotech Adv* 27:84–93.
- Aşkıım Hediye Sekmen, İsmail Türkan, Susumu Takio** (2007) Differential responses of antioxidative enzymes and lipid peroxidation to salt stress in salt-tolerant *Plantago maritima* and salt-sensitive *Plantago media*. *Physiologia Plantarum* Volume 131 Issue 3, Pages 399 – 411.
- Averina N, Rassadina V, and Leonid F.** (2002) Native state, energetic interaction of chlorophyll precursors and intraplastid location of S-adenosyl-L-methionine: Mg-protoporphyrin IX methyltransferase in etiolated leaves. *Indian J Exp Biol.* 40: 192-201.

- Babcock GT** (1987) The photosynthetic oxygen evolving process. In Amesz, J (ed) *New Comprehensive Biochemistry*, vol 15 pp 125-158, Elsevier, Amsterdam.
- Badawi GH, Kawano N, Yamauchi Y, Shimada E, Sasaki R, Kubo A and Tanaka K** (2004) Over-expression of ascorbate peroxidase in tobacco chloroplasts enhances the tolerance to salt stress and water deficit. *Physiol Plant*. 121(2): 231-238.
- Baker NR** (1991) Possible role of photosystem II in environmental perturbations of photosynthesis. *Physiologia Plantarum* 81, 563-570.
- Barber J and Andersson B.** (1992) Too much of a good thing: Light can be bad for photosynthesis. *Trends Biochem. Sci.* 17: 61-66
- Barnes SA, Nishizawa NK, Quaggio RB, Whitelam GC and Chua N-H.** (1996) Far-red light blocks greening of *Arabidopsis* seedlings via a phytochrome A-mediated change in plastid development. *Plant Cell*. 8: 601–615.
- Batschauer A and Apel K.** (1984) An inverse control by phytochrome of the expression of two nuclear genes in barley (*Hordeum vulgare* L.). *Eur J Biochem*. 143: 593–597.
- Bauer CE, Bollivar DW and Suzuki JY.** (1993) Genetic analysis of photopigment biosynthesis in Eubacteria : A guiding light for algae and plants. *J bacteriol* 175: 3919-3925.
- Baxter-Burrell A, Yang Z, Springer PS and Bailey-Serres J.** (2002) RopGAP4-dependent Rop GTPase rheostat control of Arabidopsis oxygen deprivation tolerance. *Science*. 296: 2026–2028.
- Bazzaz MB and Brereton RG.** (1982) 4-Vinyl-4desethyl chlorophyll a: a new naturally occurring chlorophyll. *FEBS Lett*. 128: 104–108.
- Bazzaz MB.** (1981) New chlorophyll chromophores isolate from a chlorophyll deficient mutant of maize. *Photobiochem. Photobiophys.* 2: 199–207.
- Beale SI** (1999) Enzymes of chlorophyll biosynthesis. *Photosynth. Res.* 60: 43–73.
- Beale SI and Weinstein JD.** (1990) Tetrapyrrole metabolism in photosynthetic organisms. In Biosynthesis of heme and chlorophyll. H.A.Dailey eds, McGraw-Hill, New York, pp. 287-291.
- Beauchamp C, Fridovich I.** (1971). Superoxide dismutase: improved assays and an assay applicable to acrylamide gels *Anal Biochem*. Nov; 44(1):276-87.
- Belanger FC and Rebeiz CA.** (1980) Chloroplast biogenesis. Detection of divinylprotochlorophyllide in higher plants. *J Biol. Chem.* 225: 1266-1272.

- Belkhodja R, Morales F, Abadia A, Gomez-Aparisi J and Abadia J.** (1994) Chlorophyll fluorescence as a possible tool for salinity tolerance screening in barley (*Hordeum vulgare* L.) *Plant Physiology* 31, 491-543.
- Benli M, Schulz R and Apel K.** (1991) Effect of light on the NADPH-Pchlide oxidoreductase (POR) of *A. thaliana*. *Plant Mol Biol.* 16: 615-625.
- Benz J and Rüdiger W.** (1981a) Incorporation of 1-¹⁴C-isopentenylidiphosphate, geraniol and farnesol into chlorophyll in plastid membrane fractions of *Avena sativa* L. *Z Pflanzenphysiol.* 102: 95-100.
- Benz J and Rüdiger W.** (1981b) Chlorophyll biosynthesis: various chlorophyllides as exogenous substrates for chlorophyll synthetase. *Z Naturforsch.* 36c: 51-57.
- Berry-Lowe S.** (1987) The chloroplast glutamate tRNA gene required for δ -aminolevulinic acid synthesis. *Carlsberg Res Commun.* 52: 197-210.
- Bhattacharjee S and Mukherjee AK.** (2003) Heavy metals alter photosynthetic pigment profiles as well as activities of chlorophyllase and 5-aminolevulinic acid dehydratase (ALAD) in *Amaranthus lividus* seedlings. *J Environ Biol.* 24: 395-399.
- Binzel ML, Hess FD, Bressan RA and Hasegawa PM.** (1998) Intracellular compartmentation of ions in salt adapted tobacco cells. *Plant Physiol.* 86: 607-14.
- Birve SJ, Selstam E and Johansson LB.** (1996) Secondary structure of NADPH:protochlorophyllide oxidoreductase examined by circular dichroism and prediction methods. *Biochem J.* 317: 549-555.
- Block MA, Tewari AK, Albrieux C, Marechal E and Joyard J.** (2002) The plant S-adenosyl-L-methionine: Mg-protoporphyrin IX methyl transferase is isolated in both envelope and thylakoid chloroplast membranes. *Eur J Biochem.* 269: 240-248.
- Blumwald, E., Aharon, G.S. and Apse, M.P.** (2000) Sodium transport in plant cells. *Biochimica et Biophysica Acta* 1465, 140-151.
- Böddi B and Franck F.** (1997) Room temperature fluorescence spectra of protochlorophyllide and chlorophyllide forms in etiolated bean leaves. *J Photochem Photobiol B.* 41: 73-82.
- Böddi B, Kis-Petik K, Kaposi AD, Fidy J and Sundqvist C.** (1998) The two spectroscopically different short wavelength protochlorophyllide forms in pea epicotyls are both monomeric. *Biochim Biophys Acta.* 1365: 531-540.

- Böddi B, Lindsten A, Ryberg M, Sundqvist C** (1989) On the aggregational states of protochlorophyllide and its protein complexes in wheat etioplasts. *Physiol Plant* 76: 135-143
- Böddi B, Ryberg M and Sundqvist C.** (1992) Identification of four universal protochlorophyllide forms in dark-grown leaves by analyses of the 77K fluorescence emission spectra. *J Photochem Photobiol B Biol.* 12: 389–401.
- Böddi B, Ryberg M and Sundqvist C.** (1993) Analysis of the 77K fluorescence emission and excitation spectra of isolated etioplast inner membranes. *J Photochem Photobiol B Biol.* 21: 125–133.
- Böddi B, Ryberg M, Sundqvist C** (1991) The formation of a short-wavelength chlorophyllide form at partial phototransformation of protochlorophyllide in etioplast inner membranes. *Photochem Photobiol* 53: 667-673.
- Boese QF, Spano AJ, Li JM and Timko MP.** (1991) Aminolevulinic acid dehydratase in pea (*Pisum sativum* L.) Identification of an unusual metal binding in the plant enzyme. *J Biol Chem.* 266: 17060-17066.
- Bohnert, H.J. and Jensen, R.G.**(1996) Strategies for engineering for waterstress tolerance in plants. *Trends in Biotechnology* 14, 89-97.
- Bohnert, H.J., Nelson, D.E. and Jensen, R.G.** (1995) Adaptations to environmental stresses. *Plant Cell* 7, 1099-1111.
- Bohren KM, Grimshaw CE, Lai CJ, Harrison DH, Ringe D, Petsko GA and Gabbay KH.** (1994) Tyrosine-48 is the proton donor and histidine-110 directs substrate stereochemical selectivity in the reduction reaction of human aldose reductase: enzyme kinetics and crystal structure of the Y48H mutant enzyme. *Biochemistry.* 33: 2021-2032.
- Bollivar DW and Beale SI.** (1996) The chlorophyll biosynthetic enzyme Mg-protoporphyrin IX monomethyl ester (oxidative) cyclase. *Plant Physiol.* 112: 105–114.
- Bollivar DW, Suzuki JY, Beatty JT, Dobrowolski JM and Bauer CE.** (1994) Directed mutational analysis of bacterio-chlorophyll a biosynthesis in *Rhodobacter capsulatus*. *J Mol Biol.* 237: 622-640.
- Bollivar DW, Wang S, Allen JP and Bauer CE.** (1994b) Molecular genetic analysis of terminal steps in bacteriochlorophyll a biosynthesis: characterization of a *Rhodobacter*

capsulatus strain that synthesises geranylgeraniol esterified bacteriochlorophyll a. *Biochemistry*. 33: 12763-12768.

Bongi G and Loreto F. (1989) Gas-exchange properties of salt-stressed olive (*Olea europaea* L.) leaves. *Plant Physiology* 90, 1408-1416.

Bougri O and Grimm B. (1996) Members of a low-copy number gene family encoding glutamyl-tRNA reductase are differentially expressed in barley. *Plant J* 9: 867-878.

Bowler C and Fluhr R. (2000) The role of calcium and activated oxygens as signals for controlling cross-tolerance. *Trends Plant Sci.* 5: 241–246.

Bowler, C. et al. (1992) Superoxide dismutases and stress tolerance. *Annu. Rev. Plant Physiol. Plant Mol. Biol.* 43, 83–116.

Boyer, J.S. (1976) In *Water deficit and Plant Growth* (Kozlowski, T.T., ed.) Vol 4. pp. 153-190, Academic Press, New York.

Bradford MM. (1976) A rapid and sensitive method for the quantification of microgram quantities of protein utilizing the principle of protein-dye binding. *Anal. Biochem.* 72: 248-254.

Braun Y., Hassidim M, Learner HR and Reinhold L. (1986) Studies on H⁺-translocating ATPase in plants of varying resistance to salinity. Salinity during growth modulates the proton pump in the halophyte *Atriplex nummularia*. *Plant Physiol.* 81: 1050-56.

Bressan RA, Nelson DE, Iraki NM, LaRosa PC and Singh NK (1990). Reduced cell expansion and changes in cell walls of plants adapted to NaCl. See Ref.124a, pp.137-71.

Bressan,R.A., Hesegawa,P.M. and Prado,J.M. (1998) Plants use calcium to resolve salt stress. *Trends in Plant Sci.* 3, 411-412.

Breton R, Watson D, Yaguchi M and Lapointe J. (1990) Glutamyl-tRNA synthetases of *Bacillus subtilis* 168T and of *Bacillus stearothermophilus*. Cloning and sequencing of the *gltX* genes and comparison with other aminoacyl-tRNA synthetases. *J Biol Chem.* 265: 18248-18255.

Britt RD (1996) Oxygen evolution. In: Ort DR, Yocum CF (eds) *Oxygenic photosynthesis: The light reactions*. Dordrecht: Kluwer.

Brugnoli E and Bjorkman O. (1992) Growth of cotton under continuous salinity stress: influence on allocation pattern, stomatal and non-stomatal components of photosynthesis and dissipation of excess light energy. *Planta* 187, 335-345.

- Bruyant P and Kannangara CG.** (1987) Biosynthesis of δ -aminolevulinate in greening barley leaves. VII. Purification and characterization of the glutamate-tRNA ligase. *Carlsberg Res Comm* 52: 99-109.
- Butler, W.L.** (1978). Energy distribution in the photochemical apparatus of photosynthesis. *Ann. Rev. Plant Physiol.* 29, 345-378.
- Cahoon AB and Timko MP.** (2000) yellow-in-the-dark mutants of *Chlamydomonas* lack the CHLL subunit of light-independent protochlorophyllide reductase. *Plant Cell.* 12: 559-568.
- Camadro JM, Chamba H, Jolles J and Labbe P.** (1986) Purification and properties of coproporphyrinogen oxidase from the yeast (*Saccharomyces cerevisiae*). *Eur J Biochem.* 156: 579-587.
- Camadro JM, Matringe M, Scalla R and Labbe P.** (1991) Kinetic studies on protoporphyrinogen oxidase inhibition by diphenyl ether herbicides. *Biochem J.* 277: 17-21.
- Camadro JM, Thome F, Brpuillet N and Labbe P.** (1994) Purification and properties of protoporphyrinogen oxidase from the yeast *S. cerevisiae*. *J Biol Chem.* 269: 32085-32091.
- Casas AM, Bressan RA and Hasegawa PM.** (1991) Cell growth and water reactions of the halophytes *Atriplex nummularia* L., in response of NaCl. *Plant Cell Rep.* 10: 81-84.
- Castelfranco PA, Thayer SS, Wilkinson JQ and Bonner BA.** (1988) Labeling of porphobilinogen deaminase by radioactive 5-aminolevulinic acid in isolated developing pea chloroplasts. *Arch Biochem Biophys.* 266: 219-226.
- Cayuela I, Perez-Alfocea F, Caro M. and Bolarin M. C.** (1996) Priming of seeds with NaCl induces physiological changes in tomato plants grown under salt stress *Physiologia Plantarum* 96: 231-236.
- Chakraborty N and Tripathy B C.** (1990) Expression of 5-aminolevulinic acid induced photodynamic damage to the thylakoid membranes in dark sensitized by brief pre-illumination. *J. Biosci.* 15: 199-204.
- Chakraborty N and Tripathy B C.** (1992a) 5-aminolevulinic acid induced photodynamic reactions in thylakoid membranes of cucumber (*Cucumis sativus* L.) cotyledons. *J. Plant Biochem. Biotech.* 1: 65-68.

- Chakraborty N and Tripathy B C.** (1992b) Involvement of singlet oxygen in 5-aminolevulinic acid induced photodynamic damage of cucumber (*Cucumis sativus* L.) Chloroplasts. *Plant Physiol.* 98: 7-11.
- Chamnongpol S, Willekens H, Moeder W, Langebartels C and Sandermann H Jr.** (1998) Defense activation and enhanced pathogen tolerance induced by H₂O₂ in transgenic tobacco. *Proc. Natl. Acad. Sci. USA.* 95: 5818–23.
- Chattopadhyay M.K., Tiwari B.S., Chattopadhyay G, Bose A, Sengupta D.N. and Gosh B.** (2002) Protective role of exogenous polyamines on salinity-stressed rice (*Oryza sativa*) plants. *Physiologia Plantarum.* 116: 192-199.
- Chauhan S and O'Brian MR.** (1993a) *Bradyrhizobium japonicum* δ-aminolevulinic acid dehydratase is essential for symbiosis with soybean and contains a novel metal-binding domain. *J bacteriol* 175: 7222-7227.
- Chauhan VS, Singh B, Singh S, Gour RK and Bisen PS** (2000) Isolation and characterization of the thylakoid membranes from the NaCl-resistant (NaCl(r)) mutant strain of the cyanobacterium *Anabaena variabilis*. *Curr Microbiol.* 41(5): 321-7.
- Chaves MM, Flexas J, Pinheiro C.** (2009). Photosynthesis under drought and salt stress: regulation mechanisms from whole plant to cell. *Ann Bot (Lond).* Feb; 103(4):551-60.
- Che FS, Watnabe N, Iwano M, Inokuchi H, Takayama S, Yoshida S and Isogai A.** (2000) Molecular characterization and subcellular localization of protoporphyrinogen oxidase in spinach chloroplasts. *Plant Physiol.* 124: 59-70.
- Chekounova E, Voronetskaya V, Papenbrock J, Grimm B and Beck CF.** (2001) Characterization of *Chlamydomonas* mutants defective in the H subunit of Mg-chelatase. *Mol Genet Genomics.* 266: 363-373.
- Chen H-X, Li W-J, An S-Z and Gao H-Y** (2004) Characterization of PSII photochemistry and thermostability in salt treated *Rumex* leaves. *J. Plant Physiol.* 161, 257-264.
- Chen J Q, Meng X P, Zhang Y, Xia M, Wang X P** (2008) Over-expression of OsDREB genes lead to enhanced drought tolerance in rice. *Biotechnol Lett.* Dec; 30(12):2191-8.
- Chen MW, Jahn D, O'Neil GP and Soll D.** (1990b) Purification of the glutamyl-tRNA reductase from *Chlamydomonas reinhardtii* involved in 5-aminolevulinic acid formation during chlorophyll biosynthesis. *J Biol Chem* 265: 4058-4063.

- Chen W, Wright L, Lie S, Cosloy SD, Russell CS and Lee S.** (1998) Expression of glutamyl-tRNA reductase in *Escherichia coli*. *Biochim Biophys Acta* 1395: 361. chlorophyll b biosynthesis in chlorophyllide a oxygenase overexpressing tobacco plants. *Biochem Biophys Res Commun.* 326: 466-471.
- Chitnis PR** (1996) Photosystem I. *Plant Physiol*, 111: 661-669.
- Chitnis PR, Xu Q, Chitnis VP and Nechushtai R** (1995) Function and organization of photosystem I polypeptides. *Photosynth Res* 44: 23-40.
- Choquet Y, Rahire M, Girard-Bascou J, Erickson J and Rochaix J D.** (1992) A chloroplast gene is required for the light-independent accumulation of chlorophyll in *Chlamydomonas reinhardtii*. *EMBO J.* 11:1697-1704.
- Chory J, Reinecke D, Sim S, Washburn T and Brenner M.** (1994) A role of cytokinins in de-etiolation in *Arabidopsis*. *Plant Physiol.* 104: 339-347.
- Chory J.** (1991) Light signals in leaf and chloroplast development: photoreceptor and downstream responses in search of a transduction pathway. *New Biologist.* 3: 538-548.
- Chow K S, Singh D P, Walker A R and Smith A G.** (1998) Two different genes encode ferrochelatase in *Arabidopsis*: mapping, expression and subcellular targeting of the precursor proteins. *Plant J.* 15: 531-541.
- Clarkson DT.** (1991) Root structure and sites of ion uptake. In *Plant Roots: The Hidden Half*, ed, Y Waisel, A Eshel, U Kafkafi, pp.417-53. New York: Marcel Dekker.
- Clough SJ and Bent AF.** (1998) Floral dip: a simplified method for *Agrobacterium* mediated transformation of *Arabidopsis thaliana*. *Plant J.* 6: 735-743.
- Coelho SM, Taylor AR, Ryan KP, Sousa-Pinto I, Brown MT and Brownlee C.** (2002) Spatiotemporal patterning of reactive oxygen production and Ca²⁺ wave propagation in *Fucus* rhizoid cells. *Plant Cell.* 14: 2369-2381.
- Coemans B, Matsumura H, Terauchi R, Remy S, Swennen R and Sagi L.** (2005) SuperSAGE combined with PCR walking allows global gene expression profiling of banana (*Musa acuminata*), a non-model organism. *Theor Appl Genet.* 111: 1118-26.
- Coomber SA, Jones RM, Jordan PM and Hunter CN.** (1992) A putative anaerobic coprogen III oxidase in *R.sphaeroides* 1. Molecular cloning, transposon, mutagenesis and sequence analysis of the gene. *Mol Microbiol.* 6: 3159-3169.

- Cornah J E, Roper J M, Pal Singh D and Smith A G.** (2002) Measurement of ferrochelatase activity using a novel assay suggests that plastids are the major site of haem biosynthesis in both photosynthetic and non-photosynthetic cells of pea (*Pisum sativum* L.). *Biochem J.* 362: 423-32.
- Cushman J C, DeRocher E J and Bohnert H J.** (1990) Gene expression during adaptation to salt stress. See ref.124a, pp.173-203.
- D.J. Chadwick, K.Ackrill.** eds, John Wiley and sons, Chichester,UK, pp. 131-152.
- Dahlin C, Aronsson H, Almkvist J and Sundqvist C.** (2000) Protochlorophyllide-independent import of two NADPH: Pchlde oxidoreductase proteins (PORA and PORB) from barley into isolated plastids. *Physiol Plant.* 109: 298–303.
- Dahlin C, Aronsson H, Wilks HM, Lebedev N, Sundqvist C and Timko MP.** (1999) The role of protein surface charge in catalytic activity and chloroplast membrane association of the pea NADPH: protochlorophyllide oxidoreductase (POR) as revealed by alanine scanning mutagenesis. *Plant Mol Biol.* 39: 309–323.
- Dahlin C, Sundqvist C and Timko M P.** (1995) The *in vitro* assembly of the NADPH-protochlorophyllide oxidoreductase in pea chloroplasts. *Plant Mol Biol.* 29: 317-330.
- Dailey T A, Meissner P and Dailey H A.** (1994) Expression of a cloned protoporphyrinogen oxidase. *J Biol Chem.* 269: 813-815.
- Dalton T P, Shertzer H G and Puga A.** (1999) Regulation of gene expression by reactive oxygen. *Annu. Rev. Pharmacol. Toxicol.* 39: 67–101.
- Danon A, Miersch O, Felix G, Camp RG and Apel K.** (2005) Concurrent activation of cell death-regulating signaling pathways by singlet oxygen in *Arabidopsis thaliana*. *Plant J.* 41: 68-80
- Darrah P M, Kay S A, Teakle G R and Griffiths W T.** (1990) Cloning and sequencing of protochlorophyllide reductase. *Biochem J.* 265: 789-798.
- Dat, J. et al.** (2000) Dual action of the active oxygen species during plant stress responses. *Cell. Mol. Life Sci.* 57, 779–795
- Dau, H.** (1994). Molecular mechanisms and quantitative models of variable photosystem II fluorescence. *Photochem. Photobiol.* 60, 1-23.

- Davison P A, Schubert H L, Reid J D, Iorg C D, Heroux A, Hill CP and Hunter C N. (2005)** Structural and biochemical characterization of Gun4 suggests a mechanism for its role in chlorophyllbiosynthesis. *Biochemistry*. 44: 7603-7612.
- Day I S, Golovkin M and Reddy A S. (1998)** Cloning of the cDNA for glutamyl-tRNA synthetase from *Arabidopsis thaliana*. *Biochim Biophys Acta*. 1399: 219-224.
- Debez A, Koyro H W, Grignon C, Abdelly C, Huchzermeyer B. (2008)** Relationship between the photosynthetic activity and the performance of *Cakile maritima* after long-term salt treatment. *Physiol Plant*. Jun;133(2):373-85.
- Delaunay A M, Huault C and Balange A P. (1991)** Molecular cloning of the 5-aminolevulinic acid dehydratase gene from *Rhodobacter sphaeroides*. *J Bacteriol*. 73: 2712-2715.
- Delaunay A, Isnard A-D and Toledano M B. (2000)** H₂O₂ sensing through oxidation of the Yap1 transcription factor. *EMBO J*. 19: 5157–5166.
- Delaunay A, Pflieger D, Barrault M B, Vinh J and Toledano M B. (2002)** A thiol peroxidase is an H₂O₂ receptor and redox-transducer in gene activation. *Cell*. 111: 471–481.
- Delfine S, Alvino A, Villani M C, and Loreto F. (1998)** Salt induced changes of CO₂ conductance and photochemical properties of spinach leaves. In *Photosynthesis: Mechanisms and its effects*, vol.IV, 2621-2624.
- Demko V, Pavlovic A, Valková D, Slováková L, Grimm B, Hudák J. (2009).** A novel insight into the regulation of light-independent chlorophyll biosynthesis in *Larix decidua* and *Picea abies* seedlings. *Planta*. Jun; 230(1):165-76.
- Demmig-Adams B, Adams IIIWW. (1996).** The role of xanthophylls cycle carotenoids in the protection of photosynthesis. *Trends in Plant Science* 1, 21–26.
- Desikan R, A-H Mackerness S, Hancock JT and Neill SJ. (2001)** Regulation of the *Arabidopsis* transcriptome by oxidative stress. *Plant Physiol*. 127: 159–172.
- Desikan R, Neill SJ and Hancock JT. (2000)** Hydrogen peroxide-induced gene expression in *Arabidopsis thaliana*. *Free Rad. Biol. Med*. 28: 773–778.
- Desikin, R. et al. (2001)** Regulation of the *Arabidopsis* transcriptosome by oxidative stress. *Plant Physiol*. 127, 159–172.
- Devlin R M, Karczmarczyk S J and Zbejc I. (1983)** Influence of Norflurazon on the activation of substituted diphenyl ether herbicides by light. *Weed sci*. 31: 109-112.

- Diner B A, Petrouleas V and Wendoloski J J** (1991) The iron-quinone electron acceptor complex of photosystemII. *Physiol Plant* 81: 423-436.
- Domanski V P and Rüdiger W.** (2001) On the nature of the two pathways in chlorophyll formation from protochlorophyllide. *Photosynth Res.* 68: 131–139.
- Domanskii V, Rassadina V, Gus-Mayer S, Wanner G, Schoch S and Rudiger W.** (2003) Characterization of two phases of chlorophyll formation during greening of etiolated barley leaves. *Planta.* 216: 475-83.
- Dostani R, Meyer H E & Oettmeier W** (1998) Mapping of two tyrosine residues involved in the quinone (QB) binding site of the D1 reaction centre polypeptide of photosystem II. *FEBS Lett* 239: 207-210.
- Drozdowicz, Y M and Rea, P A** (2001) Vacuolar H⁺ P.A.(2001) Vacuolar H⁺ pyrophosphatases:from the evolutionary backwaters into the mainstream. *Trends Plant Sci.* 6,206-11.
- Dubouzet J G, Sakuma Y, Ito Y, Kasuga M, Dubouzet E G, Miura S, Seki M, Shinozaki K, Yamaguchi-Shinozaki K** (2003) OsDREB genes in rice, *Oryza sativa* L., encode transcription activators that function in drought-, high-salt- and cold-responsive gene expression. *Plant J.* Feb; 33(4):751-63.
- Duke S O and Kenyon W H.** (1987) A non-metabolic model of aciflurofen activity. *Z. Naturforsch.* 42c: 813-818.
- Duke S O and Kenyon W H.** (1986) Photosynthesis is not involved in the mechanism of action of aciflurofen in cucumber (*Cucumis sativus* L.). *Plant physiol.* 81: 882-888.
- Duke S O, Becerril J M, Sherman T D and Matsumoto H.** (1991) Photosensitizing porphyrins as herbicides. In: Naturally occurring pest Bioregulators. (Hedin, PA eds). ACS Symposium series No. 449, pp. 371-386, ACS, Washington.
- Duke S O, Vaughn K C and Meeusen R L.** (1984) Mitochondrial involvement in the mode of action of aciflurofen. *Pest. Biochem. Physiol.* 21: 368-376.
- Duncan J, Bibby T, Tanaka A and Barber J.** (2003) Exploring the ability of chlorophyll b to bind to the CP43' protein induced under iron deprivation in a mutant of *Synechocystis* PCC 6803 containing the *cao* gene. *FEBS Lett.* 541: 171-175.

- Durrant JR, Klug DR, Kwa SLS, van Grondell R, Porter G and Dekkar JP** (1995) A multiple model for P680, the primary electron donor of PSII. *Proc Natl Acad Sci, USA* 92:4798-4802.
- Dyall SD, Brown MT, Johnson PJ.** (2004). Ancient invasions: from endosymbionts to organelles. *Science*. Apr 9; 304(5668):253-7.
- Eenennaam, A. L., Lincoln, K., Durrett, T. P., Valentin, H. E., Shewmaker, C. K., et al.** (2003) Engineering vitamin E content: From Arabidopsis mutant to soy oil. *Plant Cell* 15, 3007–3019.
- Eggink LL, LoBrutto R, Brune DC, Brusslan J, Yamasato A, Tanaka A and Hooper JK.** (2004) Synthesis of chlorophyll b: localization of chlorophyllide a oxygenase and discovery of a stable radical in the catalytic subunit. *BMC Plant Biol.* 4: 5.
- Eguchi S, Takano H, Ono K and Takio S** (2002) Photosynthetic electron transport regulates the stability of the transcript for the protochlorophyllide oxidoreductase gene in the liverwort, *Marchantia paleacea* var. *diptera*. *Plant Cell Physiol.* 43: 573–577.
- Elliot T, Avissar JR, Rhie G and Beale SI.** (1990) Cloning and sequencing of the hemL gene from *Salmonella typhimurium* and identification of the missing enzyme in hemL mutants as glutamate 1-semialdehyde aminotransferase. *J Bacteriol* 172: 7071-7084.
- Ellsworth RK, Dullaghan JP and St. Pierre ME.** (1974) The reaction of S-adenosyl L-methionine: magnesium protoporphyrin IX methyltransferase of wheat. *Photosynthetica.* 8: 375-384.
- Elumalai RP, Nagpal P, Reed JW** (2002) A mutation in the Arabidopsis KT2/ KUP2 potassium transporter gene affects shoot cell expansion. *Plant Cell* 14: 119–131.
- Ensminger MP and Hess FD.** (1985a) Action spectrum of the activity of acifluorfen-methyl, a diphenyl ether herbicide, in *Chlamydomonas eugametos*. *Plant physiol.* 77: 503-505.
- Epple P, Mack AA, Morris VR and Dangl JL.** (2003) Antagonistic control of oxidative stress-induced cell death in Arabidopsis by two related, plant-specific zinc finger proteins. *Proc. Natl. Acad. Sci. USA.* 100: 6831–6836.
- Epstein E** (1961) The essential role of calcium in selective cation transport by plant cells. *Plant Physiol* 36: 437–444.

- Espineda CE, Linford AS, Devine D and Brusslan JA.** (1999) The AtCAO gene, encoding chlorophyll a oxygenase, is required for chlorophyll b synthesis in *Arabidopsis thaliana*. *Proc Natl Acad Sci U S A.* 96: 10507-11.
- Everard JD, Gussi R, Kann SC, Flore JA and Loescher WH.** (1994) Gas exchange and carbon partitioning in the leaves of celery (*Apium graveolens* L.) at various level of root zone salinity. *Plant Physiology.* 106, 281-292.
- Fairbrain, D.J., Liu, W., Schachtman, D.P., Gomez-Gallego, S., Day, S.R. and Teasdale, R.D.** (2000) characterization of two distinct HKT1-like potassium transporters from *Eucalyptus camaldulensis*. *Plant Mol Biol.* 43, 515-25.
- Falbel TG and Staehelin LA.** (1994) Characterization of a family of chlorophyll-deficient wheat (*Triticum*) and barley (*Hordeum vulgare*) mutants with defects in the magnesium-insertion step of chlorophyll biosynthesis. *Plant Physiol.* 104: 639-648.
- Falciatore A, Merendino L, Barneche F, Ceol M, Meskauskiene R, Apel K and Rochaix JD.** (2005) The FLP proteins act as regulators of chlorophyll synthesis in response to light and plastid signals in *Chlamydomonas*. *Genes Dev.* 19: 176-187.
- Fedina IS, Grigorova ID, Georgieva KM** (2003) Response of barley seedlings to UV-B radiation as affected by NaCl. *J Plant Physiol.* 160(2): 205-8.
- Feinbaum RL and Ausubel FM.** (1988) Transcriptional regulation of the *Arabidopsis thaliana* chalcone synthase gene. *Mol. Cell. Biol.* 8: 1985-1992.
- Felix F and Brouillet N.** (1990) Purification and properties of uroporphyrinogen decarboxylase from *Saccharomyces cerevisiae*. *Eur J Biochem.* 188: 393-403.
- Feng L, Bai ZY, Lu BS, Cai SW, Feng LN.** (2008) Effects of NaCl stress on *Hovenia dulcis* and *Gleditsia sinensis* seedlings growth, chlorophyll fluorescence, and active oxygen metabolism. (Article in Chinese). *Ying Yong Sheng Tai Xue Bao.* Nov; 19(11):2503-8.
- Ferjani A, Mustardy L, Sulpice R, Marin K, Suzuki I, Hagemann M and Murata N** (2003) Glucosylglycerol, a compatible solute, sustains cell division under salt stress. *Plant Physiol.* 2003 131(4): 1628-37.
- Fletcher RA and McCullagh D.** (1971) Benzyladenine as a regulator of chlorophyll synthesis in cucumber cotyledons. *Can J Bot.* 49: 2197-2201.
- Flohe L and Otting F.** (1984) Superoxide dismutase assay, *Methods in Enzymology.* 105: 93-104.

- Flowers TJ and Yeo AR.** (1992) *Solute Transport in plants*. Glasgow, Scotland:Blackie.176pp
- Flowers TJ, Troke PF and Yeo AR.** (1977) The mechanism of salt tolerance in halophytes. *Ann.Rev.Plant Physiol.* 28:89-121
- Flowers TJ, Troke PF, Yeo AR.** (1977). The mechanism of salt tolerance in halophytes. *Annu. Rev. Plant Physiol.* 28:89–121
- Flowers, T.J., Hajibagheri, M.A. and Clipson, N.J.W.** (1986) Halophytes. *The Quart. Rev. Biol.* 61, 313-337.
- Flowers,T.J. and Yeo, A.R.**(1995) Breeding for salinity resistance in crop plants:where next? *Aus.J.Plant Physiol.* 22,875-884.
- Foote CS, Shook FC and Abakerli RB.** (1984) Characterization of singlet oxygen.. *Methods Enzymol.* 105: 36-47
- Foote CS.** (1976) Photosensitized oxidation and singlet oxygen: consequences in biological systems. In *Free Radicals in Biology*, ed. WA Pryor, 2:85–133. New York: Academic.
- Ford C, Mitchell S and Wang W-Y.** (1981) Protochlorophyllide photoconversion mutants of *Chlamydomonas reinhardtii*. *Mol Gen Genet.* 184: 460–464.
- Fork, D.C. and Mohanty, P.** (1986). Fluorescence and other characteristics of blue green algae (cyanobacteria), red algae, and cryptomonads. In: *Light emission by Plants and Bacteria* (Govindjee, Ames, J. and Fork, D.C., eds). pp. 451-496.New York: Academic Press.
- Forreiter C, van Cleve B, Schmidt A and Apel K.** (1990) Evidence for a general light-dependent negative control of NADPH-protochlorophyllide oxidoreductase in angiosperms. *Planta.* 183: 126-132.
- Forreiter C, van Cleve B, Schmidt A and Apel K.** (1991) Evidence for a general light-dependent negative control of NADPH– protochlorophyllide oxidoreductase in angiosperms. *Planta.* 183: 126–132.
- Foyer CH and Harbinson J.** (1994) Oxygen metabolism and the regulation of photosynthetic electron transport. In *Causes of Photooxidative Stress and Amelioration of Defense Systems in Plants*, ed.CH Foyer, PM Mullineaux, pp. 1–42. Boca Raton: CRC Press
- Franck F, Bereza B and Böddi B.** (1999) Protochlorophyllide– NADP⁺ and protochlorophyllide–NADPH complexes and their regeneration after flash illumination in leaves and etioplast membranes of dark-grown wheat. *Photosynth Res.*59: 53–61.

- Franck F, Sperling U, Frick G, Pochert B, van Cleve B, Apel K and Armstrong GA.** (2000) Regulation of etioplast pigment– protein complexes, inner membrane architecture, and protochlorophyllide a chemical heterogeneity by light-dependent NADPH:protochlorophyllide oxidoreductases A and B. *Plant Physiol.* 124: 1678–1696.
- Freist W, Gauss DH, Ibba M and Soll D.** (1997) GlutaminyI-tRNA synthetase. *Biol Chem.* 378: 1103-1117.
- Frick G, Su Q, Apel K and Armstrong GA.** (2003) An *Arabidopsis* *porB porC* double mutant lacking light-dependent NADPH:protochlorophyllide oxidoreductases B and C is highly chlorophyll-deficient and developmentally arrested. *Plant J.* 35: 141–153.
- Frustaci JM, Sangwan I and O'Brian MR.** (1995) *gsal* is a universal tetrapyrrole synthesis gene in soybean and is regulated by a GAGA element. *J Biol Chem.* 270: 7387-7393.
- Fryer MJ, Oxborough K, Mullineaux PM and Baker NR.** (2002). Imaging of photooxidative stress responses in leaves. *J. Exp. Bot.* 53: 1249–1254.
- Fujita Y and Bauer CE.** (2000) Reconstitution of light-independent protochlorophyllide reductase from purified *bchl* and *BchN-BchB* subunits. In vitro confirmation of nitrogenase-like features of a bacteriochlorophyll biosynthesis enzyme. *J Biol Chem.* 275: 23583-23588.
- Fujita Y, Takagi H and Hase T.** (1998) Cloning of the gene encoding a protochlorophyllide reductase: the physiological significance of the co-existence of light-dependent and - independent protochlorophyllide reduction systems in the cyanobacterium *Plectonema boryanum*. *Plant Cell Physiol.* 39: 177–185.
- Fusada N, Masuda T, Kuroda H, Shimada H, Ohta H and Takamiya K.** (2005) Identification of a novel cis-element exhibiting cytokinin-dependent protein binding in vitro in the 5'-region of NADPH-protochlorophyllide oxidoreductase gene in cucumber. *Plant Mol Biol.* 59: 631-645.
- Fusada N, Masuda T, Kuroda H, Shiraishi T, Shimada H, Ohta H and Takamiya K.** (2000) NADPH–protochlorophyllide oxidoreductase in cucumber is encoded by a single gene and its expression is transcriptionally enhanced by illumination. *Photosynth Res.* 64: 147–154.
- Gamborg OL, Miller RA and Ojima K.** (1968) Nutrient requirements of suspension culture of soybean root cells. *Expt. Cell Res.* 50: 151-158.

- Gao Y, Xiong W, He MJ, Tang L, Xiang JY, Wu QY.** (2009). Action spectra of chlorophyll a biosynthesis in cyanobacteria: dark-operative protochlorophyllide oxidoreductase-deficient mutants. *Z Naturforsch [C]*. Jan-Feb; 64(1-2):117-24.
- Garcia-Maurino S, Monreal JA, Alvarez R, Vidal J and Echevarria C** (2002) Characterization of salt stress-enhanced phosphoenolpyruvate carboxylase kinase activity in leaves of *Sorghum vulgare*: independence from osmotic stress, involvement of ion toxicity and significance of dark phosphorylation. *Planta*. 216(4): 648-55. Epub 2002 Sep 17.
- Gaubier P, Wu HJ, Laudie M, Delseny M and Grellet F.** (1995) A chlorophyll synthetase gene from *Arabidopsis thaliana*. *Mol Gen Genet*. 249: 673-676.
- Gaxiola, R.A., Rao, R., Sherman, A., Grisafi, P., Alper, S.L. and Fink, G.R.** (1999) The *arabidopsis thaliana* proton transporter, At Nhx1 and Avp1, can function in cation detoxification in yeast. *Proc. Natl. Acad. Sci. USA* 96, 1480-1485.
- Ghanotakis DF, Topper JN, Babcock GT and Yocum CF** (1984) Water-soluble 17-kDa and 23 kDa polypeptides restore oxygen evolution activity by creating a high-affinity binding site for Ca^{2+} and on the oxidizing site of photosystem II. *FEBS Lett* 170: 169-173.
- Ghars MA, Parre E, Debez A, Bordenave M, Richard L, Leport L, Bouchereau A, Savoure0 A, Abdelly C** (2008) Comparative salt tolerance analysis between *Arabidopsis thaliana* and *Thellungiella halophila*, with special emphasis on K^+/Na^+ selectivity and proline accumulation. *J Plant Physiol* 165:588– 599
- Gibson KD, Neuberger A and Tait GH.** (1963) Studies on the biosynthesis of porphyrin and bacteriochlorophyll by *Rhodospseudomonas spheroides*. 4. S-adenosylmethionine-magnesium protoporphyrin methyltransferase. *Biochem J*. 88: 325–334.
- Gibson LC, Marrison JL, Leech RM, Jensen PE, Bassham DC, Gibson M and Hunter CN.** (1996) A putative Mg chelatase subunit from *Arabidopsis thaliana* cv C24. Sequence and transcript analysis of the gene, import of the protein into chloroplasts, and in situ localization of the transcript and protein. *Plant Physiol*. 111: 61-71.
- Gibson LC, Willows RD, Kannangara CG, von Wettstein D and Hunter CN.** (1995) Magnesium-protoporphyrin chelatase of *Rhodobacter sphaeroides*: reconstitution of activity by combining the products of the bchH, -I and -D genes expressed in *Escherichia coli*. *Proc Natl Aca Sci USA*. 92: 1941-1944.

- Glenn EP, Brown JJ and Blumwald E.** (1999) Salt tolerance and crop potential of halophyte. *Crit.Rev.Plant Sci.*18: 227-55
- Goslings D, Meskauskiene R, Kim C, Lee KP, Nater M and Apel K.** (2004) Concurrent interactions of heme and FLU with Glu tRNA reductase (HEMA1), the target of metabolic feedback inhibition of tetrapyrrole biosynthesis, in dark- and light-grown *Arabidopsis* plants. *Plant J.* 40: 957-67.
- Gough SP, Kannangara CG and von Wettstein D.** (1992) Glutamate 1-semialdehyde aminotransferase as a target for herbicides. In "Target assays for modern herbicides and related phytotoxic compounds". (P. Boger and G. Sandmann, eds). pp. 21-27. Lewis publishers, Chelsea.
- Gough SP, Petersen BO and Duus JQ.** (2000) Anaerobic chlorophyll isocyclic ring formation in *Rhodobacter capsulatus* requires a cobalamin cofactor. *Proc. Natl. Acad. Sci. USA* 97: 6908–6913.
- Govindjee** (1995). Sixty-three years since Kautsky: chlorophyll a fluorescence. *Aust.J.Plant Physiol.* 22,131-160.
- Govindjee and Papageorgiou,G.** (1971). Chlorophyll fluorescence and photosynthesis: fluorescence transient. *Photophysiology* 6, 1-50.
- Govindjee and Spilotro P.** (2002) An *Arabidopsis thaliana* mutant, altered in the β -subunit of ATP synthase, has a different pattern of intensity- dependent changes in non-photochemical quenching and kinetics of the P-to-S fluorescence decay. *Funct. Plant Biol.*, 2002, 29, 425-434.
- Govindjee,** (2004) Chlorophyll a fluorescence: a bit of basics and history, in: G.C. Papageorgiou, Govindjee (Eds.), Chlorophyll a Fluorescence a Signature of Photosynthesis, Springer, Dordrecht, , pp. 1–41.
- Grafe S, Saluz HP, Grimm B and Hanel F.** (1999) Mg-chelatase of tobacco: the role of the subunit CHL D in the chelation step of protoporphyrin IX. *Proc Natl Acad Sci U S A.* 96: 1941-1946.
- Graham MY.** (2005) The diphenylether herbicide lactofen induces cell death and expression of defense-related genes in soybean. *Plant Physiol.* 139: 1784-1794.

- Graham RC Jr, Karnovsky MJ.** (1965). The histochemical demonstration of monoamine oxidase activity by coupled peroxidatic oxidation. *J Histochem Cytochem.* 1965 Sep-Oct; 13(7):604-5.
- Granik S.** (1959) Magnesium porphyrins formed by barley seedlings treated with δ -aminolevulinic acid. *Plant physiol.* 34, XVIII.
- Grasses T, Grimm B, Koroleva O and Jahns P.** (2001) Loss of alpha-tocopherol in tobacco plants with decreased geranylgeranyl reductase activity does not modify photosynthesis in optimal growth conditions but increases sensitivity to highlight stress. *Planta.* 213: 620-628.
- Gray J, Close PS, Briggs SP and Johal GS.** (1997) A novel suppressor of cell death in plants encoded by the *Lls1* gene of maize. *Cell.* 89: 25-31.
- Greenfield, S. and Wasielewski, M.R.** (1996) Excitation energy transfer and charge separation in the isolated PhotosystemII reaction center. *Photosynth. Res.* 48, 83-97.
- Greenway H and Munns R.** (1980) Mechanisms of salt tolerance in nonhalophalophytes. *Ann.Rev.Plant Physiol.* 31:149-90.
- Gregenheimer, P.,** 1990. Preparation of extracts from plants. *Meth. Enzymol.* 182, 174–193.
- Griffiths WT.** (1975) Characterization of the terminal stages of chlorophyll(ide) synthesis in etioplast membrane preparations. *Biochem J.* 152: 623–655.
- Grimm B, Bull A and Breu V.** (1991) Structural genes of glutamate 1-semialdehyde aminotransferase for porphyrin synthesis in a cyanobacterium and *E.coli*. *Mol Gen Genet* 225: 1-10.
- Grimm B, Smith AJ, Kannangara CG and Smith M.** (1991) Gabaculine-resistant glutamate 1-semialdehyde aminotransferase of *Synechococcus*. Deletion of a tripeptide close to the NH₂ terminus and internal amino acid substitution. *J Biol Chem.* 266: 12495-12501.
- Grimm B.** (1990) Primary structure of a key enzyme in plant tetrapyrrole synthesis: Glutamate-1-semialdehyde aminotransferase. *Proc Natl Acad Sci USA.* 87: 4169-4173.
- Groom QJ, Torres MA, Fordham-Skelton AP, Hammond-Kosack KE, Robinson NJ and Jones JD.** (1996) *rbohA*, a rice homologue of the mammalian gp91phox respiratory burst oxidase gene. *Plant J.* 10: 515–522.
- Grusak, M. A.** (1999) Genomics-assisted plant improvement to benefit human nutrition and health. *Trends Plant Sci.* 4, 164– 166.

- Guo R, Luo M and Weinstein JD.** (1998) Magnesium-chelatase from developing pea leaves. *Plant Physiol.* 116: 605-615.
- Guo, Y., Halfter, U., Ishitani, M. and Zhu, J.-K.** (2001) Molecular characterization of functional domains in the protein kinase SOS2 that is required for plant salt tolerance. *Plant cell* 13, 149-190.
- Gupta I and Tripathy BC.** (2000) Oxidative stress in cucumber (*Cucumis sativus* L) seedlings treated with acifluorfen. *Indian J Biochem Biophys.* 37: 498-505.
- Gupta KJ, Stoimenova M, Kaiser WM.** (2005) In higher plants, only root mitochondria, but not leaf mitochondria reduce nitrite to NO, invitro and insitu. *J Exp Bot*; 56: 2601-9.
- Gupta M, Sharma P, Sarin NB, Sinha AK.** (2009). Differential response of arsenic stress in two varieties of *Brassica juncea* L. *Chemosphere.* 2009 Mar; 74(9):1201-8. Epub 2008 Dec 19.
- Gupta R and Luan S.** (2003) Redox control of protein tyrosine phosphatases and mitogen-activated protein kinases in plants. *Plant Physiol.* 132: 1149-1152.
- Hammond-Kosack, K.E. and Jones, J.D.G.** (1996) Resistance gene-dependent plant defense responses. *Plant Cell* 8, 1773-1791.
- Hanahan D.** (1983) Studies on transformation of *E.coli* with plasmid. *J.Mol.Bio.* 166: 557-580.
- Hankamer B, Barber, J and Boekema EJ** (1997) Structure and membrane organization of photosystem II in green plants. *Ann Rev Plant Physiol Plant Mol Biol* 48: 641-671.
- Hansson A, Kannangara CG, von Wettstein D and Hansson M.** (1999) Molecular basis for semidominance of missense mutations in the XANTHA-H (42-kDa) subunit of magnesium chelatase. *Proc Natl Aca Sci USA.* 96: 1744-1749.
- Hansson A, Willows RD, Roberts TH and Hansson M.** (2002) Three semidominant barley mutants with single amino acid substitutions in the smallest magnesium chelatase subunit form defective AAA+ hexamers. *Proc Natl Acad Sci U S A.* 99: 13944-13949.
- Hansson M, Rutberg L, Schroder I and Hederstedt L.** (1991) The *Bacillus subtilis* hemAXCDBL gene cluster, which encodes enzymes of the biosynthetic pathway from glutamate to uroporphyrinogen III. *J. Bacteriol.* 173: 2590-2599.
- Hara-Yokoyama M, Yokoyama S and Miyazawa T.** (1986) Conformation change of tRNA^{Glu} in the complex with glutamyl-tRNA synthetase is required for the specific binding of L-glutamate. *Biochemistry.* 25: 7031-7036.

- Harmer SL, Hogenesch JB, Straume M, Chang H-S, Han B, Zhu T, Wang X, Kreps JA and Kay SA.** (2000) Orchestrated transcription of key pathways in Arabidopsis by the circadian clock. *Science*. 290: 2110–2113.
- Harper AL, von Gesjen SE, Linford AS, Peterson MP, Faircloth RS, Thissen MM and Brusslan JA.** (2004) Chlorophyllide *a* oxygenase mRNA and protein levels correlate with the chlorophyll *a/b* ratio in *Arabidopsis thaliana*. *Photosynth. Research*. 79: 149–159.
- Hart GJ and Battersby AR.** (1985) Purification and properties of uroporphyrinogen III synthase(co-synthase) from *Euglena gracilis*. *Biochem J*. 232: 151-160.
- Hartel H, Haseloff RF, Walter G and Hanke T.** (1993b) Photoinduced damage in leaf segments of wheat (*Triticum aestivum* L.) and lettuce (*Lactuca sativa* L.) treated with 5-aminolevulinic acid. 2. Characterization of photodynamic damage by means of delayed chlorophyll fluorescence and P700 photooxidation. *J. Plant Physiol*. 142: 237-243.
- Hartel H, Walter G and Hanke T.** (1993a) Photoinduced damage in leaf segments of wheat (*Triticum aestivum* L.) and lettuce (*Lactuca sativa* L.) treated with 5-aminolevulinic acid. 1. Effect on structural components of photosynthetic apparatus. *J. Plant Physiol*. 142: 230-236.
- Hasegawa PM, Bressan RA, Zhu J-K, Bohnert HJ** (2000) Plant cellular and molecular responses to high salinity. *Annu Rev Plant Physiol Plant Mol Biol* 51: 463–499.
- Hasegawa,P.M., Bressan R.A. and Prado,J.M.** (2000a) The dawn of plant salt to tolerance genetics. *Trends in Plant Sci*. 5,317-319
- Hasegawa,P.M., Bressan,R.A. Zhu,J.-K. and Bohnert,H.J.** (2000b). Plant cellular and molecular responses to high salinity. *Annu.Rev.Plant Physiol.Plant Mol.Biol.* 51,463-499.
- Havaux M, Eymery F, PorWrova S, Rey P, Dörmann P** (2005) Vitamin E protects against photoinhibition and photooxidative stress in *Arabidopsis thaliana*. *Plant Cell* 17:3451–3469.
- Havaux M, Lutz C and Grimm B.** (2003) Chloroplast membrane photostability in chlP transgenic tobacco plants deficient in tocopherols. *Plant Physiol*. 132: 300-310.
- Haworth P and Hess FD.** (1988) The generation of singlet oxygen by the Nitrodiphenyl ether herbicide Oxyfluorefen is independent of photosynthesis. *Plant physiol*. 86: 672-676.

- Hayaishi O.** (1987) General properties and biological functions of oxygenases. In *Molecular Mechanisms of Oxygen Activation* (Edited by O.Hayaishi), pp.1-28. Academic press. London.
- He ZH, Li J, Sundqvist C and Timko MP.** (1994) Leaf development age controls expression of genes encoding enzymes of chlorophyll and heme biosynthesis in pea (*Pisum sativum* L.). *Plant Physiol.* 106: 537-546.
- He Z-H, Li J, Sundqvist C, Timko MP** (1994) Leaf developmental age controls expression of **Helfrich M, Schoch S, Lempert U, Cmiel E and Rudiger W.** (1994) Chlorophyll synthetase cannot synthesize chlorophyll a'. *Eur J Biochem.* 219: 267-275.
- Hermann CA, Im C and Beale SI.** (1999) Light-regulated expression of gsa gene encoding the chlorophyll biosynthetic enzyme glutamate 1-semialdehyde aminotransferase in carotenoid-deficient *Chlamydomonas reinhardtii* cells. *Plant Mol Bio.* 1 39: 289-297.
- Hernandez J.A., Olmos E., Corpas F.J., Sevilla F and Rio del L.A.** (1995) Salt-induced oxidative stress in chloroplasts of pea plants. *Plant Science* 105, 151-167.
- Hess WR, Blank-Huber M, Fieder B, Borner T and Rudiger W.** (1992) Chlorophyll synthetase and chloroplast tRNA_{glu} are present in heat bleached, ribosome-deficient plastids. *J Plant Physiol.* 139: 427-430.
- Heyes DJ and Hunter CN.** (2002) Site-directed mutagenesis of Tyr- 189 and Lys-193 in NADPH:protochlorophyllide oxidoreductase from *Synechocystis*. *Biochem Soc Trans.* 30: 601–604.
- Heyes DJ and Hunter CN.** (2004) Identification and characterization of the product release steps within the catalytic cycle of protochlorophyllide oxidoreductase. *Biochemistry.* 43: 8265–8271
- Heyes DJ, Heathcote P, Rigby SE, Palacios MA, van Grondelle R, Hunter CN.** (2006). The first catalytic step of the light-driven enzyme protochlorophyllide oxidoreductase proceeds via a charge transfer complex. *J Biol Chem.* Sep 15; 281(37):26847-53.
- Heyes DJ, Kruk J and Hunter CN.** (2006) Spectroscopic and kinetic characterization of the light-dependent enzyme protochlorophyllide oxidoreductase (POR) using monovinyl and divinyl substrates *Biochem. J.* 394: 243–248.
- Heyes DJ, Menon BR, Sakuma M, Scrutton NS.** (2008). Conformational events during ternary enzyme-substrate complex formation are rate limiting in the catalytic cycle of the light-

- driven enzyme protochlorophyllide oxidoreductase. *Biochemistry*. Oct 14; 47(41): 10991-8.
- Heyes DJ, Ruban AV and Hunter CN.** (2003) Protochlorophyllide oxidoreductase: spectroscopic characterization of the 'dark' reactions. *Biochemistry*. 42: 523–528
- Heyes DJ, Ruban AV, Wilks HM and Hunter CN.** (2002) Enzymology below 200 K: the kinetics and thermodynamics of the photochemistry catalyzed by protochlorophyllide oxidoreductase. *Proc. Natl. Acad. Sci. USA* . 99: 11145–11150
- Hideg E, Kalai T, Hideg K and Vass I.** (1998) Photoinhibition of photosynthesis in vivo results in singlet oxygen production. Detection via nitroxide-induced fluorescence quenching in broad bean leaves. *Biochemistry*. 37: 11405–11411.
- Higuchi M and Bogorad L.** (1975) The purification and properties of uroporphyrinogen I synthase and uroporphyrinogen III cosynthase. Interactions between the Enzymes. *Ann N.Y. Acad Sci.* 244: 401-418.
- Hinchigeri SB and Richards WR.** (1982) The reaction mechanism of S -adenosyl-L-methionine: magnesium protoporphyrin methyltransferase from *Euglena gracilis*. *Photosynthetica*. 16: 554–560.
- Hiriart JB, Lehto K, Tyystjarvi E, Junttila T and Aro EM.** (2002) Suppression of a key gene involved in chlorophyll biosynthesis by means of virus-inducing gene silencing. *Plant Mol Biol*. 50: 213-224.
- Hodges DeLong JM, Forney CF and Prange RK.** (1999) Improving the thiobarbituric acid-reactive-substances compounds. *Planta*. 207: 604-611.
- Höfgen R, Axelsen KB, Kannangara CG, Schuttke I, Pohlenz, Willmitzer L, Grimm B and von Wettstein D.** (1994) A visible marker for antisense mRNA expression in plants: Inhibition of chlorophyll biosynthesis with a glutamate 1-semialdehyde aminotransferase antisense gene. *Proc Natl Acad Sci USA* 91: 1726-1730.
- Holtorf H and Apel K.** (1996a) Transcripts of the two NADPH– protochlorophyllide oxidoreductase genes *PorA* and *PorB* are differentially degraded in etiolated barley seedlings. *Plant Mol Biol*. 31: 387–392
- Holtorf H and Apel K.** (1996b) The regulation of NADPH– protochlorophyllide oxidoreductase *a* and *b* in green barley plants kept under a diurnal light dark cycle. *Planta*. 199: 289–295.

- Holtorf H, Reinbothe S, Reinbothe C, Bereza B and Apel K.** (1995) Two routes of chlorophyllide synthesis that are differentially regulated by light in barley (*Hordeum vulgare* L.). *Proc Natl Acad Sci USA*. 92: 3254-3258.
- Hong CY, Hsu YT, Tsai YC, Kao CH.** (2007). Expression of ASCORBATE PEROXIDASE 8 in roots of rice (*Oryza sativa* L.) seedlings in response to NaCl. *J Exp Bot*. 58(12):3273-83.
- Hooper JK, Kahn A, Ash DE, Gough SP and Kannagara CG.** (1988) Biosynthesis of δ -aminolevulinate in greening barley leaves.IX. Structure of the substrate, mode of gabaculine inhibition, and the catalytic mechanism of Glutamate-1-semialdehyde aminotransferase. *Carlsberg Res Com* 53:11-25.
- Horie,T., Yoshida,K., Nakayama,H., Yamada,K., Oiki,S. and Shinmyo,A.** (2001) Two types of HKT transporters with different properties of Na⁺ and K⁺ transport in *Oryza sativa*.*Plant J*.27,129-38.
- Horlow E and Lane D.** (1988) In: Antibodies: A Laboratory Manual (Cold Spring Harbour Laboratory)
- Horsch RB, Rogers SG and Fraley RT.** (1985) Transgenic plants. *Cold Spring Harb Symp Quant Biol*. 50: 433-437.
- Horton P and Hague A** (1988) Studies on the induction of chlorophyll fluorescence in isolated barley protoplasts: IV. Resolution of non-photochemical quenching. *Biochim Biophys Acta* 932: 107-115.
- Horton P, Ruban AV.** (1992). Regulation of photosystem II. *Photosynthesis Research* 34, 375–385.
- Hsiao TC** (1973) Plant responses to water stress. *Annu Rev Plant Physiol* 24: 519-570.
- Hsu WP and Miller GW.** (1970) Coproporphyrinogenase in tobacco (*Nicotiana tabacum* L.). *Biochem J*. 117: 215-220.
- Hu G, Yalpani N, Briggs SP and Johal GS.** (1998) A porphyrin pathway impairment is responsible for the phenotype of a dominant disease lesion mimic mutant of maize. *Plant Cell*. 10: 1095-1105.
- Hu X, Bidney DL, Yalpani N, Duvick JP, Crasta O, Folkerts O and Lu G.** (2003) Overexpression of a gene encoding hydrogen peroxide-generating oxalate oxidase evokes defense responses in sunflower. *Plant Physiol*. 133:170–181

- Hu X, Bidney DL, Yalpani N, Duvick JP, Crasta O, Folkerts O and Lu G. (2003)** Overexpression of a gene encoding hydrogen peroxide-generating oxalate oxidase evokes defense responses in sunflower. *Plant Physiol.* 133: 170-181.
- Huang DD, Wang WY, Gough SP and Kannangara CG. (1984)** Delta-Aminolevulinic acid-synthesizing enzymes need an RNA moiety for activity. *Science.* 225: 1482-1484.
- Huang L and Castelfranco PA. (1989)** Regulation of 5-ALA synthesis in developing chloroplasts. I. Effect of light/dark treatments in vivo and in organello. *Plant Physiol.* 93: 996-1002.
- Huang L and Castelfranco PA. (1990)** Regulation of 5-ALA synthesis in developing chloroplasts. III Evidence for functional heterogeneity of the ALA pool. . *Plant Physiol.* 92: 172-178.
- Huang YS, Li HM. (2009).** Arabidopsis CHL2 can substitute for CHL1. *Plant Physiol.* Apr 10.
- Hukmani P and Tripathy BC. (1992)** Spectrofluorometric estimation of intermediates of chlorophyll biosynthesis: Protoporphyrin IX, Mg- Protoporphyrin, and Protochlorophyllide. *Anal Biochem.* 206: 125-130.
- Hukmani P and Tripathy BC. (1992).** Involvement of Singlet Oxygen in 5-Aminolevulinic Acid-Induced Photodynamic Damage of Cucumber (*Cucumis sativus* L.) Chloroplasts. *Plant Physiol.* 1992 Jan; 98(1):7-11.
- Hukmani P and Tripathy BC. (1994).** Chlorophyll Biosynthetic Reactions during Senescence of Excised Barley (*Hordeum vulgare* L. cv IB 65) Leaves. *Plant Physiol.* Aug;105(4):1295-1300.
- Huq E, Al-Sady B, Hudson M, Kim C, Apel K and Quail PH. (2004)** Phytochrome-interacting factor 1 is a critical bHLH regulator of chlorophyll biosynthesis. *Science.* 305: 1937-41.
- Hurt E and Hauska G (1981)** A cytochrome b_6/f complex of the polypeptides with plastoquinol-plastocyanin oxidoreductase activity from spinach chloroplasts. *Eur J Biochem* 117: 591-599.
- Iglesias DJ, Levy Y, Gomez-Cadenas A, Tadeo FR, Primo-Millo E and Talon M (2004)** Nitrate improves growth in salt-stressed citrus seedlings through effects on photosynthetic activity and chloride accumulation. *Tree Physiol.* 24(9): 1027-34.

- Ikegami A, Yoshimura N, Motohashi K, Takahashi S, Romano PG, Hisabori T, Takamiya K, Masuda T.** (2007). The CHL11 subunit of *Arabidopsis thaliana* magnesium chelatase is a target protein of the chloroplast thioredoxin. *J Biol Chem.* 2007 Jul 6; 282(27): 19282-91.
- Ilag LL, Kumar AM and Soll D.** (1994) Light reduction of chlorophyll biosynthesis at the level of 5-aminolevulinate formation in *Arabidopsis*. *Plant Cell.* 6: 265-275.
- Im C and Beale SI.** (2000) Identification of possible signal transduction components mediating light induction of the Gsa gene for an early chlorophyll biosynthesis step in *Chlamydomonas reinhardtii*. *Planta.* 210: 999-1005.
- Ishikawa A, Okamoto H, Iwasaki Y and Asahi T.** (2001) A deficiency of coproporphyrinogen III oxidase causes lesion formation in *Arabidopsis*. *Plant J.* 27: 89-99.
- Ishitani, M., Liu, J., Halfter, U., Kim, C.-S., Shi, W. and Zhu, J.-K.** (2000) SOS3 function in plant salt tolerance requires N-myristoylation and calcium binding. *Plant Cell* 12,1667-1677.
- Ito H and Tanaka A.** (1996) Determination of the activity of chlorophyll b to chlorophyll a conversion during greening of etiolated cotyledons by using protochlorophyllide b. *Plant Physiol Biochem.* 34: 35-40.
- Ito H, Yokono M, Tanaka R, Tanaka A.** (2008). Identification of a novel vinyl reductase gene essential for the biosynthesis of monovinyl chlorophyll in *Synechocystis* sp. PCC6803. *J Biol Chem.* Apr 4; 283(14):9002-11.
- Iwamoto K, Fukuda H and Sugiyama M.** (2001) Elimination of POR expression correlates with red leaf formation in *Amaranthus tricolor*. *Plant J.* 27: 275–284.
- J.E. Mullet, J.J. Burke, C.J. Arntzen,** (1980) Chlorophyll proteins of Photosystem I, *Plant Physiol.* 65 814–822.
- J.E. Mullet, J.J. Burke, C.J. Arntzen,** (1980) Chlorophyll proteins of Photosystem I, *Plant Physiol.* 65 814–822.
- Jacobs JM and Jacobs NJ.** (1987) Oxidation of protoporphyrinogen to protoporphyrin, a step in chlorophyll and haem biosynthesis. Purification and partial characterization of the enzyme from barley organelles. *Biochem J.* 244: 219-224.

- Jacobs JM and Jacobs NJ.** (1993) Porphyrin accumulation and export by isolated barley (*Hordeum vulgare*) plastids- Effect of diphenyl ether herbicides. *Plant physiol.* 101: 1181-1187.
- Jacobs JM and Jacobs NJ.** (1995) Terminal enzyme of heme biosynthesis in the plant plasma membrane. *Arch Biochem Biophys.* 323: 274-278.
- Jacobs NJ and Jacobs JM.** (1979) Microbial oxidation of protoporphyrinogen: an intermediate in heme and chlorophyll biosynthesis. *Arch Biochem Biophys.* 197: 396-403.
- Jahn D.** (1992) Complex formation between glutamyl-tRNA synthetase and glutamyl-tRNA reductase during the tRNA-dependent synthesis of 5-aminolevulinic acid in *Chlamydomonas reinhardtii*. *FEBS Lett.* 314: 77-80.
- Jain M and Gadre RP.** (2004) Inhibition of 5-amino levulinic acid dehydratase activity by arsenic in excised etiolated maize leaf segments during greening. *J Plant Physiol.* 161: 251-255.
- James RA, Munns R, von Caemmerer S, Trejo C, Miller C, Condon AG.** (2006). Photosynthetic capacity is related to the cellular and subcellular partitioning of Na⁺, K⁺ and Cl⁻ in salt-affected barley and durum wheat. *Plant Cell Environ.* 29:2185-97
- Jang IC, Oh SJ, Seo JS, Choi WB, Song SI, Kim CH, Kim YS, Seo HS, Choi YD, Nahm BH and Kim JK** (2003) Expression of a bifunctional fusion of the *Escherichia coli* genes for trehalose-6-phosphate synthase and trehalose-6-phosphate phosphatase in transgenic rice plants increases trehalose accumulation and abiotic stress tolerance without stunting growth. *Plant Physiol.* 131(2): 516-24.
- Jarvis P and Soll J.** (2001) Toc, Tic, and chloroplast protein import. *Biochim Biophys Acta.* 1541: 64-79.
- Jarvis P, Chen L-J, Li H-M, Peto CA, Fankhauser C and Chory J.** (1998) An *Arabidopsis* mutant defective in the plastid general protein import apparatus. *Science.* 282: 100-103.
- Jarvis P, Soll J.** (2002) Toc, tic, and chloroplast protein import. *Biochim Biophys Acta.* Jun 12; 1590(1-3):177-89.
- Jefferson RA.** (1987) Assaying chimeric genes in plants: the GUS fusion system. *Plant Mol. Biol. Rep.* 5: 387-405.
- Jensen PE, Gibson LCD, Shephard F, Smith V and Hunter CN.** (1999) Introduction of a new branchpoint in tetrapyrrole biosynthesis in *Escherichia coli* by co-expression of genes

encoding the chlorophyll-specific enzymes magnesium chelatase and magnesium protoporphyrin methyltransferase. *FEBS Lett.* 455, 349–354

- Jensen PE, Willows RD, Petersen BL, Vothknecht UC, Stummann BM, Kannangara CG, von Wettstein D and Henningsen KW.** (1996) Structural genes for Mg-chelatase subunits in barley: Xantha-f, -g, and -h. *Mol Gen Genet.* 250: 383-394.
- Jia YX, Sun L, He F, Wan LQ, Yuan QH, Li XL.** (2008). Analysis of effects of salt stress on absorption and accumulation of mineral elements in *Elymus* spp. using atomic absorption spectrophotometer *Guang Pu Xue Yu Guang Pu Fen Xi.* Dec; 28(12):2984-8.
- Jilani A., Kar S., Bose S., and Tripathy B.C.** (1996). Regulation of the carotenoid and chloroplast development by levulinic acid. *Physiol Plant* 96: 139-145.
- Joliot P, Barbier IG and Chabaud R** (1969) Un nouveau module des centres photochimique du systeme II. *Photochem Photobiol* 10: 309-329.
- Jonak C, O'kresz L, Bo'gre L and Hirt H.** (2002) Complexity, cross talk and integration of plant MAP kinase signaling. *Curr. Opin. Plant Biol.* 5: 415–424.
- Jones DT.** (1999) GenTHREADER: an efficient and reliable protein fold recognition method for genomic sequences. *J. Mol. Biol.* 287: 797-815.
- Jones GTG.** (1968) Ferrochelatase of spinach chloroplasts. *Biochem J.* 107: 113-119.
- Jones RM and Jordan PM.** (1993) Purification and properties of the uroporphyrinogen decarboxylase from *Rhodobacter sphaeroides*. *Biochem J.* 293: 703-712.
- Jones RM and Jordan PM.** (1994) Purification and properties of porphobilinogen deaminase from *Arabidopsis thaliana*. *Biochem J.* 299: 895-902.
- Jordan PM and Shemin D.** (1980) Mechanism of action of 5-aminolevulinic acid dehydratase: Stepwise order of addition of the two molecules of 5-aminilevulinic acid in the enzymatic synthesis of porphobilinogen. *J. Chem. Soc. Chem. Comm.* 240-242.
- Joshi PC and Pathak MA.** (1984) The role of active oxygen (1O₂ and O₂) induced by crude coal tar and its ingredients used in spinach thylakoids. *Photochem. Photobiol.* 52: 1003-1009.
- Joshi, M.K. & Mohanty, P.** (1995) Probing photosynthetic performance by chlorophyll a fluorescence: analysis and interpretation of fluorescence parameters. *J. Sci, Ind. Res.* 54, 154-174.

- Jukant AA, Seubert A, Seubert S and Ippen H.** (1989) Studies on uroporphyrinogen decarboxylase from *Rhodobacter sphaeroides*. *Biochem J.* 179: 423-428.
- Jung KH, Hur J, Ryu CH, Choi Y, Chung YY, Miyao A, Hirochika H and An G.** (2003) Characterization of a rice chlorophyll-deficient mutant using the T-DNA gene-trap system. *Plant Cell Physiol.* 44: 463-472.
- Jung S, Lee HJ, Lee Y, Kang K, Kim YS, Grimm B, Back K.** (2008). Toxic tetrapyrrole accumulation in protoporphyrinogen IX oxidase-overexpressing transgenic rice plants. *Plant Mol Biol.* 2008 Jul; 67(5):535-46.
- Jung Y-S, Yu L and Golbeck JH** (1995) Reconstitution of iron-sulfur centre FB results in complete restoration of NADP⁺ photoreduction by heated *Euglena* chloroplasts. *Arch Biochem Biophys* 122: 144-152.
- Kaczor CM, Smith MW, Sangwan I and O'Brian MR.** (1994) Plant delta-aminolevulinic acid dehydratase. Expression in soybean root nodules and evidence for a bacterial lineage of the Alad gene. *Plant Physiol.* 104: 1411-1417.
- Kada S, Koike H, Satoh K, Hase T and Fujita Y.** (2003) Arrest of chlorophyll synthesis and differential decrease of Photosystems I and II in a cyanobacterial mutant lacking light-independent protochlorophyllide reductase. *Plant Mol Biol.* 51: 225-235.
- Kagan RM and Clarke S.** (1994) Widespread occurrence of three sequence motifs in diverse S-adenosylmethionine-dependent methyltransferases suggests a common structure for these enzymes. *Arch Biochem Biophys.* 310: 417-427.
- Kanematsu S, Sakuraba Y, Tanaka A, Tanaka R.** (2008). Characterization of Arabidopsis mutants defective in the regulation of chlorophyllide a oxygenase. *Photochem Photobiol Sci.* 2008 Oct; 7(10):1196-205.
- Kanjo N, Nakahigashi K, Oeda K and Inokuchi H.** (2001) Isolation and characterization of a cDNA from soybean and its homolog from *Escherichia coli*, which both complement the light sensitivity of *Escherichia coli* hemH mutant strain VS101. *Genes Genet Syst.* 76: 327-334.
- Kannagara CG, Gough SP, Bruyant P, Hooper JK, Kahn A and Wettstein DV.** (1988) tRNA^{glu} as a cofactor on δ -aminolevulinic acid biosynthesis: Steps that regulate chlorophyll synthesis. *Trends Biol Sci* 13: 139-143.

- Kannangara CG, Andersen RV, Pontoppidan B, Willows R and von Wettstein D.** (1994) Enzymic and mechanistic studies on the conversion of glutamate to 5- aminolaevulinate. *Ciba Found Symp.* 180: 3-20.
- Kannangara CG, Gough SP, Oliver RP and Rasmussen SK.** (1984) Biosynthesis of 5-ALA in greening barley leaves. VI. Activation of glutamate by ligation to RNA. *Carlsberg Res.Com.* 49: 417-437.
- Kannangara CG, Vothknecht UC, Hansson M and von Wettstein D.** (1997) Magnesium chelatase: association with ribosome and mutant complementation studies identify barley subunit Xantha-G as a functional counterpart of Rhodobacter subunit BchD. *Mol Gen Genet.* 254: 85-92.
- Kant S, Kant P, Raveh E, Barak S** (2006) Evidence that differential gene expression between the halophyte, *Thellungiella halophila*, and *Arabidopsis thaliana* is responsible for higher levels of the compatible osmolyte proline and tight control of Na⁺ uptake in *T. halophila*. *Plant Cell Environ* 29:1220–1234.
- Karnovsky MJ.** (1967) The ultrastructural basis of capillary permeability studied with peroxidase as a tracer. *J Cell Biol.* 35: 213-236.
- Kasinathan V and Wingler A** (2004) Effect of reduced arginine decarboxylase activity on salt tolerance and on polyamine formation during salt stress in *Arabidopsis thaliana*. *Physiol Plant.* 121(1): 101-107.
- Kato,Y., Sakaguchi,M., Mori,Y., Saito,K., Nakamura,T., Bakker.E.P., Sato,Y., Goshima,S. and Uozumi,N.**(2001) Evidence in support of a four transmembrane-pore-transmembrane topology model for the *Arabidopsis thaliana* Na⁺/K⁺ translocating AtHKT1 Protein,a member of the superfamily of K⁺ transporters. *Proc.Natl.Acad.Sci.USA* 98,6488-6493.
- Kawasaki S, Borchert C, Deyholos M, Wang H, Brazille S, Kawai K, Galbraith D and Bohnert H.J.** (2001) Gene expression profiles during the initial phase of salt stress in Rice. *Plant Cell.* 13, 889-905.
- Keller Y, Bouvier F, D'Harlingue A and Camara B.** (1998) Metabolic compartmentation of plastid prenyl lipid biosynthesis. Evidence for the involvement of a multifunctional geranylgeranyl reductase. *Eur J Biochem.* 251: 413-417.

- Kenyon WH and Duke SO.** (1985) Effects of Aciflurofen on endogenous antioxidants and protective enzymes in cucumber (*Cucumis sativus* L.) cotyledon. *Plant physiol.* 79: 862-866.
- Kervinen J, Dunbrack RI Jr, Litwin S, Martins J, Scarrow RC, Volin M, Yeung AT, Yoon E and Jaffe EK.** (2000) Porphobilinogen synthase from pea: Expression from an artificial gene, kinetic characterisation and novel implication for subunit interactions. *Biochemistry.* 39: 9018-9029.
- Kiel JAKW, Tenberg AM and Venema G.** (1992) Nucleotide sequence of *Synechococcus* sp. PCC7942 hemE gene encoding the hamalog of mammalian uroporphyrinogen decarboxylase. *J DNA Seq Mapp.* 2: 415-418.
- Kim C and Apel K.** (2004) Substrate-dependent and organ-specific chloroplast protein import in planta. *Plant Cell.* 16: 88-98.
- Kim C, Ham H and Apel K.** (2005) Multiplicity of different cell- and organ-specific import routes for the NADPH-protochlorophyllide oxidoreductases A and B in plastids of Arabidopsis seedlings. *Plant J.* 42: 329-340.
- Kim SY, Lim JH, Park MR, Kim YJ, Park TI, Seo YW, Choi KG, Yun SJ.** (2005) Enhanced antioxidant enzymes are associated with reduced hydrogen peroxide in barley roots under saline stress. *J Biochem Mol Biol.* 2005 Mar 31; 38(2):218-24.
- Kirsten Haubuhl, Bertil Andersson, and Iwona Adamska** (2001) A chloroplast DegP2 protease performs the primary cleavage of the photodamaged D1 protein in plant photosystem II. *EMBO Journal.* 20, 713-722.
- Kis-Petik K, Böddi B, Kaposi AD and Fidy J.** (1999) Protochlorophyllide forms and energy transfer in dark-grown wheat leaves. Studies by conventional and laser excited fluorescence spectroscopy between 10–100 K. *Photosynth Res.* 60: 87–98.
- Klement H, Helfrich M, Oster U, Schoch S and Rüdiger W.** (1999) Pigment-free NADPH:protochlorophyllide oxidoreductase from *Avena sativa* L. Purification and substrate specificity. *Eur J Biochem.* 265: 862–874.
- Knight H and Knight MR.** (2001) Abiotic stress signalling pathways: specificity and cross-talk. *Trends Plant Sci.* 6: 262–267.
- Knight, H. and Knight, M.R.** (2001) Abiotic stress signalling pathways: specificity and cross-talk. *Trends Plant Sci.* 6, 262–267.

- Koch M, Breithaupt C, Kiefersauer R, Freigang J, Huber R and Messerschmidt A.** (2004) Crystal structure of protoporphyrinogen IX oxidase: a key enzyme in haem and chlorophyll biosynthesis *EMBO J.* 23: 1720-1728.
- Kok B, Forbush B and McGloin M** (1970) Co-operation of charges in photosynthesis evolution 1. A linear four step-mechanism. *Photochem Photobiol* 11: 457-475.
- Kolossov VL and Rebeiz CA.** (2003) Chloroplast biogenesis 88. Protochlorophyllide b occurs in green but not in etiolated plants. *J Biol Chem.* 278: 49675-49678.
- Kolossov VL and Rebeiz CA.** (2001) Chloroplast biogenesis 84: Solubilization and partial purification of membrane-bound [4-vinyl] chlorophyllide a reductase from etiolated barley leaves. *Anal. Biochem.* 295: 214-219.
- Kovach C.W., Kurdziel J.P., Bowman R., Wagner J and Lawrence J.M** (1992) The effects of stress and disturbance on proximate composition, allocation of production, photosynthesis, respiration, and chlorophyll levels in *Hygrophila Polysperma* (ROXB.) Anders. (Acanthaceae) *Environmental and Experimental Botany* 32(4), 479-486.
- Kovtun Y, Chiu W-L, Tena G and Sheen J.** (2000) Functional analysis of oxidative stress-activated mitogen-activated protein kinase cascade in plants. *Proc. Natl. Acad. Sci. USA.* 97: 2940-2945.
- Kruse E, Mock HP and Grimm B.** (1995b) Coproporphyrinogen III oxidase from barle and tobacco-sequence analysis and initial expression studies. *Planta.* 196: 796-803.
- Kruse E, Mock HP and Grimm B.** (1997) Isolation and characterization of tobacco (*Nicotiana tabacum*) cDNA clones encoding prteins involved in magnesium chelation into protoporphyrin IX. *Plant Mol Biol.* 35: 1053-1056.
- Kruse E, Mock HP. and Grimm B.** (1995a) Reduction of coproporphyrinogen oxidase level by antisense RNA synthesis leads to deregulated gene expression of plastid proteins and affects the oxidative defense system. *EMBO J.* 14: 3712-3720.
- Kumar AM and Söll D.** (2000) Antisense HEMA1 RNA expression inhibits heme and chlorophyll biosynthesis in *Arabidopsis*. *Plant Physiol* 122: 49-56.
- Kumar AM, Csankovszki G and Söll D.** (1996) A second and differentially expressed glutamyl-tRNA reductase gene from *Arabidopsis thaliana*. *Plant Mol Biol* 30: 419-426.
- Kunert KJ and Boger P.** (1981) The bleaching effect of diphenyl ether oxyfluorefen. *Weed sci.* 29: 169-172.

- Kunert KJ, Sandmann G and Boger P.** (1987) Mode of action of diphenyl ethers. *Rev. Weed sci.* 3: 35-55.
- Kuroda H, Masuda T, Fusada N, Ohta H and Takamiya K.** (2000) Expression of NADPH– protochlorophyllide oxidoreductase gene in fully green leaves of cucumber. *Plant Cell Physiol.* 41: 226–229.
- Kuroda H, Masuda T, Fusada N, Ohta H and Takamiya K.** (2001) Cytokinin-induced transcriptional activation of NADPH– protochlorophyllide oxidoreductase gene in cucumber. *J Plant Res.* 114: 1–7.
- Kuroda H, Masuda T, Ohta H, Shioi Y and Takamiya K.** (1995) Light-enhanced gene expression of NADPH– protochlorophyllide oxidoreductase in cucumber. *Biochem Biophys Res Commun.* 210: 310–316.
- Kusnetsov V, Herrmann RG, Kulaeva ON and Oelmüller R.** (1998) Cytokinin stimulates and abscisic acid inhibits greening of etiolated *Lupinus luteus* cotyledons by affecting the expression of the light-sensitive protochlorophyllide oxidoreductase. *Mol Gen Genet.* 259: 21–28.
- L’äuchli A.** (1984). Salt exclusion: an adaptation of legumes for crops and pastures under saline conditions. In *Salinity Tolerance in Plants: Strategies for Crop Improvement*, ed. RC Staples, pp. 171–87. New York: Wiley
- Laemmli, U.K.** (1970) Cleavage of structural proteins during the assembly of the head of bacteriophage T4. *Nature* 227: 680-685.
- Lam E and Malkin R** (1982) Ferredoxin-mediated reduction of cytochrome b-563 in a chloroplast b-563/f complex. *FEBS Lett* 141: 98-101.
- Lammeli UK.** (1970) Cleavage of structural proteins during the assembly of the head of bacteriophage T4. *Nature.* 227: 680-685.
- Lapina, L.P and Popov, B.A.** (1970) *Sov. Plant Physiol.* 17, 477-481 [In Russ]
- Larissa Menezes-Benavente, Felipe Karam Teixeira, Claire Lessa Alvim Kamei, Márcia Margis-Pinheiro** (2004) Salt stress induces altered expression of genes encoding antioxidant enzymes in seedlings of a Brazilian *indica* rice (*Oryza sativa* L.). Volume 166, Issue 2, February, Pages 323-331.
- Larkin RM, Alonso JM, Ecker JR and Chory J.** (2003) GUN4, a regulator of chlorophyll synthesis and intracellular signaling. *Science.* 299: 902-906.

- Latimer,P., Bannister,T.T. & Rabinowitch. E.** (1956). Quantum yields of fluorescence of plants pigments. *Science* 124, 585-586.
- Lavergne,J. and Trissel,H.-W.** (1995). Theory of fluorescence induction in photosystem II:derivation of analytical expressions in a model including excitation –radiac-pair equilibrium and restricted energy transfer between photosynthetic units. *Biophys. J.* 68,2474-2492.
- Lebedev N, Karginova O, McIvor W and Timko MP.** (2001) Tyr275 and Lys279 stabilize NADPH within the catalytic site of NADPH:protochlorophyllide oxidoreductase and are involved in the formation of the enzyme photoactive state. *Biochemistry.* 40: 12562–12574.
- Lebedev N, Timko MP (1999)** Protochlorophyllide oxidoreductase B-catalysed protochlorophyllide photoreduction *in vitro*: insight into the mechanism of chlorophyll formation in light-adapted plants. *Proc Nat Acad Sci USA* 96: 9954-9959
- Lebedev N, van Cleve B, Armstrong G and Apel K.** (1995) Chlorophyll synthesis in a deetiolated (*det340*) mutant of *Arabidopsis* without NADPH–protochlorophyllide (PChlide) oxidoreductase (POR) a and photoactive PChlide-F655. *Plant Cell.* 7: 2081–2090.
- Lee HJ, Duke MV and Duke SO.** (1993) Cellular localization of protoporphyrinogen oxidising activities of etiolated barley (*H. vulgare* L.) leaves. Relationship to mechanism of the action of protoporphyrinogen oxidase inhibiting herbicides. *Plant Physiol.* 103: 881-889.
- Lee HJ, Lee SB, hung JS, Han SU, Han O, Guh JO, Jeon JS, An G and Back K.** (2000) Transgenic rice plants expressing a *Bacillus subtilis* protoporphyrinogen oxidase gene are resistant to diphenyl-ether herbicide acifluorfen. *Plant Cell Physiol.* 41: 743-749.
- Lee KP, Kim C, Lee DW and Apel K.** (2003) *TIGRINA d*, required for regulating the biosynthesis of tetrapyrroles in barley, is an ortholog of the *FLU* gene of *Arabidopsis thaliana*. *FEBS Lett.* 553: 119–124
- Lee S, Kim JH, Yoo ES, Lee CH, Hirochika H and An G.** (2005) Differential regulation of chlorophyll a oxygenase genes in rice. *Plant Mol Biol.* 57: 805-818.
- Leon P. Arroyo A. and Mackenzie S.** (1998) Nuclear control of plastid and mitochondrial development in higher plants. *Annu Rev Plant Physiol Plant Mol. Biol.* 49: 453-480.

- Lermintova I, Kruse E, Mock HP and Grimm B.** (1997) Cloning and characterisation of a plastidal and a mitochondrial isoform of tobacco protoporphyrinogen IX oxidase. *Proc Natl Acad Sci USA*. 94: 8895-8900.
- Lermontova I and Grimm B.** (2000) Overexpression of plastidic protoporphyrinogen IX oxidase leads to resistance to the diphenyl-ether herbicide acifluorfen. *Plant Physiol*. 122: 75-84.
- Levicán G, Katz A, de Armas M, Núñez H, Orellana O.** (2007). Regulation of a glutamyl-tRNA synthetase by the heme status. *Proc Natl Acad Sci U S A*. Feb 27; 104(9):3135-40. Epub 2007 Feb 20.
- Levican G, Katz A, Valenzuela P, Soll D and Orellana O.** (2005) A tRNA (Glu) that uncouples protein and tetrapyrrole biosynthesis. *FEBS Lett*. 579: 6383-6387.
- Li J and Timko MP.** (1996) The pc-1 phenotype of *Chlamydomonas reinhardtii* results from a deletion mutation in the nuclear gene for NADPH:protochlorophyllide oxidoreductase. *Plant Mol Biol*. 30: 15-37.
- Li J, Goldschmidt-Clermont M and Timko MP.** (1993) Chloroplast-encoded chlB is required for light-independent protochlorophyllide reductase activity in *Chlamydomonas reinhardtii*. *Plant Cell*. 5: 1817-1829.
- Li J, Spano AJ and Timko MP.** (1991) Isolation and characterisation of nuclear genes encoding the ALA dehydratase of pea (*Pisum sativum* L.). *Plant Physiol*. 96: 125-127.
- Li X-P, Bjořrkman O, Shih C, Grossman AR, Rosenquist M, Jansson S, Niyogi KK.** (2000). A pigment-binding protein essential for regulation of photosynthetic light harvesting. *Nature* 403, 391–395.
- Liedgens W, Grutzmann R and Schneider HAW.** (1980) Highly efficient purification of the labile plant Enzyme 5-aminolevulinate dehydratase (EC 4.2.1.24) by means of monoclonal antibodies. *Z. Naturforsch.* 35c: 958-962.
- Lim SH, Witty M, Wallace-Cook AD, Ilag LI and Smith AG.** (1994) Porphobilinogen deaminase is encoded by a single gene in *Arabidopsis thaliana* and is targeted to the chloroplasts. *Plant Mol Biol*. 26: 863-872.
- Lindstein A, Welch CJ, Schoch S, Ryberg M, Rüdiger W and Sundqvist C.** (1990) Chlorophyll synthetase is latent in well preserved prolamellar bodies of etiolated wheat. *Physiol Plant*. 80: 277-285.

- Lindsten A, Ryberg M, Sundqvist C** (1988) The polypeptide composition of highly purified prolamellar bodies and prothylakoids from wheat (*Triticum aestivum*) as revealed by silver staining. *Physiol Plant* 72: 167-176
- Lister R, Chew O, Rudhe C, Lee MN and Whelan J.** (2001) Arabidopsis thaliana ferrochelatase-I and-II are not imported into Arabidopsis mitochondria. *FEBS Lett.* 506: 291-295.
- Little HN and Jones GTG.** (1976) The subcellular localization and properties of the ferrochelatase of etiolated barley. *Biochem J.* 156: 309-314.
- Liu N, Yang YT, Liu HH, Yang GD, Zhang NH and Zheng CC.** (2004) NTZIP antisense plants show reduced chlorophyll levels. *Plant Physiol Biochem.* 42: 321-327.
- Liu, J., Ishitani, M., Halfter, U., Kim, C.-S. and Zhu, J.-K.** (2000) The *Arabidopsis thaliana* SOS2 gene encodes a protein kinase that is required for salt tolerance. *Proc. Natl. Acad. Sci. USA* 97, 3730-3734.
- Liu, J. and Zhu, J.-K.** (1998) A calcium sensor homolog required for plant salt tolerance. *Science* 280, 1943-1945.
- Lowery, O.H., Rosebrough, N.J., Farr, A.L. and Randall, R.J.** (1951) Protein measurement with the folin phenol reagent. *J. Biol. Chem.* 193: 265-275.
- Lu C and Vonshak A** (2002) Effects of salinity stress on photosystem II function in cyanobacterial *Spirulina platensis* cells. *Physiologia Plantarum.* 114: 405-413.
- Lu C, Qiu N, Wang B and Zhang J.** (2003) Salinity treatment shows no effect on photosystem II photochemistry, but increases the resistance of photosystem II to heat stress in halophyte *Suaeda salsa*. *Journal of Experimental Botany.* 54(383), 851-860.
- Lu C., Qiu N., Lu Q., Wang Q and Kuang T.** (2002) Does salt stress lead to increased susceptibility of photosystem II to photoinhibition and changes in photosynthetic pigment composition in halophyte *Suaeda salsa* grown outdoors *Plant Science* 163, 1063-1068.
- Luer C, Schauer S, Mobius K, Schulze J, Schubert WD, Heinz DW, Jahn D and Moser J.** (2005) Complex formation between glutamyl-tRNA reductase and glutamate-1-semialdehyde 2,1-aminomutase in *Escherichia coli* during the initial reactions of porphyrin biosynthesis. *J Biol Chem.* 280: 18568-18572.
- Luo J and Lim CK.** (1993) Order of urogen III decarboxylation on incubation of PBG and urogen III with erythrocyte UDC. *Biochem J.* 289: 529-532.

- Luo M, Weinstein JD and Walker CJ.** (1999) Magnesium chelatase subunit D from pea: characterization of the cDNA, heterologous expression of an enzymatically active protein and immunoassay of the native protein. *Plant Mol Biol.* 41: 721-731.
- Lv X, Fan J, Ge H, Gao Y, Zhang X, Teng M, Niu L.** (2006). Cloning, expression, purification, crystallization and preliminary X-ray diffraction analysis of the glutamate-1-semialdehyde aminotransferase from *Bacillus subtilis*. *Acta Crystallogr Sect F Struct Biol Cryst Commun.* May 1; 62(Pt 5):483-5.
- Lydon J and Duke SO.** (1988) Porphyrin synthesis is required for photobleaching activity of the p-nitrosubstituted diphenyl ether herbicides. *Pest. Biochem. Physiol.* 31: 74-83.
- M'Rah S, Ouerghi Z, Eymery F, Rey P, Hajji M, Grignon C, Lachaal M** (2007) Efficiency of biochemical protection against toxic effects of accumulated salt differentiates *Thellungiella halophila* from *Arabidopsis thaliana*. *J Plant Physiol* 164:375–384
- Ma H-C, Fung L., Wang S-S., Altman A and Huttermann A.** (1977) Photosynthetic response of *Populus euphratica* to salt stress. *Forest Ecology and Management* 93, 55-61.
- Maathuis FJM, Sanders D** (1996) Mechanisms of potassium absorption by higher plant roots. *Physiol Plant* 96: 158–168.
- Maathuis,F.J.M., Verlin,D., Smith,F.A., Sanders,D., Ferneabndez,J.A. and Walker,N.A.** (1996) The physiological relevance of Na⁺-coupled K⁺-transport. *Plant Physiol.* 112,1609-1616.
- Mach JM, Castillo AR, Hoogstraten R and Greenberg JT.** (2001) The *Arabidopsis*-accelerated cell death gene ACD2 encodes red chlorophyll catabolite reductase and suppresses the spread of disease symptoms. *Proc Natl Acad Sci USA.* 98: 771-776.
- Macpherson AN, Telfer A, Barber J and Truscott TG.** (1993) Direct detection of singlet oxygen from isolated photosystem II reaction centres. *Biochim. Biophys. Acta.* 1143: 301–309.
- Madsen O, Sandal L, Sandal NN and Marcker KA.** (1993) A soybean coproporphyrinogen oxidase gene is highly expressed in root nodules. *Plant Mol Biol.* 23: 35-43.
- Maeda H, Sakuragi Y, Bryant DA, DellaPenna D** (2005) Tocopherols protect *Synechocystis* sp. Strain PCC 6803 from lipid peroxidation. *Plant Physiol* 138:1422–1435.
- Maeshima, M.** (2000) Vacuolar H⁺ -pyrophosphatase. *Biochim.Biophys.Acta* 1465,37-51.

- Maeshima, M.** (2001) Tonoplast transporters: Organization and function. *Annu. Rev. Plant. Physiol. Plant. Mol. Biol.* 52, 469-497.
- Mahajan S and Tuteja N** (2005) Cold, salinity and drought stresses: An overview *Archives of Biochemistry and Biophysics* 444, 139–158.
- Mahalingam R and Fedoroff NV.** (2003) Stress response, cell death and signaling: the many faces of reactive oxygen species. *Physiol. Plant.* 119: 56–68.
- Mannan RM, He W-Z, Metzger S, Whitmarsh J, Malkin B and Pakrasi HB** (1996) Active photosynthesis in cyanobacterial mutants with directed modifications in the ligands for two iron-sulfur clusters in the PsaC protein of photosystem I. *EMBO J* 15: 1826-1833.
- Maplestone RE and Griffiths WT.** (1980) Light modulation of the activity of protochlorophyllide reductase. *Biochem J.* 189: 125-33.
- Mars BL.** (1981) Mobilization of the genes for the photosynthesis from *Rhodospseudomonas capsulatas* by a promiscuous plasmid. *J Bacteriol.* 146: 1003-1012.
- Martin W, Rujan T, Richly E, Hansen A, Cornelsen S, Lins T, Leister D, Stoebe B, Hasegawa M, Penny D.** (2002). Evolutionary analysis of Arabidopsis, cyanobacterial, and chloroplast genomes reveals plastid phylogeny and thousands of cyanobacterial genes in the nucleus. *Proc Natl Acad Sci U S A.* Sep 17; 99(19):12246-51. Epub 2002 Sep 6.
- Martins BM, Grimm B, Mock HP, Huber R and Messerschmidt A.** (2001) Crystal structure and substrate binding modeling of the uroporphyrinogen III decarboxylase from *Nicotiana tabacum*. Implications for catalytic mechanism. *J Biol Chem.* 276: 44108-44116.
- Masojidek J and Hall DO.** (1992). Salinity and drought stress are amplified by high irradiance in sorghum. *Photosynthetica* 27, 159-171.
- Masuda T and Takamiya K.** (2004) Novel Insights into the Enzymology, Regulation and Physiological Functions of Light-dependent Protochlorophyllide Oxidoreductase in Angiosperms. *Photosynth. Res.* 81: 1-29.
- Masuda T, Fusada N, Oosawa N, Takamatsu K, Yamamoto YY, Ohto M, Nakamura K, Goto K, Shibata D, Shirano Y, Hayashi H, Kato T, Tabata S, Shimada H, Ohta H and Takamiya K.** (2003) Functional analysis of isoforms of

NADPH:protochlorophyllide oxidoreductase (POR), PORB and PORC, in *Arabidopsis thaliana*. *Plant Cell Physiol.* 44: 963–974.

Masuda T, Fusada N, Shiraishi T, Kuroda H, Awai K, Shimada H, Ohta H and Takamiya K. (2002) Identification of two differentially regulated isoforms of protochlorophyllide oxidoreductase (POR) from tobacco revealed a wide variety of light and development-dependent regulations of POR gene expression among angiosperms. *Photosynth Res.* 74: 165–172.

Masuda T, Polle JE and Melis A. (2002) Biosynthesis and distribution of chlorophyll among the photosystems during recovery of the green alga *Dunaliella salina* from irradiance stress. *Plant Physiol.* 128: 603-614.

Masuda T, Suzuki T, Shimada H, Ohta H and Takamiya K. (2003) Subcellular localization of two types of ferrochelatase in cucumber. *Planta.* 217: 602-609.

Masuda T, Tanaka A and Melis A. (2003) Chlorophyll antenna size adjustments by irradiance in *Dunaliella salina* involve coordinate regulation of chlorophyll a oxygenase (CAO) and Lhcb gene expression. *Plant Mol Biol.* 51: 757-771.

Matringe M, Camadro JM, Block MA, Joyard J, Scalla R, Labbe P and Douce R. (1992a) Localisation within the chloroplasts of protoporphyrinogen oxidase, the target enzyme for diphenylether like herbicides. *J Biol Chem.* 267: 4646-4651.

Matringe M, Camadro JM, Joyard J and Douce R. (1994) Localization of ferrochelatase activity within mature pea chloroplasts. *J Biol Chem.* 269: 15010-15015.

Matringe M, Camadro JM, Labbe P and Scalla R. (1989) Protoporphyrinogen oxidase as a molecular target for diphenyl ether herbicides. *Biochem J.* 260: 231-235.

Matringe M, Mornet R and Scalla R. (1992b) Characterization of [³H] acifluorfen binding to purified pea etioplasts and evidence that protoporphyrinogen oxidase specifically binds acifluorfen. *Eur J Biochem.* 209: 861-868.

Matsuzaki M, Misumi O, Shin-I T, Maruyama S, Takahara M, Miyagishima SY, Mori T, Nishida K, Yagisawa F, Nishida K, Yoshida Y, Nishimura Y, Nakao S, Kobayashi T, Momoyama Y, Higashiyama T, Minoda A, Sano M, Nomoto H, Oishi K, Hayashi H, Ohta F, Nishizaka S, Haga S, Miura S, Morishita T, Kabeya Y, Terasawa K, Suzuki Y, Ishii Y, Asakawa S, Takano H, Ohta N, Kuroiwa H, Tanaka K, Shimizu N, Sugano S, Sato N, Nozaki H, Ogasawara N, Kohara Y and Kuroiwa T. (2004)

Genome sequence of the ultrasmall unicellular red alga *Cyanidioschyzon merolae* 10D. *Nature*. 428: 653–657.

- Matters GL and Beale SI.** (1994) Structure and light-regulated expression of the *gsa* gene encoding the chlorophyll biosynthetic enzyme glutamate 1-semialdehyde aminotransferase, in *Chlamydomonas reinhardtii*. *Plant Mol Biol* 24: 617-629.
- Matters GL and Beale SI.** (1995b) Structure and expression of the *Chlamydomonas reinhardtii* *alad* gene encoding and chlorophyll biosynthetic enzyme, δ ALA dehydratase(PBG synthetase). *Plant Mol Biol*. 27: 607-617.
- Mauzerall D, Granick S.** (1956) The occurrence and determination of delta-amino-levulinic acid and porphobilinogen in urine. *J Biol Chem*. Mar; 219(1):435-46. Foyer CH, Halliwell B (1976) The presence of glutathione and glutathione reductase in chloroplasts: a proposed role in ascorbic acid metabolism. *Planta* 133:21–25.
- Maxwell DP, Wang Y and McIntosh L.** (1999) The alternative oxidase lowers mitochondrial reactive oxygen production in plant cells. *Proc. Natl. Acad. Sci. USA*. 96: 8271– 8276.
- McCormac AC and Terry MJ.** (2002) Light-signalling pathways leading to the coordinated expression of HEMA1 and Lhcb during chloroplast development in *Arabidopsis thaliana*. *Plant J*. 32: 549-559.
- McCormac AC and Terry MJ.** (2002) Loss of nuclear gene expression during the phytochrome A-mediated far-red block of greening response. *Plant Physiol*. 130: 402–414.
- McCormac AC and Terry MJ.** (2004) The nuclear genes Lhcb and HEMA1 are differentially sensitive to plastid signals and suggest distinct roles for the GUN1 and GUN5 plastid-signalling pathways during de-etiolation. *Plant J*. 40: 672-685.
- McCormac AC, Fischer A, Kumar AM, Soll D and Terry MJ.** (2001) Regulation of HEMA1 expression by phytochrome and a plastid signal during de-etiolation in *Arabidopsis thaliana*. *Plant J*. 25: 549–561.
- McFarlane MJ, Hunter CN and Heyes DJ.** (2005) Kinetic characterisation of the light-driven protochlorophyllide oxidoreductase (POR) from *Thermosynechococcus elongatus*. *Photochem Photobiol Sci*. 4:1055-1059.
- Meinhard M and Grill E.** (2001) Hydrogen peroxide is a regulator of ABI1, a protein phosphatase 2C from *Arabidopsis*. *FEBS Lett*. 508: 443–446.

- Meinhard M, Rodriguez PL and Grill E.** (2002) The sensitivity of ABI2 to hydrogen peroxide links the abscisic acid-response regulator to redox signaling. *Planta*. 214: 775–782.
- Meloni D.A, Oliva M.A., Martinez C.A. and Cambraia J** (2003) Photosynthesis and activity of superoxide dismutase, peroxidase and glutathione reductase in cotton under salt stress. *Environmental and Experimental Botany* 49, 69-76.
- Meskauskiene R and Apel K.** (2002) Interaction of FLU, a negative regulator of tetrapyrrole biosynthesis, with the glutamyl-tRNA reductase requires the tetratricopeptide repeat domain of FLU. *FEBS Lett.* 532: 27–30.
- Meskauskiene R, Nater M, Goslings D, Kessler F, op den Camp R and Apel K.** (2001) FLU: a negative regulator of chlorophyll biosynthesis in *Arabidopsis thaliana*. *Proc Natl Acad Sci U S A.* 98: 12826-12831.
- Mishra SK, Subrahmanyam D and Singhal GS.** (1991) Interaction between salt and light stress on the primary process of photosynthesis. *Journal of Plant Physiology* 138, 92-96.
- Misra, A.N., Sahu, S and Misra, M** (1995) *Acta Physiol Plant.*, 17, 375-380.
- Misra, A.N., Sahu, S.M., Misra, M., Singh P., Meera, I., Das, N., Kar, M. and Sahu, P.** (1997) *Biol. Plant.* 39, 257-262.
- Misra, A.N., Murmu, B., Singh, P and Misra, M** (1996) *Biol. Plant.*, 17. 375-380.
- Mitchel P** (1975) The protein motive Q-cycle: A general formulation. *FEBS Lett* 59: 137-139.
- Mitsuhara, I. et al.** (1999) Animal cell-death suppressors Bcl-xL and Ced-9 inhibit cell death in tobacco plants. *Curr. Biol.* 9, 775–778.
- Mittler R, Vanderauwera S, Gollery M and Breusegem FV.** (2004) Reactive oxygen gene network of plants. *Trends Plant Sci.* 9: 490-498.
- Miyamoto K, Kanaya S, Morikawa K and Inokuchi H.** (1994) Overproduction, purification and characterization of ferrochelatase from *Escherichia coli*. *J Biochem.* 115: 545-551.
- Miyao M & Murata N** (1984b) Role of 33 kDa polypeptide in preserving Mn in the photosynthetic oxygen evolution system and its replacement by chloride ions. *FEBS Lett* 170; 350-354.
- Miyao M and Murata N** (1984a) Calcium ions can be substituted for the 24-kDa polypeptide in photosynthetic oxygen evolution. *FEBS Lett* 168: 118-120.

- Mochizuki N, Brusslan JA, Larkin R, Nagatani A and Chory J.** (2001) *Arabidopsis genomes uncoupled 5 (GUN5)* mutant reveals the involvement of Mg-chelatase H subunit in plastid-to-nucleus signal transduction. *Proc Natl Acad Sci USA*. 98: 2053–2058.
- Mock HP and Grimm B.** (1997) Reduction of uroporphyrinogen decarboxylase by antisense RNA expression affects activities of other enzymes involved in tetrapyrrole biosynthesis and leads to light dependent necrosis. *Plant Physiol*. 113: 1101-1112.
- Mock HP, Heller W, Molina A, Neubohn B, Sandermann H and Grimm B.** (1999) Expression of uroporphyrinogen decarboxylase or coproporphyrinogen oxidase antisense RNA in tobacco induces pathogen defence responses conferring increased resistance to tobacco mosaic virus. *J Biol Chem*. 274: 4231-4238.
- Mock HP, Trainotti L, Kruse E and Grimm B.** (1995) Isolation, sequencing and expression of cDNA sequences encoding uroporphyrinogen decarboxylase from tobacco and barley. *Plant Mol Biol*. 28: 245-256.
- Mohanty S, Grimm B, Tripathy BC.** (2006). Light and dark modulation of chlorophyll biosynthetic genes in response to temperature. *Planta*. Aug; 224(3):692-9.
- Molina A, Volrath S, Guyer D, Maleck K, Ryals J and Ward E.** (1999) Inhibition of protoporphyrinogen oxidase expression in *Arabidopsis* causes a lesion-mimic phenotype that induces systemic acquired resistance. *Plant J*. 17: 667-78.
- Moon H, Lee B, Choi G, Shin D and Prasad T.** (2003) NDP kinase 2 interacts with two oxidative stress-activated MAPKs to regulate cellular redox state and enhances multiple stress tolerance in transgenic plants. *Proc. Natl. Acad. Sci. USA*. 100: 358–363.
- Moon J, Zhu L, Shen H, Huq E.** (2008). PIF1 directly and indirectly regulates chlorophyll biosynthesis to optimize the greening process in *Arabidopsis*. *Proc Natl Acad Sci U S A*. Jul 8; 105(27):9433-8.
- Moradi F, Ismail AM.** (2007) Responses of photosynthesis, chlorophyll fluorescence and ROS-scavenging systems to salt stress during seedling and reproductive stages in rice. : *Ann Bot (Lond)*. 2007 Jun;99(6):1161-73.
- Morales F, Abadia A, Gomez-Aparis J and Abadia J.** (1992) Effects of combined NaCl and CaCl₂ salinity on photosynthetic parameter of barley grown in nutrient solution. *Physiologia Plantarum* 86, 419-426.

- Morant-Manceau A, Pradier E and Tremblin G** (2004) Osmotic adjustment, gas exchanges and chlorophyll fluorescence of a hexaploid triticale and its parental species under salt stress. *J Plant Physiol.* 2004 161(1): 25-33.
- Morsomme.P. and Boutry,M.** (2000) The plant plasma membrane H⁺-ATPase:structure, function and regulation. *Biochim.Biophys.Acta* 1465.1-16.
- Moseley JL, Page MD, Alder NP, Eriksson M and Quinn J.** (2002) Reciprocal expression of two candidate di-iron enzymes affecting photosystem I and lightharvesting complex accumulation. *Plant Cell.* 14: 673–688.
- Moseyko N, Zhu T, Chang HS, Wang X and Feldman LJ.** (2002) Transcription profiling of the early gravitropic response in Arabidopsis using high-density oligonucleotide probe microarrays. *Plant Physiol.* 130: 720–728.
- Mosinger E, Batschauer A, Schafer E and Apel K.** (1985) Phytochrome control of *in vitro* transcription of specific genes in isolated nuclei from barley (*Hordeum vulgare*). *Eur J Biochem.* 147: 137–142.
- Muller P., Li X-P and Niyogi KK** (2001) Non-photochemical quenching. A response to excess light energy. *Plant Physiology.* 125, 1558-1566.
- Muller-Moule P, Havaux M and Niyogi KK.** (2003) Zeaxanthin deficiency enhances the high light sensitivity of an ascorbate-deficient mutant in Arabidopsis. *Plant Physiol.* 133: 748–760.
- Munday, J.C., Jr. and Govindjee** (1969) Light induced changes in the fluorescence yield of chlorophyll a in vivo. III-The dip and the peak in the fluorescent transient of *Chlorella pyrenoidosa*. *Biophys. J.* 9, 1-21.
- Munns R and Termaat A.** (1986) Whole plant response to salinity. *Australian Journal of Plant Physiology* 13, 143-160.
- Munns R and Tester M.** (2008). Mechanism of salinity tolerance. *Annu. Rev. Plant Biol.* 59:651–81
- Munns R.** (1993) Physiological processes limiting plant growth in saline soils:some dogmas and some hypothesis. *Plant Cell Environ.* 16:15-24.
- Munns R.** (2005) Genes and salt tolerance: bringing them together. *New Phytol.* 167:645–63.
- Murashige T and Skoog F.** (1962) A revised medium for rapid growth and bio-assays with tobacco tissue cultures. *Plant Physiol.* 15: 473-497.

- Mysliwa-Kurdziel B, Amirjani MR, Strzalka K and Sundqvist C.** (2003) Fluorescence lifetimes of protochlorophyllide in plants with different proportions of short-wavelength and longwavelength protochlorophyllide spectral forms. *Photochem Photobiol.* 78: 205–212.
- Nagata N, Satoh S, Tanaka R and Tanaka A.** (2004) Domain structures of chlorophyllide a oxygenase of green plants and *Prochlorothrix hollandica* in relation to catalytic functions. *Planta.* 218: 1019-1025.
- Nagata N, Tanaka R, Satoh S and Tanaka A.** (2005) Identification of a Vinyl Reductase Gene for Chlorophyll Synthesis in *Arabidopsis thaliana* and Implications for the Evolution of *Prochlorococcus* Species. *Plant Cell.* 17: 233-240.
- Nagata N, Tanaka R, Tanaka A.** (2007). The major route for chlorophyll synthesis includes [3, 8-divinyl]-chlorophyllide a reduction in *Arabidopsis thaliana*. *Plant Cell Physiol.* Dec; 48(12):1803-8.
- Nahm MY, Kim SW, Yun D, Lee SY, Cho MJ, Bahk JD.** (2003) Molecular and biochemical analyses of OsRab7, a rice Rab7 homolog. *Plant Cell Physiol.* Dec; 44(12):1341-9.
- Nakanishi H, Nozue H, Suzuki K, Kaneko Y, Taguchi G and Hayashida N.** (2005) Characterization of the *Arabidopsis thaliana* Mutant pcb2 which Accumulates Divinyl Chlorophylls. *Plant Cell Physiol.* 46: 467–473.
- Nakano Y, Asada K.** (1981) Hydrogen Peroxide is scavenged by Ascorbate-specific Peroxidase in Spinach Chloroplasts *Plant and Cell Physiology*, 1981, Vol. 22, No. 5 867-880
- Nakayama M, Masuda T, Bando T, Yamagata H, Ohta H and Takamiya K.** (1998) Cloning and expression of the soybean chlH gene encoding a subunit of Mg-Chelatase and localization of the Mg⁺⁺ concentration-dependent chlH protein within the chloroplast. *Plant Cell Physiol.* 39: 275-284.
- Nakayama M, Masuda T, Sato N, Yamagata H, Bowler C, Ohta H, Shioi Y and Takamiya K.** (1995) Cloning, subcellular localization and expression of CHLI, a subunit of Magnesium- chelatase in soybean. *Biochem Biophys Res Com.* 215: 422-428.
- Nanba O and Satoh K** (1987) Isolation of a photosystem II reaction centre consisting of D1 and D2 polypeptides and cytochrome b-559. *Proc Natl Acad Sci, USA* 84: 109-112.
- Nandi DL and Waygood ER.** (1967) Biosynthesis of porphyrins in wheat leaves. II. 5-aminolevulinate hydrolyase. *Canad J Biochem* 45: 327-336.

- Nandi DL.** (1978) Lysine as the substrate binding site of porphobilinogen synthase of *Rhodospirillum rubrum*. *Z Naturforsch.* 33: 799-800.
- Nandihalli UB and Duke SO.** (1994) Chapter 10. Structure-Activity relationships of protoporphyrinogen oxidase inhibiting herbicides. In: *Porphyric pesticides: Chemistry, Toxicology and Pharmaceutical applications* (Eds. S. O. Duke and C. A. Rebeiz). ACS Symposium Series No. 599, pp. 133-146.
- Narita S, Tanaka R, Ito T, Okada K, Taketani S and Inokuchi H.** (1996) Molecular cloning and characterisation of a cDNA that encodes protoporphyrinogen oxidase of *Arabidopsis thaliana*. *Gene.* 182: 169-175.
- Neil R. Baker** (2008) Chlorophyll Fluorescence: A Probe of Photosynthesis In Vivo *Annual Review of Plant Biology* Vol. 59: 89-113.
- Neil R. Baker.** (2008) Chlorophyll fluorescence: a probe of photosynthesis in vivo *Annu. Rev. Plant Biol.* 59:89–113.
- Nelson DE, Shen B. and Bohnert HJ.** (1998) The Regulation of cell-specific inositol metabolism and transport in plant salinity tolerance. *Plant Cell.* 10:753-64
- Netondo GW, Onyango JC, Beck E.** (2004). Sorghum and salinity: II. Gas exchange and chlorophyll fluorescence of sorghum under salt stress. *Crop Science* 44: 806–811.
- Neubauer, C. and Schreiber, U.** (1987). The polyphasic rise of chlorophyll fluorescence upon onset of strong continuous illumination: I-Saturation characteristics and partial control by the photosystem II acceptor side. *Z.Naturforsch.* 42c, 1246-1254.
- Nielsen OF.** (1974) Macromolecular physiology of plastids. XII. *Tigrina* mutants of barley. *Hereditas.* 76: 269–304.
- Nishimura K, Nakayashi T and Inokuchi H.** (1993) Cloning and sequencing of hem E gene encoding uroporphyrinogen decarboxylase (UPD) from *Escherichia coli* K-12. *Gene.* 133: 109-113.
- Niu X, Bressan RA, Haegawa PM, and Pardo JM.** (1995) Ion homeostasis in NaCl stress environments. *Plant Physiol.*109: 735-42.
- Niu X, Bressan RA, Hasegawa PM, Pardo JM** (1995) Ion homeostasis in NaCl stress environments. *Plant Physiol* 109: 735–742.

- Niyogi KK, Grossman AR, Björkman O.** (1998). Arabidopsis mutants define a central role for the xanthophyll cycle in the regulation of photosynthetic energy conversion. *The Plant Cell* 10, 1121–1134.
- Nogaj LA, Srivastava A, van Lis R and Beale SI.** (2005) Cellular levels of glutamyl-tRNA reductase and glutamate-1-semialdehyde aminotransferase do not control chlorophyll synthesis in *Chlamydomonas reinhardtii*. *Plant Physiol.* 139: 389-396.
- Noreen S, Ashraf M, Hussain M, Jamil A.** (2009) Exogenous application of salicylic acid enhances antioxidative capacity in salt stressed sunflower (*Helianthus annuus* L.) plants. *Pak J Bot*; 41(1): 473–9.
- Norris JR, Uphans RA, Crepsi HL and Katz JJ** (1971) Electron spin resonance of chlorophyll and the origin of signal I in photosynthesis. *Proc Natl Acad Sci, USA* 68: 625-628.
- Nuccio, M.L., Rhodes, D., McNeil, S.D. and Hanson, A.D.** (1999) Metabolic engineering of plants for osmotic stress resistance. *Curr. Opin. Plant Biol.* 2, 128-34.
- Nureki O, Vassilyev DG, Katayanagi K, Shimizu T, Sekine S, Kigawa T, Miyazawa T, Yokoyama S and Morikawa K.** (1995) Architectures of class-defining and specific domains of glutamyl-tRNA synthetase. *Science.* 267: 1958-1965.
- Ohad I, Keren N, Zer H, Gong H and Mor TS.** (1994) Light-induced degradation of the photosystem II reaction center D1 protein *in vivo*: an integrative approach. Baker NR, Bowyer JR, eds.. *Photoinhibition of Photosynthesis: From Molecular Mechanisms to the Field*. Oxford: BIOS Sci. Publ. pp. 161–177.
- Oh-hama T, Stolowich NJ and Scott AI.** (1991) Characterization of the process of 5-aminolevulinic acid formation from glutamate via the C5 pathway in *Clostridium thermoaceticum*. *Int J Biochem.* 23: 1417-20.
- Ohtsuka G, Ito H and Tanaka A.** (1997) Conversion of chlorophyll b to chlorophyll a and the assembly of chlorophyll with apoproteins by isolated chloroplasts. *Plant Physiol.* 113: 137-147.
- Oliver RP and Griffiths WT.** (1980) Identification of the polypeptides of NADPH--protochlorophyllide oxidoreductase. *Biochem J.* 191: 277-280.

- Oliver RP and Griffiths WT.** (1981) Covalent labelling of the NADPH: protochlorophyllide oxidoreductase from etioplast membranes with [3H]N-phenylmaleimide. *Biochem J.* 195: 93-101.
- Oliver RP and Griffiths WT.** (1982) Pigment-protein complexes of illuminated etiolated leaves. *Plant Physiol.* 70: 1019-1025.
- O'Neill GP, Peterson DM, Schon A, Chen MW and Soll D.** (1988) Formation of the chlorophyll precursor delta-aminolevulinic acid in cyanobacteria requires aminoacylation of a tRNAGlu species. *J Bacteriol.* 170: 3810-3816.
- Oosawa N, Masuda T, Awai K, Fusada N Shimada H, Ohta H and Takamiya K.** (2000) Identification and light-induced expression of a novel gene of NADPH-potchlorophyllide oxidoreductase isoform in *Arabidopsis thaliana*. *FEBS Lett.* 474: 133-136.
- Op den Camp RGL, Przybyla D, Ochsenein C, Laloi C, Kim C, Danon A, Wagner D, Hidge E, Gobel C, Feussner I, Nater M and Apel K.** (2004) Rapid Induction of Distinct Stress Responses after the Release of Singlet Oxygen in *Arabidopsis*. *Plant Cell.* 15: 2320–2332.
- Orozco-Cardenas, M. and Ryan, C.A.** (1999) Hydrogen peroxide is generated systemically in plant leaves by wounding and systemin via the octadecanoid pathway. *Proc. Natl. Acad. Sci. U. S. A.* 96, 6553–6557.
- Orr GL and Hess FD.** (1981) Characterization of herbicidal injury by acifluorfen-methyl in excised Cucumber (*Cucumis sativus* L.) cotyledons. *Pestic. Biochem. Physiol.* 16: 171-178.
- Osmond CB, Austin MP, Berry JA, Billings WD, Boyer JS, Dacey WJH, Nobel PS, Smith SD, and Winer WE,** (1986) Stress physiology and the distribution of plants. *BioScience* 37, 38-48.
- Oster U, Tanaka R, Tanaka A and Rudiger W.** (2000) Cloning and functional expression of the gene encoding the key enzyme for chlorophyll b biosynthesis (CAO) from *Arabidopsis thaliana*. *Plant J.* 21: 305-310.
- Ouazzani Chahdi AM, Schoefs B, Franck F** (1998) Isolation and characterization of photoactive complexes of NADPH Protochlorophyllide oxidoreductase. *Planta* 206: 673-680.

- Owens TG.** (1994) Excitation energy transfer between chlorophylls and carotenoids. A proposed molecular mechanism for non-photochemical quenching; Baker NR, Bowyer JR, eds.. *Photoinhibition of Photosynthesis: From Molecular Mechanisms to the Field*. Oxford: BIOS Sci. Publ. pp. 95–109.
- P. Haworth, J.L. Watson, C.J. Arntzen,** (1983) The detection, isolation and characterization of light-harvesting complex which is specifically associated with photosystem I, *Biochim. Biophys. Acta* 724, 151–158.
- Papenbrock J, Grafe S, Kruse E, Hanel F and Grimm B.** (1997) Mg-chelatase of tobacco: identification of a Chl D cDNA sequence encoding a third subunit, analysis of the interaction of the three subunits with the yeast two-hybrid system, and reconstitution of the enzyme activity by co-expression of recombinant CHL D, CHL H and CHL I. *Plant J.* 12: 981-990.
- Papenbrock J, Mishra S, Mock HP, Kruse E, Schmidt EK, Petersmann A, Braun HP and Grimm B.** (2001) Impaired expression of the plastidic ferrochelatase by antisense RNA synthesis leads to a necrotic phenotype of transformed tobacco plants. *Plant J.* 28: 41-50.
- Papenbrock J, Mock HP, Kruse E and Grimm B.** (1999) Expression studies on tetrapyrrole biosynthesis: inverse maxima of magnesium chelatase and ferrochelatase activity during cyclic photoperiods. *Planta.* 208: 264-273.
- Papenbrock J, Mock HP, Tanaka R, Kruse E and Grimm B.** (2000b) Role of magnesium chelatase activity in the early steps of the tetrapyrrole biosynthetic pathway. *Plant Physiol.* 122: 1161-1169.
- Papenbrock J, Pfundel E, Mock HP and Grimm B.** (2000a) Decreased and increased expression of the subunit CHL I diminishes Mg chelatase activity and reduced chlorophyll synthesis in transgenic tobacco plants. *Plant J.* 22: 155-164.
- Parham R and Rebeiz CA.** (1995) Chloroplast biogenesis 72: a [4-vinyl] chlorophyllide a reductase assay using divinyl chlorophyllide a as an exogenous substrate. *Anal. Biochem.* 231: 164–169.
- Parida A. K., Das A. B. and Mohanty P.** (2004) Defense potentials to NaCl in a mangrove, *Bruguiera parviflora*: differential changes of isoforms of some antioxidative enzymes. *J. Plant Physiol.* 161, 531–542.

- Pattanayak GK and Tripathy BC.** (2002) Catalytic function of a novel protein protochlorophyllide oxidoreductase C of *Arabidopsis thaliana*. *Biochem. Biophys. Res. Commun.* 291: 921-924.
- Pattanayak GK, Biswal AK, Reddy VS and Tripathy BC.** (2005) Light-dependent regulation of chlorophyll b biosynthesis in chlorophyllide a oxygenase overexpressing tobacco plants. *Biochem Biophys Res Commun.* 326: 466-471.
- Patterson BD, Payne LA, Chen YZ, Graham D.** (1984). An Inhibitor of Catalase Induced by Cold in Chilling-Sensitive Plants. *Plant Physiol.* Dec; 76(4):1014-1018.
- Pei, Z-M. et al.** (2000) Calcium channels activated by hydrogen peroxide mediate abscisic acid signaling in guard cells. *Nature* 406, 731–734.
- Pelchat M, Lacoste L, Yang F and Lapointe J.** (1998) Overproduction of the *Bacillus subtilis* glutamyl-tRNA synthetase in its host and its toxicity to *Escherichia coli*. *Can J Microbiol.* 44: 378-381.
- Pérez-Tornero O, Tallón CI, Porras I, Navarro JM.** (2009) Physiological and growth changes in micropropagated *Citrus macrophylla* explants due to salinity. *J. Plant. Physiol.* Jul.13
- Petersen BL, Jensen PE, Gibson LC, Stummann BM, Hunter CN and Henningsen KW.** (1998) Reconstitution of an active magnesium chelatase enzyme complex from the bchl, -D, and -H gene products of the green sulfur photosynthetic electron transport chain of cucumber bacterium *Chlorobium vibrioforme* expressed in *Escherichia coli*. *J Bacteriol.* 180: 699-704.
- PintaV, Picaud M, Reiss-Husson F and Astier C.** (2002) *Rubrivivax gelatinosus acsF* (previously *orf358*) codes for a conserved, putative binuclear-iron-cluster-containing protein involved in aerobic oxidative cyclization of Mg-protoporphyrin IX monomethylester. *J. Bacteriol.* 184: 746–753.
- Pnueli L, Liang H, Rozenberg M and Mittler R.** (2003) Growth suppression, altered stomatal responses, and augmented induction of heat shock proteins in cytosolic ascorbate peroxidase (Apx1)-deficient *Arabidopsis* plants. *Plant J.* 34:185-201.
- Polking GF, Hannapel DJ and Gladon RJ.** (1995) A cDNA clone for 5-aminolevulinic acid dehydratase from tomato (*Lycopersicon esculentum* Mill.). *Plant Physiol.* 107:1033-1034

- Polle, A.** (2001) Dissecting the superoxide dismutase–ascorbate peroxidase–glutathione pathway in chloroplasts by metabolic modeling computer simulations as a step towards flux analysis. *Plant Physiol.* 126, 445–462.
- Pontoppodian B, and Kannangara CG.** (1994) Purification and partial characterization of barley glutamyl-tRNAglu reuctase, the enzyme that directs glutamate to chlorophyll biosynthesis. *Eur J Biochem* 225: 529-537.
- Porra R.J., Thompson W.A. and Kriendemann P.E.** (1989) Determination of accurate extinction coefficients and simultaneous equations for assaying chlorophylls a and b extracted with four different solvents: verification of the concentration of chlorophyll standards by atomic absorption spectroscopy. *Biochim Biophys Acta* 975: 384-394.
- Porra RJ and Iascelles J.** (1968) Studies on ferrochelatase. *Biochem J.* 108: 343-348.
- Porra RJ, Schäfer W, Katheder I and Scheer H.** (1995) The derivation of the oxygen atoms of the 131-oxo and 3-acetyl groups of bacteriochlorophyll *a* from water in *Rhodobacter sphaeroides* cells adapting from respiratory to photosynthetic conditions: evidence for an anaerobic pathway for the formation of isocyclic ring E. *FEBS Lett.* 371: 21–24.
- Porra RJ, Thompson WA and Kriedemann PE.** (1989) Determination of accurate extinction coefficients and simultaneous equations for assaying chlorophylls a and b extracted with four different solvents: verification of the concentration of chlorophyll standrads by atomic absorption spectroscopy. *Biochim Biophys Acta.* 975: 384-394.
- Porra RJW, Schäfer E, Cmiel IK and Scheer H.** (1993) Derivation of the formyl group oxygen of chlorophyll b from molecular oxygen in greening leaves of a higher plant (*Zea mays*). *FEBS Lett.* 371: 21-24.
- Poulson R and Polglasse WJ.** (1974) Aerobic and anaerobic Coproporphyrinogen oxidase activities in extract from *Saccharomyces cerevisiae*. *J Biol Chem.* 249: 6367-6371.
- Pruzinska A, Tanner G, Anders I, Roca M and Hortensteiner S.** (2003) Chlorophyll breakdown: pheophorbide a oxygenase is a Rieske-type iron-sulfur protein, encoded by the accelerated cell death 1 gene. *Proc Natl Acad Sci USA.* 100:15259-15264.
- Pugh CE, Harwood JL and John RA.** (1992) Mechanism of glutmate semialdehyde aminotransferase. *J Biol chem* 267: 1584-1588.
- Purvis AC.** (1997) Role of the alternative oxidase in limiting superoxide production by plant mitochondria. *Physiol. Plant.* 100: 165–170.

- Qing DJ, Lu HF, Li N, Dong HT, Dong DF, Li YZ.** (2009). Comparative profiles of gene expression in leaves and roots of maize seedlings under conditions of salt stress and the removal of salt stress. *Plant Cell Physiol.* Apr; 50(4):889-903.
- Quintero,F.J., and Blatt,M.R. and Prado,J.M.** (2000) Functional conservation between yeast and plant endosomal Na⁺/H⁺ antiporters. *FEBS Lett.* 471,224-228.
- Rains DW, Epstein E** (1965) Transport of sodium in plant tissue. *Science* 148: 1611.
- Rains,D and Epstein,E.** (1967) Sodium absorption by barley roots.Its mediation by mechanism 2 of alkali cation transport. *Plant Physiol.* 42.319-323.
- Ramel F, Sulmon C, Bogard M, Couée I, Gouesbet G.** (2009) Differential patterns of reactive oxygen species and antioxidative mechanisms during atrazine injury and sucrose-induced tolerance in *Arabidopsis thaliana* plantlets. *BMC Plant Biol.* Mar 13; 9:28.
- Ratajczak,R.** (2000) Structure,function and regulation of the plant vacuolar H⁺ -translocating ATPase. *Biochim,Biophys.Acta* 1465,17-36.
- Ratinaud MH, Thomes JC and Julien R.** (1983) Glutamyl-tRNA synthetases from wheat. Isolation and characterization of three dimeric enzymes. *Eur J Biochem.* 135: 471-477.
- Rebeiz CA, Montazer-Zouhoor A, Mayasich JM, Tripathy BC, Wu SM and Rebeiz CC.** (1988) Photodynamic herbicides. Recent development and molecular basis of selectivity. *CRC Crit. Rev. Plant Sci.* 6: 385-436.
- Rebeiz CA, Montazer-ZouhoorA, Hopen HJ and Wu SM.** (1984) Photodynamic herbicides: 1. Concept and phenomenology. *Enzymol. Microb. Technol.* 6: 390-401.
- Rebeiz CA, Nandihalli UB & Reddy KN.** (1991) In: Topics in Photosynthesis -Volume 10, Herbicides.
- Redondo-Gómez S, Mateos-Naranjo E, Davy AJ, Fernández-Muñoz F, Castellanos EM, Luque T, Figueroa ME.** (2007) Growth and photosynthetic responses to salinity of the salt-marsh shrub *Atriplex portulacoides*. *Ann Bot (Lond).* Sep; 100(3):555-63.
- Reinbothe C, Apel K and Reinbothe S.** (1995a) A light-induced protease from barley plastids degrades NADPH:protochlorophyllide oxidoreductase complexed with chlorophyllide. *Mol Cell Biol.* 15: 6206-6212.
- Reinbothe C, Apel K and Reinbothe S.** (1995d) A light-induced protease from barley plastids degrades NADPH:protochlorophyllide oxidoreductase complexed with chlorophyllide. *Mol Cell Biol.* 15: 6206-6212.

- Reinbothe C, Buhr F, Bartsch S, Desvignes C, Quigley F, Pesey H and Reinbothe S. (2006)** In vitro-mutagenesis of NADPH:protochlorophyllide oxidoreductase B: two distinctive protochlorophyllide binding sites participate in enzyme catalysis and assembly. *Mol Genet Genomics*. Epub ahead of print.
- Reinbothe C, Buhr F, Pollmann S and Reinbothe S. (2003a)** *In vitro* reconstitution of light-harvesting POR–protochlorophyllide complex with protochlorophyllides *a* and *b*. *J Biol Chem*. 278: 807–815.
- Reinbothe C, Lebedev N and Reinbothe S. (1999)** A protochlorophyllide light-harvesting complex involved in de-etiolation of higher plants. *Nature*. 397: 80–84.
- Reinbothe C, Lebedev N, Apel K and Reinbothe S. (1997)** Regulation of chloroplast protein import through a protochlorophyllide-responsive transit peptide. *Proc Natl Acad Sci USA*. 94: 8890-8894.
- Reinbothe C, Lepinat A, Deckers M, Beck E and Reinbothe S. (2003b)** The extra loop distinguishing POR from the structurally related short-chain alcohol dehydrogenases is dispensable for pigment binding but needed for the assembly of light-harvesting POR–protochlorophyllide complex. *J Biol Chem*. 278: 816–822.
- Reinbothe S, Mache R and Reinbothe C. (2000)** A second, substrate-dependent site of protein import into chloroplasts. *Proc Natl Acad Sci USA*. 97: 9795-9800.
- Reinbothe S, Pollmann S and Reinbothe C. (2003c)** *In situ* conversion of protochlorophyllide *b* to protochlorophyllide *a* in barley. Evidence for a novel role of 7-formyl reductase in the prolamellar body of etioplasts. *J Biol Chem*. 278: 800–806.
- Reinbothe S, Pollmann S, Springer A, James RJ, Tichtinsky G and Reinbothe C. (2005)** A role of Toc33 in the protochlorophyllide-dependent plastid import pathway of NADPH:protochlorophyllide oxidoreductase (POR) A. *Plant J*. 42: 1-12.
- Reinbothe S, Quigley F, Gray J, Schemenewitz A and Reinbothe C. (2004)** Identification of plastid envelope proteins required for import of protochlorophyllide oxidoreductase A into the chloroplast of barley. *Proc Natl Acad Sci U S A*. 101: 2197-202.
- Reinbothe S, Quigley F, Springer A, Schemenewitz A and Reinbothe C. (2004)** The outer plastid envelope protein Oep16: role as precursor translocase in import of protochlorophyllide oxidoreductase A. *Proc Natl Acad Sci U S A*. 101: 2203-2208.

- Reinbothe S, Reinbothe C, Holtorf H and Apel K.** (1995a) Two NADPH:Protochlorophyllide Oxidoreductases in Barley: Evidence for the Selective Disappearance of PORA during the Light-Induced Greening of Etiolated Seedlings. *Plant Cell*. 7: 1933-1940.
- Reinbothe S, Reinbothe C, Lebedev N and Apel K** (1996b) PORA and PORB, two light-dependent protochlorophyllide-reducing enzymes of angiosperm chlorophyll biosynthesis. *Plant Cell*. 8: 763–769.
- Reinbothe S, Reinbothe C, Neumann D and Apel K.** (1996c) A plastid enzyme arrested in the step of precursor translocation in vivo. *Proc Natl Acad Sci USA*. 93: 12026-12030.
- Reinbothe S, Reinbothe C, Runge S and Apel K.** (1995b) Enzymatic product formation impairs both the chloroplast receptor-binding function as well as translocation competence of the NADPH: protochlorophyllide oxidoreductase, a nuclear-encoded plastid precursor protein. *J Cell Biol*. 129: 299-308.
- Reinbothe S, Reinbothe C, Runge S and Apel K.** (1995c) Enzymatic product formation impairs both the chloroplast receptor-binding function as well as translocation competence of the NADPH: protochlorophyllide oxidoreductase, a nuclear-encoded plastid precursor protein. *J Cell Biol*. 129: 299-308.
- Reinbothe S, Runge S, Reinbothe C, van Cleve B and Apel K.** (1995b) Substrate-dependent transport of the NADPH:protochlorophyllide oxidoreductase into isolated plastids. *Plant Cell*. 7: 161-172.
- Rentel MC, Lecourieux D, Ouaked F, Usher SL, Petersen L, Okamoto H, Knight H, Peck SC, Grierson CS, Hirt H and Knight MR.** (2004) OX11 kinase is necessary for oxidative burst-mediated signalling in Arabidopsis. *Nature*. 427: 858–861.
- Rhodes D, and Samaras Y.** (1994) Genetic control of osmoregulation in plants .In cellular and molecular physiology of Cell Volume Regulation,ed,K Strange.pp.347-61.Boca Raton:CRCPress.
- Rhodes D.** (1987). Metabolic response to stress. In The biochemistry of plants,ed.DD Davies,pp.202-42. New York:Academic.
- Rhodes,D and Hanson,A.D.** (1993) Quaternary ammonium and tertiary sulfonium compounds in higher plants. *Annu.Rev.Plant Physiol.Plant.Mol.Biol*. 44,357-384.

- Richard M, Tremblay C and Bellemare G.** (1994) Chloroplastic genomes of *Ginkgo biloba* and *Chlamydomonas moewusii* contain a *chlB* gene encoding one subunit of a light-independent protochlorophyllide reductase. *Curr Genet.* 26: 159-165.
- Rieble S and Beale SI.** (1991) Separation and partial characterization of enzymes catalysing delta-aminolevulinic acid formation in *Synechocystis* sp. 6803. *Arch Biochem Biophys* 289: 289-297.
- Rieble S, Ormerd JG and Beale SI.** (1989) transformation of glutamate to delta-aminolevulinic acid by soluble extracts of *Chlorobium vibrioforme*. *J Bacteriol* 171: 3782-3787.
- Rigas S, Debrosses G, Haralampidis K, Vicente-Agullo F, Feldmann KA, Grabov A, Dolan L, Hatzopoulos P** (2001) TRH1 encodes a potassium transporter required for tip growth in *Arabidopsis* root hairs. *Plant Cell* 13: 139–151.
- Rissler HM, Collakova E, DellaPenna D, Whelan J and Pogson BJ.** (2002) Chlorophyll biosynthesis. Expression of a second *chl I* gene of magnesium chelatase in *Arabidopsis* supports only limited chlorophyll synthesis. *Plant Physiol.* 128: 770-779.
- Rizhsky L, Davletova S, Liang H and Mittler R.** (2004) The zinc finger protein *Zat12* is required for cytosolic ascorbate peroxidase 1 expression during oxidative stress in *Arabidopsis*. *J. Biol. Chem.* 279:11736–11743.
- Rizhsky L, Hallak-Herr E, Van Breusegem F, Rachmilevitch S and Barr JE.** (2002) Double antisense plants lacking ascorbate peroxidase and catalase are less sensitive to oxidative stress than single antisense plants lacking ascorbate peroxidase or catalase. *Plant J.* 32: 329–342.
- Rizhsky L, Liang H and Mittler R.** (2003) The water–water cycle is essential for chloroplast protection in the absence of stress. *J. Biol. Chem.* 278: 38921–38925.
- Robinson SP, Downton WJS, and Millhouse J.** (1983) Photosynthesis and ion content of leaves and isolated chloroplasts of salt-stressed spinach. *Plant Physiology* 37, 363-376.
- Robson CA and Vanlerberghe GC.** (2002) Transgenic plant cells lacking mitochondrial alternative oxidase have increased susceptibility to mitochondria-dependent and – independent pathways of programmed cell death. *Plant Physiol.* 129: 1908-1920.
- Rowe JD and Griffiths WT.** (1995) Protochlorophyllide reductase in photosynthetic prokaryotes and its role in chlorophyll synthesis. *Biochem J.* 311: 417-424.

- Roychoudhury A, Basu S, Sarkar SN, Sengupta DN.** (2008). Comparative physiological and molecular responses of a common aromatic indica rice cultivar to high salinity with non-aromatic indica rice cultivars. *Plant Cell Rep.* Aug; 27(8):1395-410.
- Rubio MC, Bustos-Sanmamed P, Clemente MR, Becana M.** (2008). Effects of salt stress on the expression of antioxidant genes and proteins in the model legume *Lotus japonicus*. *New Phytol.* Dec 29.
- Rudiger W, Benz J and Guthoff C.** (1980) Detection and partial characterization of activity of chlorophyll synthetase in etioplast membranes. *Eur J Biochem.* 109: 193-200.
- Runge S, Sperling U, Frick G, Apel K and Armstrong GA.** (1996) Distinct roles for light-dependent NADPH:protochlorophyllide oxidoreductases (POR) A and B during greening in higher plants. *Plant J.* 9: 513–523.
- Runge S, van Cleve B, Lebedev N, Armstrong G and Apel K.** (1995) Isolation and classification of chlorophyll-deficient *xantha* mutants of *Arabidopsis thaliana*. *Planta.* 197: 490–500.
- Ryberg M and Sundqvist C.** (1988) The regular ultrastructure of isolated prolamellar bodies depends on the presence of membrane-bound NADPH–protochlorophyllide oxidoreductase. *Physiol Plant.* 73: 216–226.
- Ryu JY, Suh KH, Chung YH, Park YM, Chow WS, and Park YI** (2003) Cytochrome c oxidase of the cyanobacterium *Synechocystis* sp. PCC 6803 protects photosynthesis from salt stress. *Mol Cells.* 31; 16(1): 74-7.
- Rzeznicka K, Walker CJ, Westergren T, Kannangara CG, von Wettstein D, Merchant S, Gough SP and Hansson M.** (2005) Xantha-I encodes a membrane subunit of the aerobic Mg-protoporphyrin IX monomethyl ester cyclase involved in chlorophyll biosynthesis. *Proc Natl Acad Sci U S A.* 102: 5886-5891.
- S. MANDHANIA, S. MADAN and V. SAWHNEY** (2006) Antioxidant defense mechanism under salt stress in wheat seedlings. *Biologia Plantarum* 50 (2): 227-231.
- Sairam R.K., and Srivastava G.C** (2002) Changes in antioxidant activity in sub-cellular fractions of tolerant and susceptible wheat genotypes in response to long term salt stress. *Plant Science* 162, 897-904.

- Sakuraba Y, Yamasato A, Tanaka R, Tanaka A.** (2007). Functional analysis of N-terminal domains of Arabidopsis chlorophyllide a oxygenase. *Plant Physiol Biochem.* Oct-Nov; 45(10-11):740-9.
- Sambrook J, Fritsch EF and Maniatis T. (1989) Molecular cloning: a laboratory manual.
- Sanders, D** (2000) Plant Biology: The salty tale of *Arabidopsis*. *Curr.Biol.* 10,486-488.
- Sangwan I and O'Brian MR.** (1993) Expression of the soybean (*Glycine max*) glutamate 1-semialdehyde aminotransferase gene in symbiotic root nodules. *Plant Physiol* 102: 829-834.
- Santel HJ and Apel K.** (1981) The protochlorophyllide holochrome of barley (*Hordeum vulgare* L.). The effect of light on the NADPH:protochlorophyllide oxidoreductase. *Eur J Biochem.* 120: 95-103.
- Sasmita Mohanty, Bernhard Grimm and Baishnab C. Tripathy** (2006) Light and dark modulation of chlorophyll biosynthetic genes in response to temperature *Planta* 224: 692–699.
- Satoh K** (1996) Introduction to the photosystem II reaction centre: isolation and biochemical and biophysical characterization. Ort DR, Yocum CF (eds) Oxygenic photosynthesis: The light reactions. Dordrecht, Kluwer.
- Satoh S and Tanaka A.** (2002) Chlorophyll b inhibits the formation of photosystem I trimer in *Synechocystis* sp. PCC6803. *FEBS Lett.* 528: 235-240.
- Satoh S, Ikeuchi M, Mimuro M and Tanaka A.** (2001) Chlorophyll b expressed in Cyanobacteria functions as a light-harvesting antenna in photosystem I through flexibility of the proteins. *J Biol Chem.* 276: 4293-4297.
- Schachtman, D.P.** (2000) Molecular insights into the structure and function of plant K⁺ transport mechanisms. *Biochimica et Biophysica Acta* 1465,127-139.
- Scheumann V, Klement H, Helfrich M, Oster U, Schoch S and Rüdiger W.** (1999) Protochlorophyllide *b* does not occur in barley etioplasts. *FEBS Lett.* 445: 445–448.
- Schmid HC, Rassadina V, Oster U, Schoch S and Rudiger W.** (2002) Pre-loading of chlorophyll synthase with tetraprenyl diphosphate is an obligatory step in chlorophyll biosynthesis. *Biol Chem.* 383: 1769-1778.
- Schneegurt MA and Beale SI.** (1992) Origin of the chlorophyll b formyl oxygen in *Chlorella vulgaris*. *Biochemistry.* 31: 11677-11683.

- Schoch S, Helfrich M, Wiktorsson B, Sundqvist C, Rüdiger W and Ryberg M. (1995)** Photoreduction of zinc protopheophorbide *b* with NADPH-protchlorophyllide oxidoreductase from etiolated wheat (*Triticum aestivum* L.). *Eur J Biochem.* 229: 291–298.
- Schoefs B and Bertrand M. (2000)** The formation of chlorophyll from chlorophyllide in leaves containing proplastids is a four-step process. *FEBS lett.* 486: 243-246.
- Schoefs B and Bertrand M. (2000)** The formation of chlorophyll from chlorophyllide in leaves containing proplastids is a four-step process. *FEBS Lett.* 486: 243-246.
- Schoefs B, Bertrand M and Franck F. (2000a)** Spectroscopic properties of protochlorophyllide analyzed *in situ* in the course of etiolation and in illuminated leaves. *Photochem Photobiol.* 72: 85–93.
- Schoefs B, Bertrand M and Funk C. (2000b)** Photoactive protochlorophyllide regeneration in cotyledons and leaves from higher plants. *Photochem Photobiol.* 72: 660–668.
- Schoefs B, Bertrand M, Franck F (2000a)** Spectroscopic properties of protochlorophyllide aggregational state of protochlorophyllide. *Photosynthetica* 29: 205-218
- Schoefs B, Bertrand M, Franck F (2000b)** Photoactive protochlorophyllide regeneration in
- Schoefs B, Franck F (1993)** Photoreduction of Protochlorophyllide to chlorophyllide in 2-d-old dark-grown bean (*Phaseolus vulgaris* cv. Commodore) leaves. Comparison with 10-d-old dark-grown (etiolated) leaves. *J Expt Bot* 44:1053-1057
- Schoefs B, Franck F (2003)** Protochlorophyllide reduction: mechanism and evolution. *Photochem Photobiol* 78: 543-557
- Schoefs B, Garnir HP, Bertrand M (1994)** Comparison of the photoreduction protochlorophyllide to chlorophyllide in leaves and cotyledons from dark-grown beans as a function of age. *Photosynth Res* 41: 405-417
- Schon A, Gough S and Soll D. (1992)** Chloroplast tRNA(Asp): nucleotide sequence and variation of *in vivo* levels during plastid maturation. *Plant Mol Biol.* 20: 601-607.
- Schon A, Kannangara CG, Gough S and Soll D. (1988)** Protein biosynthesis in organelles requires misaminoacylation of tRNA. *Nature.* 331: 187-190.
- Schreiber, U. and Bilger, W. (1993).** Progress in fluorescence research: majors developments during the past years in retrospect. *Prog.Bot.* 54, 151-173.

- Schubert HL, Raux E, Matthews MA, Phillips JD, Wilson KS, Hill CP, Warren MJ.** (2002) Structural diversity in metal ion chelation and the structure of uroporphyrinogen III synthase. *Biochem Soc Trans.* 30: 595-600.
- Schulz R, Steinmuller K, Klaas M, Forreiter C, Rasmussen S, Hiller C and Apel K.** (1989) Nucleotide sequence of a cDNA coding for the NADPH–protochlorophyllide oxidoreductase (PCR) of barley (*Hordeum vulgare* L.) and its expression in *Escherichia coli*. *Mol Gen Genet.* 217: 355–361.
- Schunmann PH and Ougham HJ.** (1996) Identification of three cDNA clones expressed in the leaf extension zone and with altered patterns of expression in the slender mutant of barley: a tonoplast intrinsic protein, a putative structural protein and protochlorophyllide oxidoreductase. *Plant Mol Biol.* 31: 529–537.
- Seehra JS, Jordan PM and Akhtar M.** (1983) Anaerobic and aerobic coproporphyrinogen III oxidase of *Rhodospseudomonas sphaeroides*. *Biochem J.* 209: 709-718.
- Sekine S, Nureki O, Dubois DY, Bernier S, Chenevert R, Lapointe J, Vassylyev DG and Yokoyama S.** (2003) ATP binding by glutamyl-tRNA synthetase is switched to the productive mode by tRNA binding. *EMBO J.* 22: 676-688.
- Sekmen AH, Türkan I, Takio S.** (2007) Differential responses of antioxidative enzymes and lipid peroxidation to salt stress in salt-tolerant *Plantago maritima* and salt-sensitive *Plantago media*. *Physiologia Plantarum* 131: 399–411.
- Sengupta Sand Majumder AL.** (2009) Insight into the salt tolerance factors of a wild halophytic rice, *Porteresia coarctata*: a physiological and proteomic approach. *Planta* 229:911–929
- Sergi Munné-Bosch · Elmar W. Weiler · Leonor Alegre · Maren Müller · Petra Düchting · Jon Falk** (2007) α -Tocopherol may influence cellular signaling by modulating jasmonic acid levels in plants. *Planta* 225:681–6911.
- Seyedi M, Selstam E, Timko MP and Sundqvist C.** (2001a) The cytokinin 2-isopentenyladenine causes partial reversion to skotomorphogenesis and induces formation of prolamellar bodies and protochlorophyllide₆₅₇ in the *lip1* mutant of pea. *Physiol Plant.* 112: 261–272.
- Seyedi M, Timko MP and Sundqvist C.** (2001b) The distribution of protochlorophyllide and chlorophyll within seedlings of the *lip1* mutant of pea. *Plant Cell Physiol.* 42: 931–941.

- Shafi M, Bakht J, Hassan MJ, Raziuddin M, Zhang G.** (2009) Effect of cadmium and salinity stresses on growth and antioxidant enzyme activities of wheat (*Triticum aestivum* L.). *Bull Environ Contam Toxicol.* Jun;82(6):772-6.
- Sharma,P.K. and Hall, D.O.** (1992) *J. Plant Physiol.* 140, 661-666.
- Shashidhara LS and Smith AG.** (1991) Expression and subcellular location of the tetrapyrrole synthesis enzyme porphobilinogen deaminase in light-grown *Euglena gracilis* and three nonchlorophyllous cell lines. *Proc Natl Acad Sci USA.* 88: 63-67.
- Shemin D.** (1976) 5-Aminolevulinic acid dehydratase: Structure, function and mechanism. *Philos Trans R Soc London.* 273: 109-115.
- Sheng L, Zheng X, Tong H, Liu S, Du J, Liu Q** (2004) Purification and characterization of cytosolic isoenzyme III of Cu–Zn superoxide dismutase from tobacco leaves. *Plant Sci* 167:1235-1241
- Shepherd M and Hunter CN.** (2004) Transient kinetics of the reaction catalysed by magnesium protoporphyrin IX methyltransferase. *Biochem J.* 382: 1009-1013.
- Shepherd M, McLean S and Hunter CN.** (2005) Kinetic basis for linking the first two enzymes of chlorophyll biosynthesis. *FEBS J.* 272: 4532-4539.
- Shepherd M, Reid JD and Hunter CN.** (2003) Purification and kinetic characterization of the magnesium protoporphyrin IX methyltransferase from *Synechocystis* PCC6803. *Biochem. J.* 371, 351–360
- Shetty AS and Miller GW.** (1969) Purification and general properties of δ -aminolevulinic acid dehydratase from *Nicotiana tabacum* L. *Biochem J.* 114: 331-337.
- Shi H, Lee BH, Wu SJ, Zhu JK** (2003) Overexpression of a plasma membrane Na⁺/H⁺ antiporter gene improves salt tolerance in *Arabidopsis thaliana*. *Nat Biotechnol.* 21(1): 81-5. Epub 2002 Dec 09
- Shi,H., Ishitani,M., Kim,C. and Zhu, J.-K.** (2000) The *Arabidopsis thaliana* salt tolerance gene SOS1 encodes a putative Na⁺/H⁺ antiporter. *Proc.Natl.Acad.Sci.USA* 97,6896-6901.
- Shibata H and Ochiai H.** (1977) Purification and properties of δ -aminolevulinic acid dehydratase from radish cotyledons. *Plant Cell Physiol.* 18: 420-429.
- Shibata K.** (1957) Spectroscopic studies on chlorophyll formation in intact leaves. *J. biochem.* 44: 147-

- Shinozaki K, Yamaguchi-Shinozaki K** (2000) Molecular responses to dehydration and low temperature: differences and cross-talk between two stress signaling pathways. *Curr Opin Plant Biol* 3:217–223
- Shpilyov AV, Zinchenko VV, Shestakov SV, Grimm B and Lokstein H.** (2005) Inactivation of the geranylgeranyl reductase (ChlP) gene in the cyanobacterium *Synechocystis* sp. PCC 6803. *Biochim Biophys Acta*. 1706: 195-203.
- Shuvalov VA, Nuijs AM, Van Gorkom HJ, SmithHWJ and Duysens LNM** (1986) Picoseconds absorbance changes upon selective excitation of the primary electron donor P-700 in photosystem I. *Biochim Biophys Acta* 850: 319-323.
- Siatecka M, Rozek M, Ignacak M and Barciszewski J.** (1995) Cloning and sequencing of the first plant GlnRS and GluRS genes. *Nucleic Acids Symp Ser*. 33: 160-162.
- Sickler CM, Edwards GE, Kuirats O, Gao Z, Loescher W. 2007. Response of mannitol producing *Arabidopsis thaliana* to abiotic stress. *Funct. Plant Biol*. 34:382–91
- Singh DP, and Kshatriya K** (2002) NaCl-induced oxidative damage in the cyanobacterium *Anabaena doliolum*. *Curr Microbiol*. 44(6): 411-7.
- Singh DP, Cornah JE, Hadingham S and Smith AG.** (2002) Expression analysis of the two ferrochelatase genes in *Arabidopsis* in different tissues and under stress conditions reveals their different roles in haem biosynthesis. *Plant Mol Biol*. 50: 773-788.
- Smith AG and Francis JE.** (1981) Investigations of rat liver uroporphyrinogen decarboxylase. comparisons of porphyrinogens I and III as substrate nad inhibition by porphyrins. *Biochem J*. 195: 241-250.
- Smith AG and Griffiths WT.** (1993) Enzymes of chlorophyll and heme biosynthesis. In: Dey PM, Harborne JB (eds) *Methods in plant biochemistry*. Vol 9. Academic press. London. Pp 299-343.
- Smith AG, Santana MA, Wallace-Cook AD, Roper JM and Labbe-Bois R.** (1994) Isolation of a cDNA encoding chloroplast ferrochelatase from *Arabidopsis thaliana* by functional complementation of a yeast mutant. *J Biol Chem*. 269: 13405-13413.
- Smith AG.** (1988) Subcellular localization of two porphyrin-synthesis enzymes in *Pisum sativum* (pea) and *Arum* (cuckoo-pint) species. *Biochem J*. 249: 423-428.
- Smith CA, Suzuki JY and Bauer CE.** (1996) Cloning and characterization of the chlorophyll biosynthesis gene chlM from *Synechocystis* PCC 6803 by complementation of a

- bacteriochlorophyll biosynthesis mutant of *Rhodobacter capsulatus*. *Plant Mol Biol.* 30: 1307-1314.
- Smith MA and Grimm B.** (1992) Gabaculine resistance of *Synechococcus* glutamate 1-semialdehyde aminotransferase. *Biochemistry.* 31: 4122-4127.
- Soldatova O, Apchelimov A, Radukina N, Ezhova T, Shestakov S, Ziemann V, Hedtke B and Grimm B.** (2005) An Arabidopsis mutant that is resistant to the protoporphyrinogen oxidase inhibitor acifluorfen shows regulatory changes in tetrapyrrole biosynthesis *Mol Genet Genomics* 273: 311-318.
- Soll J, Schultz G, Rüdiger W and Benz J.** (1983) Hydrogenation of geranylgeraniol. Two pathways exist in spinach chloroplasts. *Plant Physiol.* 71: 849-854.
- Solymosi K, Böddi B** (2006) Optical properties of bud scales and protochlorophyll(ide)
- Solymosi K, Bóka K, Böddi B** (2006) Transient etiolation: protochlorophyll(ide) and chlorophyll forms in differentiating plastids of closed and breaking leaf buds of horse chestnut (*Aesculus hippocastanum*). *Tree physiol* 26: 1087-1096
- Sood S, Gupta V, Tripathy BC.** (2005). Photoregulation of the greening process of wheat seedlings grown in red light. *Plant Mol Biol.* Sep;59(2):269-87.
- Southern EM.** (1975) Detection of specific sequences among DNA fragments separated by gel electrophoresis. *J. Mol. Biol.* 98: 503-517.
- Spano AJ and Timko MP.** (1991) Isolation, characterization and partial amino acid sequence of a chloroplast-localized porphobilinogen deaminase from pea (*Pisum sativum* L.). *Biochim Biophys Acta.* 1076: 29-36.
- Spano AJ, He Z, Michel H, Hunt DF and Timko MP.** (1992) Molecular cloning, nuclear gene structure, and developmental expression of NADPH:protochlorophyllide oxidoreductase in pea (*Pisum sativum* L.). *Plant Mol Biol.* 18: 967-972.
- Spencer P and Jordan PM.** (1994) 5-Aminolevulinic acid dehydratase: Characterization of the α and β metal-binding sites of the *Escherichia coli* Enzyme . In the biosynthesis of tetrapyrrole pigments. Ciba Foundation Symposium 180, D.J. Chadwick and K.Ackrill, eds (Chichester, England: John Wiley and Sons). pp.50-64.
- Spencer P and Jordan PM.** (1995) Characterization of the two 5-aminolevulinic acid binding sites of 5-aminolevulinic acid dehydratase from *Escheichia coli*. *Biochem J.* 305: 151-158.

- Sperling U, Franck F, Cleve BV, Frick G, Apel K and Armstrong GA.** (1998) Etioplast differentiation in *Arabidopsis*: Both PORA and PORB restore the prolamellar body and photoactive protochlorophyllide-F655 to the cop1 photomorphogenic mutant. *Plant Cell*. 10: 283-296.
- Sperling U, van Cleve B, Frick G, Apel K and Armstrong GA.** (1997) Overexpression of light-dependent PORA or PORB in plants depleted of endogenous POR by far-red light enhances seedling survival in white light and protects against photooxidative damage. *Plant J*. 12: 649-658.
- Spikes DK and Bommer JC.** (1991) Chlorophyll and related pigments as photosensitizers in biology and medicine. In: Chlorophylls (Ed.Scheer, H), p.1181-1204, CRC Press, Boca Raton.
- Stange-Thomann N, Thomann HU, Lloyd AJ, Lyman H and Soll D.** (1994) A point mutation in *Euglena gracilis* chloroplast tRNA (Glu) uncouples protein and chlorophyll biosynthesis. *Proc Natl Acad Sci USA*. 91: 7947-7951.
- Stephenson PG, Terry MJ.** (2008). Light signalling pathways regulating the Mg-chelatase branchpoint of chlorophyll synthesis during de-etiolation in *Arabidopsis thaliana*. *Photochem Photobiol Sci*. Oct; 7(10):1243-52.
- Stepien P, Johnson GN.** (2009) Contrasting responses of photosynthesis to salt stress in the glycophyte *Arabidopsis* and the halophyte *Thellungiella*: role of the plastid terminal oxidase as an alternative electron sink. *Plant Physiol*. Feb; 149(2):1154-65.
- Stepien P, Johnson GN.** (2009) Contrasting responses of photosynthesis to salt stress in the glycophyte *Arabidopsis* and the halophyte *Thellungiella*: role of the plastid terminal oxidase as an alternative electron sink. *Plant Physiol*. 2009 Feb;149(2):1154-65
- Stirbet A, Govindjee, Strasser B.J. and Strasser R.J.** (1998). Chlorophyll a fluorescence induction in higher plants: modeling and numerical simulation. *J.Theor. Biol.*193, 131-151.
- Stobart AK and Ameen-Bukhari I.** (1984) Regulation of delta-aminolaevulinic acid synthesis and protochlorophyllide regeneration in the leaves of dark-grown barley (*Hordeum vulgare*) seedlings. *Biochem J*. 222: 419-426.
- Strand A, Asami T, Alonso J, Ecker JR and Chory J.** (2003) Chloroplast to nucleus communication triggered by accumulation of Mg-protoporphyrinIX. *Nature*. 421: 79-83.

- Strasser,R.J. and Govindjee** (1991). The F0 and O-J-I-P fluorescence rise in higher plants and algae. In: Regulation of Chloroplast Biogenesis (Argyroudi-Akoyunoglou,J.H.,ed.),pp. 20-32.The Netherlands: Kluwer Academic publishers.
- Strasser,R.J. and Govindjee** (1992). On the O-J-I-P fluorescent transient in leaves and D1 mutants of *Chlamydomonas reinhardtii*. In: *Research in photosynthesis*, Vol.2 (Murata, N., ed), pp. 20-32. The Netherland: Kluwer Academic Publisher.
- Strasser,R.J., Eggenberg,P. and Govindjee** (1992). An equilibrium model for electron transfer in photosystem II acceptor complex: an application to *Chlamydomonas reinhardtii* cells of D1 mutants and those treated with formate. *Archs.Sci.Geneve.* 45,207-224.
- Su Q, Frick G, Armstrong G and Apel K.** (2001) POR C of *Arabidopsis thaliana*: a third light- and NADPH-dependent protochlorophyllide oxidoreductase that is differentially regulated by light. *Plant Mol. Biol.* 47: 805-813.
- Sudhir PR, Pogoryelov D, Kovacs L, Garab G, Murthy SD.** (2005) The effects of salt stress on photosynthetic electron transport and thylakoid membrane proteins in the cyanobacterium *Spirulina platensis*. *J Biochem Mol Biol.* Jul 31; 38(4):481-5.
- Susek J and Chory J.** (1992) A tale of two genomes: role of a chloroplast signal in coordinating nuclear and plastid genome expression. *Aust J Plant Physiol.* 19: 387–399.
- Susek RE, Ausubel FM and Chory J.** (1993) Signal transduction mutants of *arabidopsis* uncoupled nuclear *cab* and *rbcS* gene expression from chloroplast development. *Cell.* 74: 787–799.
- Suzuki JY and Bauer CE.** (1992) Light-independent chlorophyll biosynthesis: involvement of the chloroplast gene chlL (*frxC*). *Plant Cell.* 4: 929-940.
- Suzuki JY and Bauer CE.** (1995b) Altered monovinyl and divinyl protochlorophyllide pools in *bchJ* mutants of *Rhodobacter capsulatus*. Possible monovinyl substrate discrimination of light-independent protochlorophyllide reductase. *J Biol Chem.* 270: 3732-3740.
- Suzuki JY and Bauer CL.** (1995) Altered monovinyl and divinyl protochlorophyllide pools in *bchJ* mutants of *Rhodobacter capsulatus*. *J. Biol. Chem.* 270: 3732–3740.
- Suzuki T, Masuda T, Inokuchi H, Shimada H, Ohta H and Takamiya K.** (2000) Overexpression, Enzymatic properties and tissue localisation of a ferrenchelatase of cucumber. *Plant Cell Physiol.* 41: 192-199.

- Sweetlove LJ, Heazlewood JL, Herald V, Holtzapffel R, Day DA, Leaver CJ and Millar AH.** (2002) The impact of oxidative stress on Arabidopsis mitochondria. *Plant J.* 2002 32: 891-904.
- Sytina OA, Heyes DJ, Hunter CN, Alexandre MT, van Stokkum IH, van Grondelle R, Groot ML.** (2008). Conformational changes in an ultrafast light-driven enzyme determine catalytic activity. *Nature.* Dec 18; 456(7224):1001-4.
- T.Y. Kuang, J.H. Argyroudi-Akoyunoglou, H.Y. Nakatani, J. Watson, C.J. Arntzen,** (1984) The origin of the long-wavelength fluorescence emission band (77 degrees K) from photosystem I. *Arch. Biochem. Biophys.* 235 618–627.
- TaiZ, L. and Zeiger, E.** (1998) *Plant Physiology.* Sunderland, Massachusetts: Sinauer Associates, Inc.
- Takemura T., Hanagata N., Sugihara K., Baba S., Karube I. and Dubinsky Z.** (2000) Physiological and biochemical responses to salt stress in the mangrove, *Bruguiera gymnorhiza.* *Aquat. Bot.* 68, 15–28.
- Takio S, Nakao N, Suzuki T, Tanaka K, Yamamoto I and Satoh T.** (1998) Light-dependent expression of protochlorophyllide oxidoreductase gene in the liverwort, *Marchantia paleacea* var. *diptera.* *Plant Cell Physiol.* 39: 665-669.
- Tan FC, Cheng Q, Saha K, Heinemann IU, Jahn M, Jahn D, Smith AG.** (2008). Identification and characterization of the Arabidopsis gene encoding the tetrapyrrole biosynthesis enzyme uroporphyrinogen III synthase. *Biochem J.* Mar 1; 410(2):291-9.
- Tanaka A, Ito H, Tanaka R, Tanaka NK, Yoshida K and Okada K.** (1998) Chlorophyll a oxygenase (CAO) is involved in chlorophyll b formation from chlorophyll a. *Proc Natl Acad Sci U S A.* 95: 12719-12723.
- Tanaka R and Tanaka A.** (2005) Effects of Chlorophyllide a Oxygenase overexpression on Light acclimation in Arabidopsis thaliana. *Photosynth Res.* 85: 327-340.
- Tanaka R, Koshino Y, Sawa S, Ishiguro S, Okada K and Tanaka A.** (2001) Overexpression of chlorophyllide a oxygenase (CAO) enlarges the antenna size of photosystem II in Arabidopsis thaliana. *Plant J.* 26: 365-373.
- Tanaka R, Oster U, Kruse E, Rudiger W and Grimm B.** (1999) Reduced activity of geranylgeranyl reductase leads to loss of chlorophyll and tocopherol and to partially

- geranylgeranylated chlorophyll in transgenic tobacco plants expressing antisense RNA for geranylgeranyl reductase. *Plant Physiol.* 120: 695-704.
- Tanaka R, Yoshida K, Nakayashiki T, Masuda T, Tsuji H, Inokuchi H and Tanaka A.** (1996) Differential expression of two hemA mRNAs encoding glutamyl-tRNA reductase proteins in greening cucumber seedlings. *Plant Physiol* 110: 1223-1230.
- Tchuinmogue SJ, Bruyant P and Balange AP.** (1992) Immunological characterization of two 5-aminolevulinic acid dehydratase in radish leaves. *Plant Physiol Biochem.* 30: 255-261.
- Teakle GR and Griffiths WT.** (1993) Cloning, characterization and import studies on protochlorophyllide reductase from wheat (*Triticum aestivum*). *Biochem J.* 296: 225-230.
- Tester M, Davenport R** (2003) Na⁺ tolerance and Na⁺ transport in higher plants. *Ann Bot (Lond)* 91: 503–527
- Tewari AK and Tripathy BC.** (1998) Temperature-stress-induced impairment of chlorophyll biosynthetic reactions in cucumber and wheat. *Plant Physiol.* 117: 851-858.
- Tezara W, Martinez D, Rengifo E and Herrera A.** (2003) Photosynthetic response of the tropical spiny shrub *Lycium nodosum* (Solanaceae) to drought, soil salinity and saline spray. *Annals of Botany* 92, 1-9.
- Thomashow, M.F.** (1999). Plant cold acclimation: Freezing tolerance genes and regulatory mechanisms. *Annu. Rev. Plant Physiol. Plant Mol. Biol.* 50, 571–599.
- Thomashow, M.F.** (1999). Plant cold acclimation: Freezing tolerance genes and regulatory mechanisms. *Annu. Rev. Plant Physiol. Plant Mol. Biol.* 50, 571-599.
- Thordal-Cristensen H, Zhang Z, wei Y and Collinge DB.** (1997) Subcellular localization of H₂O₂ in plants. H₂O₂ accumulation in papillae and hypersensitive response during the barley-powdery mildew interaction. *Plant J.* 11: 1187-1194.
- Thurnaeur MC and Gast P** (1985) Q-band (35 Ghz) EPR results on the nature of A1 and electron spin polarization in photosystem I particles. *Photochem Photobiophys* 9: 29-38.
- Tiwari AK and Tripathy BC.** (1998). Temperature-Stress-Induced Impairment of Chlorophyll Biosynthetic Reactions in Cucumber and Wheat. *Plant Physiol.* 117: 851-858.
- Tomitani A, Okada K, Miyashita H, Matthijs HC, Ohno T and Tanaka A.** (1999) Chlorophyll b and phycobilins in the common ancestor of cyanobacteria and chloroplasts. *Nature.* 400: 159-62.

- Tottey S, Block MA, Allen M, Westergren T, Albrieux C, Scheller HV, Merchant S and Jensen PE.** (2003) Arabidopsis CHL27, located in both envelope and thylakoid membranes, is required for the synthesis of protochlorophyllide. *Proc Natl Acad Sci USA*. 100: 16119-16124.
- Towbin H, Staehelin T and Gordon J.** (1979) Electrophoretic transfer of proteins from polyacrylamide gels to nitrocellulose sheets: Procedure and some applications. *Proc. Natl. Acad. Sci. USA*. 76: 4350-4354.
- Townley HE, Sessions RB, Clarke AR, Dafforn TR and Griffiths WT** (2001) Protochlorophyllide oxidoreductase: a homology model examined by site-directed mutagenesis. *Proteins*. 44: 329–335.
- Traber, M. G. and Sies, H.** (1996) Vitamin E in humans: demand and delivery. *Annu. Rev. Nutr.* 16, 321–347.
- Trebst A** (1986) The topology of the plastoquinone and herbicide binding peptides of photosystem II in the thylakoid membrane. *Z Naturforsch* 41c: 240-245.
- Tripathy BC and Chakraborty N.** (1991) 5-aminolevulinic acid induced photodynamic damage of the photosynthetic electron transport chain of cucumber (*Cucumis sativus* L.) cotyledons. *Plant Physiol*. 96: 761-767.
- Tripathy BC and Mohanty P.** (1980) Zinc-inhibited electron transport of photosynthesis in isolated barley chloroplasts. *Plant Physiol*. 66: 1174-1178.
- Tripathy BC and Rebeiz CA.** (1985) Chloroplast biogenesis: quantitative determination of monovinyl and divinyl Mg-protoporphyrins and protochlorophyll(ides) by spectrofluorometry. *Anal Biochem*. 149:43-61.
- Tripathy BC and Rebeiz CA.** (1986) Chloroplast biogenesis. Demonstration of the monovinyl and divinyl monocarboxylic routes of chlorophyll biosynthesis in higher plants. *J Biol Chem*. 261: 13556-13564.
- Tripathy BC and Rebeiz CA.** (1988) Chloroplast biogenesis 60: Conversion of divinyl protochlorophyllide to monovinyl protochlorophyllide in green (ing) barley, a dark monovinyl/light divinyl plant species. *Plant Physiol*. 87: 89–94.
- Tripathy BC, Bhatia B, Mohanty P** (1981) Inactivation of chloroplast photosynthetic electron transport activity by Ni²⁺. *Biochim Biophys Acta* 638: 217-224

- Tripathy BC, Bhatia B, Mohanty P** (1983) Cobalt ions inhibit electrons transport activity of photosystem II without affecting photosystem I. *Biochim Biophys Acta* 722: 88-93.
- Tripathy BC, Chakraborty N.** (1991) 5-Aminolevulinic Acid Induced Photodynamic Damage of the Photosynthetic Electron Transport Chain of Cucumber (*Cucumis sativus* L.) Cotyledons. *Plant Physiol.* Jul; 96(3):761-767.
- Tripathy BC, Mohapatra A, Gupta I.** (2007). Impairment of the photosynthetic apparatus by oxidative stress induced by photosensitization reaction of protoporphyrin IX. *Biochim Biophys Acta.* Jun;1767(6):860-8. Epub 2007 Mar 19.
- Tsai S, Bishop DF and Desnick RJ.** (1987) Purification and properties of uroporphyrinogen III synthase from human erythrocytes. *J Biol Chem.* 262: 1268-1273.
- Tsang EW, Yang J, Chang Q, Nowak G, Kolenovsky A, McGregor DI and Keller WA.** (2003) Chlorophyll reduction in the seed of *Brassica napus* with a glutamate 1-semialdehyde aminotransferase antisense gene. *Plant Mol Biol.* 51: 191-201.
- Ujwal ML, McCormac AC, Goulding A, Kumar AM, Soll D and Terry MJ.** (2002) Divergent regulation of the HEMA gene family encoding glutamyl-tRNA reductase in *Arabidopsis thaliana*: expression of HEMA2 is regulated by sugars, but is independent of light and plastid signalling. *Plant Mol. Biol.* 50: 81-89.
- Uozumi, N., Kim,E.J., Rubio,F., Yamaguchi,T., Muto,S. Tsuboi,A., Bakker,E.P. Nakamura,T. and Schroedr,J.I.** (2000) The *Arabidopsis* HKT1 gene homolog mediates inward Na⁺ currents in *Xenopus laevis* oocytes and Na⁺ uptake in *Saccharomyces cerevisiae*. *Plant Physiol.* 122,1249-1259.
- Vacula R, Steiner JM, Krajcovic J, Ebringer L and Loffelhardt W.** (2001) Plastid state- and light-dependent regulation of the expression of nucleus-encoded genes for chloroplast proteins in the flagellate *Euglena gracilis*. *Folia Microbiol (Praha).* 46: 433-441.
- Van Heyningen S and Shemin D.** (1971) Quaternary structure of δ -aminolevulinic acid dehydratase from *Rhodospirillum rubrum*. *Biochemistry.* 10: 4676-4682.
- Varughese KI, Xuong NH, Kiefer PM, Matthews DA and Whiteley JM.** (1994) Structural and mechanistic characteristics of dihydropteridine reductase: a member of the Tyr-(Xaa)₃-Lys-containing family of reductases and dehydrogenases. *Proc Natl Acad Sci US A.* 91: 5582-5586.

- Vass I, Styring S, Hundal T, Koivuniemi A, Aro E-M and Andersson B.** (1992) Reversible and irreversible intermediates during photoinhibition of photosystem II: Stable reduced QA species promote chlorophyll triplet formation. *Proc. Natl. Acad. Sci. USA.* 89: 1408–1412.
- Velikova M, Bankova V, Marcucci MC, Tsvetkova I, Kujumgiev A.** (2000). Chemical composition and biological activity of propolis from Brazilian meliponinae. *Z Naturforsch [C]*. Sep-Oct; 55(9-10):785-9.
- Verkamp E and Chelm BK.** (1989) Isolation, nucleotide sequence and preliminary characterization of *E. Coli* k-12 hemA gene. *J Bacteriol* 171: 4728-4735.
- Volkov V, Wang B, Dominy PJ, Fricke W, Amtmann A** (2004) *Thellungiella halophila*, a salt-tolerant relative of *Arabidopsis thaliana*, possesses effective mechanisms to discriminate between potassium and sodium. *Plant Cell Environ* 27:1–14
- Von Wettstein D, Gough S and Kannangara CG.** (1995) Chlorophyll biosynthesis. *Plant Cell.* 7: 1039-1057.
- Vothknecht UC, kannangara CG and von Wettstein D.** (1996) Expression of catalytically active glutamyl-tRNA^{Glu} reductase in *Escherichia coli* as a fusion protein with glutathione-S-transferase. *Proc Natl Acad Sci USA* 93: 9287-9291.
- Vothknecht UC, Westhoff P.** (2001). Biogenesis and origin of thylakoid membranes. *Biochim Biophys Acta.* Dec 12; 1541(1-2):91-101.
- Vranova E, Atchartpongkul S, Villarreal R, Van Montagu M, Inze D and Van Camp W.** (2002) Comprehensive analysis of gene expression in *Nicotiana tabacum* leaves acclimated to oxidative stress. *Proc. Natl. Acad. Sci. USA.* 99:10870–10875.
- W. Wang, B. Vinocur, A. Altman (2003).** Plant responses to drought, salinity and extreme temperatures: towards genetic engineering for stress tolerance. *Planta* 218 1–14.
- Wagner D, Przybyla D, van den Camp RGL, Kim C, Landgraf F, Lee KP, Wursch M, Laloi C, Nater M and Apel K.** (2004) The Genetic Basis of Singlet Oxygen-Induced Stress Responses of *Arabidopsis thaliana*. *Science.* 306: 1183-1185.
- Walker CJ and Weinstein JD.** (1994) The magnesium-insertion step of chlorophyll biosynthesis is a two-stage reaction. *Biochem J.* 299: 277-284.
- Walker CJ and Willows RD.** (1997) Mechanism and Regulation of Mg-chelatase. *Biochem J.* 327: 321-333.

- Walker CJ, Castelfranco PA and Whyte BJ.** (1991) Synthesis of divinyl protochlorophyllide. Enzymological properties of the Mg-protoporphyrin IX monomethyl ester oxidative cyclase system. *Biochem. J.* 276: 691–697.
- Walker CJ, Mansfield KE, Smith KM and Castelfranco PA.** (1989) Incorporation of atmospheric oxygen into the carbonyl functionality of the protochlorophyllide isocyclic ring. *Biochem. J.* 257: 599–602.
- Walters DR.** (2003) Polyamines and plant disease. *Phytochemistry.* 64: 97–107.
- Wang B, Lutge U, and Ratajczak R** (2004) Specific regulation of SOD isoforms by NaCl and osmotic stress in leaves of the C3 halophyte *Suaeda salsa* L. *J Plant Physiol.* 161(3): 285-93.
- Wang B., Lutge U. and Ratajczak R.** (2004a) Specific regulation of SOD isoforms by NaCl and osmotic stress in leaves of the C3 halophyte *Suaeda salsa* L. *J. Plant Physiol.* 161, 285–293.
- Wang P, Bouwman FG, Mariman EC.** (2009) Generally detected proteins in comparative proteomics--a matter of cellular stress response? *Proteomics.* 2009 Jun; 9(11):2955-66.
- Wang R, Chen S, Zhou X, Shen X, Deng L, Zhu H, Shao J, Shi Y, Dai S, Fritz E, Hüttermann A, Polle A.** (2008) Ionic homeostasis and reactive oxygen species control in leaves and xylem sap of two poplars subjected to NaCl stress. *Tree Physiol.* Jun; 28(6):947-57.
- Wang WH, Huang DD, Stachon D, Gough SP, and Kannagara CG.** (1984) Purification, characterisation and fractionation of the δ -ALA biosynthesizing Enzymes from light-grown *Chlamydomonas reinhardtii* cells. *Plant Physiol* 74: 569-575.
- Wang, Y. S.; Yang, Z. M.** (2005) Nitric oxide reduces aluminum toxicity by preventing oxidative stress in the roots of *Cassia tora* L. *Plant Cell Physiol.*, 46, 1915–1923.
- Warabi E, Usui K, Tanaka Y and Matsumoto H.** (2001) Resistance of asoybean cell line to oxifluorfen by overproductio of mitochondrial protoporphyrinogen oxidase. *Pest Manag Sci.* 57: 743-748.
- Watanabe N, Iwano M, Inokuchi H, takayama S, Yoshida S and Isogai A.** (2000) Molecular characterization and subcellular localization of protoporphyrinogen oxidase in spinach chloroplasts. *Plant Physiol.* 124: 59-70.

- Waters MT, Fray RG, Pyke KA.** (2004). Stromule formation is dependent upon plastid size, plastid differentiation status and the density of plastids within the cell. *Plant J.* Aug; 39(4):655-67.
- Weinstein JD and Beale SI.** (1985) RNA is required for enzymatic conversion of glutamate to delta-aminolevulinate by extracts of *Chlorella vulgaris*. *Arch Biochem Biophys.* 239: 87-93.
- Weinstein JD, Mayer SM and Beale SI.** (1987) Formation of δ aminolevulinic acid from glutamic acid in algal extracts. Separation into an RNA and three required enzyme componenets by serial affinity chromatography. *Plant Physiol* 84: 244-250.
- Welburn AR and Lichanthaler H.** (1984) Formulae and program to determine total carotenoids and Chl a and b of leaf extracts in different solvents. In *Advances in photosynthesis research* (Sybesma, C. ed), Martinus Nijoff/Dr. W.Junk Publishers, The Hague/Boston/Lancaster Vol.II: pp 9-12.
- Welburn, A.R. and Lichanthaler, H.** (1984) Formulae and program to determine total carotenoids and Chla and b of leaf extracts in different solvents. *In Advances in Photosynthesis research (Sylbesma, C.ed), Martinus Nijoff/Dr. W. Junk Publishers, The Hague/Boston/Lancaster Vol.II:* pp 9-12.
- Whitmarsh J and Govindjee** (2002) PhotosystemII. In *Encyclopedia of life sciences*.
- Whyte BJ and Castelfranco PA.** (1993) Further observations on the Mg-protoporphyrin IX monomethyl ester (oxidative) cyclase system. *Biochem. J.* 290: 355–359.
- Wiktorsson B, Engdahl S, Zhong LB, Böddi B, Ryberg M, Sundqvist C** (1993) The effect of cross-linking of the subunits of NADPH-protochlorophyllide oxidoreductase of the aggregational state of protochlorophyllide. *Photosynthetica* 29: 205-218.
- Wilde A, Mikolajczyk S, Alawady A, Lokstein H and Grimm B.** (2004) The *gun4* gene is essential for cyanobacterial porphyrin metabolism. *FEBS Lett.* 571: 119-123.
- Wilks HM and Timko MP.** (1995) A light-dependent complementation system for analysis of NADPH: protochlorophyllide oxidoreductase: identification and mutagenesis of two conserved residues that are essential for enzyme activity. *Proc Natl Acad Sci USA.* 92: 724-728.

- Williams P, Hardeman K, Fowler J and Rivin C.** (2006) Divergence of duplicated genes in maize: evolution of contrasting targeting information for enzymes in the porphyrin pathway. *Plant J.* 45: 727-739.
- Willows RD, Gibson LC, Kanangara CG, Hunter CN and von Wettstein D.** (1996) Three separate proteins constitute the magnesium chelatase of *Rhodobacter sphaeroides*. *Eur J Biochem.* 235: 438-443.
- Witty M, Jones RM, Robb MS, Jordan PM and Smith AG.** (1996) Subcellular location of the tetrapyrrole synthesis enzyme porphobilinogen deaminase in higher plants: an immunological investigation. *Planta.* 199: 557-564.
- Wong Y-S, Castelfranco PA, Goff DA and Smith KM.** (1985) Intermediates in the formation of the chlorophyll isocyclic ring. *Plant Physiol.* 79: 725-729.
- Wood PM and Bendall DS** (1976) The reduction of plastocyanin by plastquinol-1 the presence of chloroplasts: a dark electron transfer reaction involving components between the two photosystems. *Eur J Biochem* 61: 337-344.
- Woodbury, W.; Spencer, A. K.; Stahmann, M. A.** (1971) An improved procedure using ferricyanide for detecting catalase isozymes. *Anal. Biochem*, 44, 301-305.
- Wu Q and Vermaas WF.** (1995) Light-dependent chlorophyll a biosynthesis upon *chlL* deletion in wild-type and photosystem I-less strains of the cyanobacterium *Synechocystis* sp. PCC 6803. *Plant Mol Biol.* 29: 933-945.
- Wyn Jones RG.** (1981) Salt tolerance. In *Physiological Processes Limiting Plant Productivity*, ed. CB Johnson. Pp.271-92. London: Butterworth.
- Xiao X, Yang F, Zhang S, Korpelainen H, Li C.** (2009) Physiological and proteomic responses of two contrasting *Populus cathayana* populations to drought stress. *Physiol Plant.* 2009 Jun; 136(2):150-68.
- Xiong,L., and Zhu,J.K.** (2001) Abiotic stress signal transduction in plants: Molecular and genetic perspectives. *Physiol Plant.* 112,152-166.
- Xiong,L., and Zhu,J.K.** (2002). Molecular and genetic aspects of plant responses to osmotic stress. *Plant Cell Environ.* 25,131-139.
- Xu H, Vavilin D and Vermaas W.** (2001) Chlorophyll b can serve as the major pigment in functional photosystem II complexes of cyanobacteria. *Proc Natl Acad Sci U S A.* 98: 14168-14173.

- Xu K, Delling J and Elliott T.** (1993) The genes required for heme synthesis in *Salmonella typhimurium* include those encoding alternative functions for aerobic and anaerobic coprogen oxidation. *J bacterial.* 175: 4990-4999.
- Yamamoto HY, Bugos RC, Hieber AD.** 1999. Biochemistry and molecular biology of the xanthophyll cycle. In: Frank HA, Young AJ, Britton G, Cogdell RJ, eds. The photochemistry of carotenoids. Dordrecht: Kluwer Academic Publishers, 293–303.
- Yamasato A, Nagata N, Tanaka R and Tanaka A.** (2005) The N-terminal domain of chlorophyllide a oxygenase confers protein instability in response to chlorophyll B accumulation in Arabidopsis. *Plant Cell.* 17: 1585-1597.
- Yamasato A, Tanaka R, Tanaka A.** (2008). Loss of the N-terminal domain of chlorophyllide a oxygenase induces photodamage during greening of Arabidopsis seedlings. *BMC Plant Biol.* Jun 12; 8:64.
- Yamato S, Ida T, Katagiri M and Ohkawa H.** (1995) A tobacco soluble protoporphyrinogen-oxidising enzyme similar to plant peroxidase in their amino acid sequences and immunochemical reactivity. *Biosci Biotech Biochem.* 59: 558-559.
- Yeo AR.** (1998) Molecular biology of the salt tolerans in the context of whole- plant physiology. *J.Exp.Bot.*49: 915-29.
- Yong Xiang, Yuemin Huang, and Lizhong Xiong** (2007) Characterization of stress-responsive CIPK genes in rice for stress tolerance improvement. *Plant Physiology*, July, Vol. 144, pp. 1416–1428.
- Yoshimoto T and Matsunakas.** (1982) The mode of action of diphenyl ether herbicides: The scavenging of active oxygen is not inhibited by diphenyl ethers. In: “Abstracts of the 5th International Congress of Pesticide chemistry”, Vol. 5, p.62.
- Zahra Noreen and Muhammad Ashraf.** (2009) Assessment of variation in antioxidative defense system in salt-treated pea (*Pisum sativum*) cultivars and its putative use as salinity tolerance markers. doi:10.1016/j.jplph.2009.05.005.
- Zavgorodnyaya A, Papenbrock J and Grimm B.** (1997) Yeast 5-aminolevulinate synthase provides additional chlorophyll precursor in transgenic tobacco. *Plant J.* 12: 169-178.
- Zhang J, Tan W, Yang XH, Zhang HX.** (2008) Plastid-expressed choline monooxygenase gene improves salt and drought tolerance through accumulation of glycine betaine in tobacco. *Plant Cell Rep.* Jun; 27(6):1113-24.

- Zhang, H.X. and Blumwald, E.** (2001) Transgenic salt-tolerant tomato plants accumulate salt in foliage but not in fruit. *Nat Biotechnol.* 19, 765-8.
- Zhao X-C, and Scahaller G.E.** (2004) Effects of salt and osmotic stress upon expression of ethylene receptor ETR1 in *Arabidopsis thaliana* *FEBS Letts* 562, 189-192.
- Zheng M, Aslund F and Storz G.** (1998) Activation of the OxyR transcription factor by reversible disulfide bond formation. *Science.* 279: 1718–1721.
- Zhu J-K** (2003) Regulation of ion homeostasis under salt stress. *Curr Opin Plant Biol* 6: 441–445.
- Zhu, J-K.** (2000) Genetic analysis of plant salt tolerance using *Arabidopsis*. *Plant Physiol.* 124, 941-948.
- Zhu, J-K.** (2001) Plant salt tolerance. *Trends in Plant Sci* 6, 66-71.
- Zsebo KM and Hearst JE.** (1984) Genetic-physical mapping of a photosynthetic gene cluster from *R. capsulatus*. *Cell.* 37: 937-947.

